

Dissertation

submitted to the
Combined Faculties for the Natural Sciences and for
Mathematics of the Ruperto-Carola University of Heidelberg,
Germany

for the degree of
Doctor of Natural Sciences

presented by

Dipl. Biol. Arman Allboje Samami
born in Rasht, Iran

Oral examination: December 15th, 2011

**Lowered sulfite reduction
affects metabolism and
seed composition
in *Arabidopsis thaliana***

Referees: Prof. Dr. Rüdiger Hell

Prof. Dr. Thomas Rausch

Dedicated to my father.

از آموختن یک زمان نغوی
بدانی که دانش نیاید به بن

ز هر دانشی چون سخن بشنوی
چو دیدار یابی به شاخ سخن

فردوسی (۳۱۹ تا ۳۹۷ خورشیدی)

And when thou hearest any man of lore
Discourse, sleep not, increase thy wisdom's store;
But mark, while gazing at the boughs of speech,
How much the roots thereof are out of reach.

Ferdowsi (940 - 1020 CE)

Table of contents

Index of figures.....	III
Index of tables.....	IV
Index of supplemental data.....	IV
Table of abbreviations.....	V
Summary.....	VII
Zusammenfassung.....	VIII
1 Introduction.....	1
1.1 Importance of sulfur for life.....	1
1.2 Sulfate uptake in plants.....	2
1.3 Sulfate assimilatory reduction.....	5
1.4 Sulfite reduction by SiR.....	7
1.5 Arabidopsis sulfite reductase versus others.....	8
1.6 SAT and OAS-TL complete sulfate assimilation.....	9
1.7 Cysteine synthase complex regulates the last step of sulfate assimilation.....	10
1.8 Seeds contain storage compounds.....	11
1.8.1 Triacylglycerides as major lipid storage compounds in Arabidopsis seeds.....	13
1.8.2 Seed storage proteins.....	15
1.9 Aims of the project.....	16
2 Material and methods.....	18
2.1 Technical equipment, materials and IT.....	18
2.1.1 Technical equipment.....	18
2.1.2 Chemicals.....	20
2.1.3 Consumables.....	23
2.1.4 Kits.....	24
2.1.5 Enzymes.....	24
2.1.6 Primers.....	25
2.1.7 Software.....	27
2.2 Plant material and growth conditions.....	28
2.2.1 Plant material.....	28
2.2.2 Surface sterilization of seeds.....	28
2.2.3 Growth conditions.....	28
2.2.3.1 Growth on soil.....	28
2.2.3.2 Hydroponic cultures.....	29
2.2.3.3 Growth of Arabidopsis under sterile conditions.....	30
2.2.3.4 Chemical complementation under sterile conditions.....	30
2.2.4 Detection of phenotypic differences between <i>sir1-1</i> and Col-0 plants.....	31
2.2.5 Pollen viability test.....	31
2.2.6 Crossing of <i>Arabidopsis thaliana</i> lines <i>sir1-1</i> and <i>sir1-2</i> with SOX-OE and <i>sox-k.o.</i>	32
2.2.7 Stress induction using sulfite.....	32
2.2.8 Stable transformation of <i>Arabidopsis thaliana</i>	32
2.3 Bacteriological methods.....	33
2.3.1 Bacterial strains.....	33
2.3.2 Preparation of competent cells for electroporation.....	33
2.3.3 Transformation of bacteria.....	33
2.3.4 Bacterial growth.....	33
2.3.4.1 Plasmid isolation from <i>E.coli</i>	34
2.3.4.2 Glycerol stocks of bacteria.....	34
2.3.5 Growth of <i>Agrobacterium tumefaciens</i>	34
2.4 Molecular Biology Methods.....	34
2.4.1 Isolation of genomic DNA from <i>Arabidopsis thaliana</i>	34
2.4.2 Polymerase Chain Reaction.....	35
2.4.3 DNA gel electrophoresis.....	36
2.4.4 Cloning using endonucleases and ligase.....	36
2.5 Biochemical methods.....	37
2.5.1 Purification of soluble proteins from Arabidopsis vegetative tissues.....	37
2.5.2 Purification of proteins from Arabidopsis generative tissues.....	37
2.5.2.1 Purification of soluble proteins from seeds.....	37
2.5.2.2 Purification of total proteins from seeds.....	38
2.5.3 Protein quantification.....	38
2.5.4 2-D gel electrophoresis of seed proteome.....	39
2.5.4.1 Total seed protein extraction and 2-D electrophoresis.....	39
2.5.4.2 Protein staining and quantification.....	40
2.5.4.3 Protein identification.....	40
2.5.5 Protein separation by electrophoresis and immunoblotting.....	41
2.5.5.1 SDS-polyacrylamide gel electrophoresis.....	41
2.5.5.2 Coomassie staining of protein.....	41
2.5.5.3 Protein transfer from SDS-gels to PVDF membranes.....	41
2.5.5.4 Immunological detection of proteins on PVDF membranes.....	42
2.5.6 Activity Assays.....	42
2.5.6.1 Determination of SiR activity.....	42

2.5.6.2	Determination of APR activity.....	43
2.6	Microscopic methods	43
2.6.1	Silique and pollen imaging	43
2.6.2	Electron microscopy.....	44
2.7	Metabolomics.....	45
2.7.1	Acidic extraction of metabolites.....	45
2.7.2	Determination of amino acids and other metabolites	45
2.7.3	Determination of thiols	46
2.7.4	Determination of adenosines.....	47
2.7.5	Extraction, isolation and quantification of jasmonates, hydroxyjasmonic acid (12-OH-JA), and hydroxyjasmonic acid sulfate (12-HSO ₄ -JA)	47
2.7.6	Isolation of lipids from Arabidopsis seeds for determination of total lipid content	48
2.7.7	Lipid extraction for triacylglyceride determination	48
2.7.7.1	Determination of TAG levels in Arabidopsis seeds	49
2.7.8	In situ staining of starch	49
2.7.9	Quantitative measurement of starch and soluble sugars	50
2.7.9.1	Determination of sugars	50
2.7.9.2	Starch determination.....	50
2.7.9.3	Quantitative measurement of starch using peroxidase	51
2.7.10	Determination of sulfolipids	51
2.7.11	Quantification of leaf chlorophyll contents	52
2.8	Transcriptomics.....	52
2.8.1	mRNA Isolation.....	52
2.8.2	Examination of RNA degradation and determination of concentration	54
2.8.3	Quantitative real time-PCR.....	54
2.8.3.1	cDNA synthesis.....	54
2.8.3.2	qRT-PCR	54
2.8.4	Microarray analysis	55
2.8.4.1	Labeling, hybridization, staining and scanning.....	55
2.8.4.2	Normalization and data analysis.....	55
2.9	Principal component analysis (PCA)	56
2.10	Statistical Analyses	56
3	Results.....	57
3.1	Complementation and stress induction of the T-DNA insertion lines <i>sir1-1</i> and <i>sir1-2</i>	57
3.1.1	Genetic complementation of homozygous <i>sir1-2</i>	57
3.1.2	Tissue-specific genetic complementation of <i>sir1-1</i>	58
3.1.3	Chemical complementation of <i>SiR</i> mutant lines.....	60
3.1.4	Sulfite treatment of <i>sir1-1</i> to assess stress resistance	62
3.2	Phenotypic and metabolic characterization of <i>sir1-1</i>	63
3.2.1	Growth-based phenotypic analysis of <i>sir1-1</i>	63
3.2.2	Determination of chlorophyll amounts in leaves.....	68
3.2.3	Determination of starch levels in leaves	69
3.2.4	Metabolite changes in leaves of soil-grown plants	72
3.2.5	Determination of <i>APR2</i> transcript and APR activity	75
3.2.6	Detection of sulfide	76
3.2.7	Effects of sulfur availability on metabolites in vegetative tissues of hydroponically grown plants.....	76
3.2.7.1	Effects of sulfur availability on metabolites in leaves	77
3.2.7.2	Effects of sulfur availability on metabolites in roots.....	84
3.3	Whole transcriptome analysis of <i>sir1-1</i>	89
3.3.1	Impact of <i>SiR</i> mutation on gene expression in wild-type and <i>sir1-1</i> plants of same age.....	89
3.3.2	Impact of <i>SiR</i> mutation on gene expression in wild-type and <i>sir1-1</i> of same developmental stage.....	91
3.3.3	Comparative transcriptomic analysis between wild-type and <i>sir1-1</i> of wild-type-age and wild- type-development	93
3.3.4	Affected genes related to sulfolipids and jasmonic acid.....	96
3.4	Analysis of generative tissue in <i>sir1-1</i>	98
3.4.1	Impact of <i>SiR</i> mutation on bolting time	99
3.4.2	Silique characterization in <i>sir1-1</i> and wild-type plants.....	100
3.4.3	Impact of <i>SiR</i> mutation on seed yield	103
3.4.4	Impact of sulfur availability on seed yield of <i>sir1-1</i> and wild-type plants.....	106
3.4.5	<i>SiR</i> transcript, protein and activity in <i>sir1-1</i> seeds	108
3.4.6	Effects of decreased sulfite reduction on the <i>sir1-1</i> seed composition	111
3.4.7	Effects of decreased sulfite reduction on the sulfur assimilatory reduction pathway in <i>sir1-1</i> and wild-type seeds	114
3.4.8	Effects of decreased sulfite reduction on the <i>sir1-1</i> proteome.....	115
4	Discussion.....	120
4.1	Effects of <i>SiR</i> mutation on the whole genome and metabolites	120
4.2	Effects of decreased sulfite reduction on the generative growth	126
4.3	Effects of decreased sulfite reduction on the seed proteome.....	127
	References.....	131
	Supplemental data.....	152
	General statement.....	175
	Acknowledgment	176

Index of figures

Fig. 1 Complementation of <i>sir1-2</i> with <i>SiR</i> restores wild-type phenotype.	58
Fig. 2 Complementation of <i>sir1-1</i> with tissue-specific <i>SiR</i> expressing constructs.	60
Fig. 3 Chemical complementation of <i>sir1-1</i> and <i>sir1-2</i>	61
Fig. 4 <i>sir1-1</i> is sensitive to sulfite stress.	63
Fig. 5 Rosette-based phenotypic analyses reveal contracted growth of <i>sir1-1</i>	65
Fig. 6 On full media <i>sir1-1</i> has a lower germination rate than wild-type.	66
Fig. 7 <i>sir1-1</i> has a lower germination rate than wild-type on deficient media.	67
Fig. 8 Total chlorophyll is decreased in <i>sir1-1</i> leaves compared to wild-type.	69
Fig. 9 <i>sir1-1</i> leaves have lower diurnal starch amount compared to wild-type leaves.	70
Fig. 10 <i>sir1-1</i> can synthesize and degrade starch.	71
Fig. 11 Metabolic analysis of soil-grown <i>sir1-1</i> and wild-type plants.	73
Fig. 12 Adenosine levels were changes in <i>sir1-1</i> compared to wild-type plants.	74
Fig. 13 <i>APR2</i> transcript and total <i>APR</i> activity is reduced in <i>sir1-1</i> leaves.	75
Fig. 14 Sulfide detection in leaf tissue reveals no changes in <i>sir1-1</i> compared to wild-type.	76
Fig. 15 Thiol contents of soil- and hydroponically grown plants were similar.	77
Fig. 16 Leaf metabolic analysis of <i>sir1-1</i> and WT plants grown hydroponically on +S.	79
Fig. 17 Leaf metabolic analysis of <i>sir1-1</i> and WT plants after transfer to -S.	80
Fig. 18 Leaf +S:-S ratios of wild-type and <i>sir1-1</i> plants.	82
Fig. 19 PCA on WT and <i>sir1-1</i> leaf metabolites from +S and -S conditions.	83
Fig. 20 Root metabolic analysis of <i>sir1-1</i> and WT plants grown hydroponically on +S.	85
Fig. 21 Root metabolic analysis of <i>sir1-1</i> and WT plants after transfer to -S.	86
Fig. 22 Root +S:-S ratios of wild-type and <i>sir1-1</i> plants.	87
Fig. 23 PCA on WT and <i>sir1-1</i> root metabolites from +S and -S conditions.	88
Fig. 24 Altered gene expression in 7-week-old <i>sir1-1</i> leaf compared to wild-type.	90
Fig. 25 Categorized altered genes in 7-week-old <i>sir1-1</i> compared to wild-type.	91
Fig. 26 Altered gene expression in 10-week-old <i>sir1-1</i> leaf compared to 7-week-old wild-type.	92
Fig. 27 Categorized altered genes in 10-week-old <i>sir1-1</i> compared to wild-type.	93
Fig. 28 Venn diagram shows unique and shared genes which were changed between and among 7-week-old wild-type, <i>sir1-1</i> and 10-week-old <i>sir1-1</i>	94
Fig. 29 Sulfolipids seemed to be unchanged in <i>sir1-1</i> leaves.	97
Fig. 30 Jasmonic acid and 12-hydroxyjasmonic acid in leaves of wild-type and <i>sir1-1</i> plants.	98
Fig. 31 <i>sir1-1</i> needs a longer period to start bolting.	99
Fig. 32 <i>sir1-1</i> has less siliques than wild-type.	100
Fig. 33 <i>sir1-1</i> siliques contain less seeds than wild-type siliques.	102
Fig. 34 <i>sir1-1</i> has more aborted pollen grains than the wild-type.	103
Fig. 35 <i>sir1-1</i> has lower seed yield with wild-type-like 100-seed-weight.	105
Fig. 36 <i>sir1-1</i> seed yield is negatively affected by sulfur deprivation to a higher degree than wild-type.	107
Fig. 37 <i>SiR</i> transcript and protein is reduced in <i>sir1-1</i> vegetative and generative tissues.	110
Fig. 38 <i>sir1-1</i> seeds contain higher protein amounts.	111
Fig. 39 <i>sir1-1</i> seeds have more free amino acids compared to wild-type.	112
Fig. 40 <i>sir1-1</i> seeds have less fat compared to wild-type.	113
Fig. 41 <i>sir1-1</i> shows seed sugar and starch levels comparable to wild-type.	114
Fig. 42 Effects of <i>SiR</i> mutation on the sulfur assimilation and reduction pathway in seeds.	115
Fig. 43 2-D analysis of the seed proteome reveals changes in <i>sir1-1</i>	116
Fig. 44 Affected metabolic pathways in <i>sir1-1</i> seeds.	119

Index of tables

Tab. 1 Affected gene sets due to <i>SiR</i> mutation are linked to DNA repair and stress.	95
Tab. 2 Polypeptides with changed abundance in <i>sir1-1</i> seeds.	118

Index of supplemental data

Suppl. data 1 Raw data of leaf metabolites of soil-grown <i>sir1-1</i> and wild-type plants.	152
Suppl. data 2 Raw data of leaf metabolites of <i>sir1-1</i> and WT plants grown hydroponically on +S.	153
Suppl. data 3 Raw data of leaf metabolites of <i>sir1-1</i> and WT plants after transfer to -S.	154
Suppl. data 4 Raw data of root metabolites of <i>sir1-1</i> and WT plants grown hydroponically on +S.	155
Suppl. data 5 Raw data of root metabolites of <i>sir1-1</i> and WT plants after transfer to -S.	156
Suppl. data 6 In vitro detection of sulfide via HPLC using OAS-TL activity.	157
Suppl. data 7 In vitro detection of cysteine via HPLC using OAS-TL activity.	158
Suppl. data 8 399 genes that were altered in 7-week-old <i>sir1-1</i> in comparison to wild-type of same age.	159
Suppl. data 9 721 genes that were altered in 10-week-old <i>sir1-1</i> in comparison to wild-type of same size (7-week-old).	161
Suppl. data 10 Mutation-specific regulated genes in <i>sir1-1</i>	165
Suppl. data 11 Constantly altered genes in all three groups.	166
Suppl. data 12 GSEA results for gene set 'nucleobase, nucleoside and nucleic acid metabolic process'.	167
Suppl. data 13 GSEA results for gene set 'DNA metabolic process'.	168
Suppl. data 14 GSEA results for gene set 'DNA repair'.	169
Suppl. data 15 GSEA results for gene set 'response to endogenous stimulus'.	170
Suppl. data 16 GSEA results for gene set response to 'DNA damage stimulus'.	171
Suppl. data 17 Detailed information about LC-MS/MS protein identification.	172

Table of abbreviations

AcCoA	acetyl-coenzymeA
ADP	adenosine diphosphate
APR	adenosine-5'-phosphosulfate reductase
APS	adenosine 5'-phosphosulfate
A.th.	<i>Arabidopsis thaliana</i>
AT	<i>Arabidopsis thaliana</i>
ATP	adenosine triphosphate
ATPS	adenosine triphosphate sulfurylase
BASTA	glufosinate ammonium
BCIP	5-bromo-4-chloro-3-indolyl phosphate toluidin salt
bp	basepairs
BSA	bovine serum albumin
CaMV	cauliflower mosaic virus
CHAPS	3-[(3-Cholamidopropyl)dimethylammonio]-1-propanesulfonate
Col-o	<i>Arabidopsis thaliana</i> ecotype Columbia-o
CSC	cysteine synthase complex
Cys	cysteine
DAF	days after flowering
DEPC	diethylpyrocarbonate
DMSO	dimethyl sulfoxide
dNTP	deoxynucleotide solution mix
DTT	1,4-dithiothreitol
DW	dry weight
EDTA	ethylenediamine tetraacetic acid
EGTA	glycol-bis(2-aminoethylether)-N,N,N',N'-tetraacetic acid
ER	endoplasmic reticulum
FW	fresh weight
GABA	4-amino-butric acid
GFP	green fluorescent protein
GR	glutathione reductase
GSH	reduced glutathione
GSH1	γ -glutamylcysteine ligase
GST	glutathione-S-transferase
HEPES	4-(2-hydroxyethyl)-1-piperazineethanesulfonic acid
HPLC	high performance liquid chromatography
HRP	horse radish peroxidase
IEF	isoelectric focusing
IPG	immobilized pH gradient
IPTG	isopropyl-D-1-thiogalactopyranoside
JA	jasmonate
Kan	kanamycin
kDa	kilo Dalton
K _m	Michaelis constant

LC	liquid chromatography
MBB	monobromobimane
MOPS	3-(N-morpholino)propanesulfonic acid
MS	Murashige & Skoog
n.a.	not applicable
n.d.	not detected
NADPH	nicotinamide adenine dinucleotide phosphate
OAS	<i>O</i> -acetylserine
OAS-TL	<i>O</i> -acetylserine(thiol)lyase
OD	optical density
12-OH-JA	hydroxyjasmonic acid
PAGE	polyacrylamide gelelectrophoresis
paraquat	N,N'-dimethyl-4,4'-bipyridinium dichloride or methylviologen
PCA	principal component analysis
PCR	polymerase chain reaction
PLP	pyridoxal 5'-phosphate
PMS	phospahte buffered saline
PMSF	phenylmethansulphonylfluoride
PR	pathogenesis related
PVP	polyvinylpyrrolidone
qRT-PCR	quantitative realtime polymerase chain reaction
ROS	reactive oxygen species
rpm	round per minute
SAT (serat)	serine acetyltransferase
SDS	sodiumdedocylsulfate
SiR	sulfite reductase
SOD	superoxide dismutase
SOX	sulfite oxidase
SQD	sulfoquinovose synthase
SSP	seed storage protein
Suc	sucrose
TAG	triacylglyceride
TAIR	The Arabidopsis information resource
TBS	tris buffered saline
TCA	trichloroacetic acid
T-DNA	transferred DNA used for insertional mutagenesis
TEMED	N,N,N',N'-Tetramethylethylenediamine
TES	N-Tris(hydroxymethyl)methyl-2-aminoethanesulfonic Acid
Tris	2-amino-2-(hydroxymethyl)propane-1,3-diol
v/v	volume per volume
VPE	vacuolar processing enzyme
VSR	vacuolar sorting receptor
w/v	weight per volume
WT	wild-type
(4Fe-4S)	iron-sulfur cluster type 4

Summary

Sulfite reductase (SiR) plays an exclusive role in the assimilatory sulfur reduction pathway by catalyzing the reduction of sulfite to sulfide. The T-DNA insertion mutant line *sir1-1* shows lower amounts of SiR transcript, protein and lower activity in vegetative and generative tissues and is severely affected in growth. However, *sir1-1* plants flower and set viable seeds, albeit later than wild-type plants and with lower yield. A T-DNA insertion with even less SiR transcript (*sir1-2*) causes early seedling lethality.

It was found that *sir1-1* is less tolerant to sulfite treatment. Death of *sir1-2* plants and the severe growth phenotype of *sir1-1* could be caused by the lack of reduced downstream products (cysteine, GSH) or/and the accumulation of toxic sulfite. Mutant plants could be partially complemented by cysteine and GSH. Despite the earlier observation of reduced flux of sulfur into cysteine and GSH the steady state concentration of sulfide was found to be unchanged in *sir1-1*. In addition to chlorosis observed in *sir1-1* the contents of sugars and starch were reduced. The large scale quantification of metabolites in *sir1-1* leaf and root compared to wild-type revealed that *sir1-1* resides in a sulfur deprivation stage. However, the response of *sir1-1* in leaves to sulfur deprivation was different from wild-type, whereas in roots the response of both *sir1-1* and wild-type plants were similar.

The consequences of the severe changes in leaf growth and metabolism prompted the investigation of the transcriptome using Affymetrix arrays. *sir1-1* plants of the same age and the same size as compared wild-type revealed numerous changes in expression of several functional groups of genes. Gene set enrichment analysis revealed up-regulation of pathways related to DNA damage. In seeds of *sir1-1* the transcription of the *SiR* gene and levels and activity of the SiR protein were even more reduced compared to leaves, resulting in severe effects on seed production. With respect to seed composition protein and free amino acid contents were increased while oil contents were decreased. The seeds were found to respond to this limitation of sulfate assimilation by comprehensive changes in their proteome. Precursors of sulfur-poor globulins accumulated but not the mature forms, while a sulfur-rich albumin decreased in content. Thus, reduced expression of sulfite reductase has profound consequences for primary metabolism of vegetative and generative organs.

Zusammenfassung

Sulfite-Reductase (SiR) spielt eine exklusive Rolle in der assimilatorischen Schwefelreduktion, indem sie die Reduktion von Sulfit zu Sulfid katalysiert. Die T-DNA-Insertionsmutante *sir1-1* hat weniger SiR-Transkript, -Protein und -Aktivität sowohl in vegetativem als auch in generativem Gewebe und ist in ihrem Wachstum stark beeinträchtigt. Allerdings blühten die *sir1-1*-Pflanzen und produzierten Samen, wenn auch später als Wildtyppflanzen und in geringeren Mengen. Eine T-DNA-Insertion, die noch weniger SiR-Transkription zulässt (*sir1-2*), hat zu Folge, dass die Pflanzen bereits im Keimling-Stadium sterben.

Es wurde festgestellt, dass *sir1-1*-Pflanzen weniger tolerant gegenüber Sulfit-Behandlung sind. Der Tod der *sir1-2*-Pflanzen und der schwerwiegende Wachstumsphänotyp von *sir1-1*-Pflanzen könnten durch den Mangel der reduzierten Folgeprodukten (Cystein, GSH) und/oder die Anhäufung von toxischem Sulfit verursacht worden sein. Trotz früherer Beobachtung der reduzierten Flussrate von Schwefel zu Cystein und GSH war die Steady-state-Konzentration von Sulfid in *sir1-1* unverändert. Zusätzlich zur beobachteten Chlorose in *sir1-1* waren die Zucker- und Stärke-Mengen reduziert. Umfangreiche Metabolitanalysen aus *sir1-1*-Blättern und -Wurzeln im Vergleich zum Wildtypen zeigten, dass *sir1-1* sich in einem Zustand des Schwefelmangels befindet. Allerdings war die Reaktion der *sir1-1*-Pflanzen auf Schwefelentzug in Blättern unterschiedlich von der der Wildtyp-Pflanzen, während die Reaktionen in den Wurzeln von *sir1-1*- und Wildtyp-Pflanzen ähnlich waren.

Die Folgen der gravierenden Veränderungen in Blattwachstum und -Stoffwechsel veranlassten die Untersuchung des Transkriptoms mit Hilfe von Affymetrix-Arrays. *sir1-1*-Pflanzen des gleichen Alters und der gleichen Größe im Vergleich zum Wildtypen zeigten zahlreiche Veränderungen in der Expression von Genen aus mehreren funktionellen Gruppen. *Gene set enrichment analysis* zeigte eine Hochregulation der Signalwege, die im Zusammenhang mit DNA-Schäden stehen. In *sir1-1*-Samen waren SiR-Transkript, -Protein und -Aktivität noch stärker reduziert als in den Blättern. Dies hatte schwere Auswirkungen auf die Samenproduktion. Die Zusammensetzung der Samen veränderte sich: Die Menge der Proteine und der freien Aminosäuren wurde erhöht, während der Ölanteil verringert wurde. Auf diese Einschränkung von Sulfatassimilation reagierten die *sir1-1*-Samen durch umfangreiche Änderungen in ihrem Proteom. Vorstufen von schwefelarmen Globulinen sammelten sich an, nicht aber die reifen Formen, während die Menge eines schwefelreichen Albumins vermindert war. Die verringerte Expression von Sulfit-Reduktase hat tiefgreifende Konsequenzen für den Primärmetabolismus in vegetativen und generativen Organen.

1 Introduction

1.1 Importance of sulfur for life

In higher plants sulfur is the most important macronutrient after carbon, phosphorus and nitrogen. Sulfur is present in the oxidized and the reduced form and due to its redox potential, it plays as divalent anion a significant role in plant metabolism. Furthermore, oxidized sulfur is essential for proper function of several molecules, e.g. glucosinolates. The break-down of glucosinolates by myrosinases results in several biologically active molecules like isothiocyanates, thiocyanates, and nitriles (Graser et al., 2001; Reichelt et al., 2002) which can protect plants against herbivores. They also might have preventive functions against cancer in humans (Schnug, 1993; Wittstock and Halkier, 2002). Hydrolysis of methylsulfinylalkyl glucosinolate results in sulforaphane (an isothiocyanate) that promotes apoptosis and cell cycle arrest in HT29 human colon cancer cells in vitro (Gamet-Payraastre et al., 2000). Another situation, in which an oxidized form of sulfur is utilized, are sulfolipids (Schiff et al., 1993; Benning, 1998). However, most sulfur in plants is found in the reduced form due to the assimilatory sulfur reduction pathway (1.2). Reduced sulfur is found in several coenzymes including biotin, vitamin B₁, coenzyme A, or in iron-sulfur clusters (Beinert et al., 1997; Leustek and Saito, 1999). Reduced sulfur is also a component of cysteine and methionine which are essential for human nutrition. Together with glycine and glutamic acid, cysteine builds the tripeptide glutathione (GSH). It can be seen as the transport form of (reduced) sulfur in plants and also has redox buffering functions. GSH is involved in detoxification of xenobiotics (Howden et al., 1995) and serves as a substrate in phytochelatin synthesis (Grill et al., 1989). Thiols' sulfur is of nucleophile nature and serves as an electron donor in redox processes. S-containing disulfide bridges play an important role in generating the tertiary and quaternary structure of proteins (Grill et al., 1989; Schröder et al., 1990; May et al., 1998; Noctor et al., 1998; Noctor and Foyer, 1998). Anthropogenic worldwide contribution to sulfur deposition in the atmosphere has been reduced in the last decades, especially in western

Europe (McGrath et al., 2002), for example in United Kingdom, it was decreased from 70 kg per ha per year in the 1970's to less than 10 kg per ha per year in the early 2000's (Zhao et al., 2008). Hence, sulfur deficiency has become a problem and there is an increased need for sulfur fertilization. Multiple-cut grasses and especially Brassica crops are more susceptible to sulfur deficiency compared to other crops (Zhao et al., 2008). Based on the versatile functions of sulfur in its reduced and oxidized form, sulfur deficiency causes growth retardation in plants. Also chlorophyll contents are reduced by sulfur deficiency (Burke et al., 1986; Dietz, 1989; Imsande, 1998). Chlorosis appears in young leaves as a first symptom and later older ones also develop it (Freney et al., 1978). Sulfur nutrition influences protein quality and composition (Randall and Wrigley, 1986). Due to the need of humans and animals for sulfur-containing amino acids and the low levels of cysteine and methionine in seed proteins of crops, one of the biggest goals in nutrient biotechnology is to increase methionine levels via genetic engineering (Molvig et al., 1997). Sulfur, carbon and nitrogen assimilation are tightly related to each other (Hesse et al., 2003; Wang et al., 2003; Kopriva and Rennenberg, 2004; Kopriva, 2006), so sulfur deficiency can cause inefficient nitrogen utilization. This could be proved when a sulfur-deficient grassland site was applied with sulfur and the nitrate leaching to drainage water was reduced up to 72% (Brown et al., 2000). Thus, sufficient sulfur availability for crops has at least two advantages: positive effects on yield and a benefit for the environment.

1.2 Sulfate uptake in plants

Like most microorganisms and some fungi, plants are autotrophic with regard to sulfur. Although 0.24% of the human body mass consists of sulfur (Steudel, 1998), neither humans nor animals are able to reduce sulfate to sulfide and therefore they are forced to take up reduced sulfur compounds via nutrition (Ravanel et al., 1998; Tabe and Higgins, 1998; Noji and Saito, 2002).

Sulfate is taken up from soil by proton/sulfate cotransporters located in the roots of plants (Mengel, 1991; Takahashi et al., 1997; Leustek et al., 2000; Buchner et al., 2004). Some of these sulfate transporters are able to acclimate to the external sulfate supply and are regulated at the transcript level. In the model plant *Arabidopsis thaliana*, there are 14 sulfate transporters, which are classified in 5 groups according to their sequence homology (Clarkson and Hawkesford, 1993; Hawkesford and Smith, 1997; Hell, 1997; Honda et al., 1998; Hawkesford and Wray, 2000; Saito, 2000; Westerman et al., 2000; Hawkesford, 2003; Yoshimoto et al., 2003; Yoshimoto et al., 2007).

Members of the first group of sulfate transporters (Sultr1) are exclusively expressed in the roots. Expression of Sultr1;1 and Sultr1;2 is induced by sulfate deficiency via O-acetylserine (OAS) and can be repressed via GSH. They are additionally post-transcriptionally regulated and called high-affinity transporters because they allow the plant to react to reduced external sulfur availability (Smith et al., 1997; Saito, 2000; Maruyama-Nakashita et al., 2004; Yoshimoto et al., 2007). Sultr1;1 has a K_m value of $3.6 \pm 0.6 \mu\text{M}$ for sulfate and is expressed in root tips, root hairs, the root epidermis and in the root cortex (Takahashi et al., 2000).

Group 2 sulfate transporters are expressed in roots as well as in the leaves and have low affinity for sulfate: Sultr2;1 ($K_m = 0.41 \pm 0.07 \text{ mM}$) can be found in pericycle and xylem parenchyma of root cells and in the leaf phloem; Sultr2;2 ($K_m = 1.2 \text{ mM}$) is expressed in the root phloem and in the bundle-sheath cells of leaves. Like Sultr1, members of the Sultr2 family are inducible by sulfur deficiency: increased mRNA levels of Sultr2;1 in the roots, and Sultr2;2 in the leaves were measured when plants were exposed to sulfur withdrawal (Takahashi et al., 2000). Sultr2;1 is involved in the translocation of sulfate into the siliques since it is located in the funiculus of *Arabidopsis thaliana* and therefore, it probably plays a role in modulating the sulfate status in seeds (Awazuhara et al., 2005).

The members of the Sultr3 family show no induction by sulfur deficiency. Kataoka et al. (2004a) could show that Sultr3;1 is involved in sulfate transport between root and shoot. There are indications that group 3

sulfate transporters are involved in sulfate translocation within developing seeds (Zuber et al., 2010b).

Sultr4;1 and Sultr4;2 are located in the tonoplast membrane and are responsible for export of sulfate out of vacuoles. Recent evidence revealed that in *Brassica oleracea* Sultr4;1 transcription is induced when sulfur is not available (Koralewska et al., 2007). When it is suffering from sulfur withdraw, Sultr4;1 pumps sulfate out of vacuole to supply sulfate for whole plant via xylem elements in a symplastic manner. Sultr4;2 is expressed in roots at sulfur deficiency (Kataoka et al., 2004b). Sultr4;1 is shown to be involved in sulfate transport in developing seeds (Zuber et al., 2010a).

Little is known about the Sultr5 family. Hesse et al. (2004) could show that Sultr5;1 transcript levels were increased in leaves and roots under sulfur-deficient conditions, and decreased again after sufficient sulfur had been applied. Analysis of MOT2 (molybdate transporter 2; previously annotated as Sultr5;1) fused to GFP indicated a vacuolar location of this carrier protein and it was concluded from *mot2* T-DNA mutant that it is important for vacuolar molybdate export in the leaves and accumulation of molybdate in Arabidopsis seeds (Gasber et al., 2011). Sultr5;2 (now annotated as MOT1) has been reported to act as a high affinity molybdenum transporter rather than a sulfate transporter (Tomatsu et al., 2007).

Translocators in xylem and phloem elements are responsible for long-distance transport of sulfate from roots where it is taken up to the leaf mesophyll cells for reduction (Saito, 2000). In the leaves, sulfate is transported into vacuoles via Sultr4 members for storage. Vacuoles can contain up to 99% of total cell sulfate (Rennenberg, 1984; Bell et al., 1994).

The majority of sulfur assimilation steps take place in chloroplasts, so there must be transporters for its import into chloroplasts. However, no chloroplast-specific sulfate transporters have been identified yet (Davidian and Kopriva, 2010). It has been suggested that this function could be carried out by phosphate-/triose-phosphate translocators

localized in the inner membrane of chloroplasts, or by proton-/sulfate symporters (Flügge et al., 1989; Leustek and Saito, 1999).

1.3 Sulfate assimilatory reduction

After uptake of sulfate its assimilation starts with an activation reaction resulting in adenosine 5'-phosphosulfate (APS) (Balharry and Nicholas, 1970; Renosto et al., 1993). This reaction is catalyzed by ATP sulfurylase (ATPS; EC 2.7.7.4) whereby sulfate is coupled with a phosphate residue by ATP cleavage which releases a pyrophosphate. ATPS reaction takes place in cytosol and plastids. It is likely that in Arabidopsis all isoforms encode plastidic enzymes. The cytosolic isoform could be derived from an alternative transcriptional start codon produced from one of these 4 genes (Hatzfeld et al., 2000a). The physiological role of cytosolic ATPS remains unclear since the sulfite reduction to sulfide (next step of sulfur reduction pathway) is carried out in plastids. Rotte and Leustek (2000) speculated that APS produced in cytosol might be further activated via PAPS.

ATPS gene expression is induced upon sulfur deficiency (Logan et al., 1996) and inhibited when nitrogen starvation occurs (Reuveny et al., 1980; Smith, 1980) or when GSH levels increase (Lappartient and Touraine, 1996; Lappartient et al., 1999).

APS inhibits ATPS and therefore it must be metabolized quickly (Renosto et al., 1993; Schwenn, 1994; Hell, 1998; Hatzfeld et al., 2000a; Rotte and Leustek, 2000). APS can either be directed into the sulfur reduction pathway or further activated (Lee and Leustek, 1998; Lillig et al., 2001; Droux, 2004). In the latter pathway APS is phosphorylated to 3'-phosphoadenosyl 5'-phosphosulfate (PAPS) by APS kinase (APK). There are 4 APKs in the cytosol and plastids (Lunn et al., 1990; Rotte and Leustek, 2000; Mugford et al., 2009). PAPS serves as a sulfate donor for sulfotransferases (SOT) that catalyze sulfation of several molecules including glucosinolates, saccharides, proteins, flavonoids, and jasmonates. Due to the high number of substrates, multiple isoforms of SOT can be found in plants (Klein and Papenbrock, 2004). PAPS can also be considered as an intermediary storage form of APS that can be (e.g.

upon oxidative stress) re-transformed to APS. This reaction step is catalyzed by 3'(2'),5'-diphosphonucleoside 3'(2')-phosphohydrolase (DNPase; EC 3.1.3.7) (Peng and Verma, 1995).

The next possibility for metabolizing APS is its reduction to sulfite by GSH-dependent double electron transfer to APS (Suter et al., 2000). This reaction is catalyzed by APS reductase (APR; EC 1.8.4.9). APR is located in plastids and exhibits a homodimer structure (Kopriva and Koprivova, 2004). One catalytic domain of APR is similar to the PAPS reductases of microorganisms and has a cysteine binding motif. The other carboxy terminal domain is homologous to the thioredoxin superfamily and serves as the acceptor of electron from GSH (Gutierrez-Marcos et al., 1996; Setya et al., 1996; Bick et al., 1998; Gao et al., 2000; Suter et al., 2000; Kopriva et al., 2002).

In Arabidopsis, there are 3 APR isoforms of which APR2 is the major form making up 80% of the total intracellular APR activity. APR is highly regulated in assimilatory sulfate reduction: APR2 transcript levels are reduced upon exposure to reduced sulfur compounds such as sulfide, cysteine, and GSH (Kopriva and Koprivova, 2004). APR expression is up-regulated when plants are stressed with heavy metals, salinity, high light, or cold (Lee and Leustek, 1999; Kopriva et al., 2008; Queval et al., 2009). APR is subjected to a diurnal rhythm whereas at day time its activity is higher than at night (Kopriva et al., 1999). Addition of sugars into plant media increased APR activity, too (Hesse et al., 2003).

Nitrogen deficiency causes a decrease of APR activity and exposure to amino acids or ammonium results in an increase of APR activity, highlighting the connection between sulfate and nitrogen assimilation (Brunold and Suter, 1984; Koprivova et al., 2000).

Sulfite can be re-oxidized to sulfate through a reaction catalyzed by a molybdenum enzyme, sulfite oxidase (SOX) utilizing oxygen as an electron acceptor in the peroxisomes (Eilers et al., 2001; Hänsch et al., 2006). Due to spatial separation, SOX rather protect plants against access to sulfur dioxide and is involved in sulfite detoxification, than in sulfur assimilation in plastids (Brychkova et al., 2007; Lang et al., 2007).

1.4 Sulfite reduction by SiR

To convert sulfite into sulfide, sulfite reductase (SiR; EC 1.8.7.1) needs 6 electrons. In higher plants, these are provided by ferredoxins, whereas chemotrophic organisms utilize electrons from NADPH. SiR is the only single-copy gene in the assimilatory sulfate reduction pathway of *Arabidopsis* (Bork et al., 1998; Nakayama et al., 2000). SiR has a bottleneck function in the assimilatory reduction pathway and is involved in regulation of sulfate assimilation and the control of sulfur flux (Khan et al., 2010). Plant SiR protein is soluble and exhibits a molecular mass of 65 kDa. SiR contains one siroheme and a (4Fe-4S) cluster as prosthetic groups (Krueger and Siegel, 1982; Nakayama et al., 2000). The physiological electron donor for SiR is an iron-containing protein called ferredoxin which carries one electron with a (2Fe-2S) cluster (Yonekura-Sakakibara et al., 2000). Two interaction sites of ferredoxin are crucial for interaction with SiR: region 1 containing Glu-29, Glu-30, Asp-34 and region 2 including Glu-92, Glu-93, Glu-94 (Saitoh et al., 2006). The 1:1 stoichiometry of the transient electron transfer complex between ferredoxin and SiR (Akashi et al., 1999) and the high affinity of SiR for sulfite ($K_m \sim 10 \mu\text{M}$) enable efficient sulfite reduction (Leustek and Saito, 1999). Since the electrons of PSI in photosynthetic cells are carried forward to ferredoxin, there is a connection between sulfate assimilation and photosynthesis.

SiR is exclusively located in plastids (Brunold and Suter, 1989), and for pea and maize, it has been shown that SiR interacts with the plastidic DNA-protein complex named nucleoid (Sekine et al., 2007). Sekine et al. (2002) suggested that SiR can regulate plastid nucleoid transcription via DNA compaction: When SiR is not bound to nucleoids, plastidic DNA can relax and transcription occurs; addition of exogenous SiR, makes plastidic DNA more compact resulting in repression of transcription. In plastids of heterotrophic tissues, regeneration of reduced ferredoxin is possible due to NADPH (Brühl et al., 1996; Leustek and Saito, 1999; Leustek et al., 2000; Nakayama et al., 2000).

SiR transcript levels increase when OAS is fed to nitrogen-deficient *Arabidopsis* (Koprivova et al., 2000) or when methyl jasmonate is added (Jost et al., 2005).

1.5 Arabidopsis sulfite reductase versus others

Sekine et al. (2007) compared the amino acid sequence homology of pea SiR (PtSiR) to SiR of other organisms. PtSiR was similar to *Nicotiana tabaccum* SiR (NtSiR, 91%), *Arabidopsis thaliana* SiR (AtSiR, 85%), *Oryza sativa* SiR (OsSiR, 79%), and *Zea mays* SiR (ZmSiR, 79%). Compared to *E. coli* and the red alga *Cyanidioschyzon merolae*, the similarity of PtSiR was lower: to the hemoprotein subunit (CysI) of *E. coli* (EcCys, 48%), SiR A of *C. merolae* (CmSiRA, 59%), and SiR B (CmSiRB, 57%).

In *E. coli*, four cysteine ligands (Cys-434, Cys-440, Cys-479, and Cys-483) hold siroheme and (4Fe-4S) cluster within the active site of CysI (Crane et al., 1995). The observation that four basic amino acids (Arg-83, Arg-153, Lys-215, and Lys-217) involved in the coordination of sulfite to the siroheme, are conserved in all SiRs gives rise to the statement that all SiRs of flowering plants are monophyletic in their origin (Sekine et al., 2007), and originated from cyanobacterial SiR (Kopriva et al., 2008).

Kopriva et al. (2008) also suggested that AtSiR and *Arabidopsis* nitrite reductase (AtNiR) have the same evolutionary origin due to their 19% identity. Phylogenetic analysis could reveal that both SiR and NiR arose from an ancient gene duplication in Eubacteria before primary endosymbiosis resulting in emergence of plastids. Also their functions are similar: NiR catalyzes an equivalent reduction step in nitrate assimilation, namely reduction of nitrite to ammonia, using ferredoxin as the donor of six electrons. Maize SiR changes substrate specificity from sulfite to nitrite, when its amino acid residue Arg-193 is converted into glutamate (Nakayama et al., 2000). SiR from *C. merolae* exposes preferred substrate specificity for nitrite (Sekine et al., 2009). Endogenous NiR in *Arabidopsis* is not able to rescue the reduced activity of SiR in a SiR T-DNA insertion mutant (Khan et al., 2010).

1.6 SAT and OAS-TL complete sulfate assimilation

Most sulfur-autotroph organisms incorporate reduced sulfur into cysteine (Giovanelli et al., 1980; Schmidt and Jäger, 1992). Therefore, a distinct two-step reaction occurs (Rabeh and Cook, 2004; Wirtz and Droux, 2005; Kopriva, 2006). In the first step, an acetyl residue of acetyl coenzyme A (AcCoA) is transferred to the hydroxyl group of serine by serine acetyltransferase (SAT; Serat; EC 2.3.1.30). O-acetylserine (OAS) is the product of this first reaction step.

The Arabidopsis Genome Initiative (2000) identified 5 genes for *SAT* and *SAT*-like isoforms located in several cell compartments. According to their position on 5 chromosomes of Arabidopsis, they were named *SAT1* to *SAT5* (Noji et al., 1998; Hell et al., 2002). *SAT1* and *SAT3* are targeted to plastids and mitochondria, respectively, and *SAT5* is localized in the cytosol (Bogdanova et al., 1995; Murillo et al., 1995; Howarth et al., 1997; Kawashima et al., 2005). These three SATs are considered to be the major isoforms with K_m values for serine and AcCoA between 1 and 3 mM (Davidian and Kopriva, 2010). Due to analysis of amino acid sequences, *SAT4* was considered to be targeted to plastids (Droux, 2004). However, it turned out that both *SAT2* and *SAT4* are located in the cytosol and have a K_m value for serine between 40 and 120 mM (Noji et al., 1998; Kawashima et al., 2005; Watanabe et al., 2008b). Levels of *SAT2* and *SAT4* transcript are lower than the other three major isoforms (eFP Browser: bbc.botany.utoronto.ca), however, after 4 days of sulfur deprivation, the mRNA amount of *SAT2* and *SAT4* was increased 2- and 45-fold, respectively, indicating that these isoforms may play a role upon sulfur starvation (Zimmermann et al., 2004; Kawashima et al., 2005).

The last reaction in the assimilation of sulfate into cysteine is carried out by O-acetylserine (thiol)lyase (OAS-TL; EC 2.5.1.47): by a β -elimination reaction of the acetyl moiety of the nitrogen and carbon containing skeleton of OAS by sulfide produced by SiR cysteine is formed (Bertagnolli and Wedding, 1977; Lunn et al., 1990).

Arabidopsis has 9 *OAS-TL* and *OAS-TL*-like isoforms belonging to the superfamily of β -substituting alanine synthases (Hatzfeld et al., 2000b). There are three major isoforms, i.e. OAS-TL A1, OAS-TL B, and OAS-TL C

which were identified as true OAS-TLs (Wirtz et al., 2004) and are localized in the cytosol, the plastids and the mitochondria, respectively. True OAS-TLs have been defined due to their ability to produce cysteine and to interact with SAT (Bogdanova and Hell, 1997; Droux et al., 1998; Wirtz et al., 2001; Bonner et al., 2005; Heeg et al., 2008). OAS-TL A1, OAS-TL B, and OAS-TL C contribute 50%, 40%, and 10%, respectively, to the total OAS TL activity in an Arabidopsis cell (Heeg et al., 2008; Watanabe et al., 2008a). Heeg et al. (2008) suggested that the cytosol is the major compartment for cysteine synthesis. OAS-TL A1 shows highest activity there and also both OAS and sulfide can be transported to the cytosol: The volatile form of sulfide (H_2S) can pass the plastidic membranes (Mathai et al., 2009) and OAS can leave the mitochondria, the major OAS synthesis compartment (Haas et al., 2008). Synthesized cysteine is the terminal product of sulfur assimilation and reduction pathway and can be used for the production of a variety of compounds such as methionine, GSH and vitamins that contain reduced sulfur (1.1).

1.7 Cysteine synthase complex regulates the last step of sulfate assimilation

SAT and OAS-TL can form the cysteine synthase complex (CSC; Hell et al., 2002) that acts as a regulatory complex (Wirtz and Hell, 2006). OAS-TLs from *Haemophilus influenzae*, *Salmonella typhimurium* and *Arabidopsis thaliana* show a dimeric structure (Burkhard et al., 1998; Burkhard et al., 1999; Bonner et al., 2005) and SATs from *H. influenzae* and *E. coli* a dimer of trimers (Gorman and Shapiro, 2004; Pye et al., 2004). Similar arrangements for Arabidopsis mitochondrial and cytosolic SATs have been demonstrated (Wirtz et al., 2010).

It was suggested that in *S. typhimurium*, *Spinacia oleracea*, *Nicotiana tabacum* and *Arabidopsis thaliana* a decameric CSC exist consisting of two OAS-TL dimers interacting with a SAT hexamer (Kredich et al., 1969; Droux et al., 1992; Wirtz and Hell, 2007; Heeg et al., 2008; Wirtz et al., 2010).

Bacterial and Arabidopsis SATs interact with OAS-TL via their C-terminus and consequently, a deletion of the C-terminus results in no more interaction within the CSC (Mino et al., 1999, 2000; Francois et al., 2006; Wirtz and Hell, 2006).

While SAT within the CSC shows high activity and is stabilized due to OAS-TL binding (Ruffet et al., 1994; Droux et al., 1998; Francois et al., 2006), bacterial OAS-TL bound to SAT in the CSC exhibits only 40% remaining activity (Kredich, 1996; Mino et al., 2000) and plant OAS-TL is even inactivated when bound to SAT (Droux et al., 1998). It was shown that the binding of the C-terminus of SAT to the active site of the OAS-TL causes OAS-TL inactivation (Huang et al., 2005; Francois et al., 2006).

OAS competes with the C-terminus of SAT for the active site of OAS-TL (Campanini et al., 2005; Huang et al., 2005) and therefore, high OAS concentration dissociates the CSC (Kredich et al., 1969; Droux et al., 1998). On the contrary, sulfide stabilizes the CSC promoting synthesis of OAS (Wirtz and Hell, 2006; Wirtz and Hell, 2007).

1.8 Seeds contain storage compounds

Plant seeds are of major industrial as well as economic interest. Considering the exhaustion of fossil combustible materials as energy sources during the next century, the storage compounds and biomass of some plants could be utilized as biofuels and biomaterials. Indeed, plant oil is one of the most energy-rich and abundant forms of reduced carbon available in nature. Therefore, plants could be seen as possibly sustainable alternative substitutes for conventional diesel. There are also other application fields that show successful production of industrially interesting compounds via seed engineering, i.e. mucilage as a source of pectin (Willats et al., 2006), flavonoids as antioxidants for foods (Yilmaz, 2006), nutraceuticals and pharmaceuticals (Ramos, 2007) and enriched cellulose fibre yield and quality from cotton (Lee et al., 2007).

But seed production is also very important for animal feed and human nutrition. Seed genetic engineering is considered to be an attractive strategy to enhance seed yield and quality and to produce various

metabolites and proteins (Moise et al. 2005). Since cysteine and methionine are essential for human nutrition and they have to be absorbed via nutrition (1.2), their over-accumulation was adjusted in lupines and maize seeds (Tabe and Higgins, 1998). Enhanced amino acid transport from source to sink by overexpressing genes for Asn synthase or amino acid transporters increased the amount of endogenous seed proteins (Lam et al., 2003; Rolletschek et al., 2005). Hood et al. (2007) could increase the amounts of cellulase in maize seeds. Production of yellow-seeded *Brassica* genotypes led to higher oil contents and meal nutritional value (Marles et al., 2003). Rice plants were enabled to synthesize provitamin A in the endosperm (Ye et al., 2000). In rapeseed, enhanced levels of the saturated fatty acid lauric acid could be achieved (Voelker et al., 1996).

Different plant species arouse interest depending on their major storage compounds: Most grain seeds have > 85% starch, whereas many oilseeds contain 50 to 70% oil, and some legumes such as soybeans include 40% of their seed dry weight as protein (Ruuska et al., 2002).

In many crops such as *Pisum sativum*, *Vicia faba*, wheat and maize, starch represents the most important storage compound. Therefore, and because of its importance for human nutrition, the corresponding biosynthetic pathway is well documented. Glucose-6-phosphate (G6P) is imported to the plastid from the cytosol and phosphoglucomutase transforms it into G1P. Next, production of ADP-glucose is catalyzed by ADP-glucose pyrophosphorylase. ADP-glucose is the constituent of both amylose and amylopectin (Zeeman et al., 2002).

However, in oilseeds, starch is only transiently accumulated and its amount is reduced in mature *Arabidopsis* seeds (King et al., 1997; Baud et al., 2002). The role of starch in seeds is highly debated (Vigeolas et al., 2004).

The role of sugar metabolism in the regulation of storage function is not understood, however, it is clear that sugar-sensing pathways interact with hormonal signaling (Varin et al., 1997; León and Sheen, 2003; Avonce et al., 2004). In legume seeds, the sucrose-to-hexose ratio is known to promote the synthesis of storage compounds, although the involved

molecular regulatory mechanisms are to date not fully understood (Weber et al., 2005). In *Brassicaceae*, the sucrose-to-hexose ratio remains a matter of debate. Also little is known about trehalose-6-phosphate. Nonetheless, it is thought to play a crucial role in developing Arabidopsis embryos, but the regulatory mechanism involved is unknown (Gómez et al., 2006).

However, major focus in Arabidopsis seeds or rapeseed is on other storage compounds, i.e. lipids (1.8.1) and storage proteins (1.8.2).

1.8.1 Triacylglycerides as major lipid storage compounds in Arabidopsis seeds

As a *Brassicaceae*, *Arabidopsis thaliana* is related to *Brassica* oilseed crops such as rapeseed, the world's major oilseed crop. Therefore, and since one third of Arabidopsis seed is filled with storage oil and proteins, respectively, Arabidopsis is an optimal model organism to understand pathways related to storage compounds.

In mature Arabidopsis seeds, triacylglycerides (TAGs) represent the major oil component (Baud et al., 2002). TAGs are energy-rich carbon storage molecules. As mentioned above, Arabidopsis is an ideal model plant for these kinds of studies.

Two TAG precursors are synthesized in different compartments:

In the cytosol, dihydroxyacetone phosphate (DHAP) is converted to glycerol-3-phosphate (G3P) by glycerol-3-phosphate dehydrogenases (G3PDH) providing the glycerol backbones for TAG synthesis (Baud and Lepiniec, 2010). G3P can alternatively be synthesized by phosphorylation of glycerol by glycerol kinase. G3P seems to be the restrictive molecule in TAG synthesis (Perry et al., 1999). Additional proof was given by the overexpression of a yeast gene encoding cytosolic G3PDH in *Brassica napus* that increased G3P levels in seeds, and resulted in a 40% increase in the final lipid content of seeds (Vigeolas et al., 2007). In *Brassicaceae*, embryos have to import sucrose which is transformed to phosphoenolpyruvate (PEP) via the cytosolic glycolytic pathway. PEP is imported into the plastids, where it is transphosphoylated irreversibly to

pyruvate by plastidic pyruvate kinase (Andre et al., 2007; Baud et al., 2007). In plastids, the oxidative decarboxylation of pyruvate by the pyruvate dehydrogenase complex (PDC) occurs producing CO₂ and AcCoA (Johnston et al., 1997; Lutziger and Oliver, 2000; Lin et al., 2003).

For de novo synthesis of fatty acids, AcCoA and bicarbonate are transformed to malonyl-CoA by AcCoA carboxylase (ACC) in the plastids (Turnham and Northcote, 1983; Harwood, 1996). This reaction is considered to be a key regulatory step in fatty acid biosynthesis (Thelen and Ohlrogge, 2002).

On the outer membrane of the chloroplast, fatty acids are then activated by long-chain AcCoA synthetases (LACS) forming CoA esters. They are then transported into the ER, where they join a larger AcCoA pool, or can be transformed to membrane phospholipids (Li-Beisson et al., 2010). Assembly of TAG takes place in the ER. Several pathways interconnected with TAG biosynthesis have been described in maturing oilseeds (Bates et al., 2009). AcCoAs, as provided directly from de novo fatty acid synthesis and from other sources, are used for the sequential acylation of three fatty acids at positions *sn*-1, *sn*-2 and *sn*-3 of a G3P moiety (Kennedy, 1961; Cao and Huang, 1986, 1987). TAG can also interact with reactions related to phosphatidylcholine (PC), an important membrane lipid (Li-Beisson et al., 2010).

After TAGs have been synthesized in the ER, they are stored in dedicated subcellular organelles, the oil bodies or oleosomes. TAGs in the oil bodies are surrounded by a phospholipid monolayer, whereby the phosphate groups are oriented towards the cytosol and the aliphatic chains towards the TAG lumen (Yatsu and Jacks, 1972). It is assumed that oil bodies arise from microdomains of the ER, however, the mechanisms of their biogenesis is controversially discussed (Murphy and Vance, 1999; Robenek et al., 2004; Robenek et al., 2006). The lipid monolayer of oil bodies contains proteins making up 1–4% of the weight of these organelles (Huang, 1992; Tzen and Huang, 1992; Tauchi-Sato et al., 2002). Among them, oleosins are the most abundant ones (Murphy, 1993). Covering the surface of oil bodies, oleosins improve the stability of these organelles by means of electronegative repulsion and steric hindrance, so that oil bodies

never coalesce or aggregate in the cells of mature seeds (Leprince et al., 1998; Murphy and Vance, 1999; Siloto et al., 2006).

1.8.2 Seed storage proteins

A second major group of storage compounds in *Arabidopsis* seeds are the seed storage proteins (SSP). There are two predominant classes of SSPs stored in *Arabidopsis* seeds: legumin-type globulins, referred to as 12S globulin or cruciferin (Sjodahl et al., 1991; Li et al., 2007), and napin-type albumins, referred to as 2S albumin or arabin (Krebbers et al., 1988; van der Klei et al., 1993). *Arabidopsis*, ecotype Col-0, has four genes encoding 12S globulin precursors: *CRA1* (S4; At5g44120), *CRB* (S3; At1g03880), *CRC* (S1; At4g28520), and *CRU2* (At1g03890) (Pang et al., 1988; Gruis et al., 2002; Gruis et al., 2004). 2S albumins contain two subunits, small and large, that are generated by cleavage of the precursor form and linked by disulfide bridges (Krebbers et al., 1988; Guerche et al., 1990). Five genes that encode 2S albumin precursors have been identified: *At2S1* (At4g27140), *At2S2* (At4g27150), *At2S3* (At4g27160), *At2S4* (At4g27170), and *At2S5* (At5g54740).

Both groups of SSPs are synthesized on the rough ER as precursor forms and then transported into protein storage vacuoles (PSVs) by a vesicle-mediated pathway, where they are converted into mature forms. PSVs are electron dense vacuolar compartments surrounded by the tonoplast, a lipid bilayer (Gillespie et al., 2005). Otegui et al. (2006) could show that *Arabidopsis* exhibits a Golgi-dependent pathway for the transport of the storage proteins and their processing enzymes to the PSV. However, during Golgi trafficking, different cisternal domains are responsible for SSPs and processing enzymes (Hillmer et al., 2001). Asn-specific endopeptidases (or vacuolar processing enzymes, VPEs) and aspartic proteases are chiefly involved in processing of SSPs. The VPE gene family in *Arabidopsis* has four genes: namely α VPE (At2g25940), β VPE (At1g62710), γ VPE (At4g32940), and δ VPE (At3g20210) (Kinoshita et al., 1995b, a; Kinoshita et al., 1999; Gruis et al., 2002). The *vpe* quadruple mutant of *Arabidopsis* showed alternatively processed forms of SSPs

cleaved at sites other than the conserved Asn residues targeted by VPEs, demonstrating that maturing seeds can tolerate variations in the protein content of PSVs (Gruis et al., 2004). Hence, VPE activity is not obligatory for processing of SSPs and probably, there are Asn-independent proteases (e.g. aspartic protease; Hiraiwa et al., 1997).

Processing enzymes are concentrated in clathrin-coated vesicles reaching prevacuolar compartments called multivesicular bodies (MVBs).

In the PVS, the precursor forms of SSPs are converted into their respective mature forms via limited proteolysis at specific sites. Globulin proforms are converted into the disulfide-linked mature α - and β -polypeptides after proteolytic processing at a conserved Asn-Gly peptide bond by an asparaginyl endopeptidase (Barton et al., 1982). The more complex proteolytic processing of albumins implies the removal of three propeptide regions, resulting in two disulfide-linked mature polypeptides (Krebbbers et al., 1988). A conserved Asn residue seems to be involved in several proteolytic steps, however, it cannot be excluded that other aspartic endopeptidases may be involved in the processing of the propeptides (Krebbbers et al., 1988; D'Hondt et al., 1993).

1.9 Aims of the project

Protein-rich seeds such as legume seeds are one of the major sources for human nutrition. Several attempts were made to enhance sulfur-containing amino acids cysteine and methionine in such seeds. It is known, that lupine seeds are able to reduce sulfate to cysteine (Tabe and Higgins, 1998). However, still little is known about the role of sulfate reduction in seeds of Arabidopsis: Cairns et al. (2006) could show that reduced sulfur in the form of GSH can be transported towards maturing seeds, at least to the funiculus. Mutation in *GSH1* encoding the first enzyme of GSH biosynthesis, gamma-glutamyl-cysteine synthetase caused reduction in GSH amounts within the seeds compared to wild-type seeds, indicating that developing Arabidopsis seeds are able to synthesize GSH autonomously. Expression data from developing and mature seeds (<http://bar.utoronto.ca/efp/cgi-bin/efpWeb.cgi>) also indicate that the

sulfur assimilation and reduction pathway is enabled. To investigate, whether SiR has an exclusive role in Arabidopsis seeds and exhibits a bottleneck effect, *sir1-1* mutant is utilized.

Therefore, also seeds will be in the focus. Since SSPs contain cysteine and methionine, we are interested in finding out, if SiR mutation in seeds and reduction of sulfur flux in vegetative tissue effect SSP composition and quality. Therefore, seed proteome will be investigated with special respect to SSPs. Generative tissues will be characterized to figure out if restricted sulfite reduction affects seed yield and quality.

It is known that *sir1-1* mimics a sulfur-deficient situation and that sulfur-related genes are affected in leaf as well as in root (Khan et al., 2010). To investigate the assumed effects on other pathways related to sulfur metabolism and in general, we will perform a whole genome transcriptomic analysis.

Also, a large scale quantification of metabolites from leaf and root and under sulfur-efficient and sulfur-deficient conditions will be performed to investigate the changes in metabolic levels and to compare those to gene expression changes.

Transcriptomic analysis from leaf tissues, metabolomic analysis from vegetative tissues under internal sulfur starvation (mutation in *sir1-1*) and external sulfur withdrawal (-S), and investigation of seed proteome will enlighten important aspects of sulfur reduction in plants.

2 Material and methods

2.1 Technical equipment, materials and IT

2.1.1 Technical equipment

6890N gas chromatograph	Agilent, Waldbronn
Autoclave Sanoklav	Sanoklav, Bad Überkingen-Hausen
Chromabond-SiOH-column, 500 mg	Macherey-Nagel, Düren
Cooling / Heating block Thermostat KBT-2 133	HLC, Bovenden
Electroporator MicroPulser	Bio-Rad, Munich
Fraction collector LKB FRAC-100	Pharmacia, Freiburg
Gel-Dokumentation Gel Jet Imager 2000	Intas, Göttingen
GeneChip Fluidics Station 450	Affymetrix, Santa Clara, CA (USA)
GeneChip Hybridization Oven 640	Affymetrix, Santa Clara, CA (USA)
GeneChip Scanner 3000 7G	Affymetrix, Santa Clara, CA (USA)
Growth chambers	Waiss, Gießen
Heating block Thermostat HBT-2 132	HLC, Bovenden
Horizontal shaker The Belly Dancer	Stovall, Greensboro, NC (USA)
Incubation shaker Innova 4300	New Brunswick Scientific, Nürtingen
Incubation shaker Multitron	Infors, Bottmingen
IPGphor system	GE Healthcare, Freiburg
Light Conditioning cabinet Percival Intellus	CLF Laborgeräte GmbH, Emersacker
LightCycler 480	Roche Applied Science, Mannheim
MicroGrid II	Isogen Lifescience, De Meern (Netherlands)
Microscope Leica DM IRB	Leica, Bensheim
Mini-Protean III electrophoresis and blot system	Bio-Rad, Munich
NanoDrop 2000 spectrophotometer	Peqlab, Erlangen
Odyssey Infrared Imaging System	LI-COR Biosciences, Lincoln, NE (USA)

Material and methods

Pegasus III time-of-flight mass spectrometer Photometer UvikonXL	Leco Instruments, St. Joseph, MI (USA) Secoman, Kandsberg
PlateReader Fluostar Optima	BMG Labtechnologies, Offenburg
Rotor-Gene Q	Qiagen, Hilden
Q-TOF-Ultima Global equipped with a nano-ESI source coupled with a Cap LC nanoHPLC Slidebooster	Waters Micromass, Saint Quentin en Yvelines (France) Advantix, Munich
Spectral photometer LKB Ultraspec III	Pharmacia, Freiburg
Stereomicroscope Leica MZ FLIII	Leica, Bensheim
Sterile bench Lamin Air 2448 and HB 2472 Ultrasonicator Sonoplus GM 70 with tip UW 70 Ultrasound waterbath Transsonic 460	Heraeus Instruments, Osterode Bandelin Electronic, Berlin Elma, Singen
Uvikon® 900	Goebel Instrumentelle Analytik GmbH, Au i.d.H.
HPLC-Systems:	
W600 controller	Waters, Milford (USA)
W600E pump multisolvent delivery system Column Nova-Pak™C18 3,9 × 150 mm	Waters, Milford (USA) Waters, Milford (USA)
Column Nova-Pak™C18 4,6 × 250 mm	Waters, Milford (USA)
W717plus autosampler	Waters, Milford (USA)
FP-920 fluorescence detector	Jasco, Groß-Umstadt
2. ICS 1000	Dionex, Idstein
AS 50 autosampler	Dionex, Idstein
Column Ion Pak® AS9-HC 2x250 mm	Dionex, Idstein
Column LiChroCART® 125-4 LiChrospher® 60 RP-select B (5 µm) Column Eurospher 100-C18 (5 µm, 250 × 4 mm)	Merck, Darmstadt Knauer, Berlin

Centrifuges:

Beckman J2-21 with JA-20 rotor	Beckman, Munich
or with SS-34 rotor	DuPont, Bad Homburg
Biofuge pico	Heraeus Instruments, Osterode
Megafuge 1.0 R with BS 4402/A Rotor	Heraeus Instruments, Osterode
Microcentrifuge 5415C and 5417R	Eppendorf, Hamburg
Sorvall RC5C with GSA Rotor	DuPont, Bad Homburg
SpeedVac Alpha RVC cmc-1 with Alpha 2-4 Loc-1m	Christ, Osterode

Further devices corresponded to the usual laboratory equipment.

2.1.2 Chemicals

2-D SDS-PAGE Standards	Bio-Rad, Hercules, CA (USA)
2-log DNA ladder	New England Biolabs, Beverly (USA)
AccQ-Tag™	Waters, Milford (USA)
Acid fuchsin	AppliChem, Karlsruhe
Agar	Fluka Biochemika, Fuchs
Agarose	Serva, Heidelberg
Albumin fraction V (BSA)	Roth, Karlsruhe
Ampicillin	Roth, Karlsruhe
Ampholytes pH 3-10 for IEF	Amersham, Braunschweig
Ascorbic acid	AppliChem, Darmstadt
Bacto trypton	BD Biosciences, Heidelberg
Bacto yeast extract	BD Biosciences, Heidelberg
Boric acid	Merck, Darmstadt
Bovine serum albumine	Sigma-Aldrich, Steinheim
5-bromo-4-chloro-3-indolyl phosphate (BCIP)	Roche, Mannheim
Bromophenol blue	Feinchemie Kallies, Sebnitz
Carbicillin	AppliChem, Darmstadt
Chloral hydrate	Riedel-de Haën, Seelze

Material and methods

3-[(3-cholamidopropyl)dimethylammonio]-1-propanesulfonate (CHAPS)	Amersham Pharmacia Biotech, Orsay (France)
Coomassie Brilliant Blue G-250	Merck, Darmstadt or Bio-Rad, Hercules, CA (USA)
L-Cysteine	Duchefa, Haarlem (Netherlands)
DEAE-Sephadex A25	Amersham Pharmacia Biotech AB, Uppsala (Sweden)
4',6-diamidino-2-phenylindole (DAPI)	Calbiochem, La Jolla, CA (USA)
Diethylpyrocarbonate (DEPC)	Roth, Karlsruhe
Dimethyl sulfoxide (DMSO)	Roth, Karlsruhe
Dithiothreitol (DTT _{red})	AppliChem, Karlsruhe
DNA loading buffer	Peqlab, Erlangen
Deoxynucleotide Solution Mix (dNTP)	New England Biolabs, Beverly (USA)
dNTPs (dATP, dGTP, dTTP, dCTP) for cDNA synthesis	Invitrogen, Karlsruhe
ECL Advance Blocking Reagent	GE Healthcare, Freiburg
Ethylene diaminetetraacetic acid (EDTA)	Roth, Karlsruhe
Ethylene glycol tetraacetic acid (EGTA)	AppliChem, Karlsruhe
Ethanol	Merck, Darmstadt
Ethidium bromide	Sigma-Aldrich, Steinheim
Formaldehyde	Sigma-Aldrich, Steinheim
Formamid	Merck, Darmstadt
Glufosinate ammonium (Basta)	Bayer Crop Science, Leverkusen
Glutathione ethyl ether	Sigma-Aldrich, Steinheim
Glycerol	Roth, Karlsruhe
Imidazole	Sigma-Aldrich, Steinheim
Immobiline dry strip pH 3-10 NL, 24cm	Amersham Pharmacia Biotech, Orsay (France)
Iodoacetamine	Sigma-Aldrich, Steinheim
Isopropyl-D-1-thiogalactopyranoside (IPTG)	Duchefa, Haarlem (Netherlands)
Isopropanol	Roth, Karlsruhe
Kanamycin	Duchefa, Haarlem (Netherlands)
Malachite green	Fluka Biochemika, Seelze

Material and methods

Murashige Skoog (MS) incl. vitamins	Duchefa, Haarlem (Netherlands)
Magnesium chloride	AppliChem, Karlsruhe
Magnesium sulfate	Merck, Darmstadt
β -mercaptoethanol	Merck, Darmstadt
MES	AppliChem, Karlsruhe
MOPS	AppliChem, Karlsruhe
Monobromobimane (MBB)	Invitrogen, Karlsruhe
Micro agar	Duchefa, Haarlem (Netherlands)
Nitroblue tetrazolium (NBT)	Roche, Mannheim
Nuclease free water	Ambion, Austin, TX (USA)
<i>O</i> -acetylserine	Bachem, Bubendorf (Switzerland)
Oil (mineral)	Sigma-Aldrich, Steinheim
Orange G	Sigma-Aldrich, Steinheim
Paraquat	Sigma-Aldrich, Steinheim
Pharmalytes pH 3-10	Amersham Pharmacia Biotech, Orsay (France)
Phenol	Fluka Biochemika, Seelze
<i>O</i> -phenylene dihydrochloride	Sigma-Aldrich, Steinheim
Phenylmethanesulphonylfluoride (PMSF)	Serva, Heidelberg
Phytigel	Sigma-Aldrich, Steinheim
Polyvinylpolypyrrolidone (PVPP)	Serva, Heidelberg
Polyvinylpyrrolidone 40,000 (PVP-40)	Sigma-Aldrich, Steinheim
Potassium dihydrogenphosphate	Fluka Biochemika, Seelze
Potassium hydrogenphosphate	Fluka Biochemika, Seelze
Protease inhibitor mix	Sigma-Aldrich, Steinheim
Protein Standard Mark12™	Invitrogen, Karlsruhe
PVDF membrane	AppliChem, Darmstadt
Rifampicillin	Duchefa, Haarlem (Netherlands)
Rotiphorese® Gel 30	Roth, Karlsruhe
Roti®-Quant Bradford reagent	Roth, Karlsruhe

Material and methods

Silwet L-77	OSi Specialities, Danbury (USA)
Sodium azide	AppliChem, Darmstadt
Sodium chloride	AppliChem, Karlsruhe
Sodium dodecyl sulfate (SDS)	Fluka Biochemika, Seelze
Sodium dithionite	Merck, Darmstadt
Sodium pyrophosphate	Merck, Darmstadt
Sodium succinate	Sima-Adrich, Steinheim
Sodium sulfide	Sigma-Aldrich, Steinheim
Sodium thiosulfate	Sigma-Aldrich, Steinheim
Starch (soluble)	Sigma-Aldrich, Steinheim
Sucrose, D+	AppliChem, Darmstadt
TEMED	Roth, Karlsruhe
TES (2-((tris(hydroxymethyl) methyl)amino) ethanesulfonic acid)	AppliChem, Darmstadt
Thiourea	AppliChem, Darmstadt
Triton-X 100	Sigma-Aldrich, Steinheim
Tween-20	Sigma-Aldrich, Steinheim
Urea	Gerbu, Heidelberg

All not listed chemicals were obtained in *pro analysis* grade from providers listed above or from AppliChem, Biomol, Boehringer-Ingelheim, Riedel-de Haën or Sigma-Aldrich.

2.1.3 Consumables

384-well plate, white	Roche, Applied Science, Mannheim
96-well	Greiner, Frickenhausen
Affymetrix array	Affymetrix, Santa Clara, CA (USA)
Immobiline DryStrip, 24 cm	GE Healthcare, Freiburg
Microscope Slides	Marienfeld, Laude-Königshofen
Membrane Desalting Filters	Millipore, Eschborn
Miracloth	Calbiochem, La Jolla, CA (USA)

NAP5™ columns	Amersham, Braunschweig
Nitrocellulose transfer membrane	AppliChem, Darmstadt
Protean IEF system electrode wigs	Bio-Rad, Munich
ReadyStrip™ IPG strips	Bio-Rad, Munich
Rotilabo aseptic filters (0,45 µm and 0,22 µM)	Roth, Karlsruhe
SILGUR-25 thin layer chromatography plate	Macherey-Nagel, Düren

Further consumables corresponded to usual laboratory equipment.

2.1.4 Kits

2-D Quant Kit	GE Healthcare, Freiburg
3' IVT Express Kit	Affymetrix, Santa Clara, CA (USA)
EXPRESS SYBR® GreenER™ qPCR SuperMix Universal Hybridization Wash and Stain Kit	Invitrogen, Karlsruhe
SensiMix™ SYBR No-ROX Kit	Affymetrix, Santa Clara, CA (USA)
QIAEX II Gel Extraction Kit®	Bioline, Luckenwalde
QIAprep Spin Miniprep Kit®	Qiagen, Hilden
QIAquick PCR Purification Kit®	Qiagen, Hilden
RevertAid™ H Minus First Strand cDNA Synthesis Kit	Qiagen, Hilden
RNeasy Plant Mini Kit®	Fermentas, St. Leon-Rot
RNase free DNase Mini Kit®	Qiagen, Hilden
Serum Triglyceride Determination Kit	Qiagen, Hilden
SuperScript® VILO™ cDNA Synthesis Kit	Sigma-Aldrich, Steinheim
SuperScript®III First-Strand Synthesis System for RT-PCR	Invitrogen, Karlsruhe
SuperSignal West Dura Extended Duration Substrate	Invitrogen, Karlsruhe
	ThermoScientific, Rockford, IL (USA)

2.1.5 Enzymes

α-Amylase	Sigma-Aldrich, Steinheim
-----------	--------------------------

α -Amyloglucosidase	Sigma-Aldrich, Steinheim
<i>Bam</i> HI	New England Biolabs, Beverly, MA (USA)
<i>Eco</i> RI-HF	New England Biolabs, Beverly, MA (USA)
Glucose oxidase	Sigma-Aldrich, Steinheim
Glucose-6-phosphate dehydrogenase	Roche, Mannheim
Hexokinase	Roche, Mannheim
<i>Hind</i> III	New England Biolabs, Beverly, MA (USA)
Invertase	Sigma-Aldrich, Steinheim
<i>Kpn</i> I	New England Biolabs, Beverly, MA (USA)
<i>Nco</i> I	New England Biolabs, Beverly, MA (USA)
<i>Not</i> I-HF	New England Biolabs, Beverly, MA (USA)
Peroxidase (type VI)	Sigma-Aldrich, Steinheim
Phosphoglucose isomerase	Roche, Mannheim
Phusion® High-Fidelity DNA Polymerase	Finnzymes, New England Biolabs, MA (USA)
<i>Sal</i> I	New England Biolabs, Beverly, MA (USA)
T4 DNA Ligase	New England Biolabs, Beverly, MA (USA)
<i>Taq</i> DNA Polymerase	New England Biolabs, Beverly, MA (USA)
<i>Xho</i> I	New England Biolabs, Beverly, MA (USA)
<i>Xma</i> I	New England Biolabs, Beverly, MA (USA)

2.1.6 Primers

Primers for qRT-PCR

Primer No	Description	Sequence
1727	EFalfa_f	GATTGCCACACCTCTCACATTGCAG
1728	EFalfa_r	GTCCTTCTCAATCTCCTTACCAG
1729	ubiquitin_f	CCAAGGTGCTGCTATCGATCTGT
1730	ubiquitin_r	AGGTCCGAGCAGTGGACTCG
1731	proteinphosphatase_f	ATCGCTTCTCGCTCCAGTAATG
1732	proteinphosphatase_r	GACTATCGGAATGAGAGATTGC
2546	SiR_RT_f	TTGAAAAGGTTGGTCTGGACTAC
2547	SiR_RT_r	GGTGTTCCTCCTAGCCAAAC
1429	sir-real-f	ACTGCAATGGCTTGCCCAGCTTT
1430	sir-real-r	TCCCGCGCTCTGCCTCAGTTATT
569	SIR_RT_PCR_for	ATCGACGTTTTCGAGCTCCGG
570	SIR_RT_PCR_rev	GCAGGAGTGGAGACGGCTT

Material and methods

1713	APR2_RT_fw	GATCGAACCCATTTGTCTCAGAGAC
1714	APR2_RT_rev	TTCAACTTCTCCTCCTTTCTCTTCAACT
1852	Sultr4;if	CACTTGACAATAGCAAGATCAGG
1853	Sultr4;r	CTCTGTACGTATTGTAGACACAC
1713	APR2_RT_fw	GATCGAACCCATTTGTCTCAGAGAC
1714	APR2_RT_rev	TTCAACTTCTCCTCCTTTCTCTTCAACT
1164	SAT1-f	CACATGCCGAACCGGTAATAC
1165	SAT1-r	GGTGAATCTTCCGGTTTACAGAGA
1166	SAT2-f	ACGCTAAGGGAACTCATAAGTCAGA
1167	SAT2-r	TCTTCTTTATAGCATCCCAAATAGGA
1168	SAT3-f	AATGGAACCCAGACCAAACC
1169	SAT3-r	GCCCAAACATCATCGACTTCA
1170	SAT4-f	CTCTTCCAATGATTGTCTCCCG
1171	SAT4-r	CCTCTCGAAAGGAACTCGTCA
1172	SAT5-f	TGGACACAGATCAAGGCGG
1173	SAT5-r	ATGAGAAAGAATCGTCAATATAGATAGC
303	oasA1_9E	GGAATATCATCCGGTGCAGCAG
653	oasA1-3'neu	GTCATGGCTTCCGCTTCTTTC
406	AtOAS-TLB-N	TCAAGAGACAGAGCCGGAGTGA
407	AtOAS-TLB-C	CACAGCCCTTGACTACATTGTTCA
408	AtOAS-TLC-N	GTTTTGCTGATGGTTCGGA
409	AtOAS-TLC-C	GTACACCATAGGAGTTTTTC

Primers for cloning

Primer No	Description	Sequence
1772	P1.R-sp_fNot	GGCGGCCGCATTAGGTGTGATATCCCG
1773	P1.R-sp_rXma	GGACCCGGGTGTTTTGGTTTATTTGATTTT
1774	SiR_fXma	GGTCCCGGGATGTCATCGACGTTTCGA
1775	SiR_rHindIII	GGAAGCTTTCATTGAGAAACTCCTTTGTA

Primers for sequencing

Primer No	Description	Sequence
334	M13 r	TTCACACAGGAAACAG
335	M13 u	GTAAAACGACGGCCAGT
911	Seq Primer middle_f	CAGACGTTTCAGCTTCATGGTG
2344	SiR_r_with promoter	GGAGCCTCTGTAAAAGCTC
2345	leaf spec promoter_SiR	GTTCTTCCAAGGAAGAGATAAG

Primers for genotyping

Primer No	Description	Sequence
1981	SiR endogene for	CGCTTCTTCTGGCTAGCC
432	GA_LB1	CCCATTTGGACGTGAATGTAGACAC
605	G_550A09_LP	TCTTTGATTAAGCATGAAACATTG
606	G_550A09_RP	AGGCGATTCAAAAAGCATCTC
1037	T-DNA sir1-2	ATATTGACCATCATACTCATTGC
1038	SiR Gene specific	TAGCACCAGCAAAAACACTCACATAC
1192	BASTA_for	GACACCGCGCGGATAATTTAT
1193	BASTA_rev	CAAGCCGTTTTACGTTTGGAAC
1832	SOX_f	TGTATCTCTCCATCAAGCA
1833	SOX_r	GTCTTCACAGAAGAAACAC
1850	SOX_r_exon	CCTTAACGGAAATCCGTGATCC
2098	SOXcDNA_f	AAATGGGGGCCCTTATAAGG
2099	SOXcDNA_r	ATCCTCCACAGAGCAGATTGC

2.1.7 Software

CTC Combi PAL and PAL Cycle Composer Software 1.5.0	CTC Analytics AG, Zwingen (Switzerland)
EndNote X4	Thomson Reuters, New York, NY (USA)
Fluostar Optima 1.30	BMG Labtechnologies, Offenburg
Gel-Pro Express Media	Cybernetics, Silver Spring, USA
Intas GDS Application 1.51	Intas, Göttingen
JMP Genomics 4	SAS, Cary, NC (USA)
LightCycler® 480 Software 1.0	Roche Applied Science, Mannheim
Millenium ³² Waters	Waters, Milford MA, USA
Photoshop CS 8.0.1	Adobe Systems GmbH, Munich
Progenesis SameSpots 3.0	Nonlinear Dynamics, Newcastle upon Tyne (UK)
Rotor-Gene® Q Series Software	Qiagen, Hilden
SigmaPlot 8.0	SPSS Inc., Munich
SigmaPlot Enzyme Kinetic Module	SPSS Inc., Munich
SigmaStat 3.0.1	SPSS Inc., Munich
Vector NTI 9	Invitrogen, Karlsruhe
Zeiss LSM 510 Software	Zeiss, Jena

Web based software tools and websites:

Brainarray	http://brainarray.mbni.med.umich.edu/Brainarray/Database/CustomCDF/genomic_curated_CDF.asp
eFP Browser	bbc.botany.utoronto.ca/efp/cgi-bin/efpWeb.cgi
ExPASy	http://web.expasy.org
Gene Investigator	www.geneinvestigator.com
GSEA	www.broadinstitute.org/gsea/index.jsp
MASCOT	http://www.matrixscience.com
Primer calc	www.basic.northwestern.edu/biotools/oligocalc.htm
R	www.r-project.org
TAIR	www.arabidopsis.org

2.2 Plant material and growth conditions

2.2.1 Plant material

For all experiments, *Arabidopsis thaliana* ecotype Col-o (family: *Brassicaceae*, order: *Capparales*, class: *Dicotyledonae*, subdivision: *Angiospermae*) was used as the wild-type control. Focus of the studies in this work was on two T-DNA insertion lines for *SiR* (AT5G04590): *sir1-1* (550A09) and *sir1-2* (727B08) obtained from the GABI-Kat collection center (Khan et al., 2010).

2.2.2 Surface sterilization of seeds

Arabidopsis seeds were sterilized for growth on plates and hydroponic cultures as described in Meyer and Fricker (2000): Seeds were sterilized with 70% ethanol for 5 min., incubated then with 0.6% hypochloride, followed by five times washing with ddH₂O.

2.2.3 Growth conditions

2.2.3.1 Growth on soil

Arabidopsis seeds were sowed on humid soil (Tonsubstrat from Ökohum, Herbertingen) appended with 20% (v/v) vermiculite and stratified at 4°C in the dark for three days. Plants germinated in short day conditions (8.5 h day light) at 50% relative humidity and a light intensity of 0.1 mmol m⁻² s⁻¹. During the day the temperature was kept at 22°C and lowered to 18°C at night. Plants were pricked out after two weeks to individual pots and grown under short day conditions until the desired age. After seven weeks, Col-o and *sir1-1* plants were conveyed to long day condition (14 h of day light, same environmental parameters as in short day) for the propagation of seeds. For examination of seed production of *sir1-1* in the size of 7-week-old wild-type, after 10 weeks *sir1-1* were transported to long day condition. For analysis of growth plants were grown on short day condition.

2.2.3.2 Hydroponic cultures

Hydroponic cultures were established for the discovery of *SiR* transcript and protein in root tissue and for the application of sulfate deficiency and investigation of its effects on seed yield. Col-0 and *sir1-1* seeds were sterilized (2.2.2) and germinated in microcentrifuge tubes on AT medium (2.2.3.3) as described in Tocquin et al. (2003). 56 microcentrifuge tubes were placed into sterilized pipet tip boxes filled with 0.4 l of 1/2 Hoagland medium (see below). After two weeks, plants were transferred to pots with 6 l or 15 l of modified 1/2 Hoagland medium that was replaced every two weeks to provide optimal supply of nutrition. Plants were harvested after four weeks for detection of *SiR* transcript (2.8.3), *SiR* protein (2.5.5.4) and activity (2.5.6.1) in leaf and root tissues. For sulfate deficiency experiments, media were exchanged weekly due to reduced sulfur availability. The seeds were collected daily until seed production was ceased.

Modified 1/2 Hoagland medium:

Macroelements:

2.5 mM Ca(NO₃)₂

2.5 mM KNO₃

0.5 mM MgSO₄ / MgCl₂

0.5 mM KH₂PO₄

Microelements (all without sulfate):

40 μM Fe-EDTA

25 μM H₃BO₃

2.25 μM MnCl₂

1.9 μM ZnCl₂

0.15 μM CuCl₂

0.05 μM (NH₄)₆Mo₇O₂₄

For sulfate deficiency experiments MgSO₄ was replaced by MgCl₂:

Full medium (500S): 0.5 mM MgSO₄; 5S: 5 μM MgSO₄ and 495 μM MgCl₂; 2.5 μM MgSO₄ and 497.5 μM MgCl₂.

The pH of all 1/2 Hoagland media was set to 5.8 with KOH.

2.2.3.3 Growth of Arabidopsis under sterile conditions

Seeds from Col-0, *sir1-1* and *sir1-2* were sterilized (2.2.2) and sowed on Arabidopsis medium (AT medium; Haughn and Somerville, 1986).

AT-medium composition:

<u>Macroelements:</u>	<u>Microelements (all without sulfate):</u>
2 mM Ca(NO ₃) ₂ × 4H ₂ O	51 μM Fe-EDTA
5 mM KNO ₃	70 μM H ₃ BO ₃
2 mM MgSO ₄ / MgCl ₂	14 μM MnCl ₂ × 4H ₂ O
2.5 mM KH ₂ PO ₄	1 μM ZnSO ₄ / ZnCl ₂
	0.5 μM CuSO ₄ / CuCl ₂
	0.2 μM NaMoO ₄
	10 μM NaCl
	0.01 μM CoCl ₂

For sulfur-deficient AT plates (2.2.3.4), the sulfate containing chemicals were replaced by their chloride equivalents as indicated in the table above. Solid medium for hydroponic cultures or agar plates was achieved by addition of 0.6% (w/v) microagar (2.1.2). The pH of medium was adjusted to 5.8 with KOH and then the medium was sterilized.

Stratification of seeds on plates was carried out for three days at 4°C in the dark. Afterwards, plates were incubated in Percival growth chambers under short day conditions. For germination rate experiments, the plants were grown under long day conditions (2.2.3.1) on AT and MS plates (2.1.2).

2.2.3.4 Chemical complementation under sterile conditions

sir1-1 and *sir1-2* were analyzed for chemical complementation on AT plates (2.2.3.3) by addition of 1 mM of cysteine or glutathione ethyl ester under normal and sulfur deficiency conditions. Col-0 was used as the control. Seeds germinated under short day conditions (2.2.3.1) in vertically arranged plates in Percival growth chambers.

2.2.4 Detection of phenotypic differences between *sir1-1* and Col-0 plants

The following morphological parameters for characterization of *sir1-1* according to Boyes et al. (2001) were analyzed weekly and documented: Rosette diameter was measured three times per plant; number of leaves per plant; and exposed leaf area. Documentation of plant growth/phenotype was performed with Canon Powershot 660 on a black velvet. The following settings for the camera were used: macro function, 2 sec light exposure, no flash in automatic mode. Images were rearranged and treated in the same way in Adobe Photoshop CS 8.0.1: Leaf area was selected via “Magic Wand” and the pixel number was noted from the “Histogram” window and transferred to cm². The data were plotted against time to gain a growth curve. Finally, fresh weight of leaves was determined at time point of harvest.

Also, total seed yield and the weight of 100 seeds per plant were determined. Dry weight of seeds was determined after incubation at 120°C for two days.

For investigation of silique development, wild-type and mutant plants were grown under short day conditions (2.2.3.1): After flowering, the length of siliques was measured daily (DAF, days after flowering) until the seeds matured. Finally, the silique was opened and the seeds within each silique were counted.

2.2.5 Pollen viability test

Plants were grown under short day conditions (2.2.3.1) for seven weeks and transferred to long day conditions (2.2.3.1) for bolting. After the flowers were visible, the petals were removed and the pollen sacs taken off the stamen. Pollen were released from the sac by putting them on a microscope slide. Pollen viability test was performed with Alexander’s staining solution: 10 ml of 95% ethanol, 10 mg malachite green, 25 ml glycerol, 5 g phenol, 5 g chloral hydrate, 50 mg acid fuchsin, 5 mg orange G, 2 ml glacial acetic acid, and 50 ml ddH₂O according to Alexander (1969). After staining the pollen in the solution, the slides were covered

with a cover slip and held for a few seconds in fire. The staining solution was removed and samples were documented by light microscopy (2.6.1). 100 pollen per plant were counted and the percentage of viable pollen determined.

2.2.6 Crossing of *Arabidopsis thaliana* lines *sir1-1* and *sir1-2* with *SOX-OE* and *sox-k.o.*

Plants grown in short day conditions (2.2.3.1) for eight weeks were transferred to long day conditions (2.2.3.1) to induce bolting. Petals and stamens of the maternal cross parent were removed and the anther of the paternal plant was used as pollen donor. Pollen was transferred by rubbing the anthers on the prepared, carefully wet-sprayed carpels. Crosses were genotyped by PCR (2.4.2) in the F₁ and F₂ generation with respective primers (2.1.6).

2.2.7 Stress induction using sulfite

For sulfite treatment of plants, leaf discs were die-cut from seven weeks old Col-o, *sir1-1* and complemented *sir1-1* (Kahn et al., 2010) plants grown under short day conditions (2.2.3.1). As a developmental stage control plant for *sir1-1*, 5-week-old Col-o plants were grown under same conditions and implemented in this experiment. Leaf discs with 75 mm diameter were allowed to float on 50% MS salt solution (2.1.2) in plates with or without 50 mM Na₂SO₃, for 12 h under constant illumination (0.1 mmol m⁻²s⁻¹).

2.2.8 Stable transformation of *Arabidopsis thaliana*

Transformation of *Arabidopsis* was performed according to the floral dip method described by Clough and Bent (1998). Transformants for complementation studies were screened by spraying a 0.2 g/l glufosinate ammonium solution (BASTA®; 2.1.2) on four-leaf stage plants. The treatment was repeated one week later.

2.3 Bacteriological methods

2.3.1 Bacterial strains

Following bacterial strains were used in this study: For cloning, *Escherichia coli* strain XL-1 Blue (Stratagene) was used (recA1, endA1, gyrA96, thi-1, hsdR17, supE44, relA1, lac- [F', proAB, lacIqlacZΔM15::Tn10(Tet^r)]; Bullock et al., 1987). Transformation of Arabidopsis plants with AtSiR was carried out with *Agrobacterium tumefaciens* strain AGL1 (C58, RecA) with pTiBo542DT-DNA Ti plasmid.

2.3.2 Preparation of competent cells for electroporation

Bacteria were grown in 25 ml LB media (1% tryptone, 0.5% yeast extract, 1% NaCl, pH 7.0 with NaOH) overnight. 10 ml of this culture were transferred in 0.25 l of pre-warmed LB media and grown to an optical density (OD) at 600 nm of 0.8. Bacterial cells were cooled down on ice for 30 min and centrifuged at 650 g for 10 min at 4°C. The harvested bacterial sediment was washed twice in 0.25 l and 125 ml pre-sterilized ddH₂O followed by two wash steps with 125 ml and 50 ml 10% glycerol. Resuspended bacteria were frozen in liquid nitrogen in aliquots of 40 μl and stored at -80°C until transformation.

2.3.3 Transformation of bacteria

E.coli strains were transformed by electroporation at 2500V and 15μF and incubated in 1 ml LB medium for one hour at 37°C and 220 rpm. The bacterial suspension was plated on solid LB medium plate (1% tryptone, 0.5% yeast extract, 1% NaCl, 1% agar, pH 7.0 with NaOH) containing antibiotics (ampicillin, 0.1 mg/ml or kanamycin, 50 μg/ml) at 37°C.

2.3.4 Bacterial growth

Single colonies from *E.coli* were transferred into 1 ml LB medium for plasmid preparation or 4 ml of LB medium for the preparation of glycerol

stocks. The culture was grown at 220 rpm in a horizontal shaker for 16 h at 37°C.

2.3.4.1 Plasmid isolation from *E.coli*

E. coli cells containing the plasmid were grown in 4 ml LB supplemented with the selective antibiotic for 16 h. The plasmid was extracted with a Miniprep Kit (2.1.4) according to manufacturer's protocol.

2.3.4.2 Glycerol stocks of bacteria

Bacteria were grown overnight in LB media containing selective antibiotics. 0.8 ml from the liquid culture was mixed with 0.2 ml of 80% glycerol, frozen in liquid nitrogen and stored at -80°C.

2.3.5 Growth of *Agrobacterium tumefaciens*

Agrobacterium tumefaciens was grown like *E.coli* but with the following modifications: Bacterial cultures were grown at 28°C for two days. After transformation, bacteria were incubated for 3 h at 28°C.

2.4 Molecular Biology Methods

2.4.1 Isolation of genomic DNA from *Arabidopsis thaliana*

Genomic DNA (gDNA) was isolated from 30 mg rosette leaf. According to (Edwards et al., 1991), leaves were grinded and suspended in 0.4 ml Edwards buffer (0.2 M Tris-HCL pH 7.5, 250 mM NaCl, 25 mM EDTA, 0.5% SDS) for 10 sec and incubated at room temperature (RT) for 10 min. The mixture was centrifuged for 5 min at RT and 13,000 g. 0.3 ml of supernatant was transferred into a fresh tube and DNA was precipitated by addition of 0.3 ml isopropanol. After incubation at room temperature for 2 min, the solution was centrifuged at 13,000 g for 10 min and the supernatant discarded. The resulting sediment was washed in 0.7 ml of

70% ethanol, pelleted again at 13,000 g for 3 min. Ethanol was discarded and the DNA sediment was air-dried for at least 30 min and resolved in 25 µl TE buffer (10 mM Tris-HCl pH 8.0, 1 mM EDTA).

2.4.2 Polymerase Chain Reaction

Specific DNA fragments were amplified using the polymerase chain reaction (PCR) as described in Mullis et al. (1986).

Amplification of DNA for cloning in vectors was performed in a total volume of 25 µl in High Fidelity buffer (Fermentas) with final concentration of 2 µM for each primer, 0.2 mM for dNTPs using 2.5 U Phusion High Fidelity DNA Polymerase (2.1.5) according to manufacturer's protocol. The optimal temperature for primer binding was calculated using the Oligo Calc algorithm (2.1.7).

Plants were screened by PCR amplification of the respective fragment for complementation constructs or T-DNA insertion. The PCR reaction was performed in a total volume of 25 µl in 1 × Thermopol buffer (NEB) with Taq DNA Polymerase (2.1.5). 1 - 2 µl of isolated gDNA (2.4.1) from the plant of interest were added to the reaction as template.

A typical PCR program was set up as following:

Step	Description	Temperature	Time
1	Initial denaturing	95°C	3 min
2	Denaturing	95°C	30 sec
3	Annealing	58 - 61°C	30 sec
4	Elongation	68°C	90 sec
5	Repeat 34 × steps 2-4		
6	Final elongation	68°C	10 min
7	Hold	12°C	∞

2.4.3 DNA gel electrophoresis

DNA fragments were separated by electrophoresis in 0.8% - 2% agarose gels. For preparation of gels, agarose was melted in 1× TBE buffer (90 mM Tris-HCl pH 8.0, 90 mM boric acid, 0.5 mM EDTA). The melted agarose was cooled down to 45°C and ethidium bromide was added to a final concentration of 0.8 µg/ml.

DNA was mixed with loading buffer (0.25% bromophenol blue, 0.25% xylene cyanole, 40% glycerol) prior loading of the sample on the gel. 2-log DNA ladder (2.1.2) served as a molecular weight standard. Separation of DNA fragments was achieved by applying a voltage of 85 – 130 V for approximately 1 h, using 1× TBE as running buffer.

2.4.4 Cloning using endonucleases and ligase

DNA digestions:

The reaction contained 5 µg of plasmid. For DNA restriction, 10 U of restriction enzymes from NEB (2.1.5) in 1× suitable restriction buffer and a total volume of 25 µl according to manufacturer's protocols were used. Restriction was implemented at 37°C for 2 h.

Extraction of DNA from agarose gels:

After separation by gel electrophoresis (2.4.3), DNA fragments of interest were sliced out precisely of the agarose gels using a scalpel. The DNA was extracted with the QUIAEX II Kit (2.1.4) according to the manufacturer's protocol.

Ligation of DNA, desalting and transformation:

The concentration of DNA was determined with the NanoDrop 2000 spectrophotometer (2.1.1) and adjusted to 1:3 vector to insert ratio. The ligation was performed in a total volume of 20 µl containing 1× ligation buffer, 3 U of T4 DNA ligase (2.1.5), and fragments of DNA. The ligation was carried out overnight at 14°C or for 1 h at RT. As a negative control, ligation without adding the insert was performed.

The whole ligation samples were desalted on Millipore filters (2.1.3) floating on ddH₂O for 30 min according to manufacturer's protocol. Competent cells (2.3.2) were transformed with 0.5 - 1.5 µl of desalted ligation sample before electroporation (2.3.3).

2.5 Biochemical methods

2.5.1 Purification of soluble proteins from Arabidopsis vegetative tissues

Soluble proteins were extracted from 0.1 g or 50 mg grinded leaf or root tissues, respectively, from four weeks old plants (2.2.3.2) with 0.5 ml extraction buffer (50 mM HEPES-KOH, pH 7.4, 10 mM KCl, 1 mM EDTA, 1 mM EGTA, 10% glycerin, 10 mM DTT, 0.5 mM PMSF) detection of SiR transcript (2.8.3), SiR protein (2.5.5.4) and activity (2.5.6.1). The extraction was achieved by shaking the samples for 15 min on ice. The cellular debris was removed by two centrifugation steps, each for 10 min at 25,000 g and 4°C.

2.5.2 Purification of proteins from Arabidopsis generative tissues

In order to optimize the extraction of proteins from mature seeds, different protein extraction methods were used:

2.5.2.1 Purification of soluble proteins from seeds

25 mg mature seeds were grinded and taken in 250 µl of protein extraction buffer (PEB; 0.1 M TES, 0.5 M NaCl, 1 mM EDTA, 1 mM PMSF, 2% β-mercaptoethanol). 250 µl and then 0.5 ml PEB were added successively and the samples were grinded again. The suspension was centrifuged at 13,000 g for 5 min. 250 µl of the supernatant was transferred to a fresh tube and 1 ml of precooled acetone (-20°C) was added to the sample. After 30 min of incubation on ice, the solution was centrifuged at 4°C with 13,000 g for 5 min. The supernatant was

discarded, the sediment washed with 0.3 ml 80% acetone, and a centrifugation step (13,000 g, 2 min) followed. The supernatant was removed and the sediment was air-dried and afterwards resuspended in SDS gel loading buffer (2.5.5.1).

2.5.2.2 Purification of total proteins from seeds

100 mg seeds were grinded at RT and 1 ml extraction buffer was added. The protocol for extraction of proteins from vegetative tissues (2.5.1) was used with minor modifications; following chemicals were added: 1% Triton X-100, 2% SDS, and 15% glycerol (instead of 10%). The suspension was further grinded, poured into a fresh tube and centrifuged at RT with 13,000 g for 10 min. The supernatant was transferred into a new tube.

The second method was according to Higashi et al. (2006) without chemicals having been used for 2D gels like CHAPS and ampholine: 10 mg mature seeds were homogenized in liquid nitrogen and proteins were extracted on ice in 0.8 ml of thiourea/urea lysis buffer (7 M urea, 2 M thiourea, 65 mM DTT, protease inhibitor mix, 5% polyvinylpyrrolidone). The prepared buffer was stirred overnight at 50°C prior extraction. The protein extract was mixed for 3 min and centrifuged at 4°C for 15 min at 18,000 g. The supernatant was centrifuged as above and transferred to a new tube.

2.5.3 Protein quantification

Two methods for protein measurement were used parallelly to ensure correct resulting protein concentrations due to the different protein extraction buffers and their chemical component, including reductants, detergents, chaotropes and carrier ampholytes which could interact with protein quantification dyes like Coomassie in some protein assays.

The protein concentration was estimated after Bradford (1976) using bovineserum albumin fraction V (BSA; 2.1.2) as standard. Each sample was adequately diluted and 10 µl from sample dilution or standard were double or triple spotted in 96-well plates. 250 µl of 1:5 diluted Bradford

reagent (2.1.2) were added into the wells containing sample dilutions. After incubation for 10 min at RT, the absorbance was measured at 595 nm with the Fluostar plate reader (2.1.1) and protein sample concentrations were calculated by using the BSA standard calibration curve.

2-D Quant Kit (2.1.4) was used for quantification of protein amounts following the manufacturer's instructions. BSA served as standard. The absorbance of standards and samples was read at 480 nm.

2.5.4 2-D gel electrophoresis of seed proteome

2.5.4.1 Total seed protein extraction and 2-D electrophoresis

Total proteins were extracted from 20 mg of mature seeds collected on four individual plants (2.2.3.1). Protein concentration was measured according to Bradford (1976). A constant volume (0.3 ml) of the protein extracts (around 0.4 mg of proteins) was used for isoelectrofocusing. Proteins were separated in duplicates from the four biological seed samples using gel strips forming an immobilized non-linear pH 3 to 10 gradient (2.1.3). Strips were rehydrated in the IPGphor system (2.1.1) with the thiourea/urea lysis buffer containing 2% (v/v) Triton X-100, 20 mM DTT and the protein extracts for 7 h at 20°C. IEF was performed at 20°C in the IPGphor system for 7 h at 50 V, 1 h at 300 V, 2 h at 3.5 kV and 7 h at 8 kV. Prior to the second dimension, the gel strips were equilibrated for 2 × 20 min in 2 × 0.1 l of equilibration solution containing 6 M urea, 30% (v/v) glycerol, 2.5% (w/v) SDS, 0.15 M bis-Tris, and 0.1 M HCl. 50 mM DTT was added to the first equilibration solution, and iodoacetamide (4% [w/v]) was added to the second (Harder et al., 1999; Gallardo et al., 2002). Proteins were separated in vertical polyacrylamide gels according to Gallardo et al. (2002).

2.5.4.2 Protein staining and quantification

Gels were stained with Coomassie Brilliant Blue G-250 (Bio-Rad, 2.1.2) according to Mathesius et al. (2001). Images were acquired with the Odyssey Infrared Imaging System (2.1.1) at 700 nm with a resolution of 169 μm . Protein signals were quantified with the Progenesis SameSpots version 3.0 software (2.1.7) according to the instruction manual. For each gel, normalized spot volumes were calculated as the ratio of each spot volume to total spot volume in the gel (arbitrary unit). Eight gels (four biological replicates and two technical replicates for each biological replicate) were analyzed for Col-0 and *sir1-1*. Molecular masses (Mr) and isoelectric points (pI) were calculated according to the migration of 2-D SDS-PAGE Standards proteins (2.1.2). All data were statistically analyzed using the Progenesis SameSpots version 3.0 software (ANOVA). Differences with P values < 0.05 were defined as significant.

2.5.4.3 Protein identification

Spots were annotated using proteome reference maps previously established for Arabidopsis mature seeds (Zuber et al., 2010b). The identity of unknown spots was confirmed by nano-LC-MS/MS (2.1.1) as described by Gallardo et al. (2007). Detailed information about protein digestion, mass spectrometry data acquisition is provided in Suppl. data 17. Peak lists of precursor and fragment ions were matched to proteins in the NCBI non redundant database (January 2010, 10,274,250 sequences; 3,505,793,397 residues, taxonomy of Arabidopsis) using the MASCOT version 2.2 program (2.1.7). The MASCOT search parameters are described in Suppl. data 17. Matches with individual ion scores above 20 were considered to be true.

2.5.5 Protein separation by electrophoresis and immunoblotting

2.5.5.1 SDS-polyacrylamide gel electrophoresis

Protein separation upon their molecular weight was performed according to Laemmli (1970). Mini-Protean III system (2.1.1) was used with discontinuous gels consisting of a 4% acrylamide stacking gel (80 mM Tris pH 6.8, 0.065% (w/v) SDS, 0.026% crosslinker) and a 12.5% acrylamide separating gel (0.37 M Tris pH 8.8, 0.1% (w/v) SDS, 0.026% crosslinker). The samples were spiked with 1/5 volume 5 × Laemmli buffer (0.1 M Tris pH 7.0, 5% SDS, 3.63 M β-mercaptoethanol, 20% glycerin, 0.01% bromophenol blue) prior loading and denatured for 3 min at 95°C. Mark12 protein marker (2.1.2) served as molecular weight standard. SDS PAGE was performed in running buffer (250 mM Tris pH 8.3, 1.92 M glycine, 1% (w/v) SDS) at a voltage of 85 V for 30 min followed by 120 V until the bromophenol blue front left the gel.

2.5.5.2 Coomassie staining of protein

After protein separation by SDS PAGE (2.5.5.1), the proteins were stained in Coomassie staining solution (50% methanol, 1% acetic acid, 0.1% Coomassie Brilliant Blue G-250) for 30 min on a horizontal shaker. The background of the gels was destained four times by incubation with Coomassie destaining solution (20% ethanol, 10% acetic acid). Gels were documented by scanning after equilibration in water.

2.5.5.3 Protein transfer from SDS-gels to PVDF membranes

After separation of proteins by SDS-PAGE (2.5.5.1), they were transferred to a polyvinylidenfluorid (PVDF) membrane according to Towbin et al. (1979). Mini-Protean III chambers or PeqlabProtein chambers (2.1.1) were used for the transfer within blotting buffer (0.02 M Tris-HCl pH 8.0, 0.15 M glycine, 0.04% SDS, 20% methanol). Protein transfer was carried out for 2.5 h at 4°C at a current of 130 mA. After incubation of the membrane for 5 min with Ponceau staining solution (1% Ponceau S, 5%

acetic acid), it was washed with ddH₂O and immediately scanned. Finally, the membrane was destained with TBST buffer (0.01 M Tris-HCl pH 7.5, 0.15 M NaCl, 0.05% Tween-20).

2.5.5.4 Immunological detection of proteins on PVDF membranes

PVDF membrane was blocked for 1.5 h with either 5% BSA or 5% ECL advance block agent in TBST buffer (10 mM Tris-HCl pH 7.5, 0.15 M NaCl, 0.05% Tween-20) and subsequently washed five times with TBST buffer. The washed membrane was incubated overnight at 4°C with αSiR serum from rabbit that was 1:3,000 diluted in TBST buffer with the respective blocking agent.

The PVDF membrane was washed five times with TBST buffer and subsequently incubated with the secondary antibody (1:10,000 diluted; goat α-rabbit IgG conjugated with horse radish peroxidase (HRP) in TBST buffer) for 1.5 h. The secondary antibody was detected with SuperSignal West Dura Extended Duration Substrate (2.1.4) following manufacturer's guidelines.

2.5.6 Activity Assays

2.5.6.1 Determination of SiR activity

The measurement of SiR activity was coupled to the cysteine synthesis of OAS-TL (Khan et al., 2010). Therefore, the reaction mix was set up in a total volume of 0.1 ml containing 25 mM HEPES pH 7.8, 1 mM Na₂SO₃, 5 mM OAS, 10 mM DTT, 30 mM NaHCO₃, 15 mM Na₂S₂O₄, 5 mM paraquat, and 1 U of OAS-TL (EC 2.5.1.47; Wirtz et al., 2004). The reaction was started by addition of 59 µl protein extracts (2.5.1 and 2.5.2.1). The assay was performed at 25°C for 30 min as described by Gaitonde (1967). The reaction was stopped by precipitation of the proteins via addition of 50 µl 20% trichloroacetic acid. Precipitated proteins were centrifuged at 4°C for 5 min at 20,000 g. 150 µl supernatant was added to a premixed 0.2 ml ninhydrine solution (17.5 mM ninhydrine in 25% (v/v)

hydrochloric acid and 75% (v/v) acetic acid), and 0.1 ml 100% acetic acid. The mixture was incubated for 10 min at 99°C and allowed to cool down on ice, followed by addition of 550 µl 100% ethanol.

The produced cysteine was determined photometrically by measuring the OD at 560 nm.

2.5.6.2 Determination of APR activity

APR activity was measured as the production of radioactive sulfite (Brunold and Suter, 1990). 10 µl of the protein extracts (2.5.1 and 2.5.2.1) were added to 240 µl of the reaction assay (0.1 M Tris-HCl pH 9.0, 0.8 M MgSO₄, 8 mM dithioerythritol (DTE), 75 mM [³⁵S]APS (1 kBq/10 µl)) and incubated at 37°C for 30 min. 1 ml of 1 M triethanolamine (TEA) was added into 20 ml scintillation vials. After incubation, 0.1 ml of 1 M Na₂SO₃ was added to the reaction, mixed and transferred into the prepared scintillation vials. 0.2 ml of 1 M H₂SO₄ was added to the assay in the tubes and the assay was incubated overnight at RT. The bottom of the tubes was washed with 0.2 ml ddH₂O into the vials. After adding 3 µl scintillation cocktail to the vials and mixing, the acid-volatile radioactivity formed in the presence of [³⁵S]APS and DTE was measured.

2.6 Microscopic methods

2.6.1 Silique and pollen imaging

Siliques were carefully opened with forceps and imaged with a Leica MZ FLII stereomicroscope equipped with a DFC 320 camera.

The prepared pollen after Alexander's staining treatment (2.2.5) were analyzed with a Zeiss microscope LSM 510 and images were taken with a 25× or 40× lens.

2.6.2 Electron microscopy

Leaves were harvested from 7-week-old Col-0 and *sir1-1* plants grown under short day condition (2.2.3.1) 1 h after light onset and after 16 h darkness. Harvested leaf material was cut into 1 mm on each side and transferred immediately to primary fixative (0.5% glutaraldehyde, 1.5% paraformaldehyde in 50 mM cacodylate buffer) at 4°C in exicator overnight. The samples were washed four times with 50 mM cacodylate buffer each 10 min at RT.

Secondary fixation was in 1% osmium tetroxide in 50 mM cacodylate buffer for 4 h at RT and the samples were washed twice in the same buffer as used in the primary and secondary fixative and twice in bidistilled water, each 10 min.

Tertiary fixation of specimens took place at 4°C overnight in 1% aqueous uranyl acetate which served both as fixative and stain and can markedly enhance membranes.

Samples were washed in bidistilled water 4 times, each for 10 min and dehydrated in graded acetone series of 25%, 50%, 70%, and 90%, each for 15 min. Final dehydration was performed in 100% acetone twice, each for 15 min.

Spurr® was used as an epoxy resin embedding medium. The infiltration series diluted in acetone were used: 25%, 50%, and 75%, each for 45 min and at the end 100% Spurr® was poured over the samples and those were incubated overnight at 4°C. Specimens were transferred into embedding BEEM capsules with fresh Spurr® solution and polymerized at 60°C overnight.

Ultra-thin sections were cut and placed on grids. Samples were stained in uranyl acetate, followed by distilled water washes and lead citrate staining. Aqueous uranyl acetate/lead citrate post-stained sections were examined in a Philips CM10 transmission electron microscope operating at 80 kV.

2.7 Metabolomics

2.7.1 Acidic extraction of metabolites

Metabolites were extracted from 0.1 g or 20 mg grinded leaf or seed (2.2.3.1). The metabolites were extracted in 0.5 ml of 0.1 M HCl on ice for 15 min. Cell debris was sedimented twice by centrifugation at 20,000 g and 4°C, for 5 min. The supernatant containing the soluble metabolites was transferred to a new microcentrifuge tube and subjected for further analysis.

2.7.2 Determination of amino acids and other metabolites

For amino acid determination, two techniques were suitable: GC-MS and HPLC. As comparatively described in Allboje Samami et al. (submitted), extraction protocol for GC-MS used methanol to isolate soluble cell constituents, whereas for HPLC diluted HCl (2.7.1) was used.

The first technique was an *N*-methyl-*N*-[trimethylsilyl]trifluoroacetamide and methoxyamine hydrochloride derivatization with ribitol as an internal standard, followed by gas chromatography/mass spectrometry analysis (CTC Combi PAL and PAL cycle composer software version 1.5.0 (2.1.7), a 6890N gas chromatograph (2.1.1), and a Pegasus III time-of-flight mass spectrometer (2.1.1)) using on MDN-35 capillary column, 30-m length, 0.32-mm inner diameter, 0.25-mm film thickness at a flow rate of 1 ml/min as described by Lisec et al. (2006). This method was also used for large scale metabolite quantification.

The second technique was based on derivatization of amino acids with the fluorescent dye AccQ-Tag™ (2.1.2) in a volume of 50 µl containing 0.14 M borate buffer pH 8.8, 30 µg AccQ-Tag and 5 µl of the metabolite extract (2.7.1) according to the manufacturer's protocol. Derivatized amino acids were separated by high-performance liquid chromatography using a Nova-Pak™ C18, 3.9 × 150 mm column (2.1.1) as described in Hartmann et al. (2004). Derivatized and separated amino acid AccQ-Tag derivatives were detected with Jasco FP-920 fluorescence detector (2.1.1) at 395 nm after excitation with 250 nm. Quantification was performed using the

Waters LC control- and analysis software Millennium³² (2.1.7). Standardization was carried out by external standards for each individual amino acid.

2.7.3 Determination of thiols

25 µl of metabolite extract (2.7.1) was incubated with 270 µl of reduction buffer (68 mM Tris pH 8.3, 0.34 mM DTT, 25 µl 0.08 M NaOH) for 1 h in the dark at RT. DTT could reduce the sulfhydryl group of thiols. Reduced thiols were derivatized by addition of 0.85 mM monobromobimane and the reaction was allowed to proceed for 15 min in the dark at RT. 705 µl of 5% acetic acid were added which stopped the reaction and stabilized the thiol-bimane-derivatives. Derivatized thiols were separated by reversed phase HPLC with a Nova-PakTM C18, 4.6 × 250 mm column (2.1.1) as described in Wirtz and Hell (2003). Detection of separated thiol-derivatives was achieved by using a Jasco FP-920 fluorescence detector (2.1.1) at 480 nm after excitation with 380 nm and quantified using the Millennium³² software.

A new method for detection of sulfide was established after Fahey et al. (1981), Newton et al. (1981), and Völkel and Grieshaber (1994): 25 mg of plant tissue (2.2.3.1) was grinded and homogenized in liquid nitrogen. To avoid transition of HS⁻ to H₂S which is volatile, the sample was directly derivatized by being introduced to 160 µl alkaline extraction buffer containing monobromobimane (145 µl extraction buffer containing 160 mM HEPES pH 8.0, 16 mM EDTA, 10 µl 1 M NaOH, 5 µl 0.1 M mBB). The reaction set was shaken for 1 min and incubated for 30 min at RT in dark, whereby every 10 min the samples were shaken. After incubation, the reactions were centrifuged for 15 min at 4°C with 20,000 g. The supernatant was taken and mixed with 0.1 ml 65 mM methanesulfonic acid to stabilize mBB-derivatized products and afterwards with 740 µl 0.25% acetic acid and 12% methanol. The product was mixed and centrifuged for 60 min at 18°C with 20,000 g. Sulfide was separated from other thiols on a LiChroCART[®] 125-4 LiChrospher[®] 60 RP-select B (5µm) column (2.1.1) with a flow rate of 1.3 ml/min by increasing the

hydrophobicity of the eluent A (0.25% acetic acid) by mixture with methanol (eluent B). Detection was performed as described for thiols.

2.7.4 Determination of adenosines

150 µl of metabolite extract (2.7.1) or standards were incubated with 770 µl of CP buffer (620 mM citric acid pH 4, 760 mM disodium hydrogen phosphate) and 80 µl of 45% chloroacetaldehyde for 10 min at 80°C. The incubation was allowed to cool down on ice to RT and sedimented at 20°C for 45 min with 20,000 g. The supernatant was transferred to HPLC vials. Adenosine derivatives were separated by reversed phase HPLC with an XTerra™ MS C18, 5 µm, 3 mm × 159 mm column (2.1.1). 1× TBAS (5.7 mM TBAS, 30.5 mM potassium dihydrogen phosphate, pH 5.8) served as running buffer, acetonitrile:1× TBAS (2:1, v/v) as separation buffer. Metabolites were detected with a Jasco FP-920 fluorescence detector (2.1.1) at 410 nm after excitation with 280 nm and quantified using the Millennium³² software.

2.7.5 Extraction, isolation and quantification of jasmonates, hydroxyjasmonic acid (12-OH-JA), and hydroxyjasmonic acid sulfate (12-HSO₄-JA)

0.5 g of leaves (2.2.3.1) were frozen in liquid nitrogen, homogenized in a mortar and extracted with 10 ml 100% methanol. For quantification of jasmonate (JA), hydroxyjasmonic acid (12-OH-JA), and hydroxyjasmonic acid sulfate (12-HSO₄-JA), appropriate amounts of internal standards were added to the extract: 0.1 µg of (²H₆)JA, 0.1 µg of 2-(²H₃)OAc-JA, and 250 ng of 12-HSO₄-JA-(²H₃)ME, respectively, were added to the extract. The methanol extracts were purified by chromatographic steps as described in (Miersch et al., 2008) and the elute was evaporated and acetylated with 0.2 ml pyridine and 0.1 ml acetic acid anhydride overnight at 20°C and taken in ethyl acetate after passing a chromabond-SiOH-column, 0.5 g (2.1.1) whereas JA and 12-OH-JA could be eluted, 12-HSO₄-JA remained within the column and was eluted with methanol. Liquids

were evaporated by addition of ethyl acetate and methanol extracts, containing JA and 12-OH-JA (E1), and 12-HSO₄-JA (E2), respectively. Derivatives were suspended in 100% methanol. JA and 12-OH-JA were dissolved using a column filled with 3 ml DEAE-Sephadex A25 (2.1.2) (Ac⁻-form, methanol). The column was washed with 3 ml methanol. After washing with 3 ml 0.1 M acetic acid in methanol, eluents with 3 ml of 1 M acetic acid in methanol and 3 ml of 1.5 M acetic acid in methanol were collected and evaporated. Extract E2 was methylated with 0.2 ml ethereal diazomethane and evaporated. The final separation was performed by HPLC with a Eurospher 100-C18 column (2.1.1) as described in Miersch et al. (2008).

2.7.6 Isolation of lipids from Arabidopsis seeds for determination of total lipid content

0.1 g of mature seeds was homogenized in liquid nitrogen and 1.5 ml of isopropanol was added to the seed powder. The suspensions were shaking for 16 h at 4°C, 100 rpm. The samples were centrifuged at 13,000 g for 10 min. Fresh tubes were weighted and their weights were noted; the suspensions were transferred to the new tubes. The tubes incubated for 8 h at 60°C to let the isopropanol evaporate. The remaining suspension contained the lipids. After weighting the tubes containing the lipids, the total lipid amount was determined by subtraction from the net weight of tubes.

2.7.7 Lipid extraction for triacylglyceride determination

20 - 30 mg of seeds were homogenized in liquid nitrogen and 1.5 ml 2:1 chloroform/methanol (v/v) was added to the tissue. Samples were homogenized with a steel bead using a tissue lyzer for 1 min at a frequency of 30Hz. Lipids were extracted on a rotating wheel at RT for 20 min. Samples were centrifuged at 1200 g m for 10 min and 1 ml of the resulting supernatant was transferred to fresh tubes. The organic phase was mixed with 0.2 ml of 0.9% sodium chloride and centrifuged at 300 g for 5 min.

The aqueous solution was carefully discarded and 50 µl of the organic phase were transferred to a fresh tube and 10 µl of 1:1 Triton-X 100/chloroform (v/v) were included. The reagents were mixed and the solvent was evaporated. The residue containing the hydrophobic contents of the seeds was resuspended in 50 µl ddH₂O and used for determination of triacylglyceride (TAG) levels (2.7.7.1).

2.7.7.1 Determination of TAG levels in Arabidopsis seeds

TAG levels were determined by separating triacylglycerides into one glycerol and three fatty acid molecules and measuring the glycerol using a calorimetric assay. The Serum Triglyceride Determination Kit (2.1.4) was used for this assay. 4 µl of isolated triglycerides from seeds (2.7.7) were transferred to a 96-well plate. In order to determine a blank value, 0.1 ml of Free Glycerol Reagent were added to each well and the plate was incubated at 37°C for 5 min. Free glycerol levels were measured at 540 nm. In a second reaction (assay), 0.1 ml of Triglyceride Reagent were added that contained lipase catalyzing the release of fatty acids from triacylglycerides. Plates were incubated at 37°C for 5 min and measured at 540 nm. TAG content was determined by subtracting the free glycerol (blank) from the second measurement (assay).

2.7.8 In situ staining of starch

Leaves from 7-week-old soil-grown Col-0 and *sir1-1* plants (2.2.3.1) were used for in situ staining of starch according to (Khan et al., 2010): Leaves were incubated for 2 h at 80°C in 80% ethanol, rinsed with water, stained for 10 min in Lugol's iodine solution (5 g I₂, 10 g KI dissolved in 85 ml water, and diluted 1:10 in water for staining), rinsed again, and photographed.

2.7.9 Quantitative measurement of starch and soluble sugars

Contents of starch, sucrose, glucose, and fructose were determined according to (Smith and Zeeman, 2006): 30 mg of leaf or 10 mg of seed tissues (2.2.3.1) were harvested, homogenized in liquid nitrogen, transferred to a tube containing 2 ml 80% ethanol and incubated in a boiling water bath for 3 min. Samples were centrifuged at RT with 13,000 g for 10 min to separate starch and sugars which were in the supernatant.

2.7.9.1 Determination of sugars

0.1 ml of supernatant was added to 0.9 ml of reaction buffer (0.1 M imidazole pH 6.9, 5 mM MgCl₂, 2 mM NADP, 1 mM ATP) and 0.7 U of glucose-6-phosphate dehydrogenase (G6P-DH) grade II, from yeast (Roche). The OD was measured at 334 nm against 1 ml reaction buffer (blank) until the absorption remained constant. For measurement of glucose, 1.5 U of hexokinase (2.1.5) was added, for fructose determination, 3.5 U of phosphoglucose isomerase from yeast (2.1.5), and for measurement of sucrose, 2 µl of a saturated invertase solution (2.1.5), also until the absorption remained constant.

2.7.9.2 Starch determination

To quantify starch, ethanol was allowed to evaporate from the final sediment (2.7.9). After that, the sediment was homogenized thoroughly with 2 ml ddH₂O. 0.5 ml of the homogenate was added to each of 3 tightly sealing screw-capped microcentrifuge tubes, heated to 100°C for 10 min to gelatinize starch granules. The samples were cooled to RT and 0.5 ml 0.1 M sodium acetate (pH 4.8) was added to each tube. 6 U of α-amylglucosidase and at least 0.5 U of α-amylase (2.1.5) were added to two of the tubes and a solution of equivalent volume and composition without the enzymes to the other tube (control samples). All samples were incubated at 37°C for 2 h. To remove particulate material, the tubes were

spun down with 10,000 g for 5 min at RT. The enzymatic assay above (Stitt et al., 1989) was used in which hexokinase and glucose 6-phosphate dehydrogenase were applied to convert glucose to 6-phosphogluconate with concomitant reduction of NADP to NADPH.

2.7.9.3 Quantitative measurement of starch using peroxidase

Starch was determined also via a second method according to Ebell (1969) and Eimert et al. (1995): 50 mg of leaf tissue (2.2.3.1) were grinded and extracted in 0.5 ml 80% ethanol at 80°C for 5 min. Samples were centrifuged at RT with 13,000 g for 5 min. Supernatant was discarded and the sediment was dissolved in 0.5 ml 80% ethanol. This step was repeated three times in total and the samples were centrifuged at RT with 13,000 g for 10 min. Supernatant was discarded and the sediment was allowed to air-dry. The resulting sediment was resuspended in 0.2 ml 0.2 M KOH, and boiled for 30 min. The reaction was neutralized with 40 µl acetic acid. An aliquot (0.1 ml) was digested with 0.5 U amyloglucosidase (2.1.5), 90 mM sodium acetate buffer, pH 4.8 for 1 h at 55°C in a total volume of 1 ml. The reaction was stopped by heating to 100°C for 5 min. The resulting glucose from 0.1 ml digested starch sample was measured by adding 37.5 µl of 0.04% O-phenylene dihydrochloride and 0.1 ml sodium acetate buffer containing 0.1 U of glucose oxidase and 0.1 U of peroxidase (2.1.5). The reaction was carried out at 37°C for 30 min and stopped with 0.1 ml of 3 M HCl. The OD was measured at 492 nm. For quantification, a standard curve of 40 - 200 µg of soluble starch (2.1.2) was set which was treated like the extracted samples after resuspension in 0.2 ml 0.2 M KOH.

2.7.10 Determination of sulfolipids

First, a SILGUR-25 thin layer chromatography (TLC) plate (2.1.3) was soaked in a 0.15 M ammonium sulfate solution for 30 min and after complete drying at RT, the plate was heated for 2.5 h at 120°C. For sulfolipids analysis, 0.2 g fresh leaf material from seven weeks old soil-

grown *sir1-1*, Col-0 and *sqd2* lines (2.2.3.1) were homogenized and extracted in 0.4 ml chloroform/methanol/formic acid (10:10:1) for 10 min. In parallel, the samples were mixed vigorously, and then centrifuged with 18,000 g at 4°C for 2 min. The entire supernatant was transferred into a fresh tube, followed by the addition of 0.2 ml of 1 M KCl and 0.2 M H₃PO₄. The mixture was centrifuged at RT for 1 min with 13,000 g and 50 µl of the lipids containing lower phase was spotted on activated pre-coated TLC plate. The TLC was performed with 0.1 l running buffer (90:30:8 acetone/toluene/water) for 60 min at RT. Afterwards, TLC plates were dried at RT, sprayed with 50% H₂SO₄ and incubated at 160°C for 15 min in order to visualize the lipids.

2.7.11 Quantification of leaf chlorophyll contents

30 mg leaf tissue of eight weeks old soil grown plants were grinded in liquid nitrogen and leaf pigments were extracted in 1 ml 80% (v/v) acetone for 15 min on ice. The cell vestige was centrifuged for 10 min at 18,000 g at 4°C. The supernatant was transferred to a fresh tube. The sediment was re-extracted in 1 ml 80% acetone as described above. The resulting supernatant was combined with the first supernatant and the absorbance of the total extract was determined (80% acetone as blank) at 645 nm and 663 nm. The following formulas were used for calculation of chlorophyll a and b contents as described in Mackinney (1941) and Arnon (1949):

$$C_{chl a} = 12.7 \times A_{663 \text{ nm}} - 2.69 \times A_{645 \text{ nm}}$$

$$C_{chl b} = 22.9 \times A_{645 \text{ nm}} - 4.68 \times A_{663 \text{ nm}}$$

$$C_{chl} = C_{chl a} + C_{chl b}$$

2.8 Transcriptomics

2.8.1 mRNA Isolation

Total RNA was extracted from 150 mg and either, 30 mg or 0.1 g frozen leaf, root and seed tissue, respectively. The grinded leaf or root tissues

were extracted with RNeasy Plant Mini Kit and RNase free DNase Kit (2.1.4) according to manufacturer's protocols. For RNA extraction from seeds, following protocol according to Chang et al. (1993) was used: The extraction buffer (0.1 M Tris-HCl, pH 8.0, 2% hexadecyltrimethylammonium bromide, 2% PVP-40, 25 mM EDTA, 2 M NaCl) was preheated in a water bath at 65°C. Before extraction, 0.1 ml β -mercaptoethanol was added to 5 ml extraction buffer for each sample. After combining the seed powder and the buffer, the homogenate was mixed for 1.5 min and incubated at 65°C for 10 min. The reaction set was centrifuged at RT and 6,000 g for 20 min. The supernatant was collected and combined with 5 ml of chloroform/isoamyl alcohol (24:1). The solution was mixed and the centrifugation step was repeated as described above. The whole supernatant was transferred to a fresh tube, 5 ml of 5 M LiCl was added and RNA was precipitated overnight at 4°C. The samples were centrifuged with 6,000 g at 4°C for 30 min. The supernatant was removed and the sediment was resuspended in 0.6 ml resuspension buffer (10 mM Tris-HCl, pH 8.0, 1 M NaCl, 0.5% SDS, 1 mM EDTA) which was preheated to 60°C. The solution was transferred to a fresh tube and incubated at 60°C until the sediment was resolved in buffer. 0.6 ml of chloroform/isoamyl alcohol (24:1) was added to the sample followed by centrifugation with 14,000 g at 20°C for 10 min. The supernatant was mixed with 0.5 ml of chloroform/isoamyl alcohol (24:1) in a new tube and centrifugation was repeated as previously described for 15 min. After centrifugation, the supernatant was transferred into a new tube with 1.2 ml ice-cold 100% ethanol and incubated for 1 h at -80°C to precipitate RNA. After centrifugation at 13,000 g and 4°C for 30 min, the supernatant was discarded carefully and the sediment washed with ice-cold 70% ethanol and centrifuged twice at 13,000 g and like before for 10 min. Sediment was dried at RT and resuspended in 50 μ l RNase-free DEPC-treated water (2.1.2). For all treatments and buffers, DEPC-treated water was used. After RNA isolation, total RNA yield was measured with NanoDrop 2000 spectrophotometer (2.1.1) as described in 2.8.2.

2.8.2 Examination of RNA degradation and determination of concentration

To examine the degree of degradation after RNA isolation, a 1% agarose gel was prepared with RNase-free reagents. RNA samples were denatured using formaldehyde/ formamide. To 10 μ l of RNA sample buffer (0.5 μ l of 0.8 μ g/ml ethidium bromide, 0.5 μ l 10 \times MOPS, 5 μ l formamide, 1.75 μ l formaldehyde, 1.7 μ l 6x loading dye, 0.55 μ l RNase-free water), 1.5 μ l (0.5 - 2 μ g) of RNA sample were added and the samples were incubated for 10 min at 65°C, and 2 min on ice. After denaturation, samples were loaded onto the agarose gel and separated for at least 40 min. The quality of the RNA was determined visually by examination of the ratio between the respective ribosomal RNAs (25S, ~3.6 kb to 18S, ~1.9 kb), which should be 2:1 as sharp bands. No low molecular weight smear indicating total RNA degradation was observed. Since the mRNA represents only 1% of total cellular RNA it is not possible to directly examine its degradation status. The amount of RNA was determined spectrophotometrically at 260 nm using the NanoDrop 2000 spectrophotometer (2.1.1). The ratios $A_{260\text{ nm}}/A_{280\text{ nm}}$ and $A_{260\text{ nm}}/A_{230\text{ nm}}$ were compared to estimate protein and polysaccharide impurities. The values should be between 1.8 and 2.1.

2.8.3 Quantitative real time-PCR

2.8.3.1 cDNA synthesis

cDNA from total RNA extract was synthesized with SuperScript® VILO™ cDNA Synthesis Kit or RevertAid™ H Minus First Strand cDNA Synthesis Kit (2.1.4) according to manufacturer's protocols using 1 μ g of total RNA extract.

2.8.3.2 qRT-PCR

The qRT-PCR reaction was set up by one of the following systems: 10 ng cDNA with 1.6 pmol of each specific primer (2.1.6) were added into

onefold EXPRESS Two-Step SYBR GreenER Universal mixture (2.1.4). The reaction was performed in the LightCycler 480 (2.1.1) according to the EXPRESS Two-Step SYBR GreenER protocol and evaluated with LightCycler software 4.0 (2.1.7). For the second system, 10 ng cDNA and 2.5 pmol of each specific primer (2.1.6) were mixed with 6.25 µl SYBR solution from SensiMix™ SYBR No-ROX Kit (2.1.4). The reaction took place in the Rotor-Gene Q (2.1.1) according to the manufacturer's protocol. For quantification, Rotor-Gene® Q Series Software (2.1.7) was used. In both systems, elongation factor 1a (EF1a, At5g60390) was used for normalization as reference gene (Zuber et al., 2010a). As additional reference genes, ubiquitin (At4g27960) and protein phosphatase (At1g13320) were tested, which delivered same results. Each of at least three biological replicas was tested three times.

2.8.4 Microarray analysis

2.8.4.1 Labeling, hybridization, staining and scanning

250 ng total RNA were transferred into biotinylated aRNA using 3' IVT Express Kit (2.1.4) according to manufacturer's protocol: After cleanup, 15 µg labeled aRNA was fragmented at 94°C for 35 min and then hybridized onto the arrays (2.1.3) for 16 h at 45°C and 60 rpm using Hybridization Wash and Stain Kit (2.1.4) and GeneChip Hybridization Oven 640 (2.1.1).

Arrays were washed and stained with GeneChip Fluidics Station 450 and scanned with GeneChip Scanner 3000 7G (2.1.1).

2.8.4.2 Normalization and data analysis

In total, nine arrays were processed, three for each group: 7-week-old Col-0 as well as 7- and 10-week-old *sir1-1* (2.2.3.1). Microarray data were analyzed using a commercial software package JMP Genomics, version 4 (2.1.7). Arrays were annotated using an Entrez Gene based custom CDF file from Brainarray (2.1.7); log₂-transformed scores of all spot measures

were then subjected to quantile normalization; identification of differentially expressed genes was carried out by mixed model ANOVA, taking group and probe_id as fixed effects and array_id as random.

Pathway analysis was performed after Subramanian et al. (2005) with p-values smaller than 0.05 and false discovery rate (FDR) smaller than 0.75.

2.9 Principal component analysis (PCA)

Data normalization, visualization, and correlation analysis based on Pearson correlation were performed using R software (Ihaka and Gentleman, 1996). Used script is from bioconductor.org (library: pcaMethods).

2.10 Statistical Analyses

Means of different data sets were analyzed for statistical significance using unpaired t-test or ANOVA test. Constant variance and normal distribution of data were checked with SigmaStat 3.0 (2.1.7) prior to statistical analysis. The Mann-Whitney rank sum test was used to analyze samples that did not follow normal Gaussian distribution. Asterisks in all figures indicate the significance: *, $0.05 \geq p > 0.01$; **, $0.01 \geq p > 0.001$; ***, $p \leq 0.001$.

3 Results

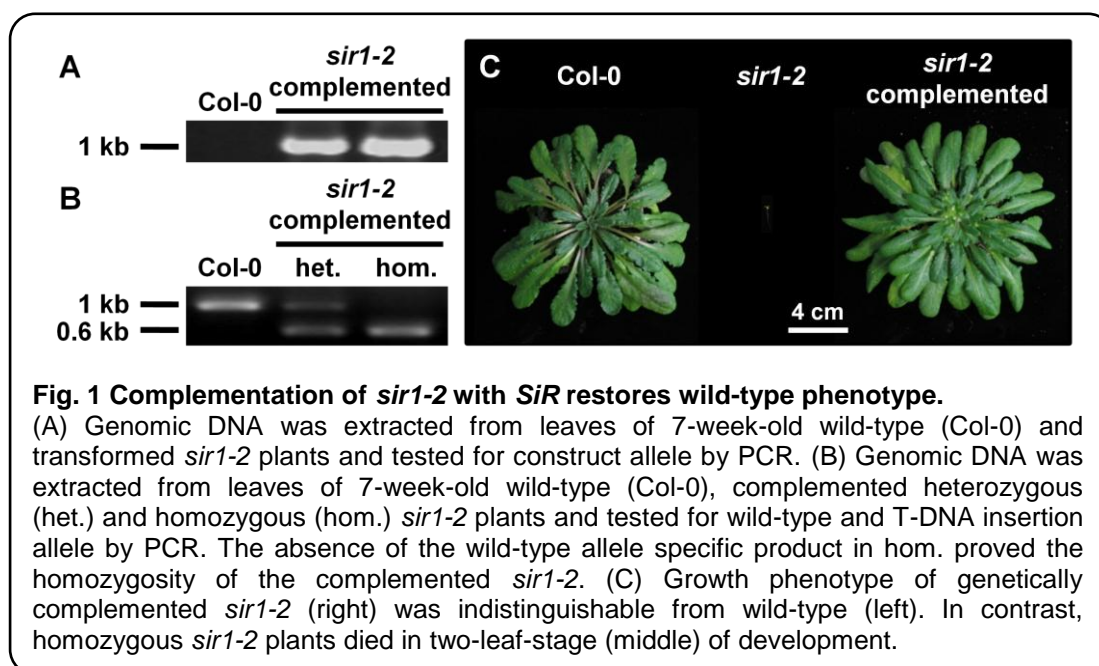
3.1 Complementation and stress induction of the T-DNA insertion lines *sir1-1* and *sir1-2*

Sulfite reductase (*SiR*, AT5G04590) is the only member of the sulfur assimilation pathway in *Arabidopsis* which is encoded by a single-copy gene (Bork et al., 1998). Two T-DNA insertion lines for *SiR* were identified and obtained from GABI-Kat collection center: *sir1-1* (550A09) and *sir1-2* (727B08). Previously, they had been characterized to a certain extent (Khan, 2008; Khan et al., 2010). More detailed analyses were performed to find out whether the phenotype of *SiR* mutants results from reduced flux of sulfur into cysteine and GSH. Therefore, chemical complementation of both mutant lines was carried out (3.1.2). Sulfite toxicity may also be possible for the phenotype of *SiR* mutants. Sulfite is accumulated in *sir1-1* (Khan et al., 2010) and is a toxic agent for cell compounds, e.g. DNA. In order to investigate the resistance of *sir1-1* to sulfite, a sulfite stress test was performed (2.2.7). Genetic complementation of *sir1-2* (3.1.1) was required to demonstrate that the effects observed in the mutant derive from the *SiR* mutation. Leaf- and root-specific complementation of *sir1-1* was carried out to demonstrate the importance of *SiR* in each of examined tissues (3.1.2).

3.1.1 Genetic complementation of homozygous *sir1-2*

For genetic complementation of the *sir1-2* mutant, the *SiR* open reading frame fused to its plastidic transit peptide was amplified from a cDNA clone and resulted in the vector described in Khan et al. (2010). Heterozygous *sir1-2* plants were transformed (2.2.7) with this vector expressing the *SiR* cDNA with its plastidic transit peptide under the control of the constitutive 35S cauliflower mosaic virus promoter. After BASTA® selection of the transformed plants, homozygous *sir1-2* mutants were identified via PCR (2.4.2) using the primers 605 and 606 which results in a 1 kb PCR product indicating the wild-type allele, and the

primers 1037 and 1038 (2.1.6) resulting in a 0.6 kb PCR fragment indicative for the *sir1-2* mutants (Fig. 1B). Successful integration of complementation vector was checked by using construct-specific primers 1192 and 1193 (2.1.6) producing a 1054 bp PCR product (Fig. 1A). The severe phenotype of *sir1-2* was completely restored (Fig. 1C) by expression of SiR under control of the 35S promoter.

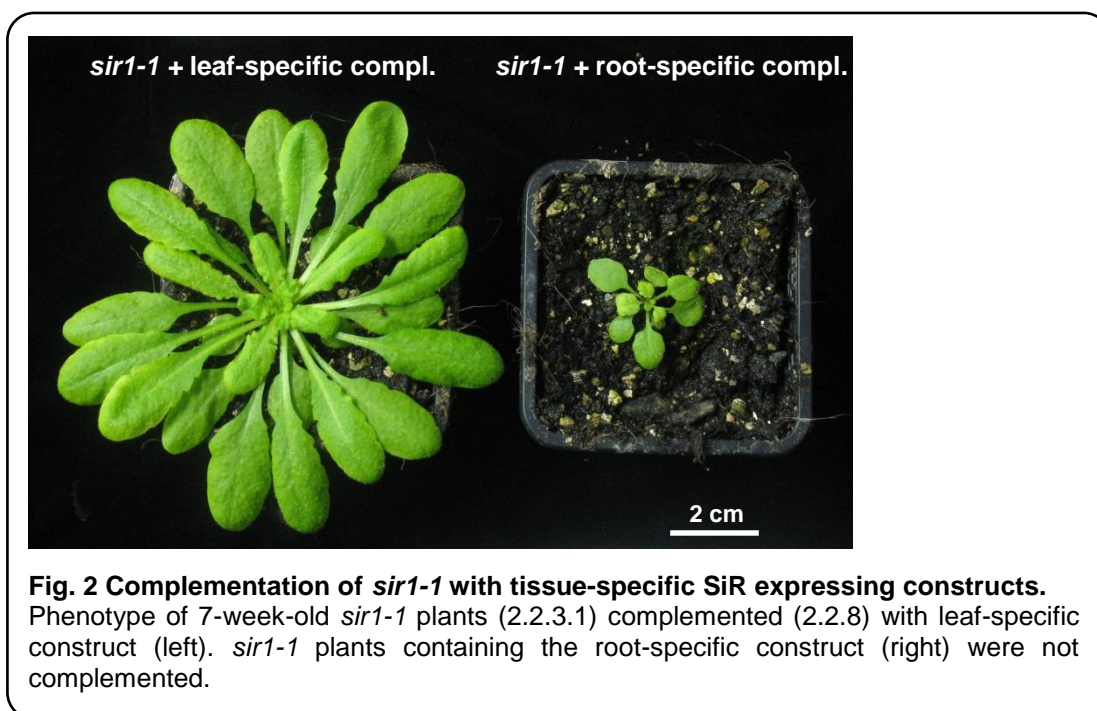


3.1.2 Tissue-specific genetic complementation of *sir1-1*

A construct with leaf-specific soybean rubisco promoter (*SRS1p*, Dhankher et al., 2002) was used for cloning of *SiR* after promoter. Therefore, *SiR* was amplified as described in 3.1.1. For *SiR* amplification the primers 1774 and 1775 were used to introduce restriction sites (2.1.6). After ligation of *SiR* to the construct (2.4.4), a sequence containing *SRS1* promoter, *SiR*, and *SRS1* terminator was cut out using restriction enzymes *NotI* and *XhoI* and introduced to Gateway® entry vector pENTR™4 Dual Selection (Invitrogen). Via a LR recombination reaction according to the supplier's instructions (Invitrogen), the expression construct was introduced to vector pMDC123 containing a BASTA® resistance gene as marker (Curtis and Grossniklaus, 2003) for expression of *SiR* in leaves of

the mutant *sir1-1*. Seed setting homozygous *sir1-1* plants were transformed with the leaf-specific construct (2.2.8). Seeds of transformed plants were sown on soil and sprayed with 0.2 g/l glufosinate ammonium solution (BASTA®; 2.1.2) on four-leaf stage plants (2.2.8). The treatment was repeated one week later.

For generation of a root-specific construct, promoter of a glycosyltransferase (At1g73160) from Arabidopsis (Vijaybhaskar et al., 2008) was amplified from wild-type gDNA (2.4.1) with restriction site introducing primers 1772 and 1773 (2.1.6). *SRS1p* was removed from the leaf-specific *SiR* complementation construct via restriction enzymes *NotI* and *XmaI* (2.1.5) and the root-specific glycosyltransferase was ligated into the final construct. Plants were transformed and screened for positive transformants with BASTA® as described for leaf-specific promoter. For each complementation construct more than ten *sir1-1* plants were tested via BASTA selection as positive, hence they contain the respective construct (Fig. 2). Expression of *SiR* in leaves could rescue the phenotype of the 7-week-old mutant fully, while *SiR* expression in roots did not change the growth phenotype of *sir1-1*. These results indicate that *SiR* expression in leaves is essential for proper growth of Arabidopsis while *SiR* expression in roots seems to have a minor role. However, to make a more certain statement, the exclusive expression of construct in the respective tissue should be demonstrated.

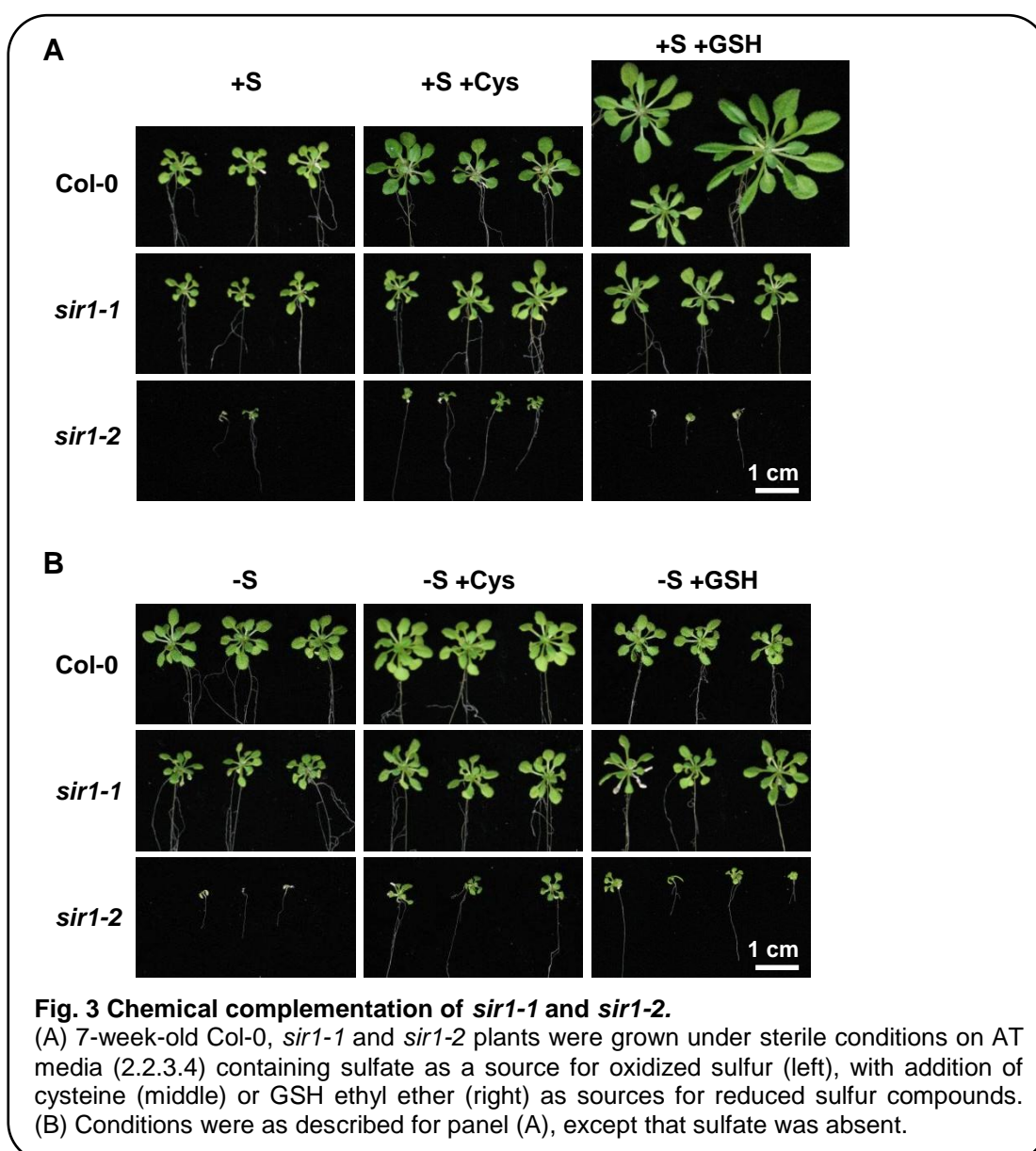


3.1.3 Chemical complementation of *SiR* mutant lines

It is known that in *Mycobacterium tuberculosis* *sirA* gene encoding for sulfite reductase is essential for growth on oxidized sulfur. However, the mutant strain could be rescued by supply with reduced sulfur like sulfide or cysteine (Pinto et al., 2007). Preliminary complementation experiments for *SiR* mutants were performed in hydroponic cultures (*sir1-1*) or on standard AT media (*sir1-2*) with 1 mM GSH and 0.1 mM sulfide, however no cysteine was applied and since *sir1-2* mutants were not able to grow, it was considered that accumulation of sulfite could cause their death, so *sir1-2* mutants were additionally grown in the absence of sulfate (Khan, 2008). Those experiments showed that the supplied sulfide or GSH could partially complement the *sir1-1* phenotype and the seedling lethal phenotype of *sir1-2* was also only partially rescued, when sulfate was absent.

The experiments were repeated to verify the observed results. Plants were grown under sterile conditions on AT media with addition of either 1 mM cysteine or 1 mM GSH ethyl ester (2.2.3.4). GSH ethyl ester was used because of its better permeability of the plasma membrane than GSH (Ito

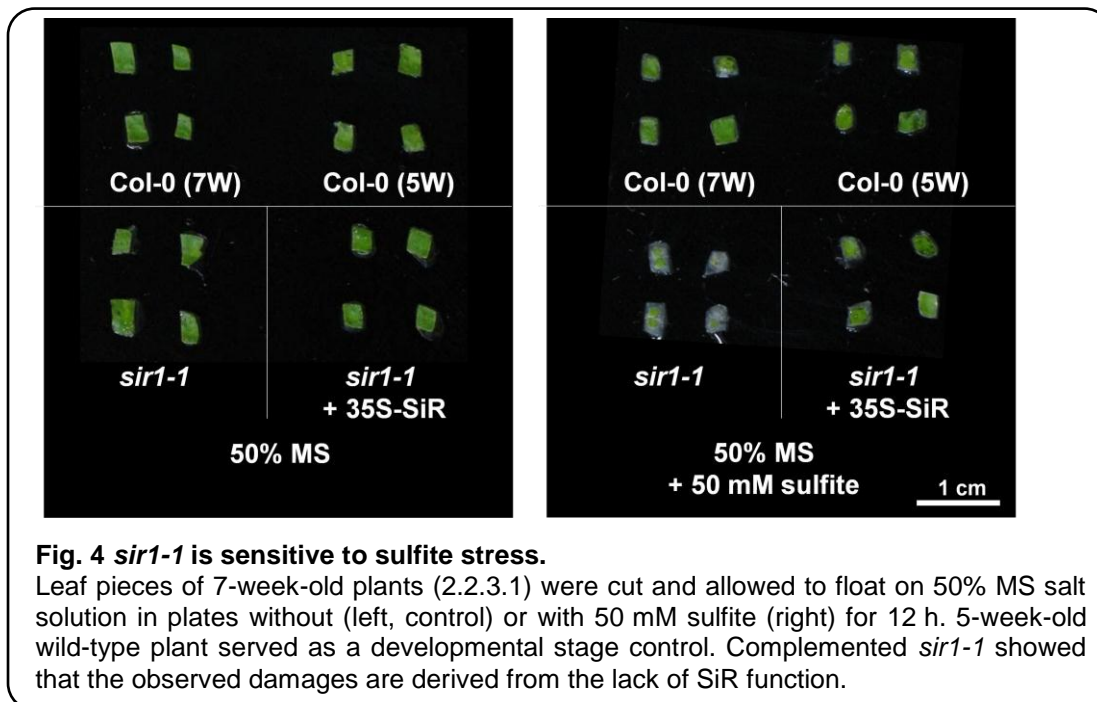
et al., 2003; Meyer et al., 2007). Plants were transferred onto new AT media every second week under sterile conditions to avoid nutrition depletion. In the presence of sulfate (+S) and cysteine Col-0 plants grew better than on sole +S and they reached up to three-fold bigger size when GSH was added (Fig. 3A). The exogenous supply of cysteine and GSH counteracted the retarded growth phenotype of *sir1-1* mutants. This was not the case for *sir1-2* mutants: while heterozygous *sir1-2* plants grew normally on +S, homozygous *sir1-2* plants died after the 2-leaf-stage as expected. The addition of GSH could not rescue the phenotype of these *sir1-2* plants and they died like on +S. Only when cysteine was provided could the lethal phenotype be rescued, but the plants never reached the wild-type size.



Col-0, *sir1-1* and *sir1-2* plants were grown on sulfate-free AT media (-S) to avoid excessive sulfite accumulation in *sir1-2* mutants (Fig. 3B). While on -S+GSH Col-0 plants did not show the huge growth phenotype on +S+GSH anymore, response of *sir1-1* plants grown on -S was similar to those grown on +S. *sir1-2* plants died at the same developmental stage when the oxidized sulfur resource was removed from growth media. However, addition of cysteine or GSH could partially rescue the *sir1-2* phenotype, and they were bigger in size compared to +S when oxidized sulfur was absent, but still 80 - 90% smaller than wild-type. These results suggest that both accumulation of sulfite and decrease of reduced sulfur compounds result in *sir1-2* phenotype and most effective complementation occur by sulfate absence and cysteine supply, followed by -S+GSH.

3.1.4 Sulfite treatment of *sir1-1* to assess stress resistance

Having shown that downstream metabolites of SiR like cysteine and GSH could rescue the *sir1-1* phenotype, it was of interest to show if the accumulation of sulfite in *sir1-1* (Khan et al., 2010) reduces *sir1-1*'s ability to defeat additional stress caused by sulfite. To assess this, 7-week-old wild-type and *sir1-1* plants were subjected to sulfite stress as described in 2.2.7. As an additional control for the developmental stage, 5-week-old wild-type plants were used. To show that the observed effects are due to reduced SiR function, a *sir1-1* complemented line was used, too. After 12 h of sulfite treatment, *sir1-1* was severely affected and showed lesions while all controls did not show remarkable damages (Fig. 4). High levels of toxic sulfite in *sir1-1* leaves and additionally, its reduced sulfur flux into cysteine and GSH impact the mutant negatively when it was forced to buffer excess of sulfite.



3.2 Phenotypic and metabolic characterization of *sir1-1*

3.2.1 Growth-based phenotypic analysis of *sir1-1*

Khan et al. (2010) previously reported that 6-week-old *sir1-1* is reduced in size and pale when compared with wild-type plants of the same age. *sir1-1* and wild-type plants were sowed on soil and grown under short day conditions (2.2.3.1) to investigate if *sir1-1* could catch up wild-type in size and if so, at which stage. The growth was documented weekly (Fig. 5A). *sir1-1* showed more pale leaves. At week 11, when wild-type plants already set flowers, *sir1-1* reached the size of 7- to 8-week-old wild-type plants and after 13 weeks it was close to wild-type plants of same age. After 11 weeks, the wild-type flowers were visible and after 13 weeks, the first wild-type leaves started the senescence program which led to reduced rosette diameter and leaf number (Fig. 5B and C). Determination of “total exposed leaf area” according to Boyes et al. (2001) showed that *sir1-1* had less leaf surface exposed to light for photosynthesis (Fig. 5D). The reduction of leaf surface from week 11 to 13 may seem astonishing, it was however due to the overlaying of leaves in the rosette while they were

photographed. The second reason for decreasing leaf surface in wild-type plants was the above-mentioned senescence.

After realizing that *sir1-1* was retarded in vegetative growth and could not reach the wild-type size, it was important to quantify the germination. Seeds of wild-type and *sir1-1* plants were stratified for 2 to 3 days at 4°C and grown in growth chamber under long day conditions on MS plates as described in 2.2.3.3. First, the germination rate of wild-type and *sir1-1* mutant plants was quantified by radicle appearance on full media consisting of MS with addition of 1% (w/v) sucrose. 3 experiments from different batches were performed; in all experiments *sir1-1* germination rate was worse than that of the wild-type (Fig. 6). After germination, the growth of *sir1-1* was slower compared to wild-type (Fig. 6D) as observed for soil-grown mutant plants (Fig. 5A).

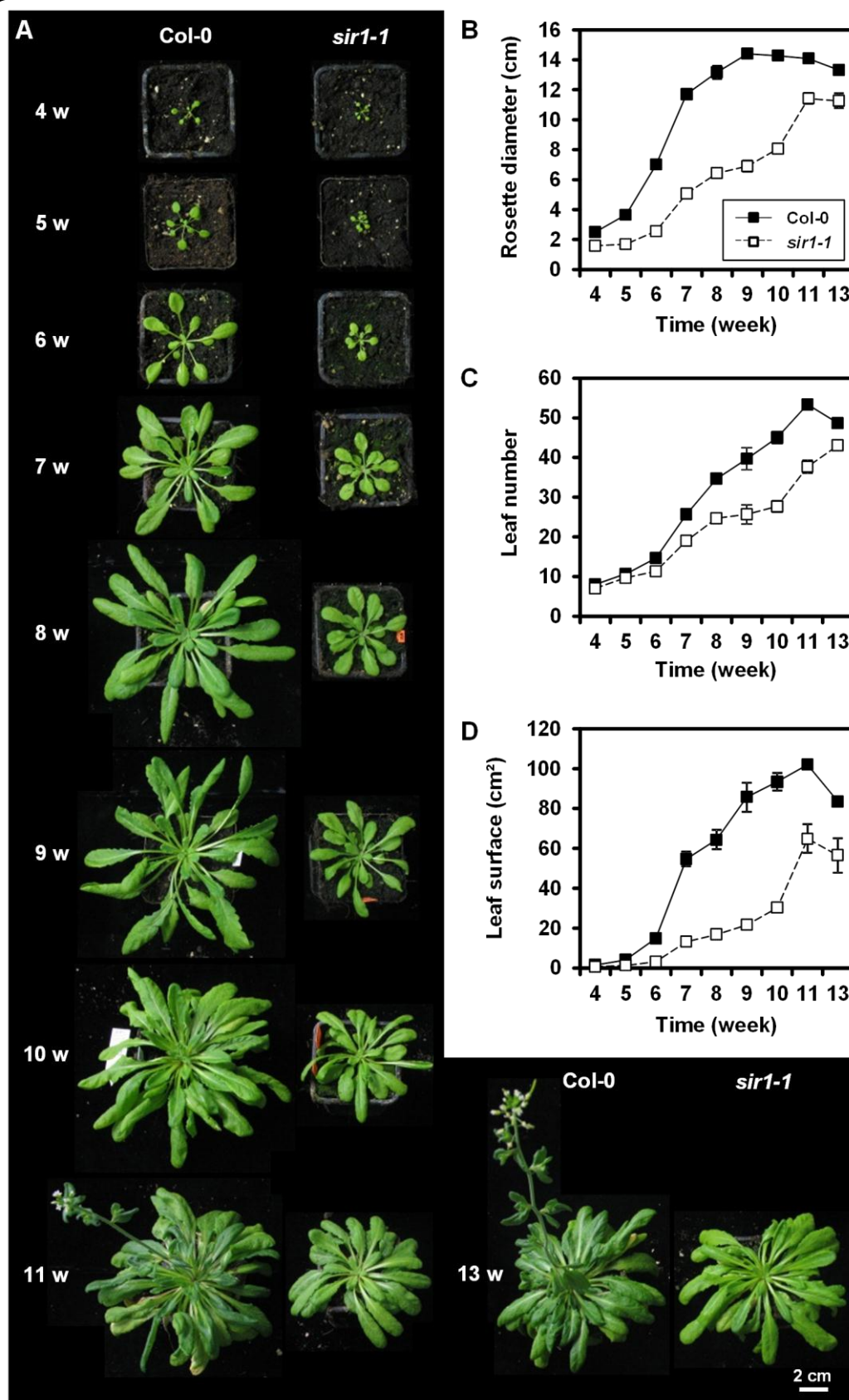


Fig. 5 Rosette-based phenotypic analyses reveal contracted growth of *sir1-1*. (A) Top view of Col-0 and *sir1-1* plants. (B) Rosette diameter, (C) leaf number, and (D) total exposed leaf area were measured weekly. *sir1-1* grew slower and reached the size of 7- to 8-week-old wild-type plants after approx. 11 weeks. Plants were grown on soil under short day conditions (2.2.3.1); (n = 3), (means \pm SEM).

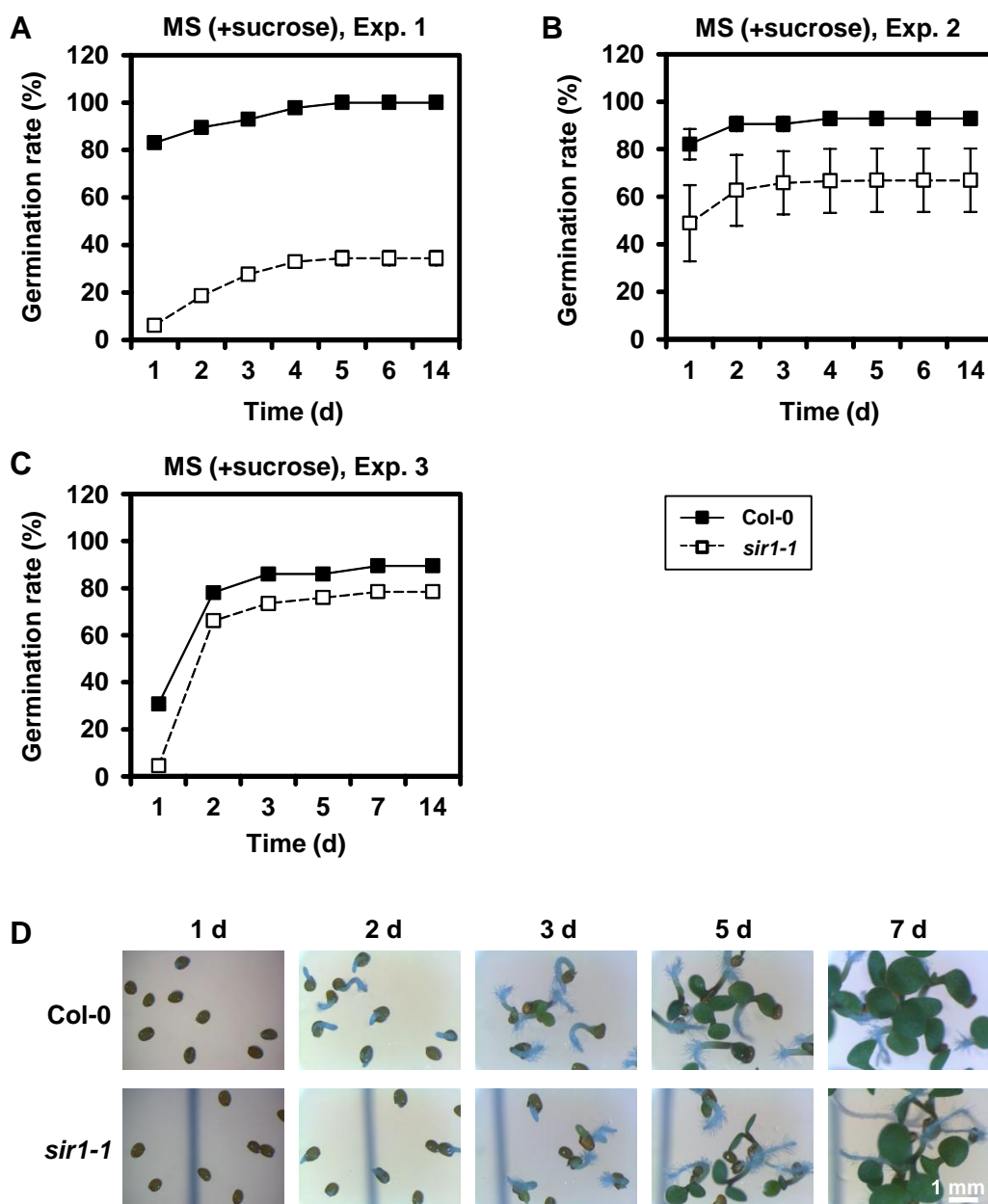


Fig. 6 On full media *sir1-1* has a lower germination rate than wild-type.

Seeds of Col-0 and *sir1-1* were put on MS media with sucrose which was defined as full media. Plants were grown under sterile long day conditions (2.2.3.3). Experiment was repeated 3 times with seeds coming from different batches. (A) *sir1-1* of this batch showed a very low germination rate. (B) and (C) *sir1-1* plants had a lower germination rate, however not as severe as in experiment 1. (D) Germination of plants from experiment 3 was documented on days 1, 2, 3, 5 and 7 in growth chamber; (n = 3), (means \pm SEM).

Germination tests were repeated without sucrose on MS media (Fig. 7A), and on 0.6% agarose (2.2.3.3) without MS or sucrose (Fig. 7B) to exclude the triggering effect of exogenously supplied nutrition on germination rate. Here also, *sir1-1* performed worse, so it could be assumed that independent from nutrient supply, *sir1-1* seeds germinate worse than wild-type seeds.

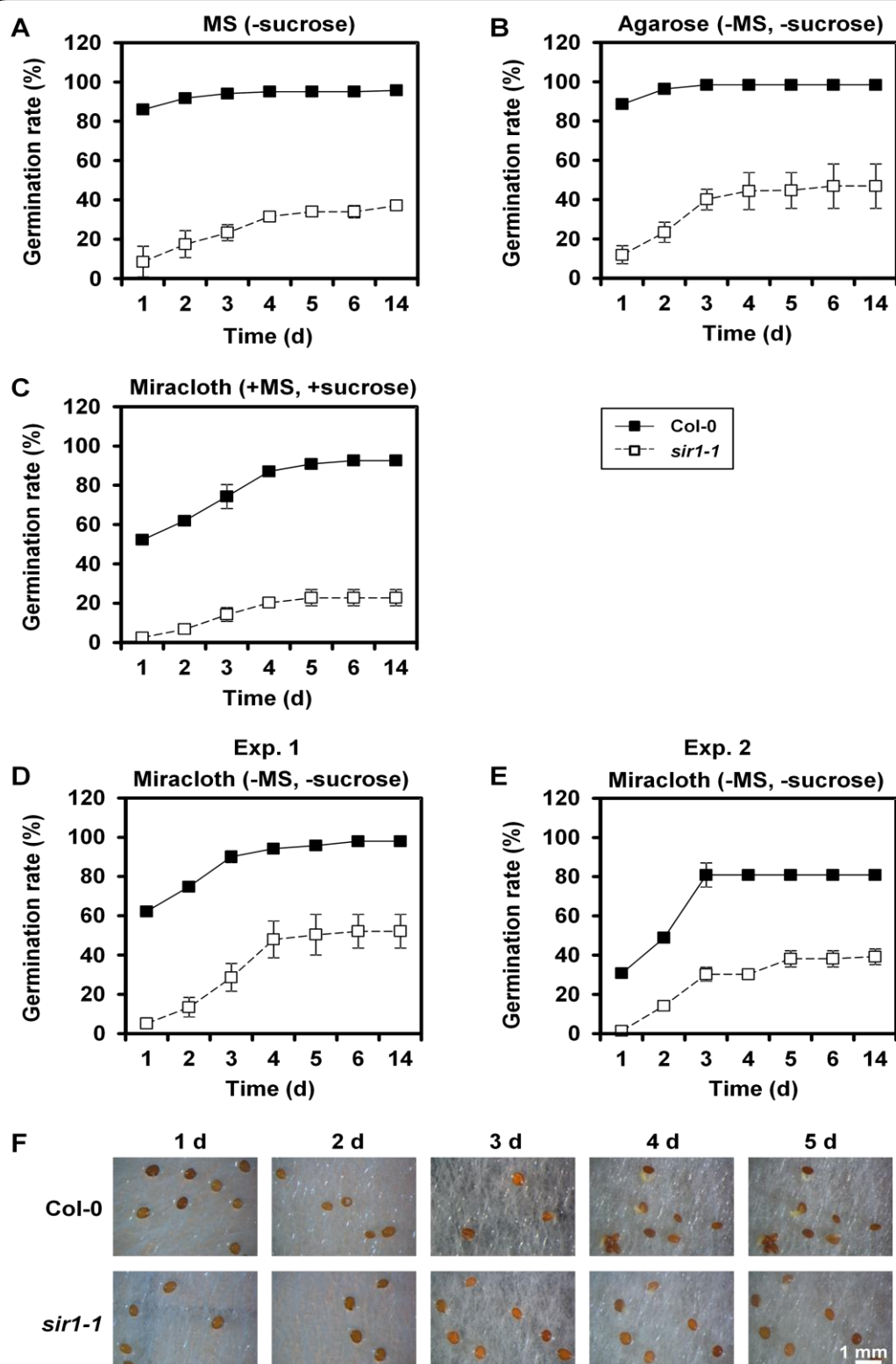


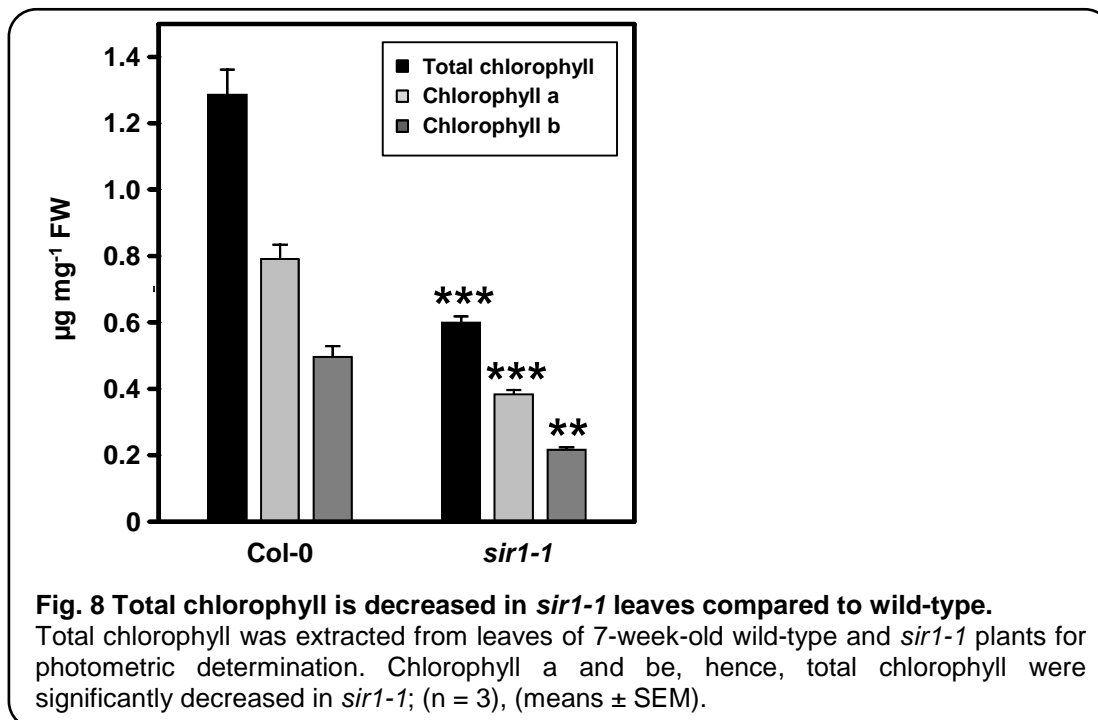
Fig. 7 *sir1-1* has a lower germination rate than wild-type on deficient media.

Plants were grown under sterile long day conditions (2.2.3.3). (A) Seeds of Col-0 and *sir1-1* were put on MS media without sucrose and (B) only on agarose gel. *sir1-1* plants had a lower germination rate. (D) and (E) To determinate the germination rate on Miraclot tissue, the experiment was repeated 2 times with seeds coming from different batches. In both experiments *sir1-1* showed lower germination rate than wild-type. (C) As a control, seeds were grown on Miraclot tissue with full media. (F) Germination of plants from experiment 1 were documented on days 1, 2, 3 and 5 in growth chamber; ($n \geq 3$), (means \pm SEM).

The germination tests were additionally performed on Miracloth tissues (2.1.3) to exclude the potential effects of polymerization chemicals. Again, *sir1-1* had a lower germination rate than Col-0 when MS and sucrose were suitable for seeds (Fig. 7C) or when the experiments were carried out in their absence after imbibition in water (Fig. 7D and E). First wild-type radicles were visible at day 2, whilst *sir1-1* radicles were first seen on day 3 (Fig. 7F). During the growth period of wild-type plants, the cotyledons were opened. This was not the case for *sir1-1*.

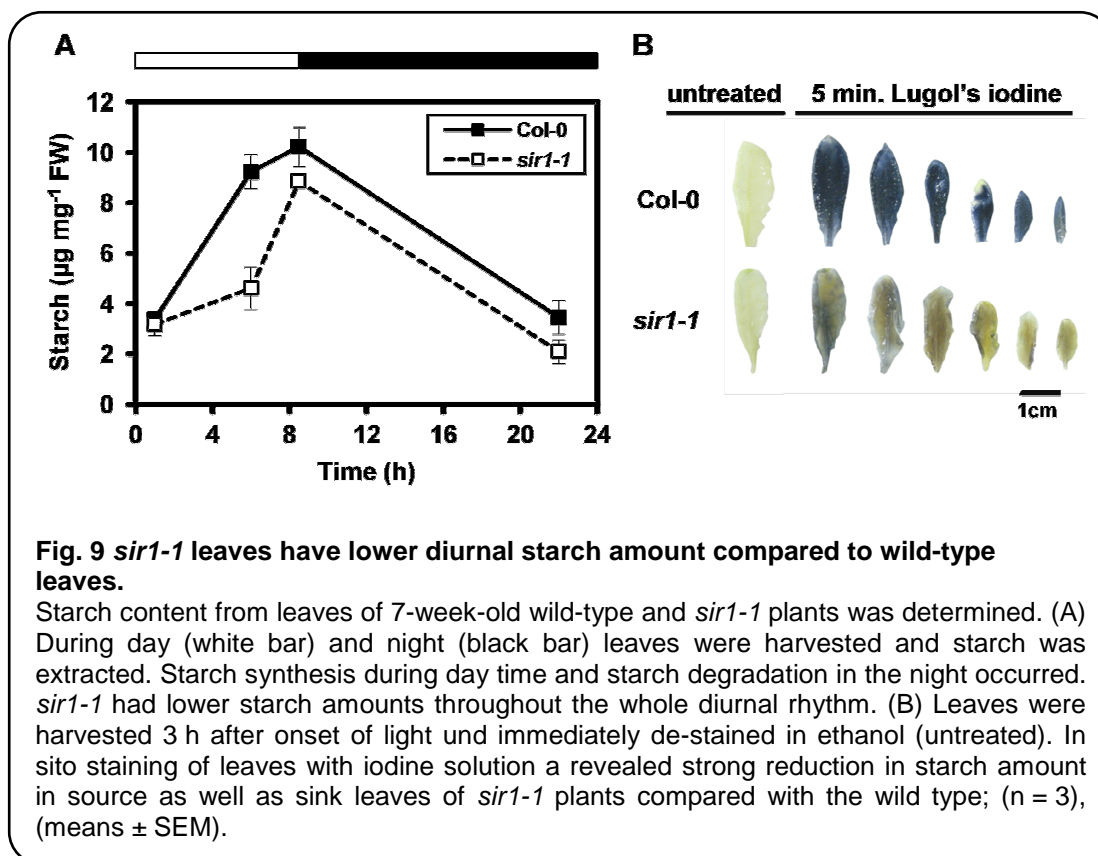
3.2.2 Determination of chlorophyll amounts in leaves

Due to the observed pale phenotype of *sir1-1* leaves (Fig. 5A) and their reduced exposed leaf area (Fig. 5D), the chlorophyll content in *sir1-1* leaves was analyzed. It was of interest to know whether the observed effects correlated with changing chlorophyll content. Total chlorophyll was extracted from 7-week-old wild-type and *sir1-1* plants for photometric determination (2.7.11). Measurement of chlorophyll a and b content revealed a significant reduction in *sir1-1*, hence total chlorophyll was reduced (Fig. 8). Interestingly, reduction of chlorophyll is also observed when Arabidopsis plants suffer from sulfur withdrawal (Nikiforova et al., 2005), a situation that is similar for *sir1-1* plants since they have a decreased flux of sulfur into reduced sulfur compounds.



3.2.3 Determination of starch levels in leaves

Assuming impaired photosynthesis and reduced carbon content in *sir1-1* leaves (Khan et al., 2010), starch levels were analyzed. In order to determine starch content, 7-week-old plants were harvested during day and night at indicated time points and starch was extracted and quantified according to 2.7.9.3. The measurement revealed that at all time points *sir1-1* had a lower starch contents (Fig. 9A). In situ staining of sink and source leaves which were harvested 3 h after onset of light showed a strong reduction of starch levels in *sir1-1* mutant (Fig. 9B). To answer the question if starch synthesis and degradation occur or de-novo starch synthesis is inhibited, leaves of *sir1-1* and wild-type plants were isolated and prepared for electron microscopy (2.6.2). Like wild-type plants, *sir1-1* was able to synthesize starch during the light period (Fig. 10A) and the accumulated starch was degraded during the night (Fig. 10B) to provide soluble sugars when no photosynthesis occurs.



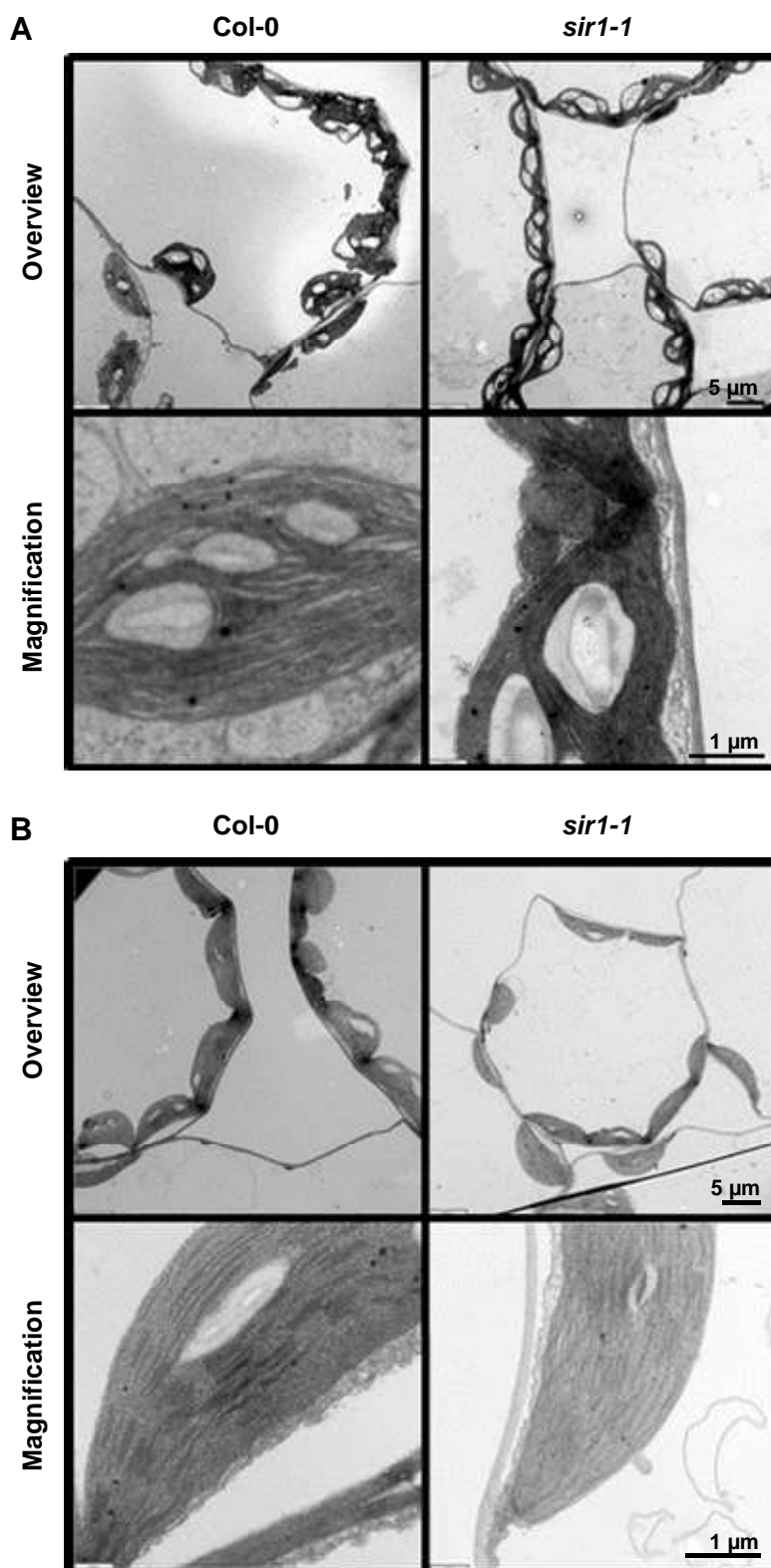


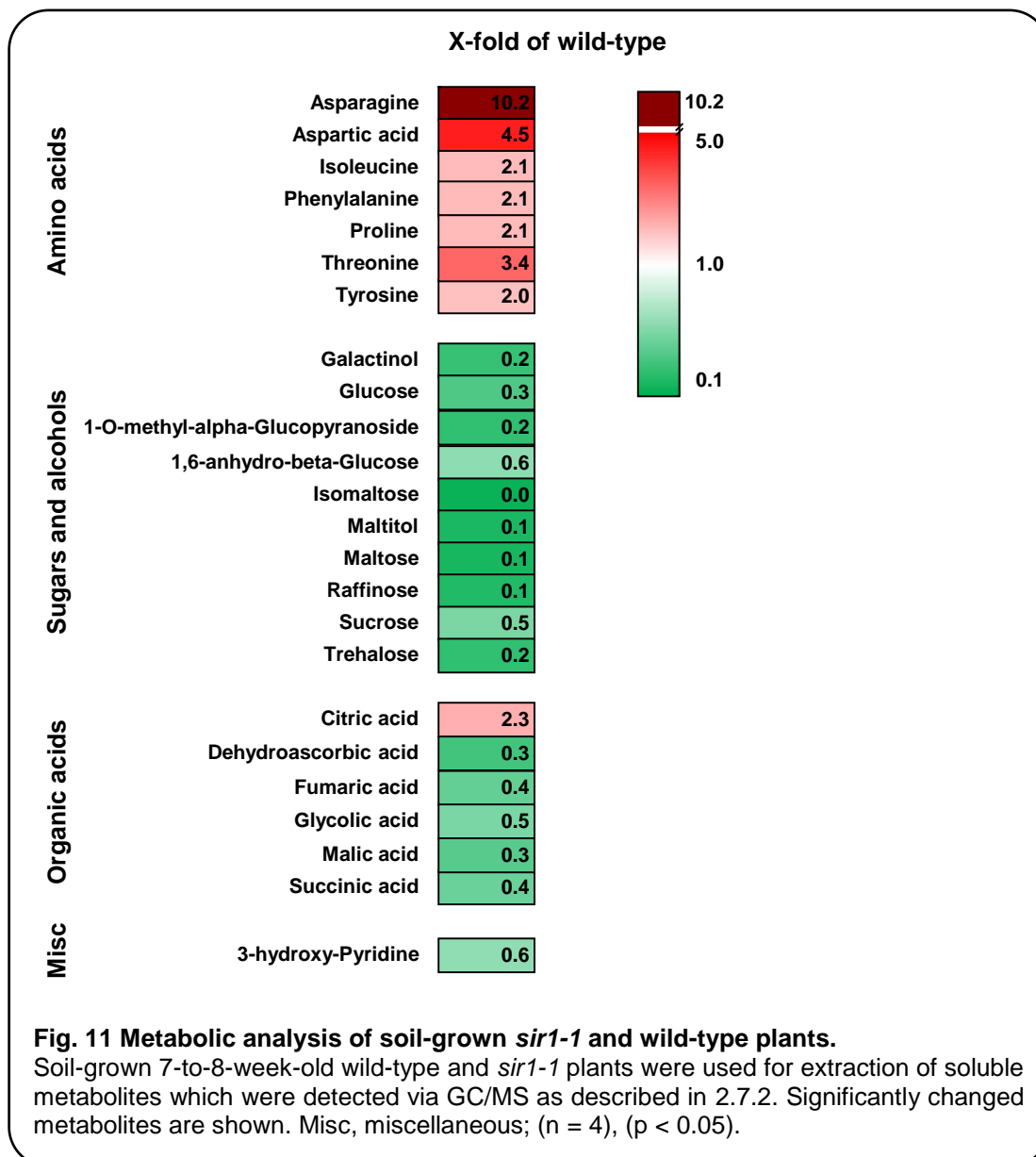
Fig. 10 *sir1-1* can synthesize and degrade starch.

Leaves of 7-week-old wild-type and *sir1-1* plants were used for electron microscopy (2.6.2). (A) Leaves of wild-type and *sir1-1* plants 1 h after onset of light. (B) Leaves of wild-type and *sir1-1* after 16 h of darkness. [Experiment was carried out in cooperation with Dr. Stefan Hillmer.]

3.2.4 Metabolite changes in leaves of soil-grown plants

Having observed changes in the level of starch and knowing that also glucose, fructose and sucrose were reduced in *sir1-1* leaves (Khan et al., 2010), large scale metabolite quantification was performed to get more insight into the mutant's response to reduced sulfide production. GC/MS analysis was used to quantify amino acids, sugars, alcohols and organic acids as described in Lisec et al. (2006) and 2.7.2.

55 metabolites were measured, of which 24 metabolites were significantly changed in *sir1-1* mutants (Fig. 11). Steady state levels of detected amino acids in leaves of *sir1-1* increase in comparison to wild-type. A complete list of measured metabolites is in Suppl. data 1. Metabolite quantification was carried out by Dr. Adriano Nunes-Nesi (MPI, Golm).



In *sir1-1* leaves, asparagine (10.2-fold) and aspartic acid (4.5-fold) showed the highest changes compared to wild-type. Sugars and alcohols were also reduced. This was also the case for glucose and sucrose as previously reported (Khan et al., 2010). As a third major group, organic acids were reduced, with exception of citric acid. The deregulation of the tricarboxylic acid cycle (TCA cycle) prompted us to investigate metabolites related to

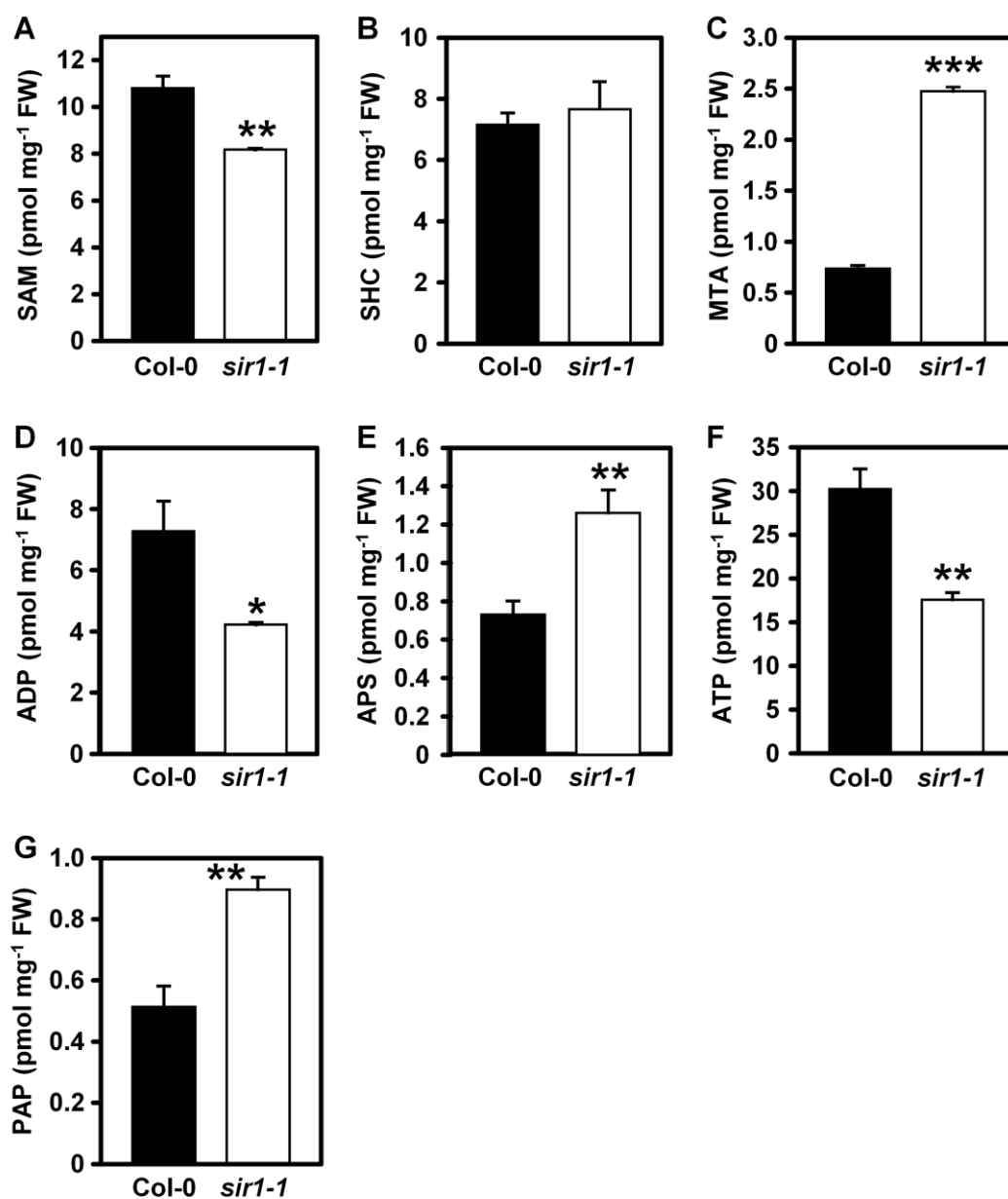


Fig. 12 Adenosine levels were changes in *sir1-1* compared to wild-type plants. 7-week-old plants were used for extraction and quantification of adenosines. (A) SAM, S-adenosyl methionine. (B) SHC, S-adenosylhomocysteine. (C) MTA, methylthio adenosine. (D) ADP, adenosine diphosphate. (E) APS, adenosine-5'-phosphosulfate. (F) ATP, adenosine triphosphate. (G) PAP, phosphoadenosine phosphate; (n = 3), (means ± SEM).

this pathway more in detail. Adenosines were extracted and determined (2.7.4). A deregulation of major compounds of adenosines was observed (Fig. 12). Only S-adenosylhomocysteine was unaffected (Fig. 12B). ADP and ATP were down-regulated (Fig. 12D and F), in accordance with the changes in citrate, succinate, fumarate and malate (Fig. 11).

3.2.5 Determination of *APR2* transcript and APR activity

Since APS accumulated in *sir1-1* leaves (Fig. 12E) and APS reduction to sulfite via APS reductase (APR) is a critical step prior to SiR (Kopriva and Koprivova, 2004), mRNA (2.9.1) was extracted from leaves of 7-week-old wild-type and *sir1-1* plants to determine levels of *APR2*, the major *APR* isoform. cDNA synthesis (2.9.3.1) and qRT-PCR (2.9.3.2) were performed with the primers 1713 and 1714 (2.1.6). The *APR2* transcript was down-regulated by approx. 80% (Fig. 13A). Proteins were extracted from the same plants as above and APR activity was determined (2.5.6.2). Also, the activity of APR isoforms was reduced in *sir1-1* leaves (Fig. 13B), indicating decreased sulfur reduction due to the lack of SiR activity (Fig. 37).

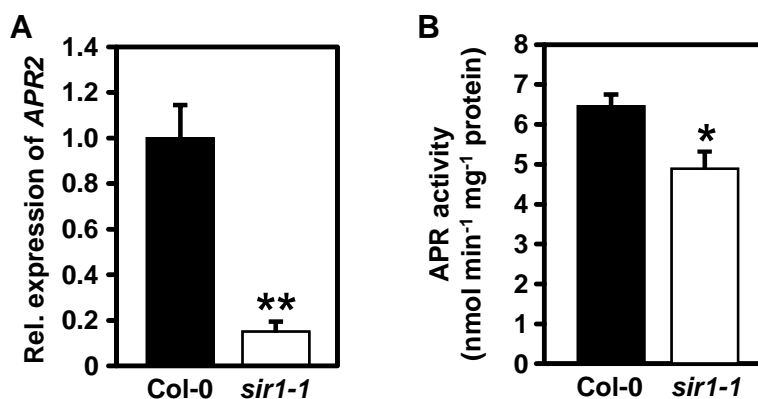


Fig. 13 *APR2* transcript and total APR activity is reduced in *sir1-1* leaves.

Plants were grown on soil under short day conditions for 7 weeks for RNA and protein extraction. (A) mRNA was extracted from leaves and submitted to cDNA synthesis and qRT-PCR; (n = 3). (B) Proteins were extracted from leaves and APR activity was performed; (n ≥ 5), (means ± SEM). [APR activity was determined by Dr. Florian Haas.]

3.2.6 Detection of sulfide

Sulfide was a metabolite of major interest since it is the direct product of the SiR, which is down-regulated in *sir1-1* (Fig. 37). To quantify sulfide from leaf tissue, we established an extraction and detection method via HPLC based on derivatization of sulfide with monobromobimane (2.7.3) and tested if the assumed evaluated signal was sulfide (Suppl. data 6). For that purpose, sulfide contents were extracted from approx. 25 mg leaf tissue and determined, in parallel to the sulfide standard (e.g., 100 pmol). The sum of the levels was set as 100% (Fig. 14A). Same amounts of sulfide standard and leaf extract were mixed and detected. We gained a recovery rate of $101.6\% \pm 6.8$ showing that the assumed sulfide peak represent indeed sulfide. Afterwards, we extracted sulfide from leaves of 7-week-old soil-grown wild-type and *sir1-1* plants (2.7.3). No significant changes were observed in the steady-state level of sulfide in *sir1-1* leaves compared to wild-type (Fig. 14B).

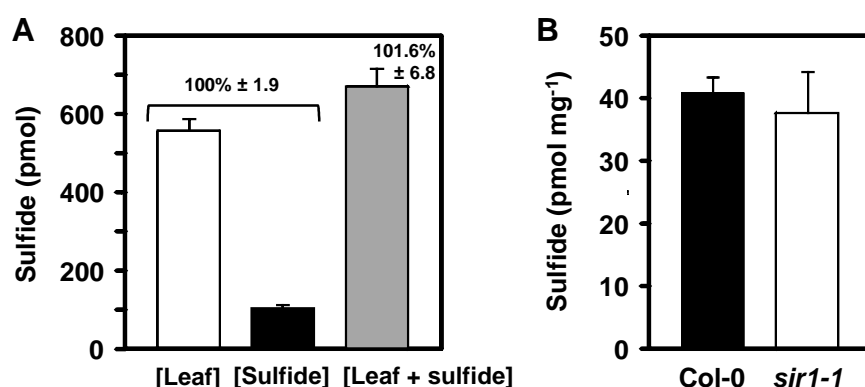


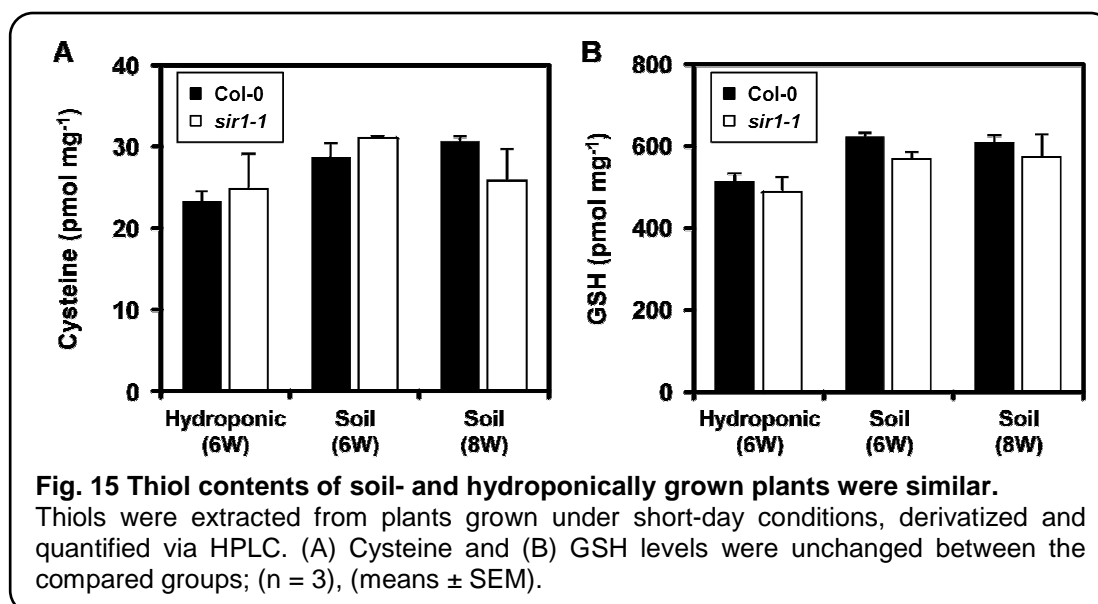
Fig. 14 Sulfide detection in leaf tissue reveals no changes in *sir1-1* compared to wild-type.

7-week-old plants were used for extraction and quantification of sulfide. (A) Recovery test proved that the peak of interest is sulfide and it could be measured. (B) Sulfide levels were unchanged in *sir1-1* leaves; (n = 3), (means \pm SEM).

3.2.7 Effects of sulfur availability on metabolites in vegetative tissues of hydroponically grown plants

In order to investigate the effects of sulfur availability on the metabolome of wild-type and *sir1-1* plants, hydroponic cultures were used (2.2.3.2). This system allows harvesting of root material for determination of

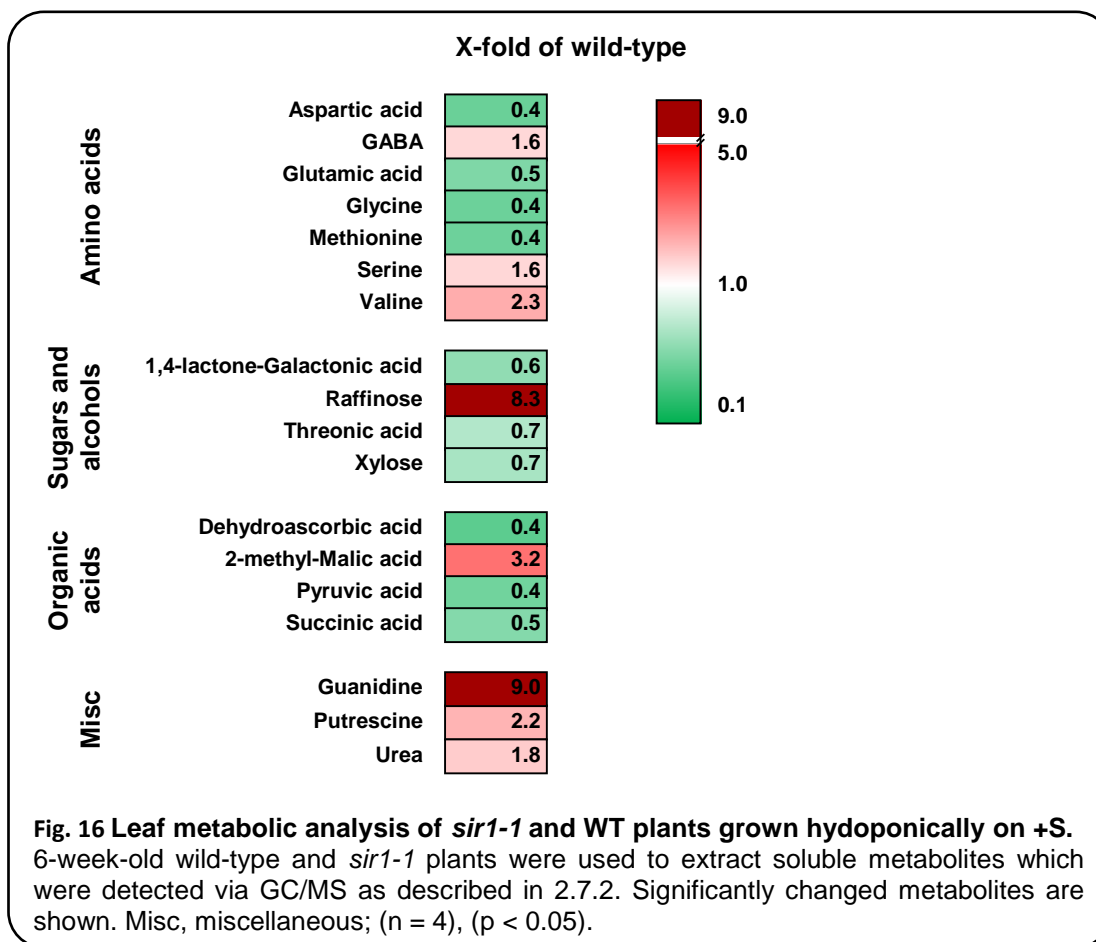
metabolites. First, thiols of soil- and hydroponically grown wild-type and *sir1-1* plants were analyzed to investigate if there were changes in metabolites due to different growth conditions. 6-week-old plants which were grown on soil or in hydroponic cultures and 7- to 8-week-old soil-grown plants were used for the analysis via HPLC (2.7.3). No significant changes were observed between the different ages of plants or the different growth systems, when cysteine levels (Fig. 15A) and GSH (Fig. 15B) were analyzed. However, differences were observed when comparing metabolite profiles from leaves of soil-grown plants (Fig. 11) with the results from hydroponic groups (Fig. 16), i.e. all significantly changed amino acids were accumulated in leaves of soil-grown *sir1-1* compared to wild-type plants, whereas some amino acids were reduced in leaves of hydroponically grown *sir1-1* in comparison to wild-type plants. The measurements showed that comparisons of results from hydroponic plants and soil-grown plants must be carried out very carefully. A complete list of measured metabolites from hydroponically grown plants is in Suppl. data 2 - 5. Metabolite quantification was carried out by Dr. Adriano Nunes-Nesi (MPI, Golm).



3.2.7.1 Effects of sulfur availability on metabolites in leaves

6-week-old wild-type and *sir1-1* plants grown in hydroponic cultures were used to determine metabolites via GC/MS as described in 3.2.4. Plants

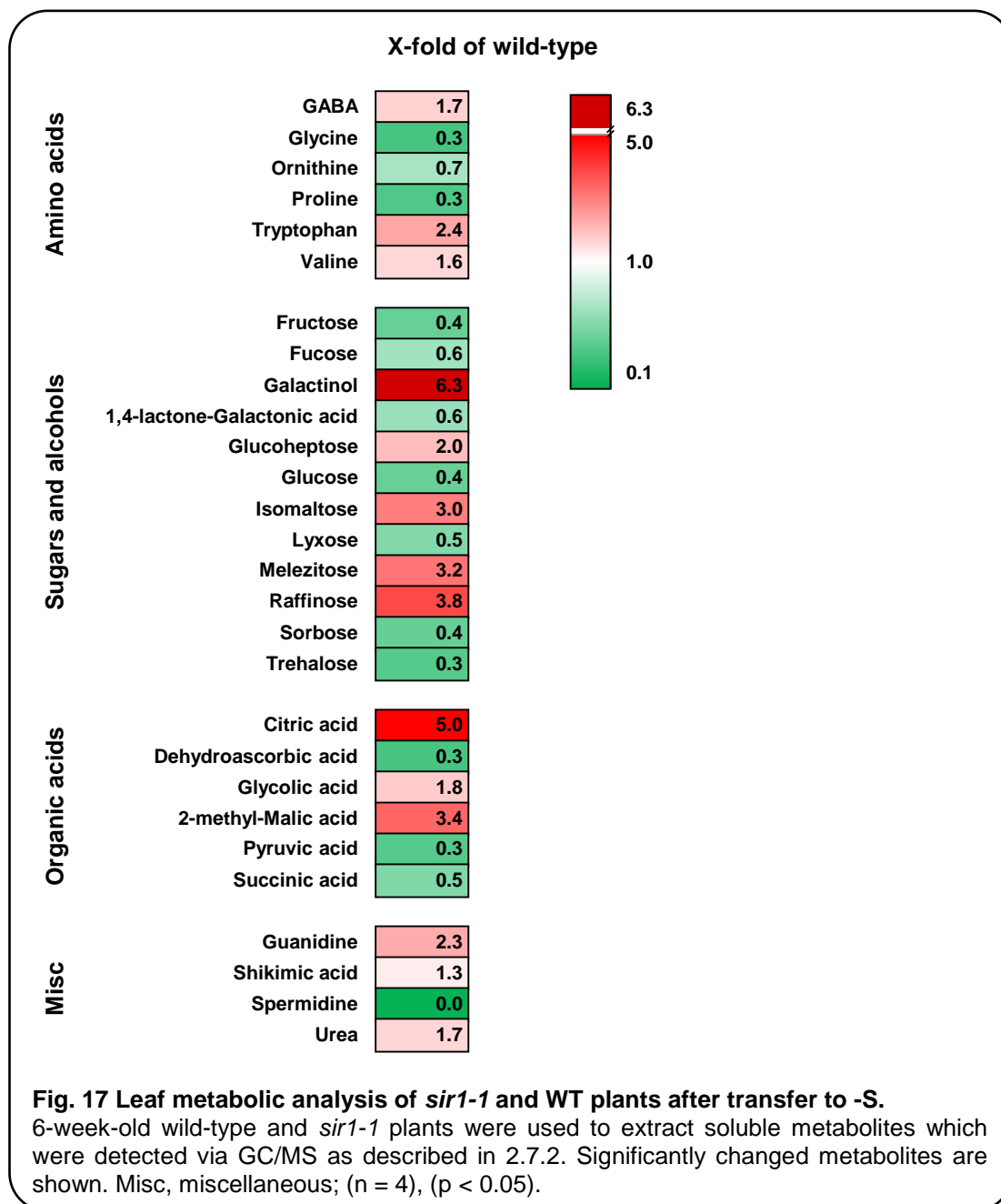
were grown on 1/2 Hoagland medium (2.2.3.2) with (+S) or without (-S) sulfate to investigate and compare the effects of sulfate on wild-type and *sir1-1* metabolites. 18 out of 52 detected metabolites from +S leaves showed significant changes when *sir1-1* was compared to wild-type (Fig. 16). As mentioned above, the pattern of changed metabolites is slightly different when the results from two different growth conditions are compared. However, 2 proteinogenic amino acids were higher in *sir1-1* (serine and valine). Guanidine, a product of protein metabolism and the functional group of arginine was elevated 9-fold in *sir1-1*. Additionally, a 1.8-fold increase in urea content indicated protein breakdown. This was supported by the 2.2-fold increase of polyamine putrescine which is produced during arginine degradation (Imai et al., 2004) and the increased expression of genes (array data) involved in arginine or putrescine breakdown (*SPDS1*, *SPDS2*, *ADC1*, *ADC2* and *ACL5*) (Hanzawa et al., 2002; Imai et al., 2004). Also the non-proteinogenic amino acid GABA (4-amino-butric acid) accumulated in leaves of *sir1-1*. The other amino acids were reduced in *sir1-1*. No statement can be made for histidine, arginine and leucine that were not detected. Less sugars and alcohols were affected than in soil-grown plants. Interestingly, neither glucose nor fructose were altered. Organic acids were disrupted indicating deregulation TCA cycle.



In order to induce sulfur deficiency, plants were transported from +S medium to S-deficient medium for 6 h and then harvested. Metabolites were extracted and determined. Under -S conditions, 28 of 59 detected metabolites were significantly changed in leaves of *sir1-1* when they were compared to wild-type (Fig. 17). Amino acid levels were changed. Valine and tryptophan were elevated 1.6- and 2.4-fold, respectively. Proline and glycine were each reduced 70%. Organic acid levels were also changed. Citric acid was increased by 5-fold in *sir1-1* leaves, 2-methyl malic acid 3.4-fold and glyconic acid 1.8-fold. Glyconic acid is an intermediate of the glycine and the serine pathway, which is believed to be the primary substrate of photorespiration (Zelitch, 1973) and reduces the net rate of photosynthesis by photorespiration (Tolbert and Ryan, 1976). Sugars and alcohol levels were also changed: Fructose, glucose and sorbose were reduced by 60%, and trehalose by 70%. Raffinose and galactinol were strongly elevated, 3.8- and 6.3-fold, respectively. Arginine can be

processed via arginase to form urea and ornithine. The latter one was reduced by 30% and urea was increased 1.7-fold.

Microarray data revealed that a putative arginase (At4g08870) was more than 2-fold expressed in *sir1-1*; however, the data are from plants under normal conditions.



After discovering the responses of *sir1-1* in comparison to wild-type under normal and -S conditions, it was of interest to investigate the metabolite ratios for wild-type as well as for *sir1-1* plants when they were transferred

from +S to -S. Many amino acids were up-regulated and none down-regulated in leaves when wild-type plants were subjected to external S deficiency; the same sulfur availability changes also caused an increase of this metabolite group in *sir1-1* leaves, however only in 5 amino acids (Fig. 18). Also among sugars and alcohols there were members which were changed in -S, including glucose (0.2-fold of +S) or glycerol (1.5-fold of +S). In *sir1-1* none of them showed any change in +S:-S ratio. Changes of organic acids were not uniform. In both groups, some were changed, however never the same metabolites.

The +S:-S responses of wild-type and *sir1-1* were compared with each other to figure out if the measured metabolites showed the same response to sulfur deficiency or not. Significantly different responses were marked with asterisks as indicated in 2.10. 15 of 23 (65.2%) changed metabolites showed different +S:-S responses when wild-type and *sir1-1* were compared. Principal Component Analysis (PCA) was performed to detect the differences between data sets of wild-type and *sir1-1* metabolites under +S and -S (Fig. 19). PCA revealed that metabolite data sets from wild-type plants (+S and -S) clustered more closely to each other. The same was the case for *sir1-1* metabolite data sets when +S and -S were scored (Fig. 19A and B), meaning that in comparing wild-type and *sir1-1* plants, leaf metabolome correlates rather endogenously after 6 h of sulfur deficiency than with change of environmental conditions.

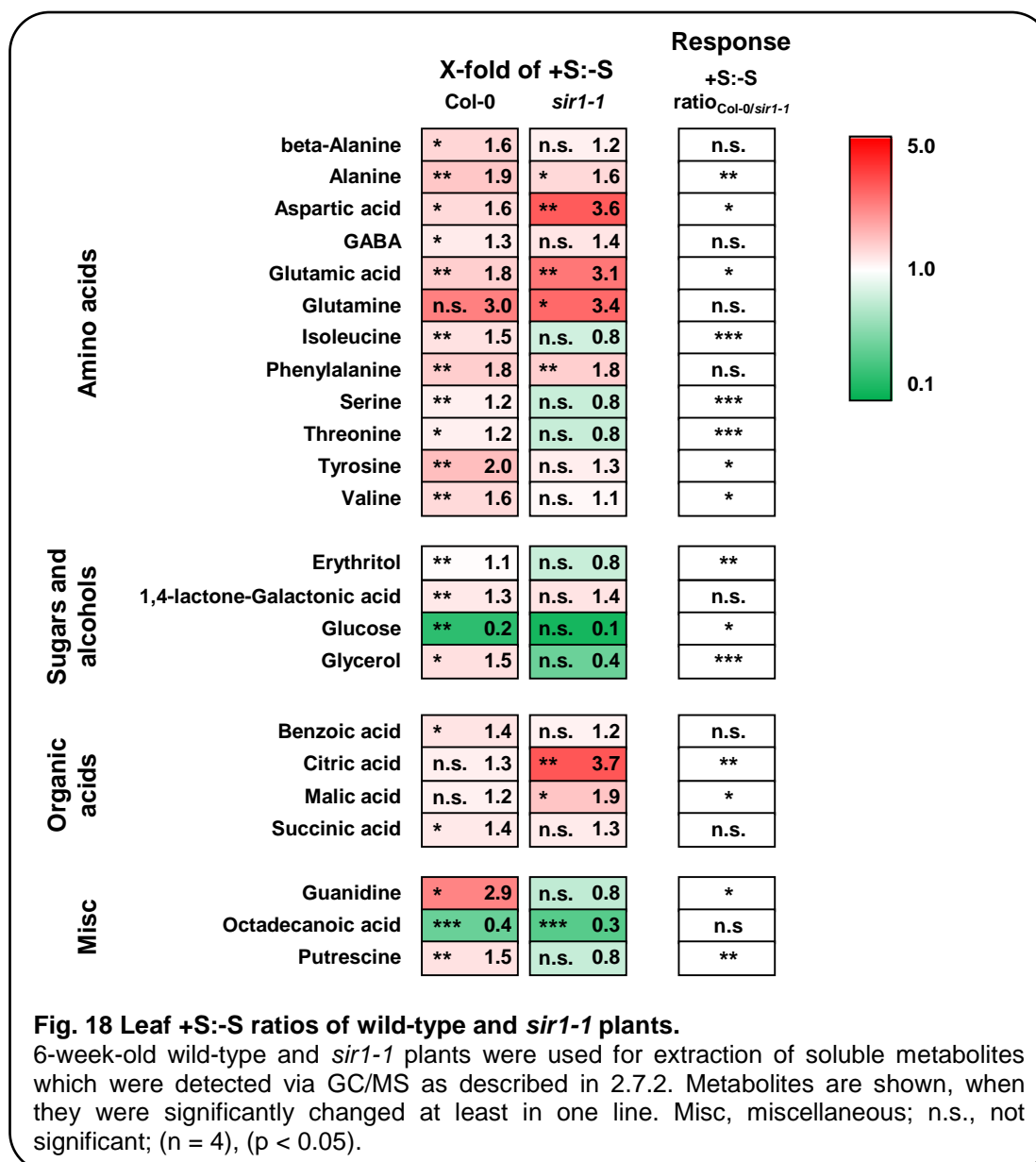
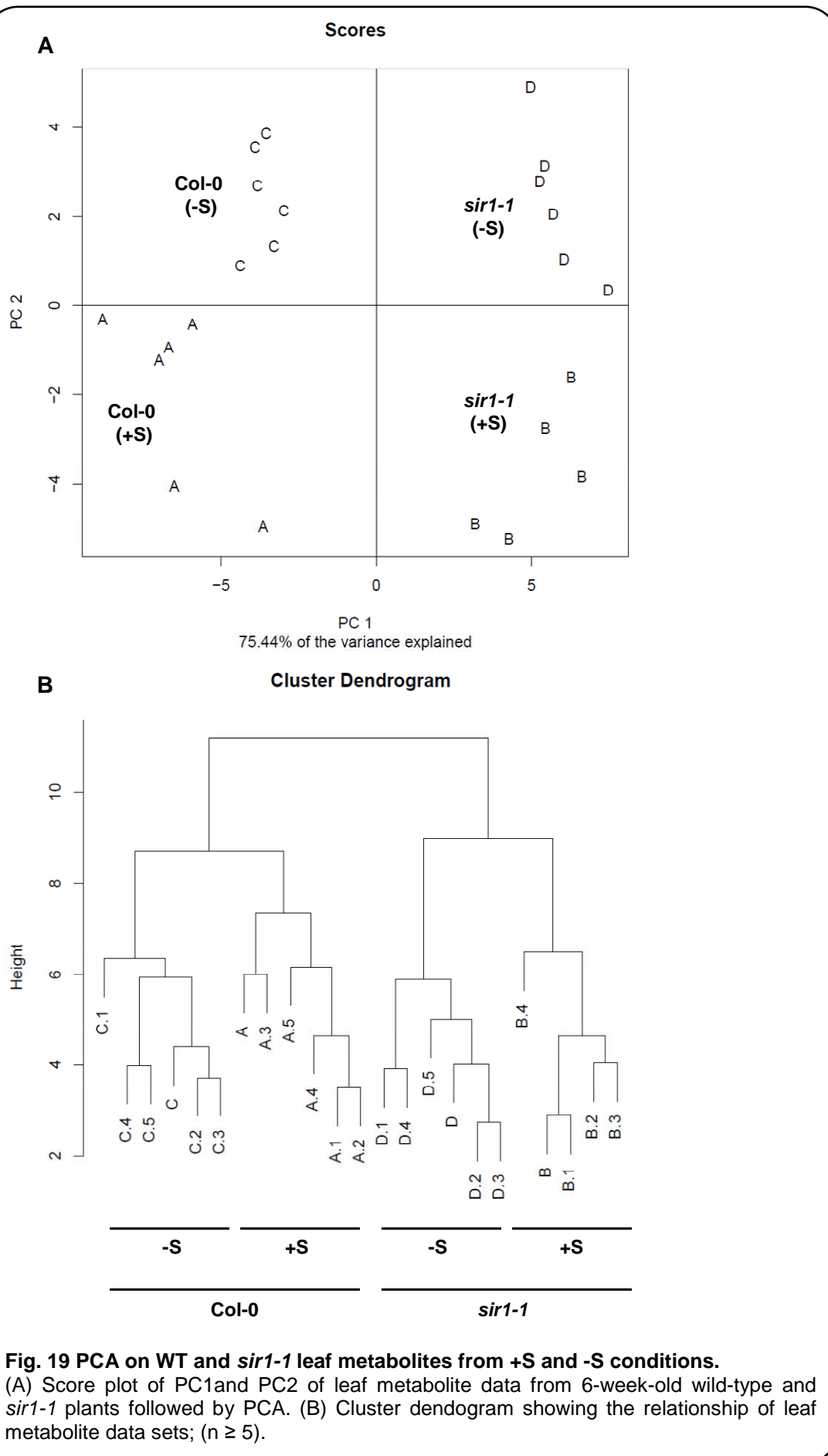


Fig. 18 Leaf +S:-S ratios of wild-type and *sir1-1* plants.

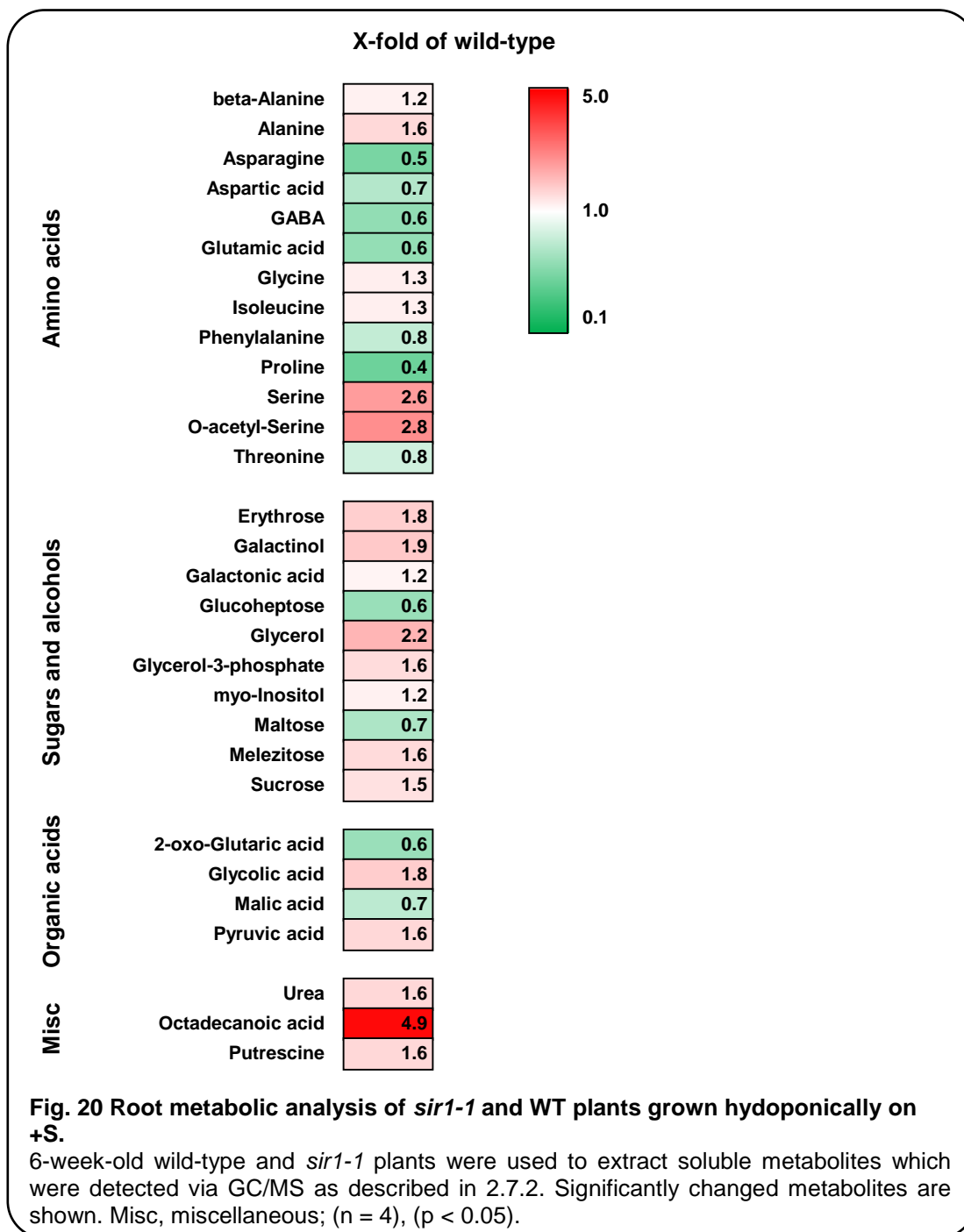
6-week-old wild-type and *sir1-1* plants were used for extraction of soluble metabolites which were detected via GC/MS as described in 2.7.2. Metabolites are shown, when they were significantly changed at least in one line. Misc, miscellaneous; n.s., not significant; (n = 4), (p < 0.05).

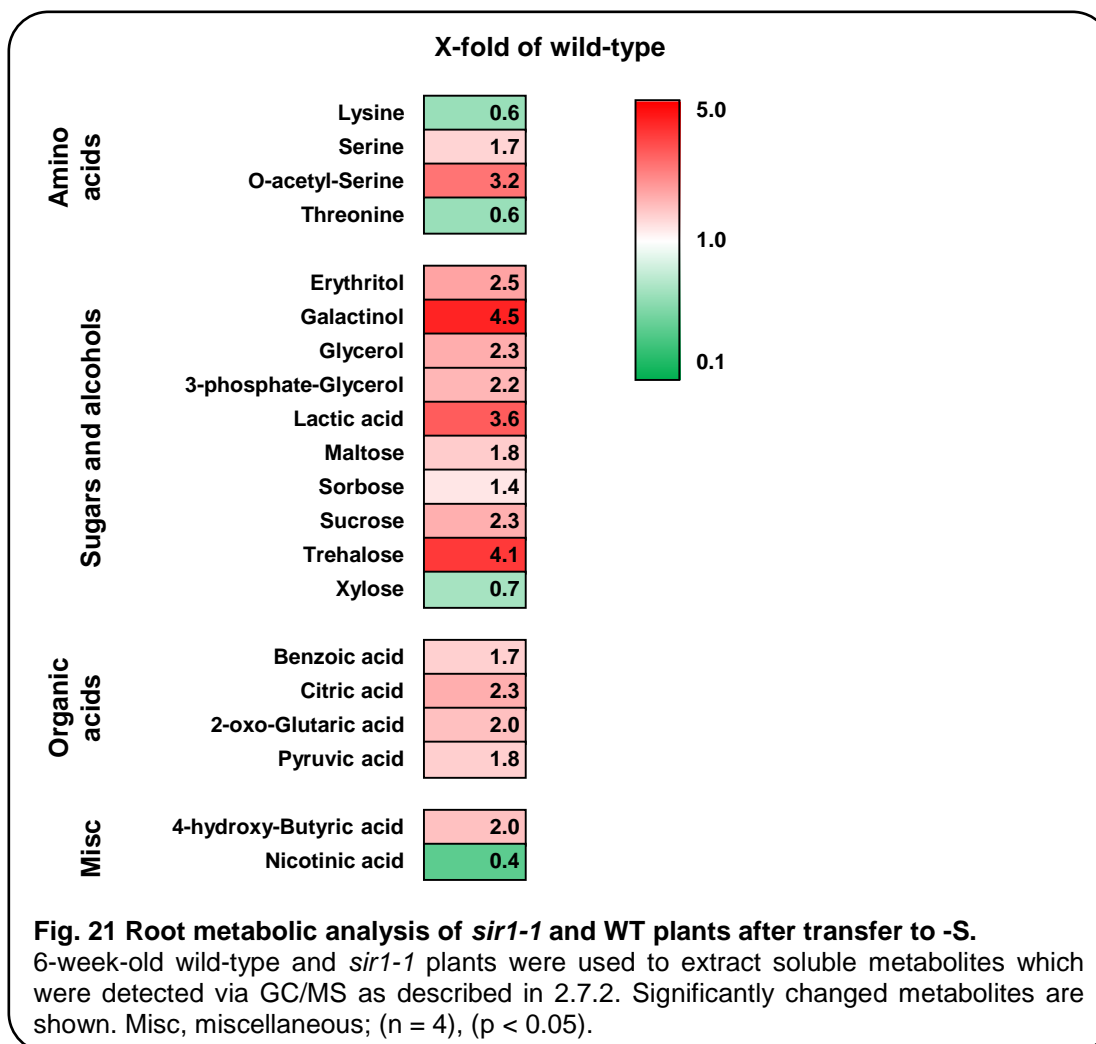


3.2.7.2 Effects of sulfur availability on metabolites in roots

In order to measure the metabolome response in roots of wild-type and *sir1-1* plants, root metabolic profiling was performed according to 3.2.7.1. The root material was taken from the same plants which were used for leaf metabolite extraction and detection. When comparing wild-type and *sir1-1* grown constantly on +S media, 30 of 56 measured metabolites from roots were significantly changed (Fig. 20). Proteinogenic amino acids glycine (1.3-fold), isoleucine (1.3-fold), alanine (1.6-fold) and serine (2.6-fold) were elevated in *sir1-1* roots and proline (0.4-fold), asparagine (0.5-fold) and glutamic acid (0.6-fold) were reduced. OAS, a cysteine precursor was also elevated (2.6-fold). Several sugars and alcohols were accumulated, including glycerol (2.2-fold), galactinol (1.9-fold) and erythrose (1.8-fold). Maltose (0.7-fold) and glucoheptose (0.6-fold) were decreased. Organic acids showed perturbation. Like in leaves, urea and putrescine were accumulated indicating protein and amino acid breakdown in the roots of *sir1-1*.

The *sir1-1* root metabolome was compared to that of the wild-type after 6 h of sulfur withdrawal to investigate the root response. 20 of 55 evaluated metabolites were significantly changed. Serine and OAS were accumulated in the mutant when it was subjected to -S (Fig. 21). All sugars and alcohols were up-regulated, except for xylose. Also, all changed organic acids were elevated in *sir1-1* roots when they were compared to the wild-type.





As had been done for leaf metabolites (3.2.7.1), +S:-S responses of wild-type and *sir1-1* for root metabolites were compared (Fig. 22): 13 of 37 (35.1%) changed metabolites showed different +S:-S responses when wild-type and *sir1-1* were compared. Principal Component Analysis (PCA) was performed to investigate the differences between data sets of wild-type and *sir1-1* metabolites under +S and -S (Fig. 23). PCA revealed that metabolite data sets from +S (wild-type and *sir1-1*) clustered more closely to each other and the same was true for -S metabolite data sets when wild-type and *sir1-1* were scored (Fig. 23A). Results shown in dendrogram supported this observation (Fig. 23B), meaning that when comparing wild-type and *sir1-1*, root metabolomes correlate with rather changed exogenous sulfur supply than genetic or metabolic guidelines. This is probably because roots are directly confronted with sulfur stress and have fewer options to adjust, hence, similar responses follow in wild-type and mutant plants.

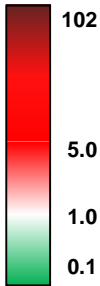
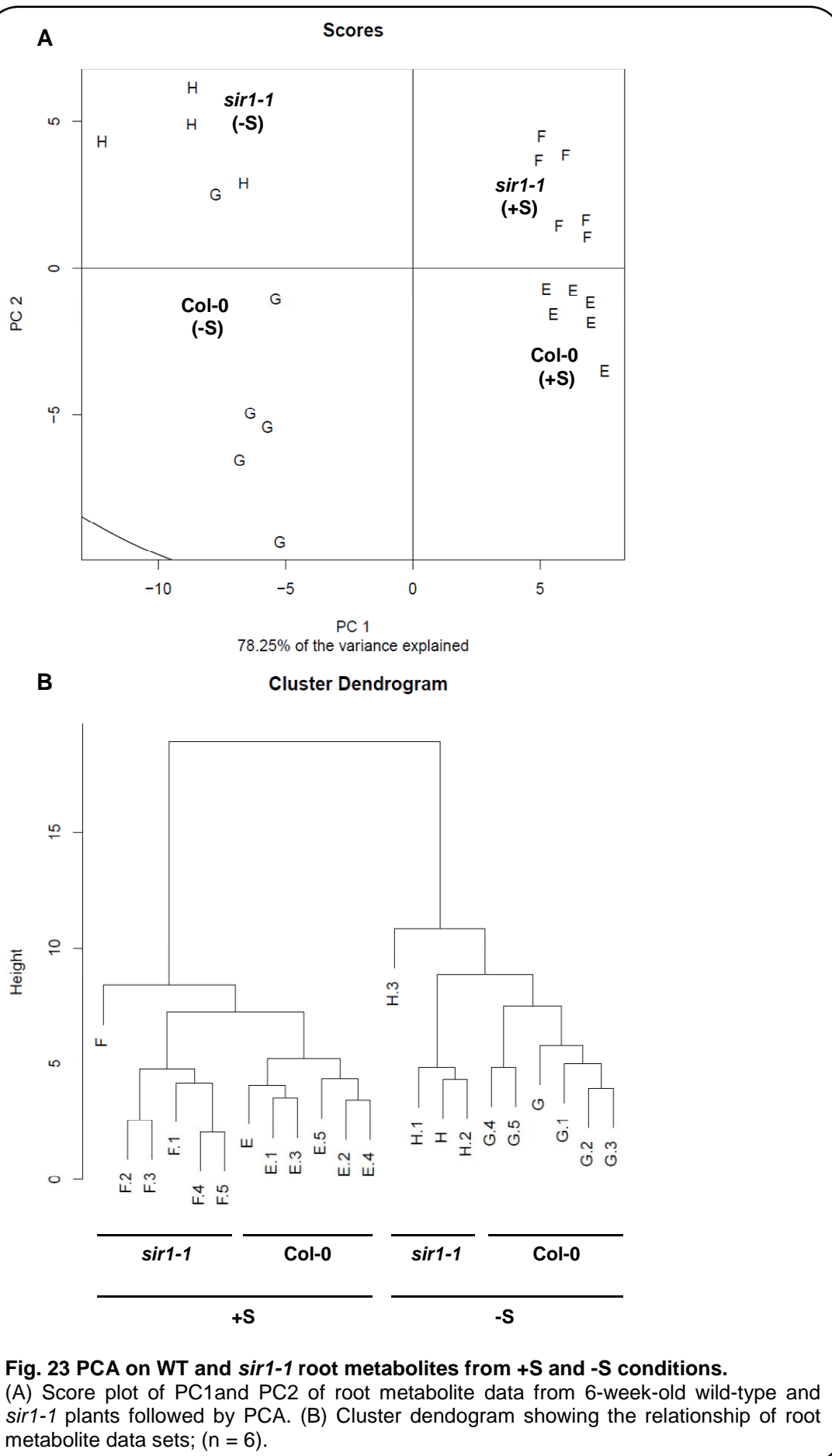
	X-fold of +S:-S		Response +S:-S ratio _{Col-0/sir1-1}	
	Col-0	<i>sir1-1</i>		
Amino acids	beta-Alanine	** 3.2	* 2.0	n.s.
	Alanine	* 3.3	n.s. 1.5	*
	Asparagine	** 5.0	*** 8.8	*
	Aspartic acid	*** 3.2	* 3.5	n.s.
	GABA	*** 2.2	** 3.1	n.s.
	Glutamic acid	*** 3.1	*** 7.0	**
	Glutamine	*** 70.4	*** 66.4	n.s.
	Glycine	* 3.1	n.s. 4.2	n.s.
	Isoleucine	*** 2.6	* 1.7	*
	Phenylalanine	*** 3.6	*** 3.8	n.s.
	Serine	*** 2.9	* 1.9	*
	O-acetyl-Serine	*** 4.0	*** 4.6	n.s.
	Threonine	*** 3.0	** 2.3	n.s.
	Tyrosine	*** 4.4	** 4.0	n.s.
Sugars and alcohols	Fructose	** 1.8	n.s. 1.4	n.s.
	Fructose-6-phosphate	** 2.8	*** 3.6	n.s.
	Galactinol	n.s. 1.3	** 3.2	*
	Glucose	** 4.2	*** 5.4	n.s.
	Glucose-6-phosphate	** 6.4	*** 8.6	n.s.
	Glycerol	*** 2.8	*** 3.0	n.s.
	Glycerol-3-phosphate	*** 2.3	** 3.1	n.s.
	myo-Inositol	*** 2.3	n.s. 1.7	n.s.
	Maltose	n.s. 2.0	*** 5.4	**
	Melezitose	* 2.8	n.s. 0.8	*
	Sucrose	n.s. 1.3	* 1.9	n.s.
	Trehalose	n.s. 31.1	*** 101.6	*
	Organic acids	Citric acid	n.s. 1.2	** 2.5
Fumaric acid		* 1.9	** 2.3	n.s.
2-oxo-Glutaric acid		*** 3.7	*** 12.1	**
Glyceric acid		** 2.5	n.s. 1.5	n.s.
Malic acid		*** 2.4	* 6.4	*
Pyruvic acid		* 2.9	* 3.2	n.s.
Succinic acid		*** 2.7	** 6.5	*
Misc	Nicotinic acid	*** 6.2	*** 5.5	n.s.
	Phosphoric acid	** 1.9	* 2.8	n.s.
	Putrescine	*** 3.8	* 4.1	n.s.
	Uracil	** 2.7	n.s. 2.6	n.s.

Fig. 22 Root +S:-S ratios of wild-type and *sir1-1* plants.

6-week-old wild-type and *sir1-1* plants were used for extraction of soluble metabolites which were detected via GC/MS as described in 2.7.2. Metabolites are shown, when they were at least in one line significantly changed. Misc, miscellaneous; n.s., not significant; (n = 4), (p < 0.05).



3.3 Whole transcriptome analysis of *sir1-1*

Sulfur metabolism is highly inter-connected to both carbon and nitrogen metabolism (Hesse et al., 2003; Wang et al., 2003; Kopriva and Rennenberg, 2004; Kopriva, 2006). Down-regulation of *SiR* as a key gene of the sulfur assimilation pathway caused a bottleneck effect in *sir1-1* and affected expression of several genes involved in the assimilatory sulfate reduction pathway (Khan et al., 2010). The whole transcriptome was analyzed by microarray assuming a down-regulation of *SiR* could also have an effect on the regulation of genes from other pathways.

Transcriptome analysis was performed using the Affymetrix array (2.9.4.1) in cooperation with Dr. Li Li and Maria Saile (ZMF, Mannheim). Total RNA was extracted (2.9.1) from leaves of soil-grown 7-week-old wild-type and *sir1-1* plants. As an additional group for wild-type-like developmental stage, 10-week-old *sir1-1* plants were used according to the similar rosette diameter and leaf number (Fig. 5B and C). For each group, three plants were applied. For each sample, 250 ng RNA was reverse-transcribed, biotinylated and labeled as aRNA (2.9.4.1). After purification, 15 µg of labeled aRNA was fragmented for 35 min. at 94 °C and then hybridized onto the arrays (2.9.4.1).

22,746 genes were assessed by the array. Only significantly ($p < 0.05$) changed genes were respected with $1 < 2\log\text{-fold-change} > -1$.

3.3.1 Impact of *SiR* mutation on gene expression in wild-type and *sir1-1* plants of same age

399 genes (136 genes up-, 263 genes down-regulated) were altered in 7-week-old *sir1-1* compared with wild-type plants of the same age (Fig. 24 and Suppl. data 8). Almost all major pathways were affected (Fig. 25). The most important gene groups with a high number of changed members are listed: signaling (43), protein (40), stress (35), RNA (34), development (22), hormone metabolism (20), secondary metabolism (10), nucleotide metabolism (10), cell (9), redox (8), lipid metabolism (4) and DNA (3). Several genes could not be categorized and were summed up in not assigned (75) and miscellaneous (44). In S-assimilation, 5 genes were

altered and all were down-regulated in *sir1-1*: *APS4* (-1.7-2log-fold), *APR3* (-2.1), *APR1* (-1.2), *APR2* (-1.7) and *SiR* (-1.3).

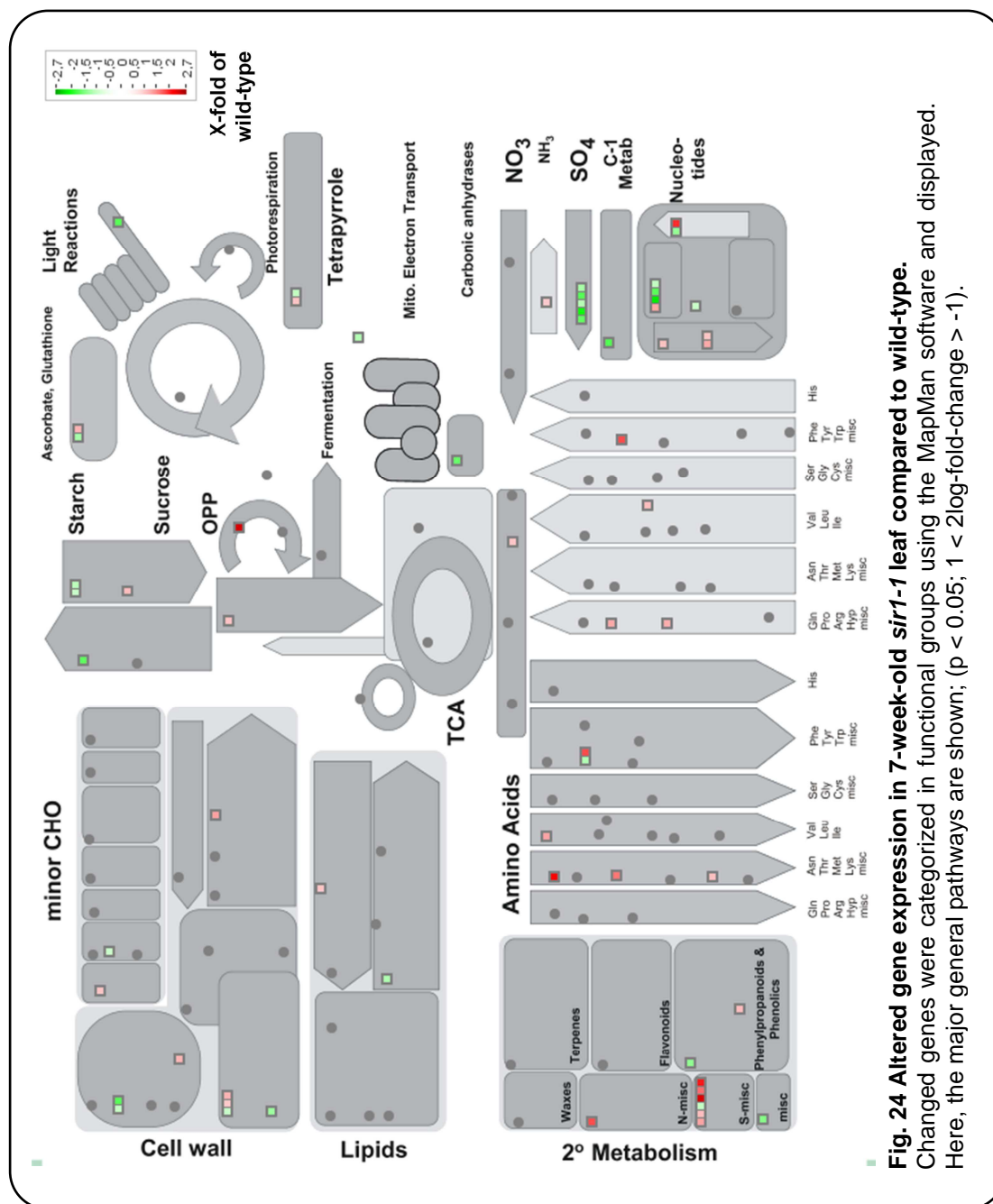
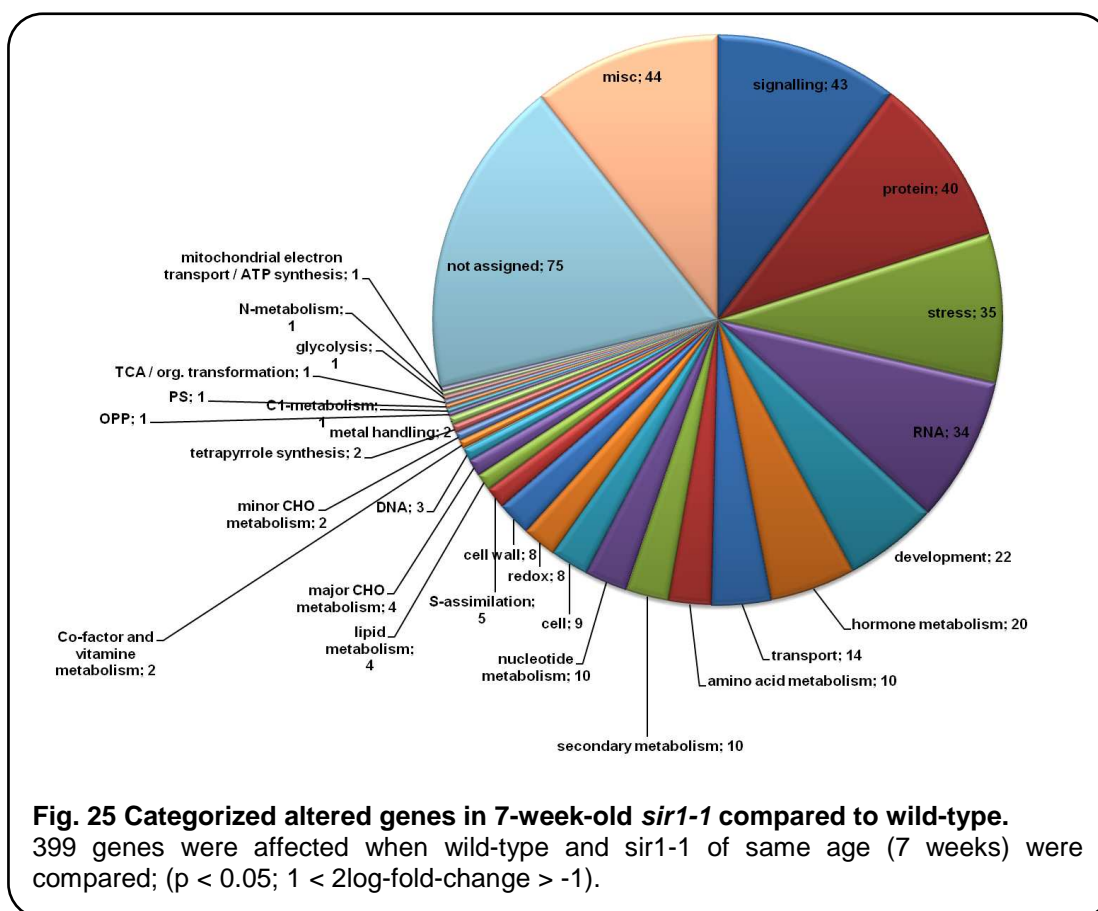


Fig. 24 Altered gene expression in 7-week-old *sir1-1* leaf compared to wild-type. Changed genes were categorized in functional groups using the MapMan software and displayed. Here, the major general pathways are shown; ($p < 0.05$; $1 < 2\log\text{-fold-change} > -1$).



3.3.2 Impact of *SiR* mutation on gene expression in wild-type and *sir1-1* of same developmental stage

To investigate if the observed changes in small *sir1-1* plants were due to the growth retardation or *SiR* dysfunction transcriptome of 10-week-old *sir1-1* mutants of wild-type size were compared to that of 7-week-old wild-type plants. 721 genes were changed (296 up- and 425 down-regulated) in 10-week-old *sir1-1* mutants compared to 7-week-old wild-type (Fig. 26 and Suppl. data 9). Like the comparison of wild-type and *sir1-1* of the same age, almost all major pathways were affected in mutant (Fig. 27): protein (70), RNA (63), transport, (54) secondary metabolism (43), stress (36) cell wall (35), redox (24), development (24), lipid metabolism (23), hormone metabolism (23), amino acid metabolism (18), signaling (17), N-metabolism (7), DNA (7), TCA / org. transformation (6), and a high number of other genes, most arranged in not assigned (141) and

miscellaneous (73). In S-assimilation 2 genes were changed: *APK4* (1.5) and *SiR* (-1.3).

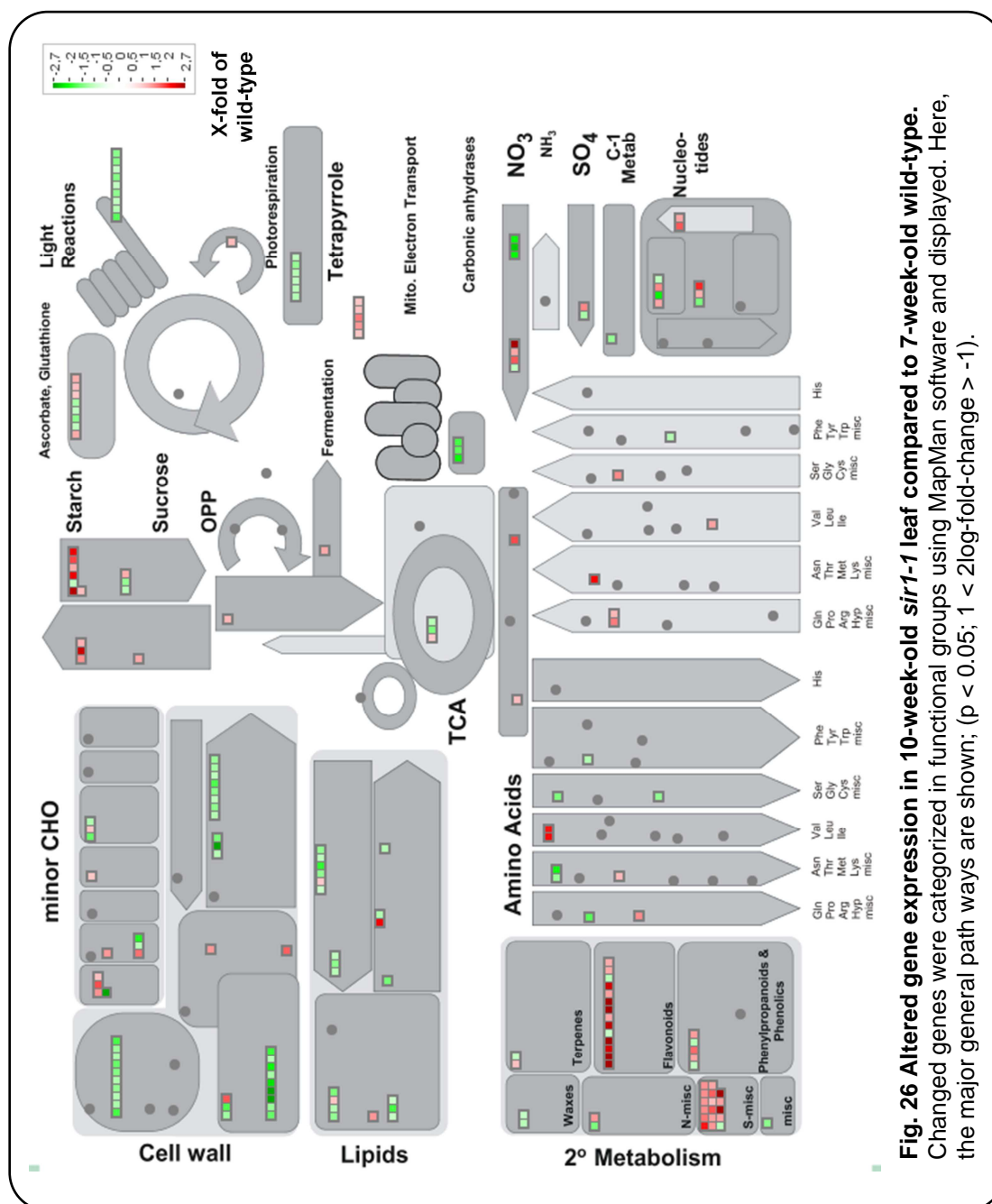
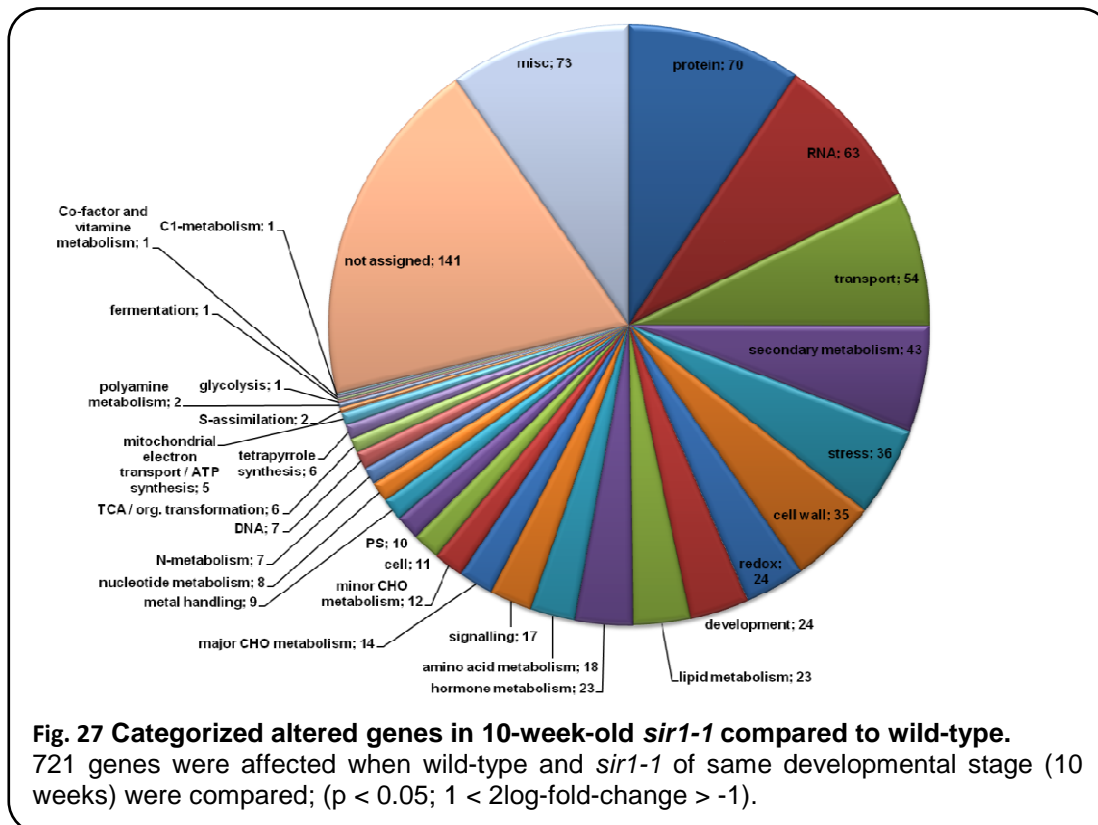


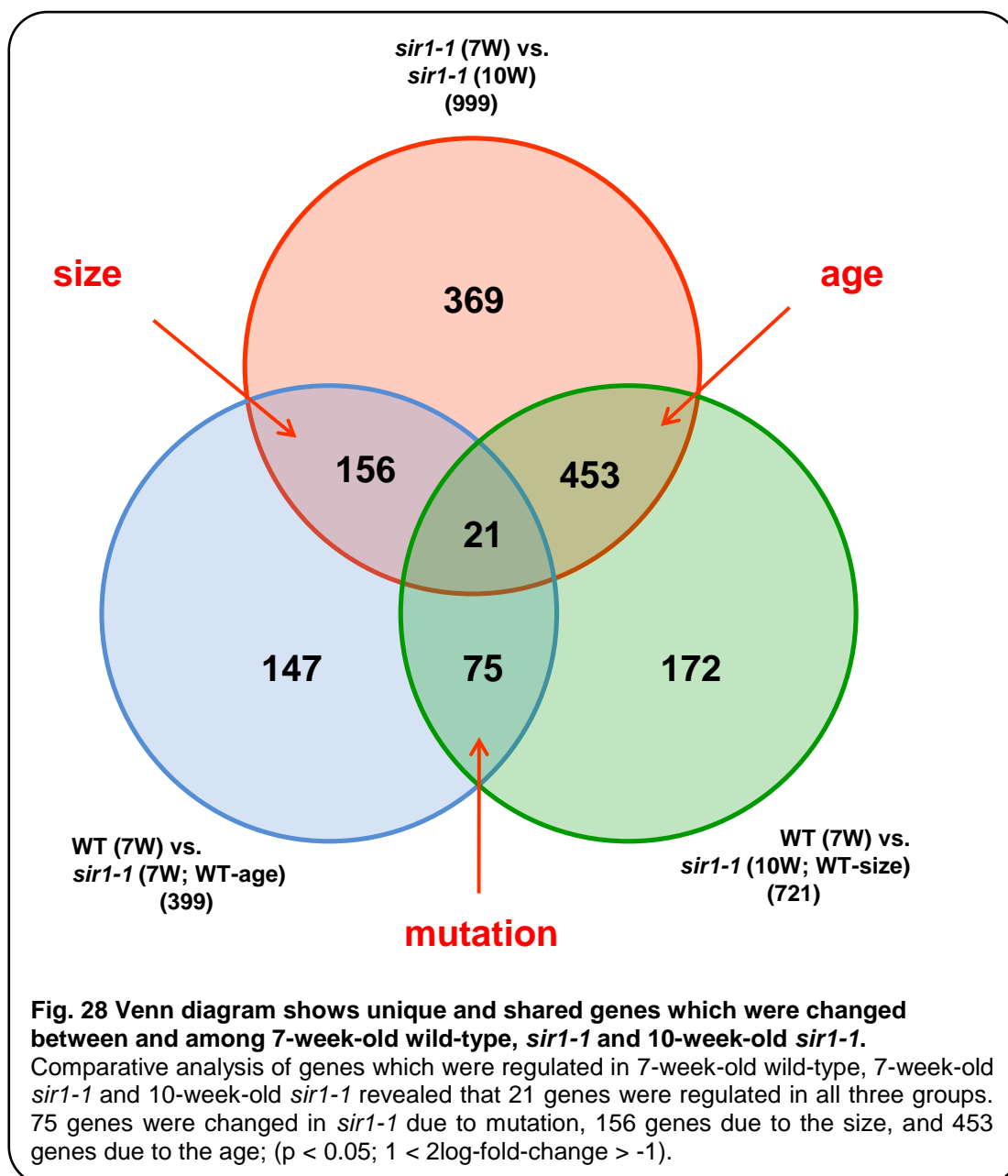
Fig. 26 Altered gene expression in 10-week-old *sir1-1* leaf compared to 7-week-old wild-type. Changed genes were categorized in functional groups using MapMan software and displayed. Here, the major general path ways are shown; ($p < 0.05$; $1 < 2\log\text{-fold-change} > -1$).



3.3.3 Comparative transcriptomic analysis between wild-type and *sir1-1* of wild-type-age and wild-type-development

Interestingly, comparing 7-week-old and wild-type-size *sir1-1* mutants (10 weeks) revealed the highest number of changed genes, namely 999. This indicates that more changes occur at the transcriptional level during *sir1-1* development than between *sir1-1* and wild-type plants. *SiR* expression was unchanged between small and big *sir1-1* plants, meaning that *SiR* down-regulation is constant during the mutant development between weeks 7 and 10. Transcriptomic analysis of wild-type versus *sir1-1* of the same age (3.3.1) revealed several affected genes. Those changes could derive from effects of *SiR* mutation and/or growth retardation, hence developmental differences between the two groups. Similar considerations had to be taken when wild-type and *sir1-1* of the same developmental stage (3.3.2) were compared. This comparison implied effects of *SiR* mutation and/or age, since *sir1-1* was of same size, but older than wild-type. A Venn diagram was assembled (Fig. 28) to investigate which genes are regulated due to mutation. Comparison of the changed gene between three groups revealed 75 genes unique to the mutation (Suppl. data 10). There were 156

changed genes unique to size, whereas there were 453 genes unique to age. Additionally, there were 21 genes that were shared among all three comparison groups (Suppl. data 11), indicating that external factors must be responsible for the expression of these genes and that all screened plants must be exposed to those factors. These factors could result from growth conditions, e.g.



Among 75 mutation-specific genes, most (11) were related to RNA, DNA and nucleotide metabolism, while some belonged to amino acid and protein metabolism (9), stress (9), development and hormone metabolism (6). Several other gene categories showed fewer numbers of affected members like secondary metabolism (4), transport (3) or signaling (2).

This strategy of identifying individual genes that were differentially regulated in mutant and wild-type plants can not detect metabolic pathways that are distributed among entire gene networks and are subtly regulated at the level of individual genes. Analysis of single genes, even if they are carefully arranged in metabolic categories, may miss important effects on pathways. Also, there are several statistically significant genes without any unifying biological theme. A high number of genes from one category does not necessarily result in up- or down-regulation of a related pathway, since the size of this certain category and its relation to connected pathways are not respected. To overcome these barriers, micro array data were submitted to a gene set enrichment analysis (GSEA) as described in Subramanian et al. (2005) and 2.8.4.2: Arrays were annotated using an Entrez Gene-based costum CDF file from Brainarray (2.1.7). The significantly affected gene sets that are constantly changed in *sir1-1* compared to wild-type are all related to DNA processing and repair (Tab. 1).

Tab. 1 Affected gene sets due to *Sir* mutation are linked to DNA repair and stress. GSEA for comparison of *sir1-1* (7- or 10-week-old) to wild-type revealed changes in pathway related to DNA metabolism and stress. Only gene sets were taken into consideration if they had an NES of same tendency (positive or negative for both comparisons). NES, normalized enrichment score; NP, normalized p-value, FDR, false discovery rate; (NP < 0.0.5; FDR < 0.75).

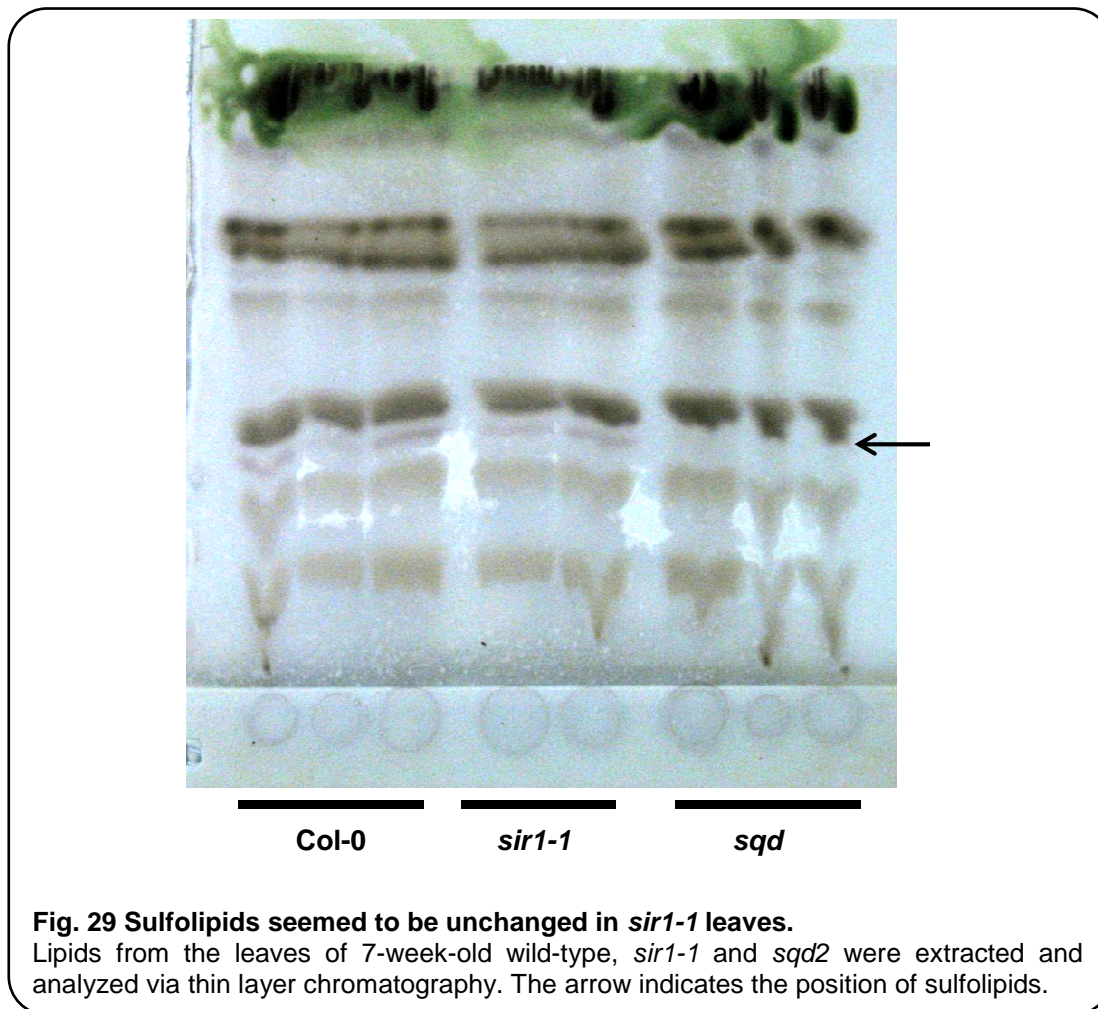
Gene set	<i>sir1-1</i> (10W) vs WT			<i>sir1-1</i> (7W) vs WT		
	NES	NP	FDR	NES	NP	FDR
Nucleobase, nucleoside, nucleotide and nucleic acid metabolic process	1.479	0.018	0.741	1.523	0.010	0.440
DNA metabolic process	1.709	0.012	0.090	1.620	0.004	0.402
DNA repair	1.865	0.002	0.021	1.495	0.040	0.497
Response to endogenous stimulus	1.865	0.002	0.041	1.520	0.037	0.423
Response to DNA damage stimulus	1.839	0.000	0.016	1.500	0.038	0.504

For each gene set, the genes contributing to core enrichment were listed in Suppl. data 12 - 16. As expected, the genes were all involved in pathways directed to nucleobase, nucleoside and nucleic acid metabolic process

(Suppl. data 12), DNA metabolic process (Suppl. data 13), DNA repair (Suppl. data 14), response to endogenous stimulus (Suppl. data 15) and response to DNA damage stimulus (Suppl. data 16).

3.3.4 Affected genes related to sulfolipids and jasmonic acid

Close investigation of the microarray data showed that both *SQD* (sulfoquinovose synthase) genes were significantly down-regulated in *sir1-1* compared to wild-type, *SQD1* (-0.49 2-log-fold) and *SQD2* (-0.22 2-log-fold). These genes are involved in sulfolipid biosynthesis: *SQD1* transfers sulfite to UDP-glucose catalyzing UDP-sulfoquinovose production (Sanda et al., 2001) and *SQD2* catalyzes the transfer of sulfoquinovose from UDP-sulfoquinovose to diacylglycerol. Since sulfite is accumulated in *sir1-1* leaves (Khan et al., 2010) and surprisingly these genes are down-regulated, sulfolipids were determined from leaves of 7-week-old wild-type and *sir1-1* plants (2.7.10). Extracts from the *sqd2* mutant (Yu et al., 2002) were used as a negative control, since commercial standards were not accessible. While no sulfolipids were detected in *sqd2* mutant, there were clear signals in wild-type and *sir1-1* plants (Fig. 29). Sulfolipids seemed to be unchanged in *sir1-1* compared to wild-type, probably to maintain the necessary composition of their photosynthetic plastidic membranes.



MYB76 (0.61 2-log-fold), and *MYB4* (-0.15 2-log-fold) were changed in *sir1-1*. Yanhui et al. (2006) reported that these transcription factors respond to jasmonic acid stimulation. Also altered *SQE3* (-0.84 2-log-fold) was reported to respond to jasmonic acid related molecules (Devoto et al., 2005), also *CEJ1* (-0.51 2-log-fold) (Nakano et al., 2006), *DWARF4* (-0.25 2-log-fold), *DHAR1* (1.19 2-log-fold) (Sasaki-Sekimoto et al., 2005), and *AGP31* (1.46 2-log-fold) (Liu and Mehdy, 2007). These observations raised our interest to find out if jasmonic acid levels were changed in *sir1-1* mutant. Furthermore, accumulated sulfite (Khan et al., 2010), and APS (Fig. 12E) indicated changes in PAPS level. PAPS can be converted from APS (Kopriva and Koprivova, 2004) and can be used for sulfonation of 12-hydroxyjasmonate into 12-hydroxyjasmonate sulfate, whereby PAP is formed (Gidda et al., 2003). Interestingly, PAP accumulated in *sir1-1* leaves (Fig. 12G). However, we were not able to measure PAPS. To investigate whether jasmonate, 12-hydroxyjasmonate and

hydroxyjasmonate sulfate levels were changed, metabolites were extracted from leaves of 7-week-old wild-type, 7-week-old *sir1-1* and 10-week-old *sir1-1* plants and quantified (2.7.5). The measurement revealed that 12-hydroxyjasmonate was accumulated in 7-week-old *sir1-1* plants and showed wild-type-like levels after reaching wild-type size (Fig. 30). Unfortunately, we could not measure hydroxyjasmonate sulfate.

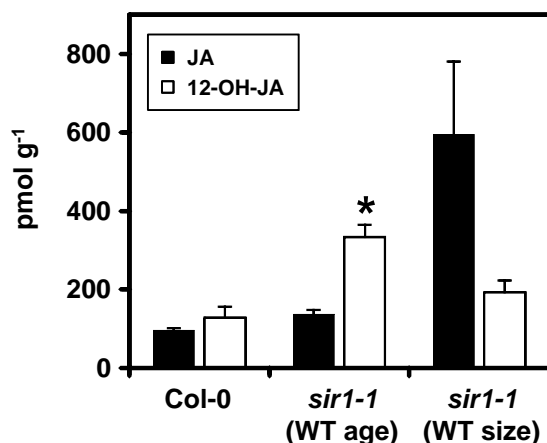


Fig. 30 Jasmonic acid and 12-hydroxyjasmonic acid in leaves of wild-type and *sir1-1* plants.

Metabolites were extracted from leaves of 7-week-old wild-type, 7-week-old *sir1-1* and 10-week-old *sir1-1*. 12-hydroxyjasmonate showed a higher level in 7-week-old *sir1-1* compared to wild-type. JA, jasmonate; 12-OH-JA, 12-hydroxyjasmonate; (n = 3), (means ± SEM). [Metabolite determination was carried out by Dr. Bettina Hause, IPB, Halle.]

3.4 Analysis of generative tissue in *sir1-1*

Having gained insight into the *sir1-1* transcriptome and metabolome in vegetative tissues, we were interested in the generative tissue. Although *sir1-1* is smaller than the wild-type, it can reach wild-type size (Fig. 5) with delayed growth, flower and set viable seeds, albeit with a lower germination rate (Fig. 6 and Fig. 7). Since *sir1-1* plants accumulate sulfate and show a reduced sulfur flux through sulfur assimilation, we decided to investigate if these regulations in vegetative tissues of *sir1-1* plants affect the generative tissues and if the seeds are able to reduce sulfate albeit *SiR* mutation.

3.4.1 Impact of *SiR* mutation on bolting time

To investigate the time *sir1-1* needs to start bolting, *sir1-1* and wild-type plants were grown under short day conditions (2.2.3.1) for 7 weeks and subsequently transferred to long day conditions to induce budding. While wild-type plants bolted after 35 days, for *sir1-1* it took 14 days longer (Fig. 31A). To allow *sir1-1* longer vegetative growth and an increase of rosette size and mass, plants were grown for 11 weeks in short day chambers till *sir1-1* had reached the size of wild-type plants. Afterwards, the plants were transported into long day condition. After 2 days, all wild-type plants had bolted. After reaching the wild-type size in week 11, *sir1-1* also reduced the bolting time from approx. 50 days to 14 days, however *sir1-1* plants bolted much later than wild-type plants.

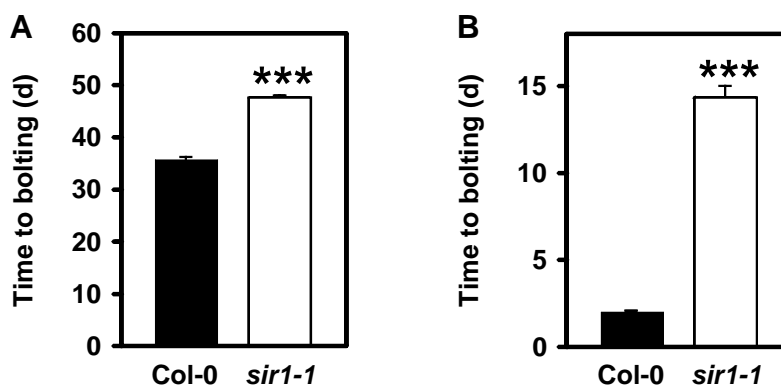


Fig. 31 *sir1-1* needs a longer period to start bolting.

(A) After 7 weeks of growth on soil under short day conditions, *sir1-1* and wild-type plants were transferred to long day condition growth chamber; (n ≥ 8). (B) After 11 weeks of growth under short day conditions, *sir1-1* and wild-type plants were transported to long day condition growth chamber; (n ≥ 6), (means ± SEM).

3.4.2 Silique characterization in *sir1-1* and wild-type plants

To investigate the reduced seed number in *sir1-1*, siliques were analyzed. Conditions for growth and seed production were as described in 3.4.2. First, siliques of *sir1-1* plants were counted and compared to the wild-type. *sir1-1* had around one third of wild-type siliques and this was also visibly detectable (Fig. 32A and C). The number of side shoots was wild-type-like (Fig. 32B).

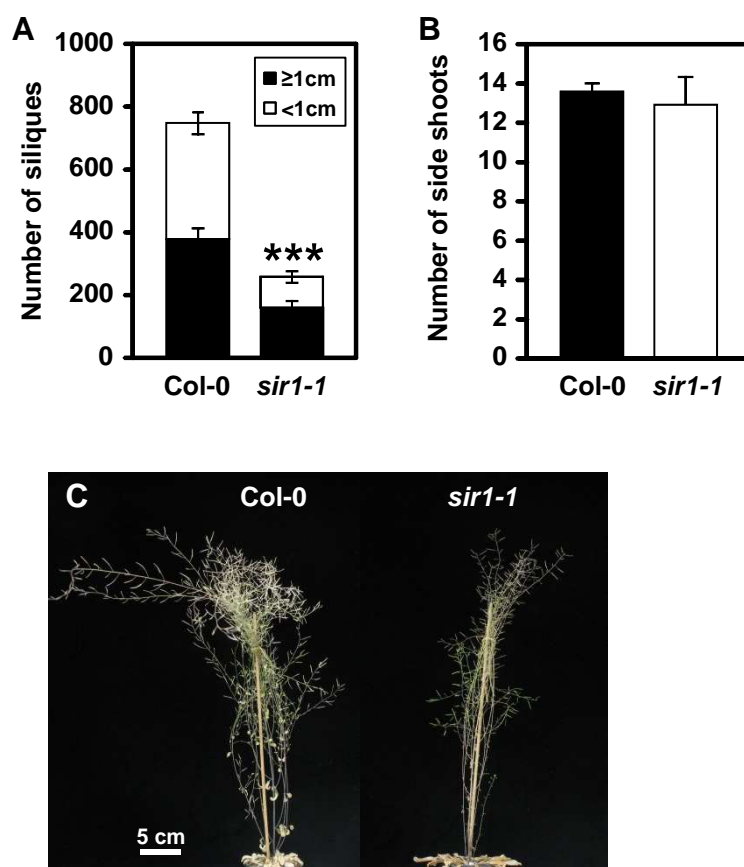


Fig. 32 *sir1-1* has less siliques than wild-type.

Plants were grown on soil under short day conditions for 6 to 7 weeks and then transferred to long day conditions for seed production. (A) Numbers of siliques (≥ 1 cm and < 1 cm) per wild-type and *sir1-1* plant were determined. (B) Side shoots number of wild-type and *sir1-1*. (C) Phenotype of seed-setting wild-type and *sir1-1* plants; ($n \geq 7$), (means \pm SEM).

One of the possible reasons for reduced seed yield could be the reduced silique size. Therefore, silique development was analyzed. Silique length of wild-type and *sir1-1* plants was measured 1, 5, 7, 10, 14 days after flowering (daf) and when seeds turned mature (approx. 21 daf). *sir1-1* was retarded in silique development until 14 daf, however at the end of silique development, it could reach the size of wild-type siliques (Fig. 33A). To uncover the number of seeds within siliques, they were opened and seeds were counted (2.6.1). *sir1-1* siliques contained less seeds than the wild-type (Fig. 33B). The reduced seed number in *sir1-1* siliques derived from an arrest of development in some seeds causing aborted seeds, which were randomly distributed along the silique (Fig. 33C and D).

Next, pollen viability of wild-type and *sir1-1* plants was investigated. To distinguish between aborted and viable pollen grains, four wild-type and *sir1-1* plants were used, which were stained according to Alexander (1969) and documented (2.6.1). For each plant, 100 pollen grains were counted and their viability was calculated in percentage. While around 90% of wild-type pollen was viable, only 25% of *sir1-1* pollen was viable (Fig. 34).

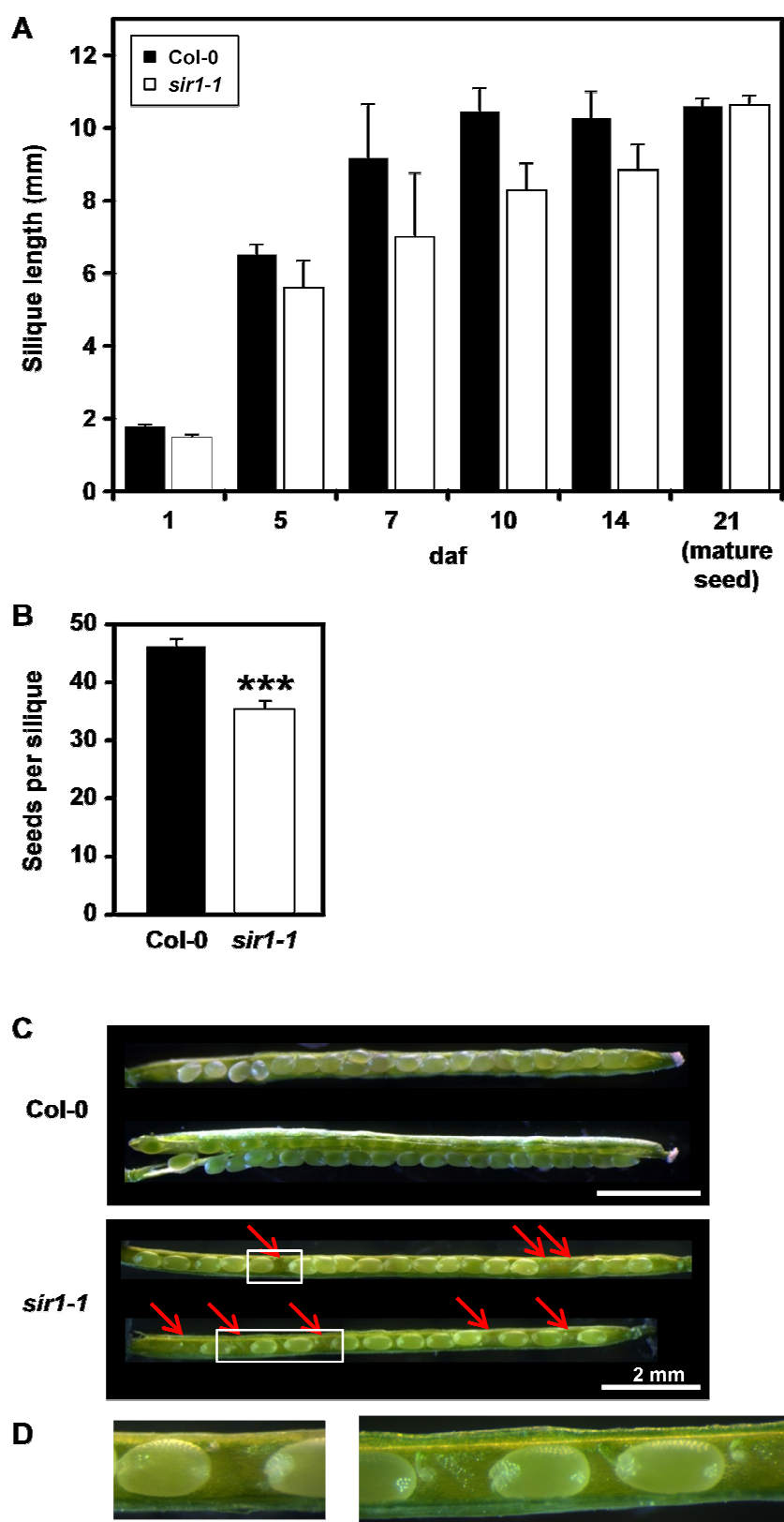


Fig. 33 *sir1-1* siliques contain less seeds than wild-type siliques.

Plants were grown on soil under short day conditions for 6 to 7 weeks and then transferred to long day conditions for seed production. (A) Length of wild-type and *sir1-1* siliques was determined on the annotated days after flowering (daf). (B) Number of wild-type and *sir1-1* seeds in siliques. (C) Phenotype of 14 daf siliques revealed developmental arrest in *sir1-1* seeds (red arrows). (D) Magnification of developmentally arrested *sir1-1* seeds; ($n \geq 3$), (means \pm SEM).

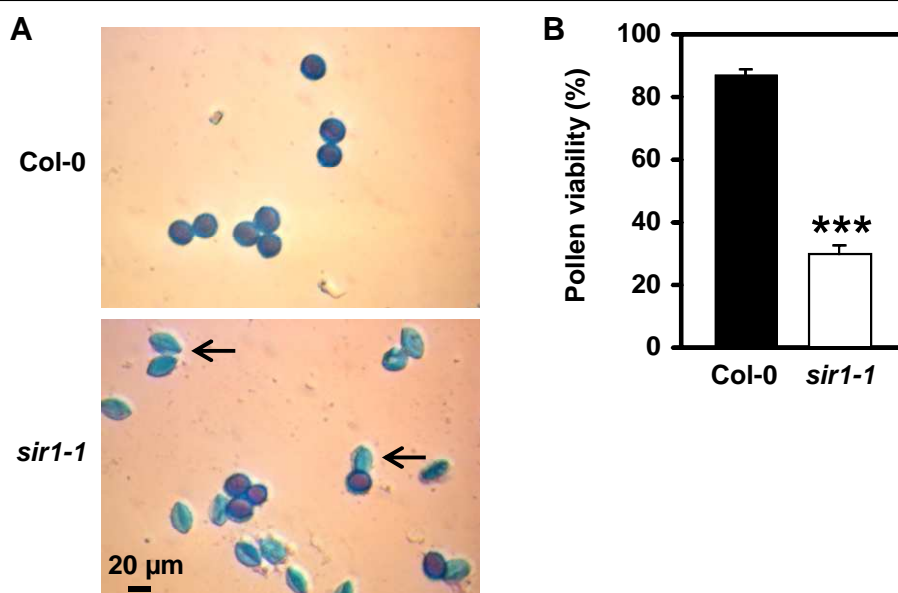


Fig. 34 *sir1-1* has more aborted pollen grains than the wild-type.

(A) Pollen grains were isolated from anthers after dehiscence and examined by differential staining of viable and aborted pollen grains. Arrows indicate aborted pollen grains that stained blue-green. Viable pollen grains are stained magenta-red. (B) 100 pollen grains were counted from each wild-type and *sir1-1* plant to investigate the pollen viability; (n = 4 plants), (means \pm SEM).

3.4.3 Impact of *SiR* mutation on seed yield

To characterize the seed yield of soil-grown wild-type and mutant plants, they were grown under short day conditions until week 6 to 7. Afterwards, the plants were transferred to long day conditions until seed maturation (2.2.3.1). Total seed yield was harvested and weighted. In average, a wild-type plant produced $230 \text{ mg} \pm 20$ seed, *sir1-1* $104 \text{ mg} \pm 17$ per plant (Fig. 35B). To allow *sir1-1* to set seeds at wild-type rosette size, plants were grown constantly under short day conditions and the seeds of short-day condition plants were analyzed. Both plant lines produced more seeds: While wild-type produced $395 \text{ mg} \pm 27$ seed per plants, *sir1-1* remained under that level and produced $163 \text{ mg} \pm 17$ seeds per plant (Fig. 35D), indicating that longer growth period under short day conditions increased seed yield. To assess whether weight of individual seeds was affected in *sir1-1*, a bulk of 100 seeds of wild-type and *sir1-1* was determined in triplicate. There were no changes in weight of 100 seeds between wild-type ($1.3 \text{ mg} \pm 0.05$) and *sir1-1* ($1.3 \text{ mg} \pm 0.04$; Fig. 35C). Knowing total seed weight of each plant and its 100-seed weight, it was possible to calculate

Results

the numbers of seeds for each plant. To demonstrate the distribution of seed yield, plants were grouped according to the number of seeds per individual plant from 1 to > 20,000 seeds in 5000-seeds groups. The number of plants in each category was presented in percentage. While most wild-type plants (46%) yielded 15,000 to 20,000 seeds and 23% produced more than 20,000 seeds, 45% of *sir1-1* plants produced 5000 to 10,000 seeds and 35% had less than 5000 seeds (Fig. 35A). To check if the balance between water content and storage compound was altered in *sir1-1* seeds, the dry weight of seeds was examined after two days at 80°C and compared to the fresh weight. There were no changes in dry weight between wild-type and *sir1-1* seeds (Fig. 35D).

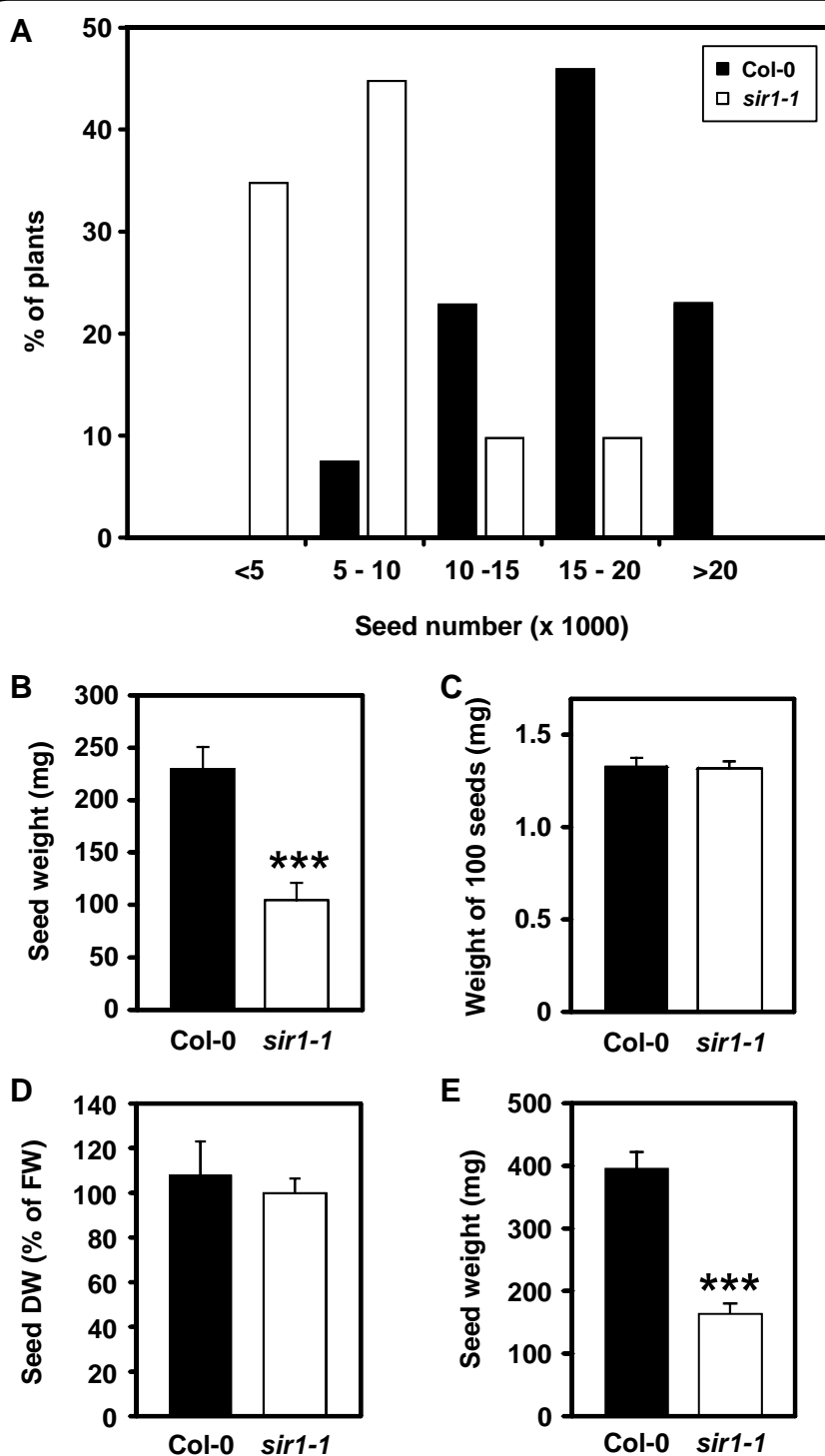


Fig. 35 *sir1-1* has lower seed yield with wild-type-like 100-seed-weight.

Plants were grown on soil under short day conditions for 6 to 7 weeks and then transferred to long day conditions. Only the results shown in (E) were from plants grown constantly under short day conditions. (A) Number of mature seeds per wild-type and *sir1-1* plant were counted and categorized; ($n \geq 13$). (B) Seed yield of wild-type and *sir1-1*; ($n \geq 13$). (C) 100-seed-weight of wild-type and *sir1-1*; ($n \geq 13$). (D) For wild-type and *sir1-1* seeds the dry weight was determined as percentage of fresh weight. ($n \geq 5$). (E) Seed yield of wild-type and *sir1-1* plants grown constantly in short day; ($n \geq 7$), (means \pm SEM).

3.4.4 Impact of sulfur availability on seed yield of *sir1-1* and wild-type plants

Wild-type and *sir1-1* plants were grown in hydroponic cultures under short day conditions until mature seeds were harvested. As a control group, plants were grown in hydroponic cultures containing 1/2 Hoagland with 500 μ M sulfate (+) and the sulfur-deprived plants were grown on 1/2 Hoagland with 5 μ M sulfate (-S) (2.2.3.2) to investigate the effects of sulfur withdrawal on seed quantity in *sir1-1* compared to wild-type. Wild-type plants with sufficient sulfur supply produced 155 mg \pm 45 seeds and with sulfur deficiency the yield was 113 mg \pm 31 of seeds per plant (Fig. 36B). However, the reduction of seed yield was not of statistical significance. *sir1-1* in +S hydroponic culture did not show significant differences (126 mg \pm 47) to wild-type grown under the same condition. Suffering from sulfur deficiency however, reduced the seed yield of *sir1-1* significantly to 19 mg \pm 3, indicating that *sir1-1* is dependent on sulfur availability for seed production, more than the wild-type. Weight of 100 seeds was determined to investigate if inefficient sulfur supply had an impact on seed weight of wild-type and *sir1-1*. 100 seeds of wild-type plants produced in hydroponic cultures weighted 1.98 mg \pm 0.04 and 1.84 mg \pm 0.03 on +S and -S, respectively (Fig. 36C). There was an increase of seed quantity compared to that of soil-grown plants (1.32 mg \pm 0.05). *sir1-1* also produced more heavy-weight seeds of 1.89 mg \pm 0.05 compared to soil-grown seeds (1.32 mg \pm 0.04). When sulfur availability was strongly reduced, in *sir1-1* the 100-seed weight was significantly lowered to 1.58 mg \pm 0.04, indicating that sulfur withdrawal affects seed weight and that these effect are more severe when *SiR* is mutated. Following the lines in 3.4.2, seed numbers were determined for each line and growth condition. 50% of wild-type plants grown on +S produced 10,000 to 15,000 seeds per plant, and 50% produced less than 5000 seeds (Fig. 36A). Under the same conditions, 43% of *sir1-1* plants produced 5000 - 10,000 seeds, 43% less than 5000 and interestingly 14% had more than 15,000 seeds. In hydroponic culture, seed weight of *sir1-1* elevates when compared with soil-grown *sir1-1* (Fig. 35).

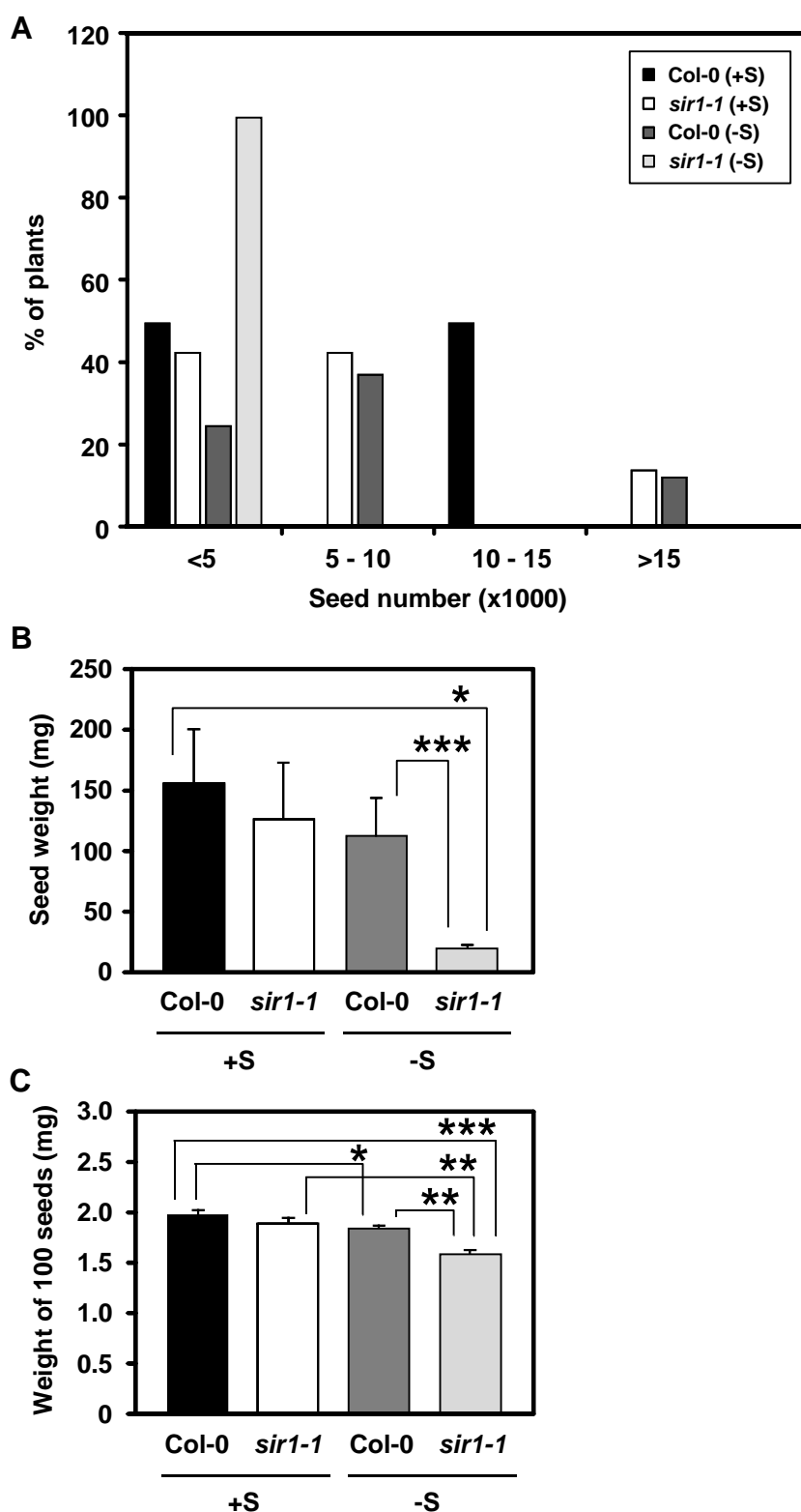


Fig. 36 *sir1-1* seed yield is negatively affected by sulfur deprivation to a higher degree than wild-type.

Plants were grown hydroponically on sulfur containing (+S) and sulfur-deficient (-S) under short day conditions until seeds were harvested. (A) Numbers of mature seeds per wild-type and *sir1-1* plant on +S and -S were counted and categorized. (B) Seed yield of wild-type and *sir1-1* on +S and -S. (C) 100-seed-weight of wild-type and *sir1-1* on +S and -S; (n ≥ 6), (means ± SEM).

Growing on -S, the wild-type plants produced seeds of a quantity similar to *sir1-1* plants grown on +S: 25% produced < 5000 seeds, 37% had 5000 to 10,000 seeds and 13% produced 15,000 to 20,000 seeds. On -S conditions, all *sir1-1* plants had less than 5000 seeds.

3.4.5 SiR transcript, protein and activity in *sir1-1* seeds

For *sir1-1* leaves, it was shown that SiR was down-regulated at transcriptional, protein and activity levels (Khan et al., 2010). It was of major importance to investigate, if T-DNA insertion in the promoter region of SiR also causes a down-regulation of *SiR* transcript, hence, SiR protein amount and activity in seeds and roots of *sir1-1*. To confirm the observations for leaf tissue and determine *SiR* transcript in the wild-type and *sir1-1* roots, mRNA was extracted (2.8.1) from pooled leaves and roots of at least eight 4-week-old plants grown in hydroponic cultures (2.2.3.2) and used for cDNA synthesis (2.8.3.1) and qRT-PCR (2.8.3.2) with primer pairs 2546 and 2547 (*SiR*) and 1727 and 1728 (*elongation factor 1 α* as reference gene; 2.1.6). *SiR* transcript was down-regulated in *sir1-1* leaf (Fig. 37A) and root tissue (Fig. 37B) to 47% ± 3 and 78% ± 1, respectively. To assess, if transcript level reduction resulted in decrease of SiR protein amounts, proteins were extracted from pooled leaves and roots (2.5.1) from the same individuals above. 40 µg leaf and 20 µg root proteins were separated via SDS-PAGE (2.5.5.1) and SiR was detected by immunoblot using a specific antiserum (2.5.5.4). Loading was controlled by amido black staining. SiR protein levels were reduced in *sir1-1* in both leaf and root tissues (Fig. 37C).

After confirming SiR down-regulation in *sir1-1* leaves and showing the same for root tissues, we investigated *SiR* transcript in mature seeds of wild-type and *sir1-1*. To gain seeds, plants were grown on soil under short day conditions for 7 weeks and then transferred to long day conditions. Seeds were collected and mRNA was extracted and used for cDNA synthesis and qRT-PCR as described above. In mature *sir1-1* seeds only 5% ± 0.6 of *SiR* transcript remained compared to the wild-type (Fig. 37D).

Results

To investigate the consequences of Sir mutation for SiR protein expression and activity, proteins were extracted from seeds (2.5.2.1) and SiR activity was measured (2.5.6.1). The SiR activity was reduced to an undetectable level (Fig. 37E). Also the immunological detection of SiR protein confirmed a strong reduction in seeds of *sir1-1* (Fig. 37F).

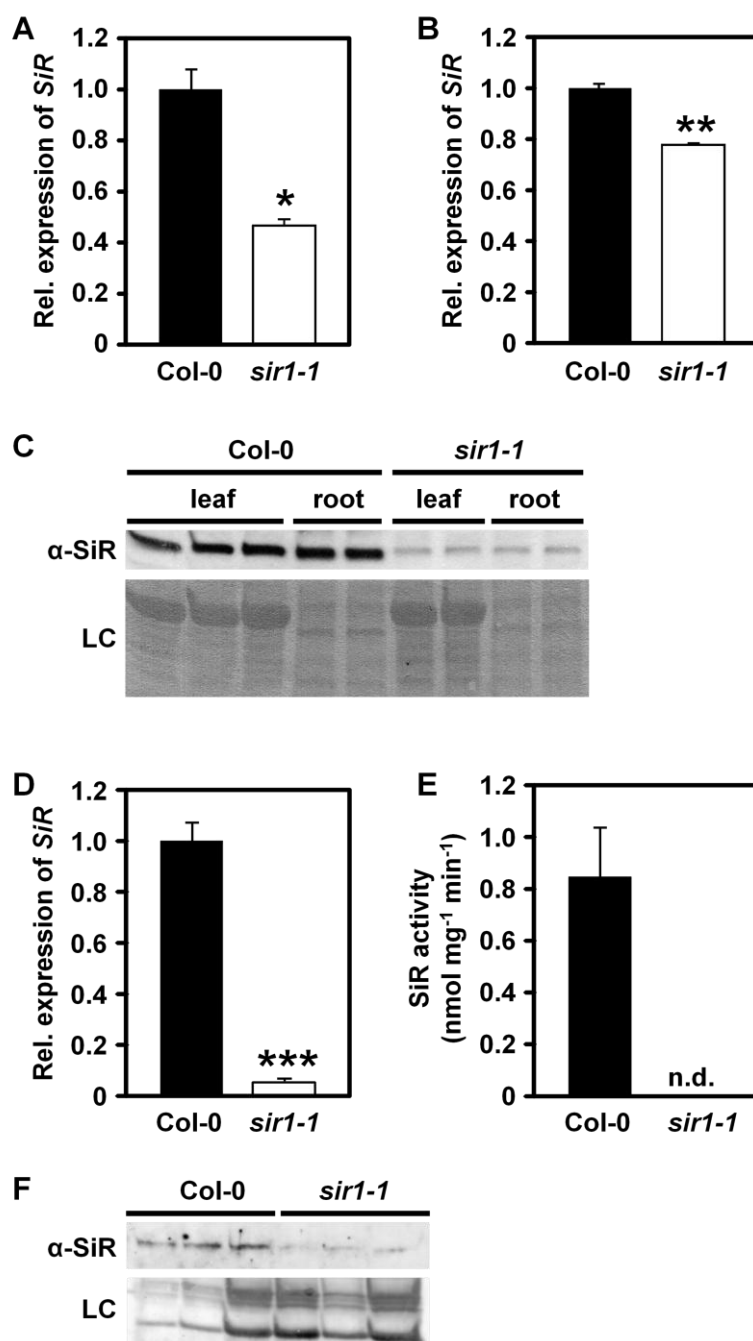
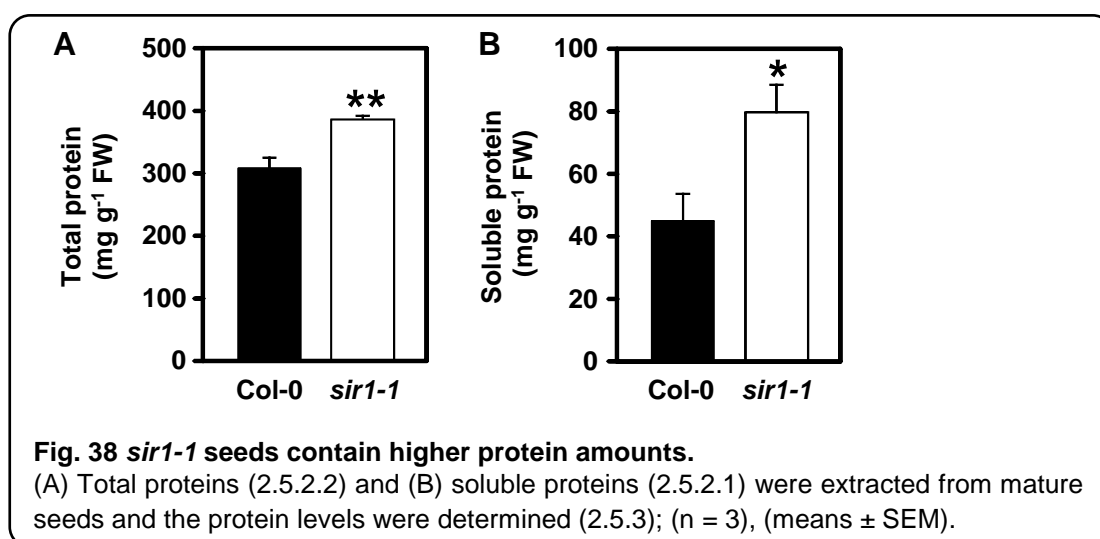


Fig. 37 SiR transcript and protein is reduced in *sir1-1* vegetative and generative tissues

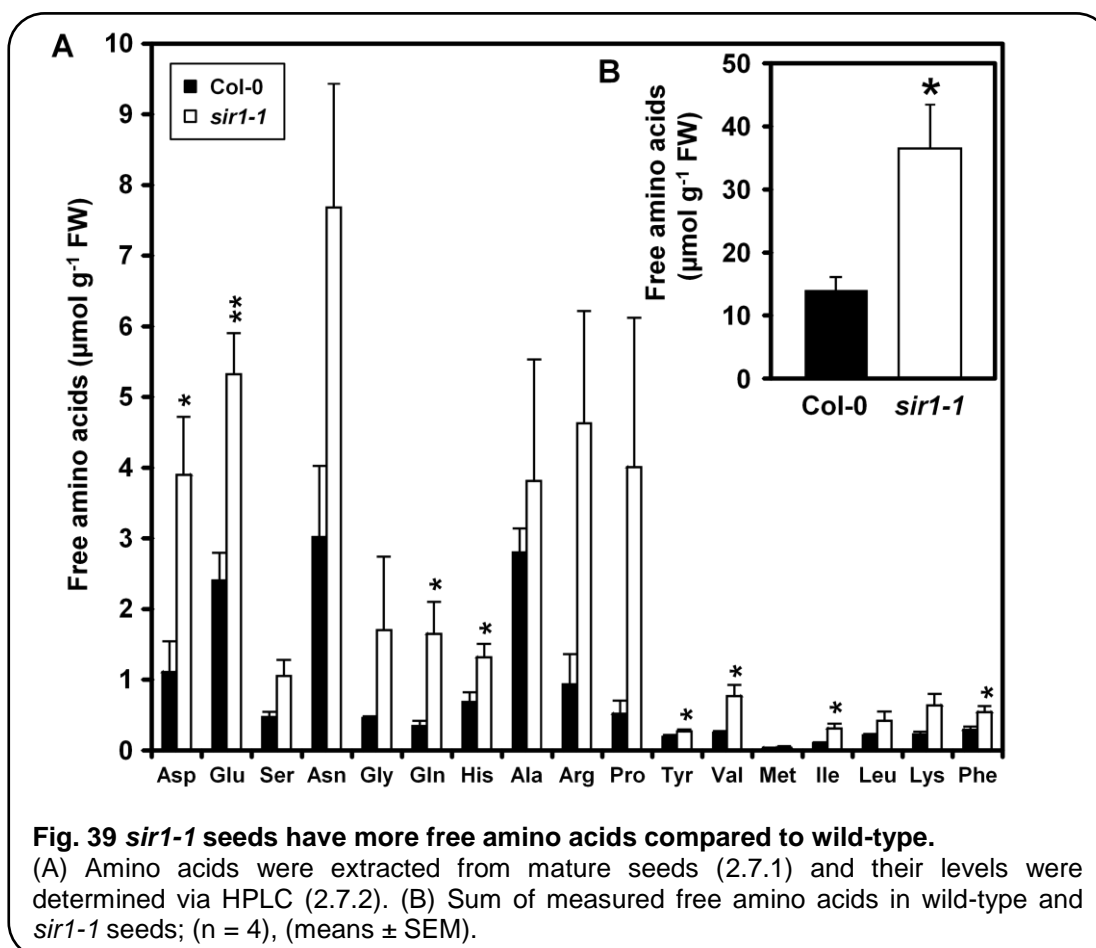
mRNA was extracted (2.8.1) from pooled leaves (A) and roots (B) of 4-week-old plants grown in hydroponic cultures (2.2.3.2) and used for cDNA synthesis (2.8.3.1) and qRT-PCR (2.8.3.2); ($n \geq 7$). (C) Proteins were extracted from pooled leaves and roots (2.5.1). 40 μg leaf and 20 μg root proteins were separated via SDS-PAGE (2.5.5.1) and SiR was detected by immunoblot using a specific antiserum (2.5.5.4). Loading was controlled by amido black staining. LC, loading control; ($n \geq 7$). (D) mRNA was extracted from seeds of plants that were grown on soil under short day conditions for 7 weeks and then transferred to long day conditions. cDNA synthesis and qRT-PCR were performed. (E) Proteins were extracted from mature seeds (2.5.2.1) and SiR activity was measured (2.5.6.1); ($n = 3$). (F) Proteins were extracted from mature seeds (2.5.2.1). From left to right: 75, 100, and 200 μg (four right lines) seed proteins were separated via SDS-PAGE (2.5.5.1) and SiR was detected by immunoblot using a specific antiserum (2.5.5.4). Loading was controlled by amido black staining. LC, loading control; ($n = 3$), (means \pm SEM).

3.4.6 Effects of decreased sulfite reduction on the *sir1-1* seed composition

To investigate the effects of the SiR mutation on the seed composition levels of proteins, amino acids and lipids were determined. Total proteins were extracted from mature seeds (2.5.2.2) and quantified (2.5.3). Seeds of *sir1-1* contained more proteins compared to the wild-type (Fig. 38A). Soluble proteins were extracted from mature seeds (2.5.2.1) and quantified as above. *sir1-1* seeds showed a higher soluble protein content (Fig. 38B).

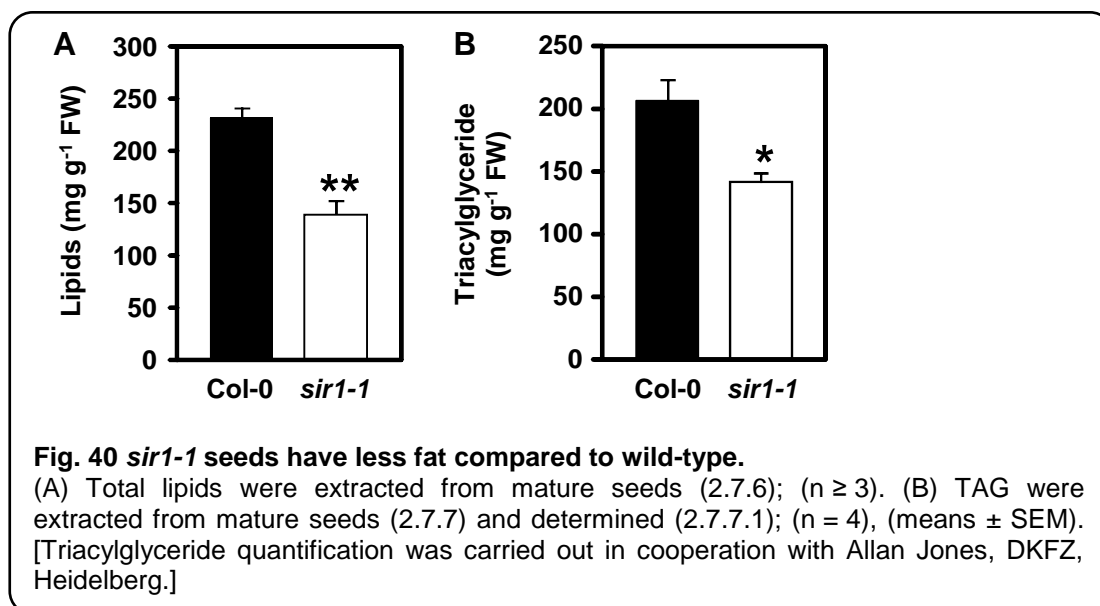


It was known that cysteine levels were unchanged in *sir1-1* seeds (Khan, 2008). Free amino acids were quantified and compared to the wild-type. Mature seeds were used for the extraction of amino acids (2.7.1), which were detected by HPLC (2.7.2). Levels of free amino acids were increased in *sir1-1* seeds (Fig. 39B). Aspartic acid (3.5-fold), glutamic acid (2.2-fold), histidine (1.9-fold), isoleucine (3-fold), phenylalanine (1.9-fold), tyrosine (1.5-fold) and valine (3.1-fold) were significantly increased.



Seeds are storage organs of plants and they have two major storage compounds: proteins and oil (Baud et al., 2008). Since an increase of protein amounts (Fig. 38) was observed and the seed weight was unchanged (Fig. 35), the lipid amount within the seeds of *sir1-1* and wild-type was measured. Lipids were extracted (2.7.6) from mature seeds and their level was determined. While wild-type seeds contained $232 \text{ mg g}^{-1} \pm 9$, *sir1-1* had a significantly lower level of $140 \text{ mg g}^{-1} \pm 12$ (Fig. 40A). In mature *Arabidopsis* seeds, almost all fatty acids are esterified to triacylglycerides (TAG) making up 90 - 95% of oil bodies (Ohlrogge and Browse, 1995; Baud et al., 2002). The remaining compounds originate from diacylglycerides and membrane lipids (Li et al., 2006; Molina et al., 2006). To investigate if the processing of oil compounds were changed in *sir1-1*, the TAG amounts were determined (2.7.7.1). Therefore, fat was extracted from mature seed (2.7.7) and determined (2.7.7.1). While *sir1-1* converted all its seed oil into TAG ($141 \text{ mg g}^{-1} \pm 7$; Fig. 40B), wild-type

seeds showed a TAG level of 203 mg g^{-1} $140 \text{ mg g}^{-1} \pm 16$ corresponding to 88% of total seed fat.



Although hexoses and their products do not contribute much to the total weight of mature *Arabidopsis* seeds, they play an important role as energy sources provided for germinating seedlings or serve as a signal controlling seed metabolism (White and Benning, 2001). Therefore, levels of fructose, glucose, sucrose and starch were measured in mature *sir1-1* and wild-type seeds (2.7.9). There were no significant changes in the amounts of measured sugars and starch (Fig. 41).

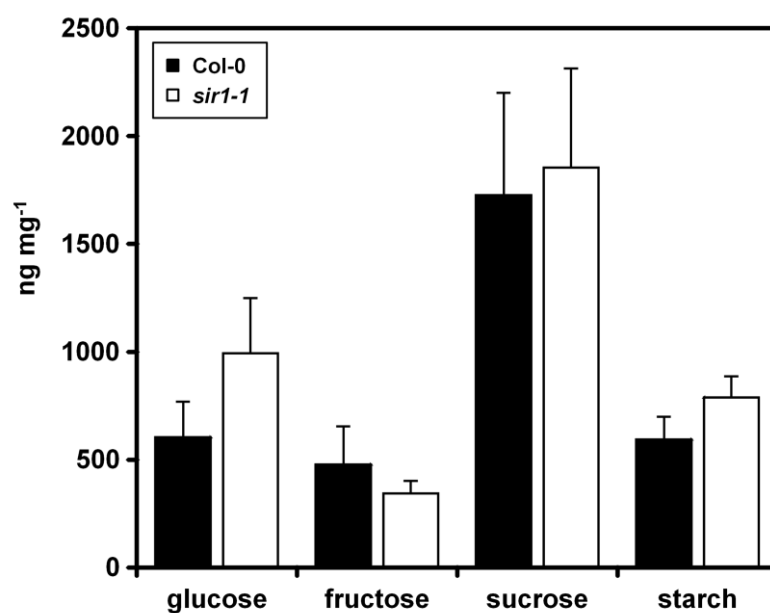


Fig. 41 *sir1-1* shows seed sugar and starch levels comparable to wild-type. Fructose, glucose, sucrose and starch were extracted from mature seeds, and their levels were determined (2.7.9); (n = 4).

3.4.7 Effects of decreased sulfite reduction on the sulfur assimilatory reduction pathway in *sir1-1* and wild-type seeds

To investigate whether the *SiR* mutation has an effect on the sulfur assimilation and reduction pathway, mRNA was extracted from mature seeds (2.8.1) and used for cDNA synthesis (2.8.3.1) and qRT-PCR (2.8.3.2) with primers listed in 2.1.6 under “Primers for qRT-PCR”. *Elongation factor 1 α* (1727 and 1728), *ubiquitin* (1729 and 1730) and *protein phosphatase* (1731 and 1732) were used as reference genes. The only significantly regulated genes were *SiR*, as shown before (Fig. 37D), and *APR2*, which was reduced to 50% of wild-type (Fig. 42). Attempts to detect APR activity in seeds failed (2.5.6.2). Down-regulation of the *APR2* transcript was also observed for leaves (Fig. 13A), indicating that the sulfur reduction pathway was slowed down due to *SiR* dysfunction.

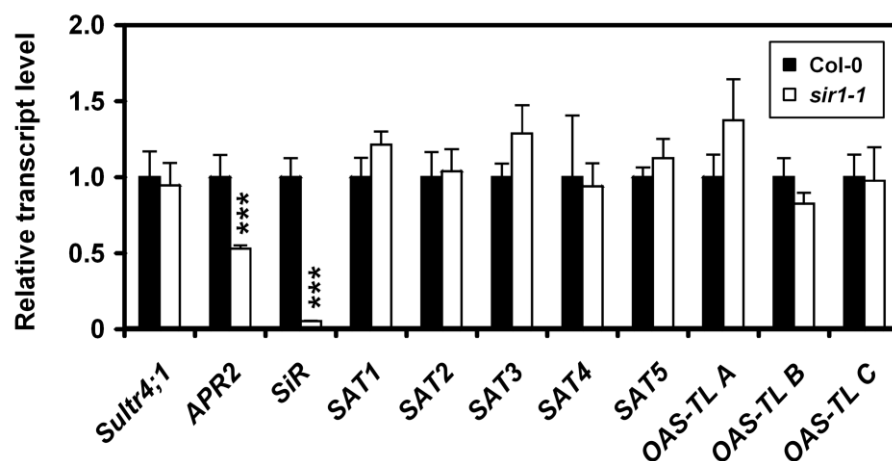
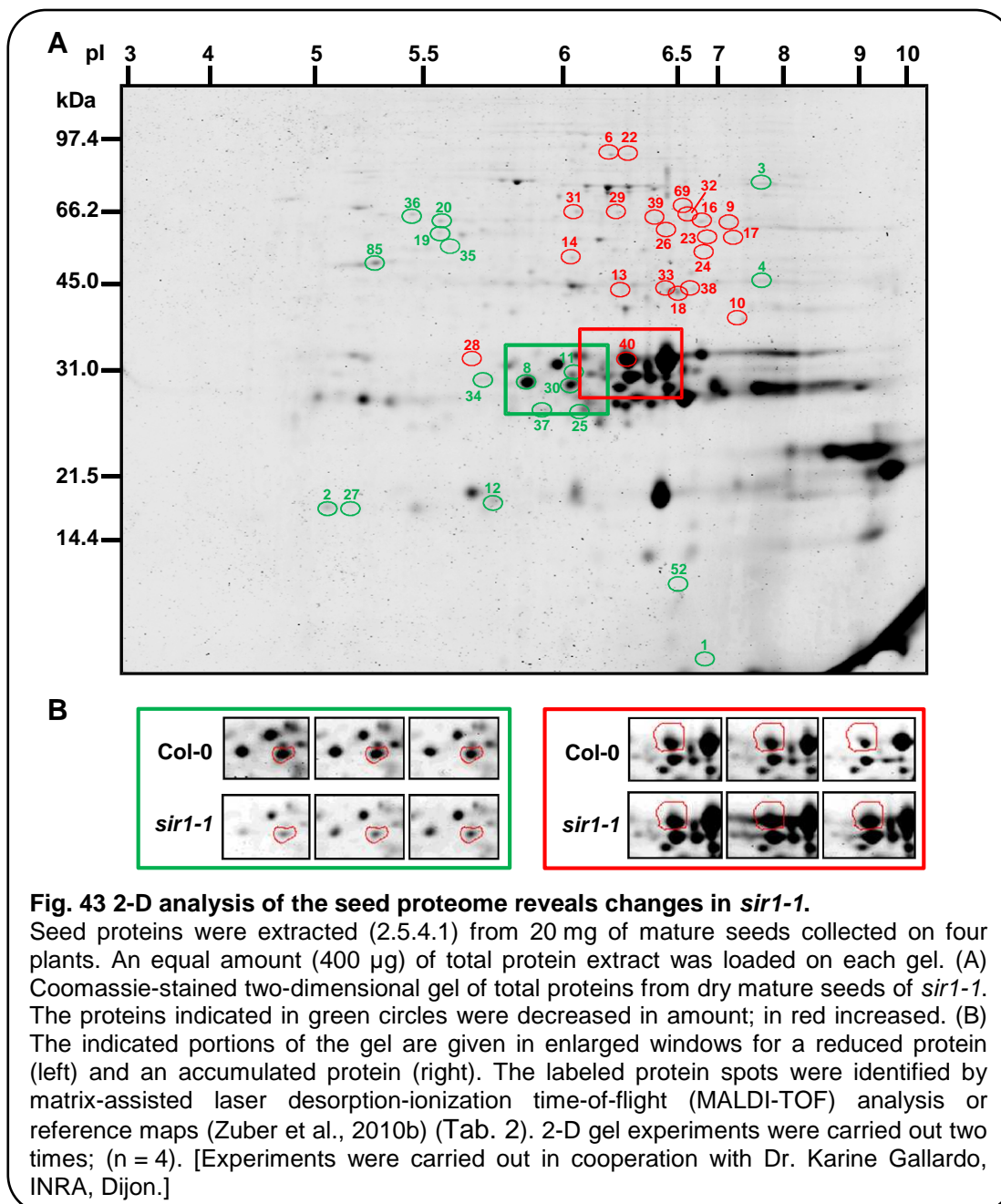


Fig. 42 Effects of *SiR* mutation on the sulfur assimilation and reduction pathway in seeds

mRNA was extracted from seeds of plants that were grown on soil under short day conditions for 6 to 7 weeks and then transferred to long day conditions. cDNA synthesis (2.8.3.1) and qRT-PCR (2.8.3.2) were performed; (n = 3).

3.4.8 Effects of decreased sulfite reduction on the *sir1-1* proteome

Seed proteome was extracted, separated and analyzed by two-dimensional gel electrophoresis (2.5.4). 180 proteins were detected; out of them 44 were significantly changed in amount in *sir1-1* ($p < 0.05$) (Fig. 43 and Tab. 2) and identified via nano-LC-MS/MS as described in Gallardo et al. (2007) (Suppl. data 17) and reference maps (Zuber et al., 2010b). The most affected protein category was the storage proteins.



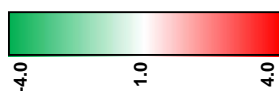
While in *sir1-1* sulfur-poor precursors of globulin (At12S1 and 12S4) were 1.3- to 1.7-fold accumulated in amount, sulfur-rich albumin (At2S) was decreased in abundance by 4-fold. Due to accumulation of precursors and probably less processing of them, the globulin α -subunits were decreased in amount. A 1.5- to 2.2-fold increase of methionine synthase was observed, indicating changes in amino acid biosynthesis. Also, proteins from glycolysis/glyconeogenesis were accumulated: fructose-bisphosphate aldolase (1.7-fold), glyceraldehyde 3-phosphate dehydrogenase (1.3- to 1.5-fold) and endolase (1.5-fold), indicating changes in energy metabolism in the mutant seeds (Fig. 44). Also changes in stress-related enzymes were observed. Isocitrate dehydrogenase amount increased 1.7-fold and GSH S-transferase was reduced 1.5-fold.

Interestingly, oleosin 2, a storage protein surrounding the oil bodies in seeds of higher plants (Murphy, 1993) was down-regulated 1.8-fold.

Tab. 2 Polypeptides with changed abundance in *sir1-1* seeds.

Protein annotation according to LC-MS/MS (Suppl. data 17) and (Zuber et al., 2010b). Function category and description after ontological classification of (Bevan et al., 1998)

Protein	Accession No.	pI	MW (kDa)	Difference	ANOVA (p)	Function category	Function description
51_A112S1 (precursor form)	AT4G28520	7.0	60.4	1.7	0.018	Storage protein	Protein destination and storage
16_A112S1 (precursor form)	AT4G28520	6.7	64.0	1.6	0.001	Storage protein	Protein destination and storage
26_A112S1 (precursor form)	AT4G28520	6.4	61.6	1.5	0.032	Storage protein	Protein destination and storage
39_A112S1 (precursor form)	AT4G28520	6.3	64.0	1.3	0.019	Storage protein	Protein destination and storage
17_A112S4 (precursor form)	AT5G44120	7.2	59.0	1.6	0.020	Storage protein	Protein destination and storage
23_A112S4 (precursor form)	AT5G44120	6.9	59.6	1.5	0.039	Storage protein	Protein destination and storage
29_A112S4 (precursor form)	AT5G44120	6.2	66.7	1.4	0.003	Storage protein	Protein destination and storage
69_Cupin family protein	AT3G22640	6.5	66.8	1.4	0.028	Storage protein	Protein destination and storage
32_Cupin family protein	AT3G22640	6.6	66.1	1.4	0.019	Storage protein	Protein destination and storage
40_A112S1 (α subunit)	AT4G28520	6.2	33.6	1.3	0.036	Storage protein	Protein destination and storage
1_2S albumin storage protein	AT4G27140	7.1	9.0	-4.0	0.019	Storage protein	Protein destination and storage
8_A112S4 (α subunit fragment)	AT5G44120	5.9	30.9	-2.0	0.000	Storage protein	Protein destination and storage
11_A112S4 (α subunit fragment)	AT5G44120	6.0	32.0	-1.8	0.000	Storage protein	Protein destination and storage
30_A112S4 (α subunit fragment)	AT5G44120	6.0	30.7	-1.4	0.005	Storage protein	Protein destination and storage
34_A112S4 (α subunit fragment)	AT5G44120	5.8	31.5	-1.4	0.003	Storage protein	Protein destination and storage
37_A112S1 (α subunit fragment)	AT4G28520	5.9	27.5	-1.4	0.001	Storage protein	Protein destination and storage
12_Oleosin 2	AT5G40420	5.8	18.0	-1.8	0.016	Storage protein	Protein destination and storage
2_Heat Shock Protein (HSP)	AT3G46230	5.1	17.7	-3.0	0.032	Protein destination and storage	Folding and stability
6_Methionine synthase	AT5G17920	6.1	86.4	2.2	0.015	Metabolism	Aminoacids
9_Methionine synthase (chain a)	AT5G17920	7.2	62.3	1.9	0.039	Metabolism	Aminoacids
22_Methionine synthase	AT5G17920	6.2	86.4	1.5	0.000	Metabolism	Aminoacids
10_ATARCA	AT1G18080	7.3	41.2	1.8	0.004	Signal transduction	G proteins
27_Phosphatidylethanolamine-binding protein	AT5G01300	5.2	17.7	-1.5	0.007	Signal transduction	Mediators
13_Fructose-bisphosphate aldolase-like protein	AT3G52930	6.2	47.1	1.7	0.016	Energy	Glycolysis / Gluconeogenesis
18_Glyceraldehyde 3-phosphate dehydrogenase C-1	AT3G04120	6.5	46.5	1.5	0.013	Energy	Glycolysis / Gluconeogenesis
33_Glyceraldehyde 3-phosphate dehydrogenase C-2	AT1G13440	6.4	46.9	1.4	0.002	Energy	Glycolysis / Gluconeogenesis
38_Glyceraldehyde 3-phosphate dehydrogenase (A subunit)	AT1G12900	6.7	47.4	1.3	0.032	Energy	Glycolysis / Gluconeogenesis
20_Enolase	AT2G36530	5.6	64.2	1.5	0.006	Energy	Glycolysis / Gluconeogenesis
31_ATP synthase (subunit α, mitochondrial)	ATMG01190	6.0	66.8	1.4	0.010	Transporters	Transport ATPases
36_ATP synthase (β chain)	AT5G08670	5.5	66.1	1.4	0.011	Transporters	Transport ATPases
14_Isocitrate dehydrogenase	AT1G65930	6.0	54.2	1.7	0.043	Disease/defence	Stress responses
25_Glutathione S-transferase	AT2G47730	6.1	27.5	-1.5	0.045	Disease/defence	Detoxification
19_Nitrile-specifier protein NSP2 / xylose isomerase	AT2G33070/ AT5G57655	5.6	60.8	1.5	0.012	Disease/defence	Stress responses
28_Dormancy related protein (aldehyde reductase)	AT1G54870	5.7	34.3	1.4	0.022	Unclassified	



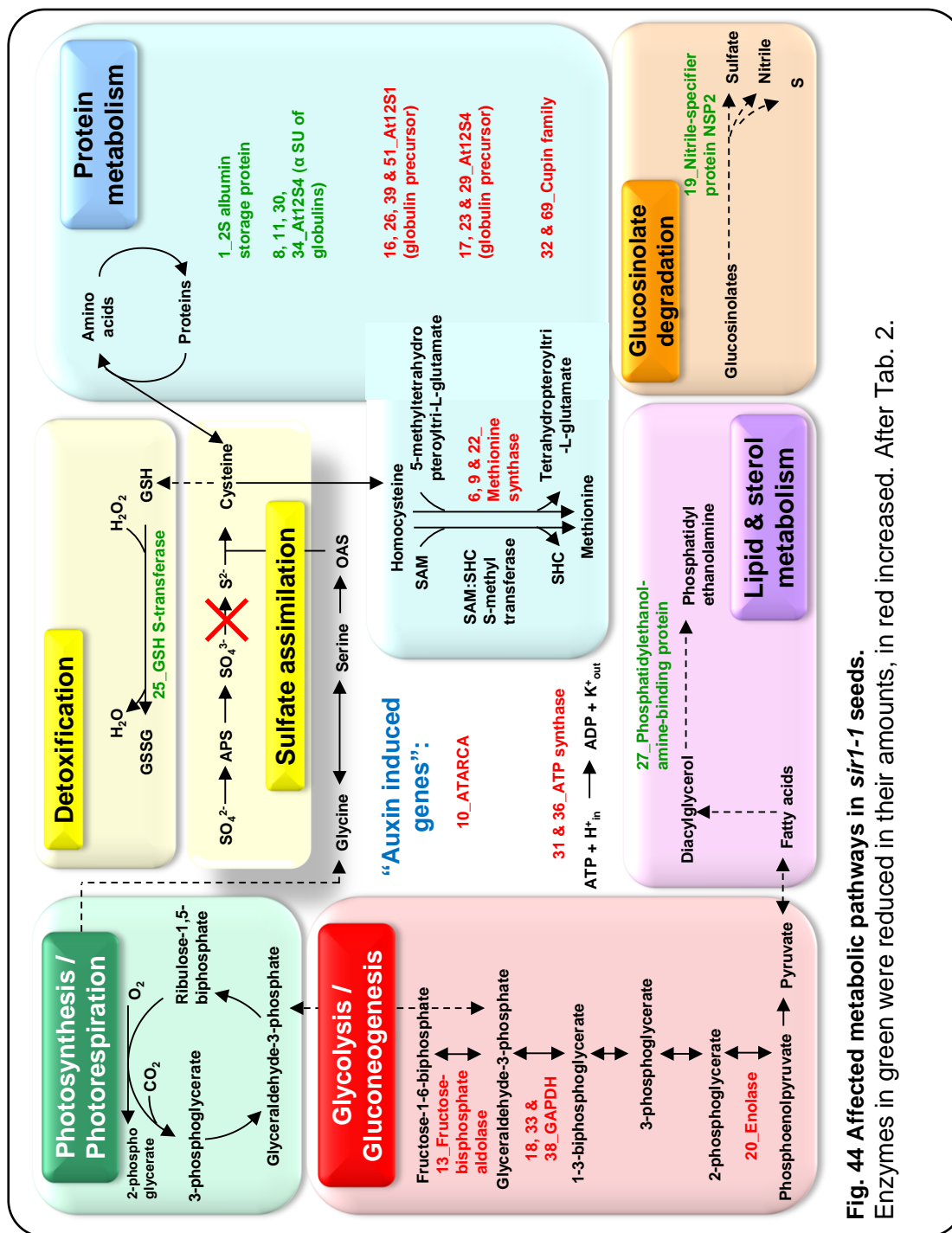


Fig. 44 Affected metabolic pathways in *sir1-1* seeds. Enzymes in green were reduced in their amounts, in red increased. After Tab. 2.

4 Discussion

4.1 Effects of SiR mutation on the whole genome and metabolites

The *sir1-1* mutant is a useful tool to investigate the sulfate assimilatory reduction pathway. At first sight, one might think that *sir1-1* plants do not really exhibit a behavior that could be seen as an adaptation to -S: Because *sir1-1* plants accumulate sulfate in leaves up to more than eight-times in comparison to the wild-type plants and also the levels of cysteine and GSH are not decreased (Khan et al., 2010, this study). However, sulfate accumulates in *sir1-1* plants for at least two reasons: For one, due to the bottleneck effect in the sulfate assimilatory reduction pathway caused by the *SiR* mutation. Secondly, OAS that together with sulfide results in cysteine, accumulates due to reduced sulfide production in *sir1-1*. OAS is believed to have a signal function, whereby its accumulation causes up-regulation of sulfate transporters (Smith et al., 1997; Hesse et al., 2004). Also, measurement of incorporation of radioactively labeled sulfate into cysteine and GSH showed a dramatic decrease of flux in sulfate assimilation pathway in *sir1-1* compared to wild-type plants (Khan et al., 2010).

This leads to a phenotype reminiscent of sulfur-deficient plants, although oxidized sulfur is available. Hence, the decreased sulfur reduction capacity is primary accountable for the phenotype. Metabolome and transcriptome analyses revealed that several metabolites were changed in *sir1-1* leaves grown under normal conditions in a manner that has been previously reported for long-term sulfate-deprived plants (Nikiforova et al., 2003; Nikiforova et al., 2005): SAM levels were reduced significantly by more than 20%. This, and a reduced sulfur flux via the sulfate assimilatory reduction pathway cause accumulation of OAS, serine, and putrescine. Also levels of chlorophyll a and b were decreased to less than 50% of wild-type levels. These changes were also observed, when plants were grown on -S (Nikiforova et al., 2005). Nikiforova et al. (2003) reported that - similar to *sir1-1* when compared to wild-type on normal media - serine and OAS, aspartic acid, SAM, chlorophyll a and b; and methionine, threonic acid,

and xylose (0.81-, 0.89-, and 0.86-fold respectively, but not significantly) were down-regulated when Col-0 was transferred to -S.

There are also some reports that show changes in the transcriptome due to sulfur availability. We compared those with our microarray data and found similarities:

Arginine is reported to be strongly down-regulated upon sulfur deficiency (Nikiforova et al., 2005). We could not detect arginine. However, there are indications for its breakdown, e.g. a putative arginase (At4g08870) was more than two 2log-fold induced in *sir1-1* compared to wild-type. Putrescine, a polyamine produced by arginine degradation (Imai et al., 2004), was increased in *sir1-1* leaves. There are several genes involved in the putrescine-related arginine breakdown pathway and some of them were up-regulated in *sir1-1* leaves: *SPD1*, *SPD2*, *ADC1*, *ADC2*, and *ACL5* (Hanzawa et al., 2002; Imai et al., 2004) indicating that arginine is also down-regulated.

Nikiforova et al. (2003) showed that hypo-sulfur stress causes down-regulation of genes encoding accessory proteins of the electron transport. We could observe changes in expression of ferredoxin genes when 7-week-old wild-type plants were compared with 10-week-old *sir1-1* plants of same developmental stage: *FED A* (At1g60950) (-0.37 2-log-fold) and *ATFD1* (At1g10960) (-0.31) were down-regulated in 10-week-old *sir1-1* plants significantly, while 7-week-old *sir1-1* did not show different expression pattern of these genes. Interestingly, a third member of ferredoxin family *ATFD3* (At2g27510) was up-regulated significantly in both, 7- and 10-week-old *sir1-1* plants, in comparison to wild-type: 0.59 and 0.63 2-log-fold, respectively.

Nikiforova et al. (2003) reported down-regulation of the Rubisco-encoding genes under sulfur deficiency and affected energy assimilation in sulfur-starved plants. Compared to 7-week-old wild-type plants, in leaves of 10-week-old *sir1-1*, the nuclear *rbcS* gene (At1g67090) encoding the small subunit of Rubisco was down-regulated -0.43-2log-fold; however no significant changes were observed in 7-week-old *sir1-1* when compared to wild-type plants of same age (-0.03). *psbA* (chloroplast gene encoding the D1 protein of photosystem II) was down-regulated in 7-week-old *sir1-1*

plants compared to wild-type plants of same age (-0.83-2log-fold). These results support the notion that photosynthesis is affected in *sir1-1* plants. As mentioned above, it has been reported that chlorophyll contents were reduced in -S plants and our results show that on +S *sir1-1* has reduced chlorophyll. Microarray data revealed that *Lhcb1B1* (chlorophyll *a/b* binding; AT2G34430) and *Lhcb3* (chlorophyll *a/b* binding; AT5G54270) were down-regulated in 10-week-old *sir1-1* compared to 7-week-old wild-type plants of same size -0.32 and -0.52 2log-fold, respectively. However, smaller, 7-week-old *sir1-1* did not show significant changes. Interestingly, there were also changes in the detected adenosine-derivate metabolites indicating affected photosynthesis and disturbed energy metabolism, i.e. reduction of glycolic acid indicating affected photorespiration.

Plastidic chaperons *Cpn60 α* and *Cpn60 β* play an important role in folding and assembly of proteins (e.g. Rubisco) and chloroplast division (Goloubinoff et al., 1989b; Goloubinoff et al., 1989a; Suzuki et al., 2009). Mutation of *ptCpn60 α* abolished greening of plastids and resulted in an albino phenotype while a weaker mutation impairs plastid division, and reduced chlorophyll levels (Suzuki et al., 2009), leading to defects in plastid development and subsequently in development of the plant embryo and seedling (Apuya et al. 2001). Transgenic tobacco plants, which expressed antisense *Cpn60 β* showed drastic phenotypic alterations including slow growth, delayed flowering, stunting and leaf chlorosis (Zabaleta et al., 1994). Although our microarray studies were carried out on mature leaves, it was of interest to examine the expression for these plastidic chaperons. *ptCpn60 β* (At1g55490) was up- (0.65-) and down- (-0.73-2log-fold) regulated in 7- and 10-week-old *sir1-1* plants, respectively, compared to 7-week-old wild-type plants. *ptCpn60 α* (At2g28000) was only significantly changed in 7-week-old *sir1-1* (0.71-2log-fold change) compared to same-age wild-type plants. It can be speculated about the altered *ptCpn60 α* and *β* transcripts' influence on the germination rate of *sir1-1*. However, the analysis must be performed on seeds and seedlings.

Transcriptome analysis showed that *sir1-1* plants suffer from stress:

Gene set enrichment analysis (GSEA) revealed up-regulation of pathways related to DNA repair in *sir1-1* plants. One reason for induction of these stress-related genes could be the elevated sulfite (Khan et al., 2010), since sulfite has damaging effects on nucleic acids (Shosuke et al., 1989; Ito and Kawanishi, 1991; Muller et al., 1997; Kawanishi et al., 2001; Alipazaga et al., 2008). It is also known that SiR binds to nucleoids in plastids and makes them more compact, hence less accessible for transcription factors (Sekine et al., 2002). When plastidic DNA is not bound to SiR, it is in the loose form. It can be speculated that decreases in SiR enzyme in plastids causes DNA relaxation making it more vulnerable for sulfite. We observed a counteracting reaction of *sir1-1* to reduce sulfite production: *APR2* transcript was reduced, hence, the protein activity also was. Also the regulatory function of CSC probably triggers deceleration of sulfur reduction: It is known that in Arabidopsis cysteine has an inhibitory function on free SATs (Wirtz et al., 2010). To avoid overproduction of OAS, *sir1-1* plants maintained the cysteine levels. Since sulfide production is decreased in *sir1-1*, OAS can not be further metabolized to cysteine. This response saves nitrogen and carbon resources that would otherwise accumulate to high excess in the form of OAS. Therefore, growth and metabolic pathways are adjusted in the *sir1-1* plants.

Arabidopsis has three ways to detoxify sulfite: First, sulfite reduction to sulfide via SiR; second, its incorporation in sulfolipids via SQD enzymes; and third, sulfide oxidation to sulfate. The latter one is carried out by SOX, an enzyme located in peroxisomes of Arabidopsis (Hänsch et al., 2006). There are no changes in sulfolipids from *sir1-1* leaves. SOX expression in 7- and 10-week-old *sir1-1* in comparison to wild-type was checked. The SOX (At3g01910) transcript was not significantly altered in any of the *sir1-1* groups compared to wild-type. However, in leaves of 7-week-old *sir1-1* plants, SOX activity was increased more than 2-fold compared to the wild-type whereas immunological analysis revealed no changes of protein amount (Khan et al., 2010), suggesting post-translational modifications. However, induction of the peroxisomal ABC (ATP-binding cassette) transporter *PXA1* (At4G39850) (0.5 2-log-fold) in 10-week-old *sir1-1* compared to 7-week-old wild-type plants could indicate

sulfite transport to peroxisomes for oxidation. Little is known about peroxisomal transporters. For spinach peroxisomes, only one porin is known to be permeable for a variety of different inorganic and organic anions which could principally facilitate sulfate or sulfite transport (Reumann et al., 1998). It has been acknowledged that the nature of the substrates handled by the different ABC transporters is less clear (Visser et al., 2007). The ultimate role of PXA1 and its potential involvement in sulfite transport to peroxisomes for oxidation reactions via SOX remain speculative. However, the fact that this ABC transporter was not significantly up-regulated in early stages of *sir1-1* development (7 week) and its transcript was increased later on in *sir1-1* plants (10 week), could derive from the accumulation of sulfite during the vegetative growth of the mutant. Seemingly, there are connections between sulfite accumulation and up-regulation of *PXA1*. However, sulfite detoxification reactions carried out by SOX have a side product, namely H₂O₂ which also has been reported to cause DNA damage (Jornot et al., 1998) and induce DNA repair genes (Desikan et al., 2000).

Since conversion of sulfite into less toxic sulfate via SOX could potentially reduce the toxic effects of sulfite and probably rescue the *sir1-1* phenotype partially or totally, we tried to cross *sir1-1* with *SOX* over-expressing Arabidopsis plants. Also, *sir1-1* should be crossed with a *sox-k.o.* line to abolish the possibility of sulfite detoxification via oxidation. One would expect a more severe phenotype in the double mutant compared to *sir1-1*. However, the attempts we made (4 times with at least 4 plants per line) remained without success in the F1 generation. We need to investigate whether the detected reduced pollen viability contributes to this phenomenon. Also the viability of female gametophytes in *sir1-1* should be investigated. However, *sir1-1* is able to self-pollinate and *sir1-1* could be crossed with *cad2* mutant (A. Speiser, unpublished). More evaluative crossing studies are of demand, i.e. pollination between female and male sexual organs from *sir1-1* and wild-type, respectively and pollination vice versa.

Interestingly, *CYP85A2* (At3g30180) transcript was reduced (-0.77) in 10-week-old *sir1-1* plants compared to wild-type plants. In 7-week-old *sir1-1*,

its expression was comparable to wild-type plants. *CYP85A1* (At5g38970) was not significantly altered in any of the mutant growth stages.

In Arabidopsis, *CYP85A1* and *CYP85A2* are two CYP85 proteins known to be involved in the final oxidation steps necessary for the biosynthesis of brassinolide (BR) and *CYP85A1* catalyzes the last oxidative reactions that lead to the biosynthesis of BR (Nomura et al., 2005). BRs are phytohormones which affect germination, root growth, cell elongation, vascular differentiation, pollen tube growth, and stress tolerance (Szekeres et al., 1996; Clouse and Sasse, 1998; Steber and McCourt, 2001; Yamamoto et al., 2001; Müssig et al., 2003). Arabidopsis mutants defective in BR synthesis show common phenotypic features including dwarfism, curly leaves, reduced apical dominance, reduced fertility, and delayed senescence (Clouse et al., 1996; Kim et al., 2005).

CYP85A1 mRNA localization studies and GUS expression under a *CYP85A1* promoter showed that within the ovule the corresponding protein is mostly active in gametophytic cells (Perez-Espana et al., 2011). T-DNA insertion lines defective in the activity of *CYP85A1* exhibit a semi-sterile phenotype, suggesting a role for the corresponding enzyme acting at the gametophytic level. In regard to some similarities between Arabidopsis BR mutants and *sir1-1*, it would be interesting to analyze the transcription levels of *CYP85A1* and *CYP85A2* in *sir1-1* seeds.

As mentioned above, raffinose and galactinol accumulate in *sir1-1* leaves compared to wild-type leaves, indicative for sulfur starvation. Knowledge of metabolic changes of raffinose and galactinol in Arabidopsis is rather limited, but they have been shown to accumulate under various kinds of stress: In wild-type leaves, treatment with 50 μ M methylviologen (MV) induces expression of *galactinol synthase 1* (*GolS1*), and increases the total activity of GolS as well as the levels of galactinol and raffinose (Nishizawa et al., 2008). High intracellular levels of galactinol and raffinose in the *GolS1*- or *GolS2*-overexpressing Arabidopsis plants compared to wild-type correlate with increased tolerance to MV treatment and salinity or chilling stress. Galactinol and raffinose effectively protect salicylate from attack by hydroxyl radicals in vitro. The authors suggested that galactinol and raffinose may scavenge hydroxyl radicals may have a

novel function in protecting plant cells from oxidative damage caused by MV treatment, salinity, or chilling. Interestingly, in leaves of 7- and 10-week-old *sir1-1* plants, the *AtGols1* (At2g47180) transcript is increased significantly 1.06 and 1.09 2log-fold, respectively, compared to 7-week-old wild-type plants. The high elevation of raffinose and galactinol, and up-regulation of *galactinol synthase 1* suggest stress in *sir1-1* leaves during vegetative growth.

It is known that *sir1-1* has an 8 times higher $^{35}\text{SO}_4^{2-}$ uptake rate compared to wild-type and that no increase of sulfate uptake takes place in *sir1-1* plants after 6 h of sulfur starvation (Haas, 2010). Therefore, it is astonishing that after 6 h of *sir1-1* growth on -S there were similar responses at the metabolic level in roots compared to equally treated wild-type plants. In contrast to *sir1-1*, wild-type plants showed increased sulfate uptake on -S (Haas, 2010). These results indicate a metabolome-associated answer independently from the regulation of sulfate uptake after short-term sulfate starvation.

4.2 Effects of decreased sulfite reduction on the generative growth

The next major aim of this project was to investigate if sulfate assimilation in Arabidopsis seeds is essential for their growth. Again, *sir1-1* is a good tool, since the growth of *sir1-1* siliques of plants is slower compared to that of wild-type plants. Also, *sir1-1* plants set less seeds. We were interested to investigate where these effects derive from: the changed metabolism of the vegetative mother tissue or the reduced sulfate reduction within seeds?

We could demonstrate that in mature seeds sulfate assimilation and reduction takes place since we detected the transcript of all major genes involved in this pathway and it has been shown that sulfur assimilation occurs in developing seeds (eFP browser), too. We also demonstrate that SiR protein shows activity in mature wild-type seeds and that SiR activity is strongly reduced to an undetectable level in seeds of *sir1-1*. Also at the transcript level, *SiR* is reduced to 7% of wild-type, a decrease much

stronger than in leaf and root. Taken together, sulfate assimilation occurs in developing and mature seeds. Like in vegetative tissues, *sir1-1* shows strong reduction of SiR due to mutation. Also the *APR2* transcript was down-regulated in mature seeds compared to wild-type seeds. To evaluate the role of maternal tissue supplying oxidized sulfur, the sulfate amounts of seeds were previously determined. There were no significant changes between *sir1-1* and wild-type (Khan, 2008). Sulfate levels in seeds were comparable to those in leaves (approx. 10 nmol mg⁻¹ FW) while nitrate content is dramatically reduced in seeds (< 1 nmol mg⁻¹ FW) compared to leaves (80 nmol mg⁻¹ FW). Reduced nitrogen must be imported into the seeds, i.e. amino acids while sulfate needs to be reduced within the seeds. Sulfate assimilation is necessary for GSH synthesis, since developing seeds need both endogenous GSH biosynthesis and maternal supply (Cairns et al., 2006). Besides GSH production, in developing seeds sulfate assimilation is needed for cysteine synthesis to produce seed storage proteins.

Our results further demonstrate that intact sulfate assimilation is required for proper development and viability of pollen grains.

4.3 Effects of decreased sulfite reduction on the seed proteome

We were interested to investigate whether alterations in the sulfate assimilation pathway affects seed composition. Storage proteins are one major group of seed storage compounds in Arabidopsis. In *sir1-1* seeds, the amount of proteins and amino acids were elevated indicating changes in protein synthesis. While *sir1-1* vegetative tissues were persevered in a condition mimicking sulfate starvation, similar -S responses were observed in the *sir1-1* seed proteome: Seed proteome of Arabidopsis plants grown under sulfur-deficient conditions revealed that 12S globulin precursors were accumulated compared to normally grown seeds (Higashi et al., 2006). 12S globulin precursors were accumulated and their fragmented and processed forms decreased in amount when the transport of sulfate in seeds was impaired (Zuber et al., 2010b).

A similar abnormal accumulation of 12S globulin precursors was observed in Arabidopsis mutants lacking vacuolar processing enzymes (Gruis et al., 2002; Shimada et al., 2003b; Gruis et al., 2004) or vacuolar sorting receptors (VSRs) (Shimada et al., 2003a) and in a rice mutant lacking protein disulfide isomerase (Takemoto et al., 2002).

In the *sir1-1* proteome, we observed changes that were similar to the seed proteome upon sulfur deficiency: Precursors of globulins were accumulated, while their processed subunit fragments were decreased in amount. Investigation of amino acid composition of seed proteins revealed that Arabidopsis seed proteins contain in average 3.1% cysteine and methionine in total and 12.7 sulfur atoms. Until today, not all the proteins in seeds have been characterized and the evaluated seed proteins (provided by Dr. Karine Gallardo, INRA, Dijon) contain only proteins that could be detected via MS/GC methods and/or reference protein maps. Therefore, the contribution of each protein to the total seed proteome could not be determined. However, 12S globulins comprise around 80% of total SSPs in Arabidopsis and the percentage of cysteine and methionine in them is 2.9%. This makes the calculation of sulfur containing amino acids for seed proteins reliable. Globulins are not sulfur-rich SSPs. This could be a reason for their accumulation, as sulfate reduction and assimilation is inefficient in *sir1-1*, as well as in shoots, roots, and seeds. One other explanation for the accumulation of their precursors could be the lack of available cysteine and methionine for biosynthesis of VPEs. The calculation of their amino acid composition revealed that the four VPEs contain in average 4.4% cysteine and methionine in total and 21.3 sulfur atoms, i.e. their sulfur content is more than average for seed proteins. Therefore, their protein expression could be down-regulated. Under -S conditions, the transcript levels of VPEs were unchanged (Higashi et al., 2006). VSRs can also be seen as sulfur-rich proteins: The average content of cysteine and methionine in seven isoforms is 7.5% and the VSRs have 47 sulfur atoms. Perhaps due to their high demand for reduced sulfur, their expression would be down-regulated, affecting transport of precursors from the ER via the Golgi to multivesicular bodies or/and protein storage vacuoles.

Assuming, that high amounts of accumulated sulfate is transported from generative tissue into the *sir1-1* seeds, the lack of sulfate for synthesis of sulfur amino acids may not be the rate-limiting aspect. Quantification of sulfate content of leaves before budding would be of interest. However, determination of sulfate and nitrate in *sir1-1* seeds revealed no changes compared to wild-type seeds (Khan, 2008). Rather the lack of sulfate assimilation capacity in *sir1-1* seeds could explain the reduction of sulfur-rich proteins.

Interestingly, oleosin 2 was decreased 1.8-fold in the *sir1-1* seed proteome compared to wild-type. Oleosins are the most abundant proteins in the lipid monolayer of oil bodies (Murphy, 1993).

Suppression of oleosin biosynthesis in seeds, increases the protein accumulation and decreases the lipid weight in an almost compensatory way, so that the total weight of seed protein and oil in combination remained constant (Siloto et al., 2006), a situation similar to *sir1-1* seed composition. In Arabidopsis seeds, there are four genes encoding for oleosins. All oleosin proteins are free of cysteine. The oleosin 2 isoform is the one with the highest methionine content (4.5%), while the other three contain 2.6 to 2.9% methionine. The lack of reduced sulfur could be responsible for the down-regulation of this isoform. Interestingly, it was shown that germination rates were positively associated with oleosin levels, suggesting that defects in germination are related to oleosin deficiency (Shimada et al., 2008).

Among the non-storage proteins that were affected in the proteome of *sir1-1*, fructose-bisphosphate aldolase, endolase, and glyceraldehyde 3-phosphate dehydrogenase were accumulated. All three are involved in catalyzing reactions of glycolysis and gluconeogenesis. With respect to the reduction of oil content and unchanged NCS ratios in *sir1-1* seeds (Khan, 2008), the detected up-regulation of these enzymes for synthesis or degradation of sugars could be a compensatory reaction of *sir1-1* seeds.

A possibility to get more insight in the supplying role of maternal tissue for *sir1-1* seeds, is a proteomic evaluation of seeds produced by hydroponically grown *sir1-1* plants in comparison to wild-type plants.

The sulfate levels of the hydroponically grown plants must be determined. Since the assumed high sulfate amounts provided by the hydroponical system (500 μM) enhance seed production of *sir1-1* plants to wild-type levels, it would be of major interest to compare the seed proteomes of wild-type and *sir1-1* with the evaluated seed proteomes of soil-grown plants in this study. Indeed, the strong reduction of seed production in *sir1-1* grown under -S conditions, support the hypothesis that the high sulfate accumulation is required for *sir1-1* to grow and develop and set viable seeds. The slower growth makes it possible for *sir1-1* to produce the required metabolites before setting seeds.

References

- Akashi, T., Matsumura, T., Ideguchi, T., Iwakiri, K.-i., Kawakatsu, T., Taniguchi, I., and Hase, T.** (1999). Comparison of the electrostatic binding sites on the surface of ferredoxin for two ferredoxin-dependent enzymes, ferredoxin-NADP⁺ reductase and sulfite reductase. *J Biol Chem* **274**, 29399-29405.
- Alexander, M.P.** (1969). Differential staining of aborted and nonaborted pollen. *Stain Technol* **44**, 117-122.
- Alipazaga, M.V., Moreno, R.G.M., Linares, E., Medeiros, M.H.G., and Coichev, N.** (2008). DNA damage by sulfite autoxidation catalyzed by cobalt complexes. *Dalton Trans*, 5636-5644.
- Allboje Samami, A., Nunes-Nesi, A., Wirtz, M., and Hell, R.** Comparative analysis of amino acids from arabidopsis wild-type and mutant *sir1-1* leaves by reverse-phase high-pressure liquid chromatography (HPLC) and gas chromatography-mass spectrometry (GC-MS). In *Sulfur metabolism in plants: mechanisms and application to food security, and responses to climate change*, L.J. De Kok, M. Tausz, M.J. Hawkesford, R. Höfgen, M.T. McManus, R.M. Norton, H. Rennenberg, K. Saito, E. Schnug, and L. Tabe, eds, (submitted).
- Andre, C., Froehlich, J.E., Moll, M.R., and Benning, C.** (2007). A heteromeric plastidic pyruvate kinase complex involved in seed oil biosynthesis in Arabidopsis. *Plant Cell* **19**, 2006-2022.
- Arnon, D.I.** (1949). Copper enzymes in isolated chloroplasts. polyphenoloxidase in *Beta vulgaris*. *Plant Physiol* **24**, 1-15.
- Avonce, N., Leyman, B., Mascorro-Gallardo, J.O., Van Dijck, P., Thevelein, J.M., and Iturriaga, G.** (2004). The Arabidopsis trehalose-6-P synthase *AtTPS1* gene is a regulator of glucose, abscisic acid, and stress signaling. *Plant Physiol* **136**, 3649-3659.
- Awazuhara, M., Fujiwara, T., Hayashi, H., Watanabe-Takahashi, A., Takahashi, H., and Saito, K.** (2005). The function of SULTR2;1 sulfate transporter during seed development in *Arabidopsis thaliana*. *Physiol Plantarum* **125**, 95-105.
- Balharay, G.J.E., and Nicholas, J.D.J.** (1970). ATP sulfurylase in spinach leaves. *Biochim Biophys Acta* **220**, 513-524.
- Barton, K.A., Thompson, J.F., Madison, J.T., Rosenthal, R., Jarvis, N.P., and Beachy, R.N.** (1982). The biosynthesis and processing of high molecular weight precursors of soybean glycinin subunits. *J Biol Chem* **257**, 6089-6095.
- Bates, P.D., Durrett, T.P., Ohlrogge, J.B., and Pollard, M.** (2009). Analysis of acyl fluxes through multiple pathways of triacylglycerol synthesis in developing soybean embryos. *Plant Physiol* **150**, 55-72.
- Baud, S., and Lepiniec, L.** (2010). Physiological and developmental regulation of seed oil production. *Prog Lipid Res* **49**, 235-249.
- Baud, S., Boutin, J.-P., Miquel, M., Lepiniec, L., and Rochat, C.** (2002). An integrated overview of seed development in *Arabidopsis thaliana* ecotype WS. *Plant Physiol Bioch* **40**, 151-160.
- Baud, S., Dubreucq, B., Miquel, M., Rochat, C., and Lepiniec, L.** (2008). Storage reserve accumulation in Arabidopsis: Metabolic and developmental control of seed filling. *The Arabidopsis Book*, e0113.
- Baud, S., Wuillème, S., Dubreucq, B., De Almeida, A., Vuagnat, C., Lepiniec, L., Miquel, M., and Rochat, C.** (2007). Function of

- plastidial pyruvate kinases in seeds of *Arabidopsis thaliana*. *Plant J* **52**, 405-419.
- Beinert, H., Holm, R.H., and Munck, E.** (1997). Iron-sulfur clusters: nature's modular, multipurpose structures. *Science* **277**, 653-659.
- Bell, C.S., Cram, W.J., and Clarkson, D.T.** (1994). Compartmental analysis of $^{35}\text{SO}_4^{2-}$ exchange kinetics in roots and leaves of a tropical legume *Macroptilium atropurpureum* cv. Siratro. *J Exp Bot* **45**, 879-886.
- Benning, C.** (1998). Biosynthesis and function of the sulfolipid sulfoquinovosyl diacylglycerol. *Annu Rev Plant Phys* **49**, 53-75.
- Bertagnolli, B.L., and Wedding, R.T.** (1977). Purification and initial kinetic characterization of different forms of *O*-acetylserine sulfhydrylase from seedlings of two species of *Phaseolus*. *Plant Physiol* **60**, 115-121.
- Bevan, M., Bancroft, I., Bent, E., Love, K., Goodman, H., Dean, C., Bergkamp, R., Dirkse, W., Van Staveren, M., Stiekema, W., Drost, L., Ridley, P., Hudson, S.A., Patel, K., Murphy, G., Piffanelli, P., Wedler, H., Wedler, E., Wambutt, R., Weitzenegger, T., Pohl, T.M., Terryn, N., Gielen, J., Villarroel, R., De Clerck, R., Van Montagu, M., Lecharny, A., Auborg, S., Gy, I., Kreis, M., Lao, N., Kavanagh, T., Hempel, S., Kotter, P., Entian, K.D., Rieger, M., Schaeffer, M., Funk, B., Mueller-Auer, S., Silvey, M., James, R., Montfort, A., Pons, A., Puigdomenech, P., Douka, A., Voukelatou, E., Milioni, D., Hatzopoulos, P., Piravandi, E., Obermaier, B., Hilbert, H., Dusterhoft, A., Moores, T., Jones, J.D., Eneva, T., Palme, K., Benes, V., Rechman, S., Ansorge, W., Cooke, R., Berger, C., Delseny, M., Voet, M., Volckaert, G., Mewes, H.W., Klosterman, S., Schueller, C., and Chalwatzis, N.** (1998). Analysis of 1.9 Mb of contiguous sequence from chromosome 4 of *Arabidopsis thaliana*. *Nature* **391**, 485-488.
- Bick, J.A., Aslund, F., Chen, Y., and Leustek, T.** (1998). Glutaredoxin function for the carboxyl-terminal domain of the plant-type 5'-adenylylsulfate reductase. *P Natl Acad Sci USA* **95**, 8404-8409.
- Bogdanova, N., and Hell, R.** (1997). Cysteine synthesis in plants: protein-protein interactions of serine acetyltransferase from *Arabidopsis thaliana*. *Plant J* **11**, 251-262.
- Bogdanova, N., Bork, C., and Hell, R.** (1995). Cysteine biosynthesis in plants: isolation and functional identification of a cDNA encoding a serine acetyltransferase from *Arabidopsis thaliana*. *FEBS Lett* **358**, 43-47.
- Bonner, E.R., Cahoon, R.E., Knapke, S.M., and Jez, J.M.** (2005). Molecular basis of cysteine biosynthesis in plants: structural and functional analysis of *O*-acetylserine sulfhydrylase from *Arabidopsis thaliana*. *J Biol Chem* **280**, 38803-38813.
- Bork, C., Schwenn, J.D., and Hell, R.** (1998). Isolation and characterization of a gene for assimilatory sulfite reductase from *Arabidopsis thaliana*. *Gene* **212**, 147-153.
- Boyes, D.C., Zayed, A.M., Ascenzi, R., McCaskill, A.J., Hoffman, N.E., Davis, K.R., and Grolach, J.** (2001). Growth stage-based phenotypic analysis of *Arabidopsis*: a model for high throughput functional genomics in plants. *Plant Cell* **13**, 1499-1510.
- Bradford, M.M.** (1976). A rapid and sensitive method for the quantitation of microgram quantities of protein utilizing the principle of protein-dye binding. *Anal Biochem* **72**, 248-254.

- Brown, L., Scholefield, D., Jewkes, E.C., Preedy, N., Wadge, K., and Butler, M.** (2000). The effect of sulphur application on the efficiency of nitrogen use in two contrasting grassland soils. *J Agr Sci* **135**, 131-138.
- Brühl, A., Haverkamp, T., Gisselmann, G., and Schwenn, J.D.** (1996). A cDNA clone from *Arabidopsis thaliana* encoding plastidic ferredoxin: sulfite reductase. *Biochim Biophys Acta* **1295**, 119-124.
- Brunold, C., and Suter, M.** (1984). Regulation of sulfate assimilation by nitrogen nutrition in the duckweed *Lemna minor* L. *Plant Physiol* **76**, 579-583.
- Brunold, C., and Suter, M.** (1989). Localization of enzymes of assimilatory sulfate reduction in pea roots. *Planta* **179**, 228-234.
- Brunold, C., and Suter, M.** (1990). Adenosine 5'-phosphosulfate sulfotransferase. In *Methods in plant biochemistry*, P. Lea, ed (London: Academic Press), pp. 339-343.
- Brychkova, G., Xia, Z., Yang, G., Yesbergenova, Z., Zhang, Z., Davydov, O., Fluhr, R., and Sagi, M.** (2007). Sulfite oxidase protects plants against sulfur dioxide toxicity. *Plant J* **50**, 696-709.
- Buchner, P., Takahashi, H., and Hawkesford, M.J.** (2004). Plant sulphate transporters: co-ordination of uptake, intracellular and long-distance transport. *J Exp Bot* **55**, 1765-1773.
- Bullock, W.O., Fernandez, J.M., and Short, J.M.** (1987). XL1-Blue: a high efficiency plasmid transforming *recA Escherichia coli* strain with betagalactosidase selection. *Biotechniques* **5**, 376-379.
- Burke, J.J., Holloway, P., and Dalling, M.J.** (1986). The effect of sulfur deficiency on the organisation and photosynthetic capability of wheat leaves. *J Plant Physiol* **125**, 371-375.
- Burkhard, P., Tai, C.H., Ristroph, C.M., Cook, P.F., and Jansonius, J.N.** (1999). Ligand binding induces a large conformational change in *O*-acetylserine sulfhydrylase from *Salmonella typhimurium*. *J Mol Biol* **291**, 941-953.
- Burkhard, P., Rao, G.S., Hohenester, E., Schnackerz, K.D., Cook, P.F., and Jansonius, J.N.** (1998). Three-dimensional structure of *O*-acetylserine sulfhydrylase from *Salmonella typhimurium*. *J Mol Biol* **283**, 121-133.
- Cairns, N.G., Pasternak, M., Wachter, A., Cobbett, C.S., and Meyer, A.J.** (2006). Maturation of *Arabidopsis* seeds is dependent on glutathione biosynthesis within the embryo. *Plant Physiol* **141**, 446-455.
- Campanini, B., Speroni, F., Salsi, E., Cook, P.F., Roderick, S.L., Huang, B., Bettati, S., and Mozzarelli, A.** (2005). Interaction of serine acetyltransferase with *O*-acetylserine sulfhydrylase active site: evidence from fluorescence spectroscopy. *Protein Sci* **14**, 2115-2124.
- Cao, Y.-z., and Huang, A.H.C.** (1986). Diacylglycerol acyltransferase in maturing oil seeds of maize and other species. *Plant Physiol* **82**, 813-820.
- Cao, Y.-Z., and Huang, A.H.C.** (1987). Acyl coenzyme A preference of diacylglycerol acyltransferase from the maturing seeds of *Cuphea*, maize, rapeseed, and Canola. *Plant Physiol* **84**, 762-765.
- Chang, S., Puryear, J., and Cairney, J.** (1993). A simple and efficient method for isolating RNA from pine trees. *Plant Mol Biol Rep* **11**, 113-116.
- Clarkson, D.T., and Hawkesford, M.J.** (1993). Molecular biological approaches to plant nutrition. In *Plant nutrition - from genetic engineering to field practice*, N.J. Barrow, ed (Dordrecht: Kluwer Academic Publishers), pp. 23-33.

- Clough, S.J., and Bent, A.F.** (1998). Floral dip: a simplified method for *Agrobacterium*-mediated transformation of *Arabidopsis thaliana*. *Plant J* **16**, 735-743.
- Clouse, S.D., and Sasse, J.M.** (1998). Brassinosteroids: essential regulators of plant growth and development. *Annu Rev Plant Phys* **49**, 427-451.
- Clouse, S.D., Langford, M., and McMorris, T.C.** (1996). A brassinosteroid-insensitive mutant in *Arabidopsis thaliana* exhibits multiple defects in growth and development. *Plant Physiol* **111**, 671-678.
- Crane, B.R., Siegel, L.M., and Getzoff, E.D.** (1995). Sulfite reductase structure at 1.6 Å: evolution and catalysis for reduction of inorganic anions. *Science* **270**, 59-67.
- Curtis, M.D., and Grossniklaus, U.** (2003). A gateway cloning vector set for high-throughput functional analysis of genes in planta. *Plant Physiol* **133**, 462-469.
- D'Hondt, K., Van Damme, J., Van Den Bossche, C., Leejeerajumnean, S., De Rycke, R., Derksen, J., Vandekerckhove, J., and Krebbers, E.** (1993). Studies of the role of the propeptides of the *Arabidopsis thaliana* 2S albumin. *Plant Physiol* **102**, 425-433.
- Davidian, J.C., and Kopriva, S.** (2010). Regulation of sulfate uptake and assimilation--the same or not the same? *Mol Plant* **3**, 314-325.
- Desikan, R., Neill, S.J., and Hancock, J.T.** (2000). Hydrogen peroxide-induced gene expression in *Arabidopsis thaliana*. *Free Radical Bio Med* **28**, 773-778.
- Devoto, A., Ellis, C., Magusin, A., Chang, H.-S., Chilcott, C., Zhu, T., and Turner, J.** (2005). Expression profiling reveals COI1 to be a key regulator of genes involved in wound- and methyl jasmonate-induced secondary metabolism, defence, and hormone interactions. *Plant Mol Biol* **58**, 497-513.
- Dhankher, O.P., Li, Y., Rosen, B.P., Shi, J., Salt, D., Senecoff, J.F., Sashti, N.A., and Meagher, R.B.** (2002). Engineering tolerance and hyperaccumulation of arsenic in plants by combining arsenate reductase and \square -glutamylcysteine synthetase expression. *Nat Biotechnol* **20**, 1140-1145.
- Dietz, K.-J.** (1989). Recovery of spinach leaves from sulfate and phosphate deficiency. *J Plant Physiol* **134**, 551-557.
- Droux, M.** (2004). Sulfur assimilation and the role of sulfur in plant metabolism: a survey. *Photosynth Res* **79**, 331-348.
- Droux, M., Martin, J., Sajus, P., and Douce, R.** (1992). Purification and characterization of *O*-acetylserine (thiol) lyase from spinach chloroplasts. *Arch Biochem Biophys* **295**, 379-390.
- Droux, M., Ruffet, M.L., Douce, R., and Job, D.** (1998). Interactions between serine acetyltransferase and *O*-acetylserine (thiol) lyase in higher plants-structural and kinetic properties of the free and bound enzymes. *Eur J Biochem* **255**, 235-245.
- Ebell, L.F.** (1969). Specific total starch determinations in conifer tissues with glucose oxidase. *Phytochemistry* **8**, 25-36.
- Edwards, K., Johnstone, C., and Thompson, C.** (1991). A simple and rapid method for the preparation of plant genomic DNA for PCR analysis. *Nucleic Acids Res* **19**, 1349.
- Eilers, T., Schwarz, G., Brinkmann, H., Witt, C., Richter, T., Nieder, J., Koch, B., Hille, R., Hansch, R., and Mendel, R.R.** (2001). Identification and biochemical characterization of *Arabidopsis thaliana*

- sulfite oxidase. A new player in plant sulfur metabolism. *J Biol Chem* **276**, 46989-46994.
- Eimert, K., Wang, S.M., Lue, W.I., and Chen, J.** (1995). Monogenic recessive mutations causing both late floral initiation and excess starch accumulation in *Arabidopsis*. *Plant Cell* **7**, 1703-1712.
- Fahey, R.C., Newton, G.L., Dorian, R., and Kosower, E.M.** (1981). Analysis of biological thiols: quantitative determination of thiols at the picomole level based upon derivatization with monobromobimanes and separation by cation-exchange chromatography. *Anal Biochem* **111**, 357-365.
- Fait, A., Angelovici, R., Less, H., Ohad, I., Urbanczyk-Wochniak, E., Fernie, A.R., and Galili, G.** (2006). *Arabidopsis* seed development and germination is associated with temporally distinct metabolic switches. *Plant Physiol* **142**, 839-854.
- Flügge, U.I., Fischer, K., Gross, A., Sebald, W., Lottspeich, F., and Eckerskorn, C.** (1989). The triose phosphate-3-phosphoglycerate-phosphate translocator from spinach chloroplasts: nucleotide sequence of a full-length cDNA clone and import of the in vitro synthesized precursor protein into chloroplasts. *EMBO J* **8**, 39-46.
- Francois, J.A., Kumaran, S., and Jez, J.M.** (2006). Structural basis for interaction of *O*-acetylserine sulfhydrylase and serine acetyltransferase in the *Arabidopsis* cysteine synthase complex. *Plant Cell* **18**, 3647-3655.
- Freney, J.R., Spencer, K., and Jones, M.B.** (1978). The diagnosis of sulphur deficiency in wheat. *Aust J Agr Res* **29**, 727-738.
- Gaitonde, M.K.** (1967). A spectrophotometric method for the direct determination of cysteine in the presence of other naturally occurring amino acids. *Biochem J* **104**, 627-633.
- Gallardo, K., Job, C., Groot, S.P., Puype, M., Demol, H., Vandekerckhove, J., and Job, D.** (2002). Proteomics of *Arabidopsis* seed germination. A comparative study of wild-type and gibberellin-deficient seeds. *Plant Physiol* **129**, 823-837.
- Gallardo, K., Firnhaber, C., Zuber, H., Hericher, D., Belghazi, M., Henry, C., Kuster, H., and Thompson, R.** (2007). A combined proteome and transcriptome analysis of developing *Medicago truncatula* seeds: evidence for metabolic specialization of maternal and filial tissues. *Mol Cell Proteomics* **6**, 2165-2179.
- Gamet-Payraastre, L., Li, P., Lumeau, S., Cassar, G., Dupont, M.A., Chevolleau, S., Gasc, N., Tulliez, J., and Terce, F.** (2000). Sulforaphane, a naturally occurring isothiocyanate, induces cell cycle arrest and apoptosis in HT29 human colon cancer cells. *Cancer Res* **60**, 1426-1433.
- Gao, Y., Schofield, O.M., and Leustek, T.** (2000). Characterization of sulfate assimilation in marine algae focusing on the enzyme 5'-adenylylsulfate reductase. *Plant Physiol* **123**, 1087-1096.
- Gasber, A., Klaumann, S., Trentmann, O., Tramczynska, A., Clemens, S., Schneider, S., Sauer, N., Feifer, I., Bittner, F., Mendel, R.R., and Neuhaus, H.E.** (2011). Identification of an *Arabidopsis* solute carrier critical for intracellular transport and inter-organ allocation of molybdate. *Plant Biol* **13**, 710-718.
- Gidda, S.K., Miersch, O., Levitin, A., Schmidt, J., Wasternack, C., and Varin, L.** (2003). Biochemical and molecular characterization of a

- hydroxyjasmonate sulfotransferase from *Arabidopsis thaliana*. *J Biol Chem* **278**, 17895-17900.
- Gillespie, J., Rogers, S.W., Deery, M., Dupree, P., and Rogers, J.C.** (2005). A unique family of proteins associated with internalized membranes in protein storage vacuoles of the Brassicaceae. *Plant J* **41**, 429-441.
- Giovanelli, J., Mudd, S.H., and Datko, A.H.** (1980). Sulfur amino acids in plants. In *The biochemistry of plants*, B.J. Mifflin, ed (New York: Academic Press), pp. 453-505.
- Goloubinoff, P., Gatenby, A.A., and Lorimer, G.H.** (1989a). GroE heat-shock proteins promote assembly of foreign prokaryotic ribulose biphosphate carboxylase oligomers in *Escherichia coli*. *Nature* **337**, 44-47.
- Goloubinoff, P., Christeller, J.T., Gatenby, A.A., and Lorimer, G.H.** (1989b). Reconstitution of active dimeric ribulose biphosphate carboxylase from an unfolded state depends on two chaperonin proteins and Mg-ATP. *Nature* **342**, 884-889.
- Gómez, L.D., Baud, S., Gilday, A., Li, Y., and Graham, I.A.** (2006). Delayed embryo development in the *ARABIDOPSIS TREHALOSE-6-PHOSPHATE SYNTHASE 1* mutant is associated with altered cell wall structure, decreased cell division and starch accumulation. *Plant J* **46**, 69-84.
- Gorman, J., and Shapiro, L.** (2004). Structure of serine acetyltransferase from *Haemophilus influenzae* Rd. *Acta Crystallogr D* **60**, 1600-1605.
- Graser, G., Oldham, N.J., Brown, P.D., Temp, U., and Gershenzon, J.** (2001). The biosynthesis of benzoic acid glucosinolate esters in *Arabidopsis thaliana*. *Phytochemistry* **57**, 23-32.
- Grill, E., Löffler, S., Winnacker, E.L., and Zenk, M.H.** (1989). Phytochelatins, the heavy-metal-binding peptides of plants, are synthesized from glutathione by a specific gamma-glutamylcysteine dipeptidyl transpeptidase (phytochelatin synthase). *P Natl Acad Sci USA* **86**, 6838-6842.
- Gruis, D., Schulze, J., and Jung, R.** (2004). Storage protein accumulation in the absence of the vacuolar processing enzyme family of cysteine proteases. *Plant Cell* **16**, 270-290.
- Gruis, D.F., Selinger, D.A., Curran, J.M., and Jung, R.** (2002). Redundant proteolytic mechanisms process seed storage proteins in the absence of seed-type members of the vacuolar processing enzyme family of cysteine proteases. *Plant Cell* **14**, 2863-2882.
- Guerche, P., Tire, C., De Sa, F.G., De Clercq, A., Van Montagu, M., and Krebbers, E.** (1990). Differential expression of the Arabidopsis 2S albumin genes and the effect of increasing gene family size. *Plant Cell* **2**, 469-478.
- Gutierrez-Marcos, J.F., Roberts, M.A., Campbell, E.I., and Wray, J.L.** (1996). Three members of a novel small gene-family from *Arabidopsis thaliana* able to complement functionally an *Escherichia coli* mutant defective in PAPS reductase activity encode proteins with a thioredoxin-like domain and "APS reductase" activity. *P Natl Acad Sci USA* **93**, 13377-13382.
- Haas, F.H.** (2010). Dual function of the cysteine synthase complex in mitochondria from *Arabidopsis thaliana* (Dissertation, Heidelberg: Ruperto-Carola University of Heidelberg).

- Haas, F.H., Heeg, C., Queiroz, R., Bauer, A., Wirtz, M., and Hell, R.** (2008). Mitochondrial serine acetyltransferase functions as a pacemaker of cysteine synthesis in plant cells. *Plant Physiol* **148**, 1055-1067.
- Hänsch, R., Lang, C., Riebeseel, E., Lindigkeit, R., Gessler, A., Rennenberg, H., and Mendel, R.R.** (2006). Plant sulfite oxidase as novel producer of H₂O₂ - combination of enzyme catalysis with a subsequent non-enzymatic reaction step. *J Biol Chem* **281**, 6884-6888.
- Hanzawa, Y., Imai, A., Michael, A.J., Komeda, Y., and Takahashi, T.** (2002). Characterization of the spermidine synthase-related gene family in *Arabidopsis thaliana*. *FEBS Lett* **527**, 176-180.
- Harder, A., Wildgruber, R., Nawrocki, A., Fey, S.J., Mose Larsen, P., and Görg, A.** (1999). Comparison of yeast cell protein solubilization procedures for two-dimensional electrophoresis. *Electrophoresis* **20**, 826-829.
- Hartmann, T., Honicke, P., Wirtz, M., Hell, R., Rennenberg, H., and Kopriva, S.** (2004). Regulation of sulphate assimilation by glutathione in poplars (*Populus tremula* x *P. alba*) of wild type and overexpressing □-glutamylcysteine synthetase in the cytosol. *J Exp Bot* **55**, 837-845.
- Harwood, J.L.** (1996). Recent advances in the biosynthesis of plant fatty acids. *BBA-Lipid Met* **1301**, 7-56.
- Hatzfeld, Y., Lee, S., Lee, M., Leustek, T., and Saito, K.** (2000a). Functional characterization of a gene encoding a fourth ATP sulfurylase isoform from *Arabidopsis thaliana*. *Gene* **248**, 51-58.
- Hatzfeld, Y., Maruyama, A., Schmidt, A., Noji, M., Ishizawa, K., and Saito, K.** (2000b). □-Cyanoalanine synthase is a mitochondrial cysteine synthase-like protein in spinach and *Arabidopsis*. *Plant Physiol* **123**, 1163-1172.
- Haughn, G.W., and Somerville, C.** (1986). Sulfonylurea-resistant mutants of *Arabidopsis thaliana*. *Mol Gen Genet* **204**, 430-434.
- Hawkesford, M.J.** (2003). Transporter gene families in plants: the sulphate transporter gene family redundancy or specialization? *Physiol Plantarum* **117**, 155-163.
- Hawkesford, M.J., and Smith, F.W.** (1997). Molecular biology of plant sulphate transporters. In *Sulphur metabolism in higher plants. Molecular, ecophysiological and nutritional aspects*, W.J. Cram, L.J. De Kok, I. Stulen, C. Brunold, and H. Rennenberg, eds (Leiden: Backhuys Publ.), pp. 13-26.
- Hawkesford, M.J., and Wray, J.L.** (2000). Molecular genetics of sulphate assimilation. *Adv. Bot. Res.* **33**, 159-223.
- Heeg, C., Kruse, C., Jost, R., Gutensohn, M., Ruppert, T., Wirtz, M., and Hell, R.** (2008). Analysis of the *Arabidopsis* O-acetylserine(thiol)lyase gene family demonstrates compartment-specific differences in the regulation of cysteine synthesis. *Plant Cell* **20**, 168-185.
- Hell, R.** (1997). Molecular physiology of plant sulfur metabolism. *Planta* **202**, 138-148.
- Hell, R.** (1998). *Molekulare Physiologie des Primärstoffwechsels von Schwefel in Pflanzen.* (Aachen: Shaker).
- Hell, R., Jost, R., Berkowitz, O., and Wirtz, M.** (2002). Molecular and biochemical analysis of the enzymes of cysteine biosynthesis in the plant *Arabidopsis thaliana*. *Amino Acids* **22**, 245-257.

- Hesse, H., Nikiforova, V., Gakiere, B., and Hoefgen, R. (2004). Molecular analysis and control of cysteine biosynthesis: integration of nitrogen and sulphur metabolism. *J Exp Bot* **55**, 1283-1292.
- Hesse, H., Trachsel, N., Suter, M., Kopriva, S., von Ballmoos, P., Rennenberg, H., and Brunold, C. (2003). Effect of glucose on assimilatory sulphate reduction in *Arabidopsis thaliana* roots. *J Exp Bot* **54**, 1701-1709.
- Higashi, Y., Hirai, M.Y., Fujiwara, T., Naito, S., Noji, M., and Saito, K. (2006). Proteomic and transcriptomic analysis of *Arabidopsis* seeds: molecular evidence for successive processing of seed proteins and its implication in the stress response to sulfur nutrition. *Plant J* **48**, 557-571.
- Hillmer, S., Movafeghi, A., Robinson, D.G., and Hinz, G. (2001). Vacuolar storage proteins are sorted in the cis-cisternae of the pea cotyledon Golgi apparatus. *J Cell Biol* **152**, 41-50.
- Hiraiwa, N., Kondo, M., Nishimura, M., and Hara-Nishimura, I. (1997). An aspartic endopeptidase is involved in the breakdown of propeptides of storage proteins in protein-storage vacuoles of plants. *Eur J Biochem* **246**, 133-141.
- Honda, C., Fujiwara, T., and Chino, M. (1998). Sulfate uptake in *Arabidopsis thaliana*. *J Plant Nutr* **21**, 601-614.
- Hood, E.E., Love, R., Lane, J., Bray, J., Clough, R., Pappu, K., Drees, C., Hood, K.R., Yoon, S., Ahmad, A., and Howard, J.A. (2007). Subcellular targeting is a key condition for high-level accumulation of cellulase protein in transgenic maize seed. *Plant Biotechnol J* **5**, 709-719.
- Howarth, J.R., Roberts, M.A., and Wray, J.L. (1997). Cysteine biosynthesis in higher plants: a new member of the *Arabidopsis thaliana* serine acetyltransferase small gene-family obtained by functional complementation of an *Escherichia coli* cysteine auxotroph. *Biochim Biophys Acta* **1350**, 123-127.
- Howden, R., Andersen, C.R., Goldsbrough, P.B., and Cobbett, C.S. (1995). A cadmium-sensitive, glutathione-deficient mutant of *Arabidopsis thaliana*. *Plant Physiol* **107**, 1067-1073.
- Huang, A.H.C. (1992). Oil bodies and oleosins in seeds. *Annu Rev Plant Phys* **43**, 177-200.
- Huang, B., Vetting, M.W., and Roderick, S.L. (2005). The active site of *O*-acetylserine sulfhydrylase is the anchor point for bienzyme complex formation with serine acetyltransferase. *J Bacteriol* **187**, 3201-3205.
- Ihaka, R., and Gentleman, R. (1996). R: A language for data analysis and graphics. *J Comput Graph Stat* **5**, 299-314.
- Imai, A., Matsuyama, T., Hanzawa, Y., Akiyama, T., Tamaoki, M., Saji, H., Shirano, Y., Kato, T., Hayashi, H., Shibata, D., Tabata, S., Komeda, Y., and Takahashi, T. (2004). Spermidine synthase genes are essential for survival of *Arabidopsis*. *Plant Physiol* **135**, 1565-1573.
- Imsande, J. (1998). Iron, sulfur, and chlorophyll deficiencies: a need for an integrative approach in plant physiology. *Physiol Plantarum* **103**, 139-144.
- Ito, H., Iwabuchi, M., and Ogawa, K.i. (2003). The sugar-metabolic enzymes aldolase and triose-phosphate isomerase are targets of glutathionylation in *Arabidopsis thaliana*: detection using biotinylated glutathione. *Plant Cell Physiol* **44**, 655-660.
- Ito, K., and Kawanishi, S. (1991). Site-specific fragmentation and modification of albumin by sulfite in the presence of metal ions or

- peroxidase/H₂O₂: role of sulfate radical. *Biochem Bioph Res Co* **176**, 1306-1312.
- Johnston, M.L., Luethy, M.H., Miernyk, J.A., and Randall, D.D.** (1997). Cloning and molecular analyses of the *Arabidopsis thaliana* plastid pyruvate dehydrogenase subunits. *BBA-Bioenergetics* **1321**, 200-206.
- Jornot, L., Petersen, H., and Junod, A.F.** (1998). Hydrogen peroxide-induced DNA damage is independent of nuclear calcium but dependent on redox-active ions. *Biochem J* **335 (Pt 1)**, 85-94.
- Jost, R., Altschmied, L., Bloem, E., Bogs, J., Gershenzon, J., Hahnel, U., Hansch, R., Hartmann, T., Kopriva, S., Kruse, C., Mendel, R.R., Papenbrock, J., Reichelt, M., Rennenberg, H., Schnug, E., Schmidt, A., Textor, S., Tokuhisa, J., Wachter, A., Wirtz, M., Rausch, T., and Hell, R.** (2005). Expression profiling of metabolic genes in response to methyl jasmonate reveals regulation of genes of primary and secondary sulfur-related pathways in *Arabidopsis thaliana*. *Photosynth Res* **86**, 491-508.
- Kataoka, T., Hayashi, N., Yamaya, T., and Takahashi, H.** (2004a). Root-to-shoot transport of sulfate in *Arabidopsis*. Evidence for the role of SULTR3;5 as a component of low-affinity sulfate transport system in the root vasculature. *Plant Physiol* **136**, 4198-4204.
- Kataoka, T., Watanabe-Takahashi, A., Hayashi, N., Ohnishi, M., Mimura, T., Buchner, P., Hawkesford, M.J., Yamaya, T., and Takahashi, H.** (2004b). Vacuolar sulfate transporters are essential determinants controlling internal distribution of sulfate in *Arabidopsis*. *Plant Cell* **16**, 2693-2704.
- Kawanishi, S., Hiraku, Y., and Oikawa, S.** (2001). Mechanism of guanine-specific DNA damage by oxidative stress and its role in carcinogenesis and aging. *Mutat Res-Rev Mutat* **488**, 65-76.
- Kawashima, C.G., Berkowitz, O., Hell, R., Noji, M., and Saito, K.** (2005). Characterization and expression analysis of a serine acetyltransferase gene family involved in a key step of the sulfur assimilation pathway in *Arabidopsis*. *Plant Physiol* **137**, 220-230.
- Kennedy, E.P.** (1961). Biosynthesis of complex lipids. *Fed Proc* **20**, 934-940.
- Khan, M.S.** (2008). The role of sulfite reductase in assimilatory sulfate reduction in *Arabidopsis thaliana* (Dissertation, Heidelberg: Ruperto-Carola University of Heidelberg).
- Khan, M.S., Haas, F.H., Allboje Samami, A., Gholami, A.M., Bauer, A., Fellenberg, K., Reichelt, M., Hansch, R., Mendel, R.R., Meyer, A.J., Wirtz, M., and Hell, R.** (2010). Sulfite reductase defines a newly discovered bottleneck for assimilatory sulfate reduction and is essential for growth and development in *Arabidopsis thaliana*. *Plant Cell* **22**, 1216-1231.
- Kim, T.-W., Hwang, J.-Y., Kim, Y.-S., Joo, S.-H., Chang, S.C., Lee, J.S., Takatsuto, S., and Kim, S.-K.** (2005). *Arabidopsis* CYP85A2, a cytochrome P450, mediates the Baeyer-Villiger oxidation of castasterone to brassinolide in brassinosteroid biosynthesis. *Plant Cell* **17**, 2397-2412.
- King, S.P., Lunn, J.E., and Furbank, R.T.** (1997). Carbohydrate content and enzyme metabolism in developing canola siliques. *Plant Physiol* **114**, 153-160.
- Kinoshita, T., Nishimura, M., and Hara-Nishimura, I.** (1995a). The sequence and expression of the gamma-VPE gene, one member of a

- family of three genes for vacuolar processing enzymes in *Arabidopsis thaliana*. *Plant Cell Physiol* **36**, 1555-1562.
- Kinoshita, T., Nishimura, M., and Hara-Nishimura, I.** (1995b). Homologues of a vacuolar processing enzyme that are expressed in different organs in *Arabidopsis thaliana*. *Plant Mol Biol* **29**, 81-89.
- Kinoshita, T., Yamada, K., Hiraiwa, N., Kondo, M., Nishimura, M., and Hara-Nishimura, I.** (1999). Vacuolar processing enzyme is up-regulated in the lytic vacuoles of vegetative tissues during senescence and under various stressed conditions. *Plant J* **19**, 43-53.
- Klein, M., and Papenbrock, J.** (2004). The multi-protein family of *Arabidopsis* sulphotransferases and their relatives in other plant species. *J Exp Bot* **55**, 1809-1820.
- Kopriva, S.** (2006). Regulation of sulfate assimilation in *Arabidopsis* and beyond. *Ann Bot-London* **97**, 479-495.
- Kopriva, S., and Koprivova, A.** (2004). Plant adenosine 5'-phosphosulphate reductase: the past, the present, and the future. *J Exp Bot* **55**, 1775-1783.
- Kopriva, S., and Rennenberg, H.** (2004). Control of sulphate assimilation and glutathione synthesis: interaction with N and C metabolism. *J Exp Bot* **55**, 1831-1842.
- Kopriva, S., Patron, N., Keeling, P., and Leustek, T.** (2008). Phylogenetic analysis of sulfate assimilation and cysteine biosynthesis in phototrophic organisms. In *Sulfur metabolism in phototrophic organisms*, R. Hell, C. Dahl, and T. Leustek, eds (Dordrecht: Springer), pp. 33-60.
- Kopriva, S., Muheim, R., Koprivova, A., Trachsel, N., Catalano, C., Suter, M., and Brunold, C.** (1999). Light regulation of assimilatory sulphate reduction in *Arabidopsis thaliana*. *Plant J* **20**, 37-44.
- Kopriva, S., Buchert, T., Fritz, G., Suter, M., Benda, R., Schunemann, V., Koprivova, A., Schurmann, P., Trautwein, A.X., Kroneck, P.M., and Brunold, C.** (2002). The presence of an iron-sulfur cluster in adenosine 5'-phosphosulfate reductase separates organisms utilizing adenosine 5'-phosphosulfate and phosphoadenosine 5'-phosphosulfate for sulfate assimilation. *J Biol Chem* **277**, 21786-21791.
- Koprivova, A., Suter, M., den Camp, R.O., Brunold, C., and Kopriva, S.** (2000). Regulation of sulfate assimilation by nitrogen in *Arabidopsis*. *Plant Physiol* **122**, 737-746.
- Koralewska, A., Posthumus, F.S., Stuiver, C.E., Buchner, P., Hawkesford, M.J., and De Kok, L.J.** (2007). The characteristic high sulfate content in *Brassica oleracea* is controlled by the expression and activity of sulfate transporters. *Plant Biol* **9**, 654-661.
- Krebbes, E., Herdies, L., De Clercq, A., Seurinck, J., Leemans, J., Van Damme, J., Segura, M., Gheysen, G., Van Montagu, M., and Vandekerckhove, J.** (1988). Determination of the processing sites of an *Arabidopsis* 2S albumin and characterization of the complete gene family. *Plant Physiol* **87**, 859-866.
- Kredich, N.M.** (1996). Biosynthesis of cysteine. In *Escherichia coli* and *Salmonella typhimurium*. Cellular and molecular biology., F.C. Neidhardt, R. Curtiss, J.L. Ingraham, E.C.C. Lin, K.B. Low, B. Magasanik, W.S. Reznikoff, M. Riley, M. Schaechter, and E. Umberger, eds (Washington D.C.: ASM Press), pp. 514-527.
- Kredich, N.M., Becker, M.A., and Tomkins, G.M.** (1969). Purification and characterization of cysteine synthetase, a bifunctional protein complex, from *Salmonella typhimurium*. *J Biol Chem* **244**, 2428-2439.

- Krueger, R.J., and Siegel, L.M.** (1982). Evidence for siroheme-Fe₄S₄ interaction in spinach ferredoxin-sulfite reductase. *Biochemistry-US* **21**, 2905 - 2909.
- Laemmli, U.K.** (1970). Cleavage of structural proteins during the assembly of the head of bacteriophage T4. *Nature* **227**, 680-685.
- Lam, H.M., Wong, P., Chan, H.K., Yam, K.M., Chen, L., Chow, C.M., and Coruzzi, G.M.** (2003). Overexpression of the *ASN1* gene enhances nitrogen status in seeds of *Arabidopsis*. *Plant Physiol* **132**, 926-935.
- Lang, C., Popko, J., Wirtz, M., Hell, R., Herschbach, C., Kreuzwieser, J., Rennenberg, H., Mendel, R.R., and Hansch, R.** (2007). Sulphite oxidase as key enzyme for protecting plants against sulphur dioxide. *Plant Cell Environ* **30**, 447-455.
- Lappartient, A.G., and Touraine, B.** (1996). Demand-driven control of root ATP sulfurylase activity and SO₄²⁻ uptake in intact Canola. *Plant Physiol* **111**, 147-157.
- Lappartient, A.G., Vidmar, J.J., Leustek, T., Glass, A.D., and Touraine, B.** (1999). Inter-organ signaling in plants: regulation of ATP sulfurylase and sulfate transporter genes expression in roots mediated by phloem-translocated compound. *Plant J* **18**, 89-95.
- Lee, J.J., Woodward, A.W., and Chen, Z.J.** (2007). Gene expression changes and early events in cotton fibre development. *Ann Bot-London* **100**, 1391-1401.
- Lee, S., and Leustek, T.** (1998). APS kinase from *Arabidopsis thaliana*: genomic organization, expression, and kinetic analysis of the recombinant enzyme. *Biochem Bioph Res Co* **247**, 171-175.
- Lee, S., and Leustek, T.** (1999). The affect of cadmium on sulfate assimilation enzymes in *Brassica juncea*. *Plant Sci* **141**, 201-207.
- León, P., and Sheen, J.** (2003). Sugar and hormone connections. *Trends Plant Sci* **8**, 110-116.
- Leprince, O., van Aelst, A.C., Pritchard, H.W., and Murphy, D.J.** (1998). Oleosins prevent oil-body coalescence during seed imbibition as suggested by a low-temperature scanning electron microscope study of desiccation-tolerant and -sensitive oilseeds. *Planta* **204**, 109-119.
- Leustek, T., and Saito, K.** (1999). Sulfate transport and assimilation in plants. *Plant Physiol* **120**, 637-644.
- Leustek, T., Martin, M.N., Bick, J.-A., and Davies, J.P.** (2000). Pathways and regulation of sulfur metabolism revealed through molecular and genetic studies. *Ann Rev Plant Phys* **51**, 141-165.
- Li-Beisson, Y., Shorrosh, B., Beisson, F., Andersson, M.X., Arondel, V., Bates, P.D., Baud, S., Bird, D., DeBono, A., Durrett, T.P., Franke, R.B., Graham, I.A., Katayama, K., Kelly, A.A., Larson, T., Markham, J.E., Miquel, M., Molina, I., Nishida, I., Rowland, O., Samuels, L., Schmid, K.M., Wada, H., Welti, R., Xu, C., Zallot, R., and Ohlrogge, J.** (2010). Acyl-lipid metabolism. *The Arabidopsis Book*, e0133.
- Li, Q., Wang, B.C., Xu, Y., and Zhu, Y.X.** (2007). Systematic studies of 12S seed storage protein accumulation and degradation patterns during *Arabidopsis* seed maturation and early seedling germination stages. *J Biochem Mol Biol* **40**, 373-381.
- Li, Y., Beisson, F., Pollard, M., and Ohlrogge, J.** (2006). Oil content of *Arabidopsis* seeds: the influence of seed anatomy, light and plant-to-plant variation. *Phytochemistry* **67**, 904-915.

- Lillig, C.H., Schiffmann, S., Berndt, C., Berken, A., Tischka, R., and Schwenn, J.D.** (2001). Molecular and catalytic properties of *Arabidopsis thaliana* adenylate kinase (AK)-kinase. *Arch Biochem Biophys* **392**, 303-310.
- Lin, M., Behal, R., and Oliver, D.J.** (2003). Disruption of *ple2*, the gene for the E2 subunit of the plastid pyruvate dehydrogenase complex, in *Arabidopsis* causes an early embryo lethal phenotype. *Plant Mol Biol* **52**, 865-872.
- Lisec, J., Schauer, N., Kopka, J., Willmitzer, L., and Fernie, A.R.** (2006). Gas chromatography mass spectrometry-based metabolite profiling in plants. *Nat Protoc* **1**, 387-396.
- Liu, C., and Mehdy, M.C.** (2007). A nonclassical arabinogalactan protein gene highly expressed in vascular tissues, *AGP31*, is transcriptionally repressed by methyl jasmonic acid in *Arabidopsis*. *Plant Physiol* **145**, 863-874.
- Logan, H.M., Cathala, N., Grignon, C., and Davidian, J.C.** (1996). Cloning of a cDNA encoded by a member of the *Arabidopsis thaliana* ATP sulfurylase multigene family. Expression studies in yeast and in relation to plant sulfur nutrition. *J Biol Chem* **271**, 12227-12233.
- Lunn, J.E., Droux, M., Martin, J., and Douce, R.** (1990). Localization of ATP-sulfurylase and *O*-acetylserine(thiol)lyase in spinach leaves. *Plant Physiol* **94**, 1345-1352.
- Lutziger, I., and Oliver, D.J.** (2000). Molecular evidence of a unique lipoamide dehydrogenase in plastids: analysis of plastidic lipoamide dehydrogenase from *Arabidopsis thaliana*. *FEBS Lett* **484**, 12-16.
- Mackinney, G.** (1941). Absorption of light by chlorophyll solutions. *J Biol Chem* **140**, 315-322.
- Marles, M.A., Ray, H., and Gruber, M.Y.** (2003). New perspectives on proanthocyanidin biochemistry and molecular regulation. *Phytochemistry* **64**, 367-383.
- Maruyama-Nakashita, A., Nakamura, Y., Yamaya, T., and Takahashi, H.** (2004). Regulation of high-affinity sulphate transporters in plants: towards systematic analysis of sulphur signalling and regulation. *J Exp Bot* **55**, 1843-1849.
- Mathai, J.C., Missner, A., Kugler, P., Saparov, S.M., Zeidel, M.L., Lee, J.K., and Pohl, P.** (2009). No facilitator required for membrane transport of hydrogen sulfide. *P Natl Acad Sci USA* **106**, 16633-16638.
- Mathesius, U., Keijzers, G., Natera, S.H., Weinman, J.J., Djordjevic, M.A., and Rolfe, B.G.** (2001). Establishment of a root proteome reference map for the model legume *Medicago truncatula* using the expressed sequence tag database for peptide mass fingerprinting. *Proteomics* **1**, 1424-1440.
- May, M., Vernoux, T., Leaver, C., Van Montagu, M., and Inze, D.** (1998). Glutathione homeostasis in plants: implications for environmental sensing and plant development. *J Exp Bot* **49**, 649-667.
- McGrath, S.P., Zhao, F.J., and Blake-Kalff, M.M.A.** (2002). History and outlook for sulphur fertilisers in Europe. In *Proceeding of the international fertiliser society no. 497* (York: International Fertiliser Society), 1-22.
- Mengel, K.** (1991). *Ernährung und Stoffwechsel der Pflanze*. (Jena: G. Fischer Verlag).

- Meyer, A.J., and Fricker, M.D.** (2000). Direct measurement of glutathione in epidermal cells of intact *Arabidopsis* roots by two-photon laser scanning microscopy. *J Microsc-Oxford* **198**, 174-181.
- Meyer, A.J., Brach, T., Marty, L., Kreye, S., Rouhier, N., Jacquot, J.P., and Hell, R.** (2007). Redox-sensitive GFP in *Arabidopsis thaliana* is a quantitative biosensor for the redox potential of the cellular glutathione redox buffer. *Plant J* **52**, 973-986.
- Miersch, O., Neumerkel, J., Dippe, M., Stenzel, I., and Wasternack, C.** (2008). Hydroxylated jasmonates are commonly occurring metabolites of jasmonic acid and contribute to a partial switch-off in jasmonate signaling. *New Phytol* **177**, 114-127.
- Mino, K., Yamanoue, T., Sakiyama, T., Eisaki, N., Matsuyama, A., and Nakanishi, K.** (1999). Purification and characterization of serine acetyltransferase from *Escherichia coli* partially truncated at the C-terminal region. *Biosci Biotech Bioch* **63**, 168-179.
- Mino, K., Yamanoue, T., Sakiyama, T., Eisaki, N., Matsuyama, A., and Nakanishi, K.** (2000). Effects of bienzyme complex formation of cysteine synthetase from *Escherichia coli* on some properties and kinetics. *Biosci Biotech Bioch* **64**, 1628-1640.
- Molina, I., Bonaventure, G., Ohlrogge, J., and Pollard, M.** (2006). The lipid polyester composition of *Arabidopsis thaliana* and *Brassica napus* seeds. *Phytochemistry* **67**, 2597-2610.
- Molvig, L., Tabe, L.M., Eggum, B.O., Moore, A.E., Craig, S., Spencer, D., and Higgins, T.J.** (1997). Enhanced methionine levels and increased nutritive value of seeds of transgenic lupins (*Lupinus angustifolius* L.) expressing a sunflower seed albumin gene. *P Natl Acad Sci USA* **94**, 8393-8398.
- Mugford, S.G., Yoshimoto, N., Reichelt, M., Wirtz, M., Hill, L., Mugford, S.T., Nakazato, Y., Noji, M., Takahashi, H., Kramell, R., Gigolashvili, T., Flugge, U.I., Wasternack, C., Gershenzon, J., Hell, R., Saito, K., and Kopriva, S.** (2009). Disruption of adenosine-5'-phosphosulfate kinase in *Arabidopsis* reduces levels of sulfated secondary metabolites. *Plant Cell* **21**, 910-927.
- Muller, J.G., Hickerson, R.P., Perez, R.J., and Burrows, C.J.** (1997). DNA damage from sulfite autoxidation catalyzed by a nickel(II) peptide. *J Am Chem Soc* **119**, 1501-1506.
- Mullis, K., Faloona, F., Scharf, S., Saiki, R., Horn, G., and Erlich, H.** (1986). Specific enzymatic amplification of DNA in vitro: the polymerase chain reaction. *Cold Spring Harb Sym* **51**, 263-273.
- Murillo, M., Foglia, R., Diller, A., Lee, S., and Leustek, T.** (1995). Serine acetyltransferase from *Arabidopsis thaliana* can functionally complement the cysteine requirement of a *cysE* mutant strain of *Escherichia coli*. *Cell Mol Biol Res* **41**, 425-433.
- Murphy, D.J.** (1993). Structure, function and biogenesis of storage lipid bodies and oleosins in plants. *Prog Lipid Res* **32**, 247-280.
- Murphy, D.J., and Vance, J.** (1999). Mechanisms of lipid-body formation. *Trends Biochem Sci* **24**, 109-115.
- Müssig, C., Shin, G.-H., and Altmann, T.** (2003). Brassinosteroids promote root growth in *Arabidopsis*. *Plant Physiol* **133**, 1261-1271.
- Nakano, T., Suzuki, K., Ohtsuki, N., Tsujimoto, Y., Fujimura, T., and Shinshi, H.** (2006). Identification of genes of the plant-specific

- transcription-factor families cooperatively regulated by ethylene and jasmonate in *Arabidopsis thaliana*. *J Plant Res* **119**, 407-413.
- Nakayama, M., Akashi, T., and Hase, T.** (2000). Plant sulfite reductase: molecular structure, catalytic function and interaction with ferredoxin. *J Inorg Biochem* **82**, 27-32.
- Newton, G.L., Dorian, R., and Fahey, R.C.** (1981). Analysis of biological thiols: derivatization with monobromobimane and separation by reverse-phase high-performance liquid chromatography. *Anal Biochem* **114**, 383-387.
- Nikiforova, V., Freitag, J., Kempa, S., Adamik, M., Hesse, H., and Hoefgen, R.** (2003). Transcriptome analysis of sulfur depletion in *Arabidopsis thaliana*: interlacing of biosynthetic pathways provides response specificity. *Plant J* **33**, 633-650.
- Nikiforova, V.J., Kopka, J., Tolstikov, V., Fiehn, O., Hopkins, L., Hawkesford, M.J., Hesse, H., and Hoefgen, R.** (2005). Systems rebalancing of metabolism in response to sulfur deprivation, as revealed by metabolome analysis of *Arabidopsis* plants. *Plant Physiol* **138**, 304-318.
- Nishizawa, A., Yabuta, Y., and Shigeoka, S.** (2008). Galactinol and raffinose constitute a novel function to protect plants from oxidative damage. *Plant Physiol* **147**, 1251-1263.
- Noctor, G., and Foyer, C.H.** (1998). Ascorbate and glutathione: keeping active oxygen under control. *Annu Rev Plant Phys* **49**, 249-279.
- Noctor, G., Arisi, A., Jouanin, L., Kunert, K., Rennenberg, H., and Foyer, C.** (1998). Glutathione: biosynthesis, metabolism and relationship to stress tolerance explored in transformed plants. *J Exp Bot* **49**, 623-647.
- Noji, M., and Saito, K.** (2002). Molecular and biochemical analysis of serine acetyltransferase and cysteine synthase towards sulfur metabolic engineering in plants. *Amino Acids* **22**, 231-243.
- Noji, M., Inoue, K., Kimura, N., Gouda, A., and Saito, K.** (1998). Isoform-dependent differences in feedback regulation and subcellular localization of serine acetyltransferase involved in cysteine biosynthesis from *Arabidopsis thaliana*. *J Biol Chem* **273**, 32739-32745.
- Nomura, T., Kushiro, T., Yokota, T., Kamiya, Y., Bishop, G.J., and Yamaguchi, S.** (2005). The last reaction producing brassinolide is catalyzed by cytochrome P-450s, CYP85A3 in tomato and CYP85A2 in *Arabidopsis*. *J Biol Chem* **280**, 17873-17879.
- Ohlrogge, J., and Browse, J.** (1995). Lipid biosynthesis. *Plant Cell* **7**, 957-970.
- Otegui, M.S., Herder, R., Schulze, J., Jung, R., and Staehelin, L.A.** (2006). The proteolytic processing of seed storage proteins in *Arabidopsis* embryo cells starts in the multivesicular bodies. *Plant Cell* **18**, 2567-2581.
- Pang, P.P., Pruitt, R.E., and Meyerowitz, E.M.** (1988). Molecular cloning, genomic organization, expression and evolution of 12S seed storage protein genes of *Arabidopsis thaliana*. *Plant Mol Biol* **11**, 805-820.
- Peng, Z., and Verma, D.P.** (1995). A rice *HAL2*-like gene encodes a Ca²⁺-sensitive 3'(2'),5'-diphosphonucleoside 3'(2')-phosphohydrolase and complements yeast *met22* and *Escherichia coli cysQ* mutations. *J Biol Chem* **270**, 29105-29110.

- Perez-Espana, V.H., Sanchez-Leon, N., and Vielle-Calzada, J.P.** (2011). *CYP85A1* is required for the initiation of female gametogenesis in *Arabidopsis thaliana*. *Plant Signal Behav* **6**, 321-326.
- Perry, H.J., Bligny, R., Gout, E., and Harwood, J.L.** (1999). Changes in Kennedy pathway intermediates associated with increased triacylglycerol synthesis in oil-seed rape. *Phytochemistry* **52**, 799-804.
- Pinto, R., Harrison, J.S., Hsu, T., Jacobs, W.R., Jr., and Leyh, T.S.** (2007). Sulfite reduction in mycobacteria. *J Bacteriol* **189**, 6714-6722.
- Pye, V.E., Tingey, A.P., Robson, R.L., and Moody, P.C.** (2004). The structure and mechanism of serine acetyltransferase from *Escherichia coli*. *J Biol Chem* **279**, 40729-40736.
- Queval, G., Thominet, D., Vanacker, H., Miginiac-Maslow, M., Gakiere, B., and Noctor, G.** (2009). H₂O₂-activated up-regulation of glutathione in *Arabidopsis* involves induction of genes encoding enzymes involved in cysteine synthesis in the chloroplast. *Mol Plant* **2**, 344-356.
- Rabeh, W.M., and Cook, P.F.** (2004). Structure and mechanism of *O*-acetylserine sulfhydrylase. *J Biol Chem* **279**, 26803-26806.
- Ramos, S.** (2007). Effects of dietary flavonoids on apoptotic pathways related to cancer chemoprevention. *J Nutr Biochem* **18**, 427-442.
- Randall, P.J., and Wrigley, C.W.** (1986). Effects of sulfur supply on the yield, composition, and quality of grain from cereals, oilseeds, and legumes. *Adv Cereal Sci Technol* **8**, 171-206.
- Ravel, S., Gakiere, B., Job, D., and Douce, R.** (1998). The specific features of methionine biosynthesis and metabolism in plants. *P Natl Acad Sci USA* **95**, 7805-7812.
- Reichelt, M., Brown, P.D., Schneider, B., Oldham, N.J., Stauber, E., Tokuhisa, J., Kliebenstein, D.J., Mitchell-Olds, T., and Gershenzon, J.** (2002). Benzoic acid glucosinolate esters and other glucosinolates from *Arabidopsis thaliana*. *Phytochemistry* **59**, 663-671.
- Rennenberg, H.** (1984). The fate of excess sulfur in higher plants. *Annu Rev Plant Phys* **35**, 121-153.
- Renosto, F., Patel, H.C., Martin, R.L., Thomassian, C., Zimmerman, G., and Segel, I.H.** (1993). ATP sulfurylase from higher plants: kinetic and structural characterization of the chloroplast and cytosol enzymes from spinach leaf. *Arch Biochem Biophys* **307**, 272-285.
- Reumann, S., Maier, E., Heldt, H.W., and Benz, R.** (1998). Permeability properties of the porin of spinach leaf peroxisomes. *Eur J Biochem* **251**, 359-366.
- Reuveny, Z., Dougall, D.K., and Trinity, P.M.** (1980). Regulatory coupling of nitrate and sulfate assimilation pathways in cultured tobacco cells. *P Natl Acad Sci USA* **77**, 6670-6672.
- Robenek, H., Hofnagel, O., Buers, I., Robenek, M.J., Troyer, D., and Severs, N.J.** (2006). Adipophilin-enriched domains in the ER membrane are sites of lipid droplet biogenesis. *J Cell Sci* **119**, 4215-4224.
- Robenek, M.J., Severs, N.J., Schlattmann, K., Plenz, G., Zimmer, K.-P., Troyer, D., and Robenek, H.** (2004). Lipids partition caveolin-1 from ER membranes into lipid droplets: updating the model of lipid droplet biogenesis. *FASEB J* **18**, 866-868.
- Rolletschek, H., Hosein, F., Miranda, M., Heim, U., Gotz, K.P., Schlereth, A., Borisjuk, L., Saalbach, I., Wobus, U., and Weber, H.** (2005). Ectopic expression of an amino acid transporter (VfAAP1) in

- seeds of *Vicia narbonensis* and pea increases storage proteins. *Plant Physiol* **137**, 1236-1249.
- Rotte, C., and Leustek, T.** (2000). Differential subcellular localization and expression of ATP sulfurylase and 5'-adenylylsulfate reductase during ontogenesis of Arabidopsis leaves indicates that cytosolic and plastid forms of ATP sulfurylase may have specialized functions. *Plant Physiol* **124**, 715-724.
- Ruffet, M.L., Droux, M., and Douce, R.** (1994). Purification and kinetic properties of serine acetyltransferase free of *O*-acetylserine(thiol)lyase from spinach chloroplasts. *Plant Physiol* **104**, 597-604.
- Ruuska, S.A., Girke, T., Benning, C., and Ohlrogge, J.B.** (2002). Contrapuntal networks of gene expression during Arabidopsis seed filling. *Plant Cell* **14**, 1191-1206.
- Saito, K.** (2000). Regulation of sulfate transport and synthesis of sulfur-containing amino acids. *Curr Opin Plant Biol* **3**, 188-195.
- Saitoh, T., Ikegami, T., Nakayama, M., Teshima, K., Akutsu, H., and Hase, T.** (2006). NMR study of the electron transfer complex of plant ferredoxin and sulfite reductase: mapping the interaction sites of ferredoxin. *J Biol Chem* **281**, 10482-10488.
- Sanda, S., Leustek, T., Theisen, M.J., Garavito, R.M., and Benning, C.** (2001). Recombinant Arabidopsis SQD1 converts UDP-glucose and sulfite to the sulfolipid head group precursor UDP-sulfoquinovose *in vitro*. *J Biol Chem* **276**, 3941-3946.
- Sasaki-Sekimoto, Y., Taki, N., Obayashi, T., Aono, M., Matsumoto, F., Sakurai, N., Suzuki, H., Hirai, M.Y., Noji, M., Saito, K., Masuda, T., Takamiya, K.-I., Shibata, D., and Ohta, H.** (2005). Coordinated activation of metabolic pathways for antioxidants and defence compounds by jasmonates and their roles in stress tolerance in Arabidopsis. *Plant J* **44**, 653-668.
- Schiff, S., Stern, A.I., Saidha, T., and Li, J.** (1993). Some molecular aspects of sulfate metabolism in photosynthetic organisms. In *Sulfur nutrition and assimilation in higher plants. Regulatory, agricultural and environmental aspects*, L.J. De Kok, I. Stulen, H. Rennenberg, C. Brunold, and W.C. Rauser, eds (The Hague: SBP Acad Publ.), 21-35.
- Schmidt, A., and Jäger, K.** (1992). Open questions about sulfur metabolism in plants. *Annu Rev Plant Phys* **43**, 325-349.
- Schnug, E.** (1993). Physiological functions and environmental relevance of sulfur-containing secondary metabolites. In *Sulfur nutrition and assimilation in higher plants*, L.J. De Kok, I. Stulen, H. Rennenberg, C. Brunold, and W.E. Rauser, eds (The Hague: SPB Acad. Publ.), pp. 179-190.
- Schröder, P., Lamoureux, G.L., Rusness, D.G., and Rennenberg, H.** (1990). Glutathione S-transferase activity in spruce needles. *Pestic Biochem Phys* **37**, 211-218.
- Schwenn, J.D.** (1994). Photosynthetic sulphate reduction. *Z Naturforsch C* **49c**, 531-539.
- Sekine, K., Hase, T., and Sato, N.** (2002). Reversible DNA compaction by sulfite reductase regulates transcriptional activity of chloroplast nucleoids. *J Biol Chem* **277**, 24399-24404.
- Sekine, K., Sakakibara, Y., Hase, T., and Sato, N.** (2009). A novel variant of ferredoxin-dependent sulfite reductase having preferred substrate

- specificity for nitrite in the unicellular red alga *Cyanidioschyzon merolae*. *Biochem J* **423**, 91-98.
- Sekine, K., Fujiwara, M., Nakayama, M., Takao, T., Hase, T., and Sato, N.** (2007). DNA binding and partial nucleoid localization of the chloroplast stromal enzyme ferredoxin:sulfite reductase. *FEBS J* **274**, 2054-2069.
- Setya, A., Murillo, M., and Leustek, T.** (1996). Sulfate reduction in higher plants: molecular evidence for a novel 5'-adenylylsulfate reductase. *P Natl Acad Sci USA* **93**, 13383-13388.
- Shimada, T., Fuji, K., Tamura, K., Kondo, M., Nishimura, M., and Hara-Nishimura, I.** (2003a). Vacuolar sorting receptor for seed storage proteins in *Arabidopsis thaliana*. *P Natl Acad Sci USA* **100**, 16095-16100.
- Shimada, T., Yamada, K., Kataoka, M., Nakaune, S., Koumoto, Y., Kuroyanagi, M., Tabata, S., Kato, T., Shinozaki, K., Seki, M., Kobayashi, M., Kondo, M., Nishimura, M., and Hara-Nishimura, I.** (2003b). Vacuolar processing enzymes are essential for proper processing of seed storage proteins in *Arabidopsis thaliana*. *J Biol Chem* **278**, 32292-32299.
- Shimada, T.L., Shimada, T., Takahashi, H., Fukao, Y., and Hara-Nishimura, I.** (2008). A novel role for oleosins in freezing tolerance of oilseeds in *Arabidopsis thaliana*. *Plant J* **55**, 798-809.
- Shosuke, K., Koji, Y., and Sumiko, I.** (1989). Site-specific DNA damage induced by sulfite in the presence of cobalt(II) ion: Role of sulfate radical. *Biochem Pharmacol* **38**, 3491-3496.
- Siloto, R.M.P., Findlay, K., Lopez-Villalobos, A., Yeung, E.C., Nykiforuk, C.L., and Moloney, M.M.** (2006). The accumulation of oleosins determines the size of seed oilbodies in *Arabidopsis*. *Plant Cell* **18**, 1961-1974.
- Sjodahl, S., Rodin, J., and Rask, L.** (1991). Characterization of the 12S globulin complex of *Brassica napus*. Evolutionary relationship to other 11-12S storage globulins. *Eur J Biochem* **196**, 617-621.
- Smith, A.M., and Zeeman, S.C.** (2006). Quantification of starch in plant tissues. *Nat Protoc* **1**, 1342-1345.
- Smith, F.W., Hawkesford, M.J., Ealing, P.M., Clarkson, D.T., Vanden Berg, P.J., Belcher, A.R., and Warrilow, A.G.** (1997). Regulation of expression of a cDNA from barley roots encoding a high affinity sulphate transporter. *Plant J* **12**, 875-884.
- Smith, I.K.** (1980). Regulation of sulfate assimilation in tobacco cells. *Plant Physiol* **66**, 877 - 883.
- Steber, C.M., and McCourt, P.** (2001). A role for brassinosteroids in germination in *Arabidopsis*. *Plant Physiol* **125**, 763-769.
- Steudel, R.** (1998). Schwefel, Selen, Tellur, Polonium. In *Chemie der Nichtmetalle; mit Atombau, Molekülgeometrie und Bindungstheorie*, Y. Drozdova, ed (Berlin, New York: Walter de Gruyter), pp. 257-320.
- Stitt, M., Lilley, R., Gerhardt, R., and Heldt, H.W.** (1989). Metabolite levels in specific cells and subcellular compartments of plant leaves. *Method Enzymol* **174**, 518-552.
- Subramanian, A., Tamayo, P., Mootha, V.K., Mukherjee, S., Ebert, B.L., Gillette, M.A., Paulovich, A., Pomeroy, S.L., Golub, T.R., Lander, E.S., and Mesirov, J.P.** (2005). Gene set enrichment

- analysis: a knowledge-based approach for interpreting genome-wide expression profiles. *P Natl Acad Sci USA* **102**, 15545-15550.
- Suter, M., von Ballmoos, P., Kopriva, S., den Camp, R.O., Schaller, J., Kuhlemeier, C., Schurmann, P., and Brunold, C.** (2000). Adenosine 5'-phosphosulfate sulfotransferase and adenosine 5'-phosphosulfate reductase are identical enzymes. *J Biol Chem* **275**, 930-936.
- Suzuki, K., Nakanishi, H., Bower, J., Yoder, D., Osteryoung, K., and Miyagishima, S.-y.** (2009). Plastid chaperonin proteins Cpn60alpha and Cpn60beta are required for plastid division in *Arabidopsis thaliana*. *BMC Plant Biol* **9**, 38.
- Szekeres, M., Németh, K., Koncz-Kálmán, Z., Mathur, J., Kauschmann, A., Altmann, T., Rédei, G.P., Nagy, F., Schell, J., and Koncz, C.** (1996). Brassinosteroids rescue the deficiency of CYP90, a cytochrome P450, controlling cell elongation and de-etiolation in *Arabidopsis*. *Cell* **85**, 171-182.
- Tabe, L., and Higgins, T.J.V.** (1998). Engineering plant protein composition for improved nutrition. *Trends Plant Sci* **3**, 282-286.
- Takahashi, H., Watanabe-Takahashi, A., Smith, F.W., Blake-Kalff, M., Hawkesford, M.J., and Saito, K.** (2000). The roles of three functional sulphate transporters involved in uptake and translocation of sulphate in *Arabidopsis thaliana*. *Plant J* **23**, 171-182.
- Takahashi, H., Yamazaki, M., Sasakura, N., Watanabe, A., Leustek, T., Engler, J.A., Engler, G., Van Montagu, M., and Saito, K.** (1997). Regulation of sulfur assimilation in higher plants: a sulfate transporter induced in sulfate-starved roots plays a central role in *Arabidopsis thaliana*. *P Natl Acad Sci USA* **94**, 11102-11107.
- Takemoto, Y., Coughlan, S.J., Okita, T.W., Satoh, H., Ogawa, M., and Kumamaru, T.** (2002). The rice mutant *esp2* greatly accumulates the glutelin precursor and deletes the protein disulfide isomerase. *Plant Physiol* **128**, 1212-1222.
- Tauchi-Sato, K., Ozeki, S., Houjou, T., Taguchi, R., and Fujimoto, T.** (2002). The surface of lipid droplets is a phospholipid monolayer with a unique fatty acid composition. *J Biol Chem* **277**, 44507-44512.
- The Arabidopsis Genome Initiative.** (2000). Analysis of the genome sequence of the flowering plant *Arabidopsis thaliana*. *Nature* **408**, 796-815.
- Thelen, J.J., and Ohlrogge, J.B.** (2002). Both antisense and sense expression of biotin carboxyl carrier protein isoform 2 inactivates the plastid acetyl-coenzyme A carboxylase in *Arabidopsis thaliana*. *Plant J* **32**, 419-431.
- Tocquin, P., Corbesier, L., Havelange, A., Pieltain, A., Kurtem, E., Bernier, G., and Perilleux, C.** (2003). A novel high efficiency, low maintenance, hydroponic system for synchronous growth and flowering of *Arabidopsis thaliana*. *BMC Plant Biol* **3**, 2.
- Tolbert, N.E., and Ryan, F.J.** (1976). Glycolate biosynthesis and metabolism during photorespiration. In *CO₂-metabolism and plant productivity*, R.H. Burris and C.C. Black, eds (Baltimore: University Press), pp. 141-159.
- Tomatsu, H., Takano, J., Takahashi, H., Watanabe-Takahashi, A., Shibagaki, N., and Fujiwara, T.** (2007). An *Arabidopsis thaliana* high-affinity molybdate transporter required for efficient uptake of molybdate from soil. *P Natl Acad Sci USA* **104**, 18807-18812.

- Towbin, H., Staehelin, T., and Gordon, J.** (1979). Electrophoretic transfer of proteins from polyacrylamide gels to nitrocellulose sheets: procedure and some applications. *P Natl Acad Sci USA* **76**, 4350-4354.
- Turnham, E., and Northcote, D.H.** (1983). Changes in the activity of acetyl-CoA carboxylase during rape-seed formation. *Biochem J* **212**, 223-229.
- Tzen, J., and Huang, A.** (1992). Surface structure and properties of plant seed oil bodies. *J Cell Biol* **117**, 327-335.
- van der Klei, H., Van Damme, J., Casteels, P., and Krebbers, E.** (1993). A fifth 2S albumin isoform is present in *Arabidopsis thaliana*. *Plant Physiol* **101**, 1415-1416.
- Varin, L., Marsolais, F., Richard, M., and Rouleau, M.** (1997). Sulfation and sulfotransferases 6: biochemistry and molecular biology of plant sulfotransferases. *FASEB J.* **11**, 517-525.
- Vigeolas, H., Waldeck, P., Zank, T., and Geigenberger, P.** (2007). Increasing seed oil content in oil-seed rape (*Brassica napus* L.) by over-expression of a yeast glycerol-3-phosphate dehydrogenase under the control of a seed-specific promoter. *Plant Biotechnol J* **5**, 431-441.
- Vigeolas, H., Mohlmann, T., Martini, N., Neuhaus, H.E., and Geigenberger, P.** (2004). Embryo-specific reduction of ADP-Glc pyrophosphorylase leads to an inhibition of starch synthesis and a delay in oil accumulation in developing seeds of oilseed rape. *Plant Physiol* **136**, 2676-2686.
- Vijaybhaskar, V., Subbiah, V., Kaur, J., Vijayakumari, P., and Siddiqi, I.** (2008). Identification of a root-specific glycosyltransferase from *Arabidopsis* and characterization of its promoter. *J Bioscience* **33**, 185-193.
- Visser, W.F., van roermund, C.W.T., Ijlst, L., Waterham, H.R., and Wanders, R.J.A.** (2007). Metabolite transport across the peroxisomal membrane. *Biochem J* **401**, 365-375.
- Voelker, T.A., Hayes, T.R., Cranmer, A.M., Turner, J.C., and Davies, H.M.** (1996). Genetic engineering of a quantitative trait: metabolic and genetic parameters influencing the accumulation of laurate in rapeseed. *Plant J* **9**, 229-241.
- Völkel, S., and Grieshaber, M.K.** (1994). Oxygen dependent sulfide detoxification in the lugworm *Arenicola marina*. *Mar Biol* **118**, 137-147.
- Wang, R., Okamoto, M., Xing, X., and Crawford, N.M.** (2003). Microarray analysis of the nitrate response in *Arabidopsis* roots and shoots reveals over 1,000 rapidly responding genes and new linkages to glucose, trehalose-6-phosphate, iron, and sulfate metabolism. *Plant Physiol* **132**, 556-567.
- Watanabe, M., Kusano, M., Oikawa, A., Fukushima, A., Noji, M., and Saito, K.** (2008a). Physiological roles of the β -substituted alanine synthase gene family in *Arabidopsis*. *Plant Physiol* **146**, 310-320.
- Watanabe, M., Mochida, K., Kato, T., Tabata, S., Yoshimoto, N., Noji, M., and Saito, K.** (2008b). Comparative genomics and reverse genetics analysis reveal indispensable functions of the serine acetyltransferase gene family in *Arabidopsis*. *Plant Cell* **20**, 2484-2496.
- Weber, H., Borisjuk, L., and Wobus, U.** (2005). Molecular physiology of legume seed development. *Annu Rev Plant Biol* **56**, 253-279.
- Westerman, S., De Kok, L.J., Stuiver, C.E.E., and Stulen, I.** (2000). Interaction between metabolism of atmospheric H₂S in the shoot and

- sulfate uptake by the roots of curly kale (*Brassica oleracea*). *Physiol Plantarum* **109**, 443-449.
- White, J.A., and Benning, C.** (2001). Genomic approaches towards the engineering of oil seeds. *Plant Physiol Bioch* **39**, 263-270.
- Willats, W.G.T., Knox, J.P., and Mikkelsen, J.D.** (2006). Pectin: new insights into an old polymer are starting to gel. *Trends Food Sci Tech* **17**, 97-104.
- Wirtz, M., and Hell, R.** (2003). Comparative biochemical characterization of OAS-TL isoforms from *Arabidopsis thaliana*. In *Sulfate transport and assimilation in plants*, J.C. Davidian, D. Grill, L.J. De Kok, I. Stulen, M.J. Hawkesford, E. Schnug, and H. Rennenberg, eds (Leiden: Backhuys Publishers), pp. 355-357.
- Wirtz, M., and Droux, M.** (2005). Synthesis of the sulfur amino acids: cysteine and methionine. *Photosynth Res* **86**, 345-362.
- Wirtz, M., and Hell, R.** (2006). Functional analysis of the cysteine synthase protein complex from plants: structural, biochemical and regulatory properties. *J Plant Physiol* **163**, 273-286.
- Wirtz, M., and Hell, R.** (2007). Dominant-negative modification reveals the regulatory function of the multimeric cysteine synthase protein complex in transgenic tobacco. *Plant Cell* **19**, 625-639.
- Wirtz, M., Droux, M., and Hell, R.** (2004). *O*-acetylserine (thiol) lyase: an enigmatic enzyme of plant cysteine biosynthesis revisited in *Arabidopsis thaliana*. *J Exp Bot* **55**, 1785-1798.
- Wirtz, M., Berkowitz, O., Droux, M., and Hell, R.** (2001). The cysteine synthase complex from plants. Mitochondrial serine acetyltransferase from *Arabidopsis thaliana* carries a bifunctional domain for catalysis and protein-protein interaction. *Eur J Biochem* **268**, 686-693.
- Wirtz, M., Birke, H., Heeg, C., Muller, C., Hosp, F., Throm, C., Konig, S., Feldman-Salit, A., Rippe, K., Petersen, G., Wade, R.C., Rybin, V., Scheffzek, K., and Hell, R.** (2010). Structure and function of the hetero-oligomeric cysteine synthase complex in plants. *J Biol Chem* **285**, 32810-32817.
- Wittstock, U., and Halkier, B.A.** (2002). Glucosinolate research in the *Arabidopsis* era. *Trends Plant Sci* **7**, 263-270.
- Yamamoto, R., Fujioka, S., Demura, T., Takatsuto, S., Yoshida, S., and Fukuda, H.** (2001). Brassinosteroid levels increase drastically prior to morphogenesis of tracheary elements. *Plant Physiol* **125**, 556-563.
- Yanhui, C., Xiaoyuan, Y., Kun, H., Meihua, L., Jigang, L., Zhaofeng, G., Zhiqiang, L., Yunfei, Z., Xiaoxiao, W., Xiaoming, Q., Yunping, S., Li, Z., Xiaohui, D., Jingchu, L., Xing-Wang, D., Zhangliang, C., Hongya, G., and Li-Jia, Q.** (2006). The MYB transcription factor superfamily of *Arabidopsis*: expression analysis and phylogenetic comparison with the rice MYB family. *Plant Mol Biol* **60**, 107-124.
- Yatsu, L.Y., and Jacks, T.J.** (1972). Spherosome membranes: half unit-membranes. *Plant Physiol* **49**, 937-943.
- Ye, X., Al-Babili, S., Klotti, A., Zhang, J., Lucca, P., Beyer, P., and Potrykus, I.** (2000). Engineering the provitamin A (β -carotene) biosynthetic pathway into (carotenoid-free) rice endosperm. *Science* **287**, 303-305.
- Yilmaz, Y.** (2006). Novel uses of catechins in foods. *Trends Food Sci Tech* **17**, 64-71.

- Yonekura-Sakakibara, K., Onda, Y., Ashikari, T., Tanaka, Y., Kusumi, T., and Hase, T.** (2000). Analysis of reductant supply systems for ferredoxin-dependent sulfite reductase in photosynthetic and nonphotosynthetic organs of maize. *Plant Physiol* **122**, 887-894.
- Yoshimoto, N., Inoue, E., Saito, K., Yamaya, T., and Takahashi, H.** (2003). Phloem-localizing sulfate transporter, *Sultr1;3*, mediates redistribution of sulfur from source to sink organs in Arabidopsis. *Plant Physiol* **131**, 1511-1517.
- Yoshimoto, N., Inoue, E., Watanabe-Takahashi, A., Saito, K., and Takahashi, H.** (2007). Posttranscriptional regulation of high-affinity sulfate transporters in Arabidopsis by sulfur nutrition. *Plant Physiol* **145**, 378-388.
- Yu, B., Xu, C., and Benning, C.** (2002). Arabidopsis disrupted in *SQD2* encoding sulfolipid synthase is impaired in phosphate-limited growth. *P Natl Acad Sci USA* **99**, 5732-5737.
- Zabaleta, E., Oropeza, A., Assad, N., Mandel, A., Salerno, G., and Herrera-Estrella, L.** (1994). Antisense expression of chaperonin 60 β in transgenic tobacco plants leads to abnormal phenotypes and altered distribution of photoassimilates. *Plant J* **6**, 425-432.
- Zeeman, S.C., Tiessen, A., Pilling, E., Kato, K.L., Donald, A.M., and Smith, A.M.** (2002). Starch synthesis in Arabidopsis. Granule synthesis, composition, and structure. *Plant Physiol* **129**, 516-529.
- Zelitch, I.** (1973). Alternate pathways of glycolate synthesis in tobacco and maize leaves in relation to rates of photorespiration. *Plant Physiol* **51**, 299-305.
- Zhao, F.-J., Tausz, M., and De Kok, L.** (2008). Role of sulfur for plant production in agricultural and natural ecosystems. In *Sulfur metabolism in phototrophic organisms*, R. Hell, C. Dahl, and T. Leustek, eds (Dordrecht: Springer), pp. 425-444.
- Zimmermann, P., Hirsch-Hoffmann, M., Hennig, L., and Gruissem, W.** (2004). GENEVESTIGATOR. Arabidopsis microarray database and analysis toolbox. *Plant Physiol* **136**, 2621-2632.
- Zuber, H., Davidian, J.C., Wirtz, M., Hell, R., Belghazi, M., Thompson, R., and Gallardo, K.** (2010a). *Sultr4;1* mutant seeds of Arabidopsis have an enhanced sulphate content and modified proteome suggesting metabolic adaptations to altered sulphate compartmentalization. *BMC Plant Biol* **10**, 78.
- Zuber, H., Davidian, J.C., Aubert, G., Aime, D., Belghazi, M., Lugan, R., Heintz, D., Wirtz, M., Hell, R., Thompson, R., and Gallardo, K.** (2010b). The seed composition of Arabidopsis mutants for the group 3 sulfate transporters indicates a role in sulfate translocation within developing seeds. *Plant Physiol* **154**, 913-926.

Supplemental data

Suppl. data 1 Raw data of leaf metabolites of soil-grown *sir1-1* and wild-type plants.

Soil-grown 7-to-8-week-old wild-type and *sir1-1* plants were used for extraction of soluble metabolites which were detected via GC/MS as described in 2.7.2.

Name Analyte	Average		SE		t-test
	Col-0	<i>sir1-1</i>	Col-0	<i>sir1-1</i>	
Alanine, beta- (3TMS)	0.003	0.005	0.000	0.001	0.195
Alanine, DL- (2TMS)	0.725	1.412	0.099	0.371	0.111
Asparagine, DL- (3TMS)	0.010	0.099	0.001	0.015	0.000
Aspartic acid, L- (3TMS)	0.082	0.371	0.009	0.069	0.003
Benzoic acid (1TMS)	0.026	0.023	0.001	0.005	0.642
Butyric acid, 4-amino- (3TMS)	0.096	0.105	0.012	0.016	0.662
Cellobiose, D- (1MEOX) (8TMS)	0.024	0.006	0.009	0.001	0.078
Citric acid (4TMS)	0.105	0.236	0.033	0.022	0.011
Dehydroascorbic acid dimer (TMS)	0.481	0.125	0.097	0.016	0.007
Erythritol (4TMS)	0.011	0.010	0.001	0.001	0.366
Fructose, D- (1MEOX) (5TMS)	1.431	1.385	0.273	0.082	0.876
Fucose, DL- (1MEOX) (4TMS)	0.026	0.022	0.003	0.002	0.256
Fumaric acid (2TMS)	3.468	1.366	0.372	0.163	0.001
Galactinol (9TMS)	0.239	0.052	0.044	0.009	0.003
Galactonic acid-1,4-lactone, D(-)- (4TMS)	0.019	0.015	0.002	0.002	0.196
Galacturonic acid, D- (1MEOX) (5TMS)	0.009	0.008	0.001	0.001	0.431
Glucoheptonic acid (7TMS)	0.392	0.140	0.119	0.036	0.078
Glucoheptose (1MEOX) (6TMS)	0.013	#DIV/0!	0.002	nd	
Glucopyranoside, 1-O-methyl-, alpha-D- (4TMS)	0.319	0.063	0.014	0.007	0.000
Glucose, 1,6-anhydro, beta-D- (3TMS)	0.159	0.089	0.012	0.013	0.005
Glucose, D- (1MEOX) (5TMS)	2.939	0.917	0.321	0.076	0.000
Glutamic acid, DL- (3TMS)	1.157	1.456	0.140	0.168	0.209
Glutamine, DL- (4TMS)	0.004	0.014	0.001	0.004	0.082
Glyceric acid, DL- (3TMS)	0.006	0.004	0.001	0.000	0.189
Glycerol (3TMS)	0.150	0.105	0.011	0.021	0.091
Glycine (3TMS)	0.132	0.620	0.020	0.252	0.090
Glycolic acid (2TMS)	0.044	0.021	0.007	0.003	0.016
Inositol, myo- (6TMS)	1.612	1.166	0.179	0.163	0.102
Isoleucine, L- (2TMS)	0.057	0.118	0.009	0.022	0.034
Isomaltose (1MEOX) (8TMS)	0.389	0.014	0.097	0.002	0.005
Lactic acid, DL- (2TMS)	0.147	0.202	0.026	0.034	0.239
Malic acid, DL- (3TMS)	0.507	0.175	0.137	0.023	0.044
Maltitol (9TMS)	0.050	0.005	0.013	0.000	0.007
Maltose, D- (1MEOX) (8TMS)	0.190	0.017	0.047	0.002	0.006
Melibiose (1MEOX) (8TMS)	0.026	0.007	0.009	0.001	0.053
Octadecanoic acid, n- (1TMS)	0.349	0.400	0.020	0.052	0.385
Phenylalanine, DL- (2TMS)	0.043	0.089	0.003	0.012	0.006
Phosphoric acid (3TMS)	0.130	0.117	0.067	0.040	0.874
Proline, L- (2TMS)	0.198	0.413	0.038	0.075	0.034
Psicose, D- (1MEOX) (5TMS)	0.010	0.014	0.002	#DIV/0!	#DIV/0!
Putrescine (4TMS)	0.027	0.062	0.006	0.026	0.224
Pyridine, 3-hydroxy- (1TMS)	0.038	0.022	0.002	0.004	0.003
Raffinose (11TMS)	0.205	0.027	0.032	0.007	0.001
Rhamnose, DL- (1MEOX) (4TMS)	0.059	0.024	0.020	0.006	0.141
Salicylic acid (2TMS)	0.006	0.006	0.001	0.001	0.828
Serine, DL- (3TMS)	0.816	1.194	0.068	0.247	0.178
Spermidine (5TMS)	nd	nd	0.000	#DIV/0!	#DIV/0!
Succinic acid (2TMS)	0.048	0.020	0.006	0.002	0.003
Sucrose, D- (8TMS)	1.102	0.533	0.218	0.092	0.043
Threonine, DL- (3TMS)	0.098	0.332	0.009	0.061	0.005
Trehalose, alpha,alpha'-, D- (8TMS)	0.076	0.015	0.014	0.001	0.002
Tyrosine, DL- (3TMS)	0.028	0.056	0.002	0.006	0.002
Urea (2TMS)	0.015	0.018	0.002	0.003	0.623
Valine, DL- (2TMS)	0.126	0.221	0.012	0.048	0.093
Xylitol (5TMS)	0.021	0.027	0.005	0.002	0.321

Suppl. data 2 Raw data of leaf metabolites of *sir1-1* and WT plants grown hydroponically on +S.

6-week-old wild-type and *sir1-1* plants were used to extract soluble metabolites which were detected via GC/MS as described in 2.7.2.

Metabolite	average		SE		t-test	
	Col-0	<i>sir1-1</i>	Col-0	<i>sir1-1</i>		
Alanine, DL- (2TMS)	0.08041	0.07285	0.00707	0.01357		0.63189
Ascorbic acid, L(+)- (4TMS)	0.00004	0.00003	0.00001	#DIV/0!	#DIV/0!	
Asparagine, DL- (3TMS)	0.00060	0.00057	0.00019	0.00011		0.90582
Aspartic acid, L- (3TMS)	0.00516	0.00215	0.00064	0.00026		0.00149
Benzoic acid (1TMS)	0.00051	0.00061	0.00006	0.00007		0.27697
Butyric acid, 4-amino- (3TMS)	0.00343	0.00556	0.00020	0.00063		0.00870
Citric acid (4TMS)	0.00161	0.00280	0.00020	0.00061		0.09691
Dehydroascorbic acid dimer (TMS)	0.00200	0.00073	0.00051	0.00014		0.03566
Erythritol (4TMS)	0.00075	0.00095	0.00005	0.00014		0.19647
Fructose, D- (1MEOX) (5TMS)	0.00351	0.00454	0.00097	0.00382		0.79811
Fumaric acid (2TMS)	0.12133	0.12696	0.00928	0.01673		0.77454
Galactinol (9TMS)	0.00274	0.02804	0.00022	0.01328		0.08600
Galactonic acid-1,4-lactone, D(-)- (4TMS)	0.00036	0.00020	0.00003	0.00004		0.00800
Glucose, 1,6-anhydro, beta-D- (3TMS)	0.00854	0.00702	0.00121	0.00119		0.39040
Glucose, D- (1MEOX) (5TMS)	0.03128	0.02657	0.00470	0.01447		0.76352
Glutamic acid, DL- (3TMS)	0.00801	0.00401	0.00097	0.00140		0.04062
Glutamine, DL- (4TMS)	0.00140	0.00113	0.00045	0.00027		0.61757
Glutaric acid, 2-oxo- (1MEOX) (2TMS)	0.00010	0.00004	0.00002	0.00001		0.14486
Glyceric acid, DL- (3TMS)	0.00097	0.00092	0.00010	0.00017		0.77853
Glycerol (3TMS)	0.00245	0.00688	0.00025	0.00447		0.34531
Glycine (3TMS)	0.02104	0.00898	0.00392	0.00240		0.02538
Guanidine (3TMS)	0.00017	0.00149	0.00002	0.00023		0.00017
Inositol, myo- (6TMS)	0.02825	0.03126	0.00098	0.00182		0.18501
Isocitric acid, DL- (4TMS)	0.00166	0.00125	0.00038	0.00018		0.35611
Isoleucine, L- (2TMS)	0.00126	0.00254	0.00013	0.00068		0.09495
Lysine, L- (4TMS)	0.00044	0.00051	0.00004	0.00027		0.79006
Malic acid, 2-methyl-, DL- (3TMS)	0.00008	0.00025	0.00001	0.00003		0.00059
Malic acid, DL- (3TMS)	0.00945	0.00868	0.00156	0.00196		0.76415
Maltose, D- (1MEOX) (8TMS)	0.00009	0.00028	0.00001	0.00014		0.18917
Mannose, D- (1MEOX) (5TMS)	0.00052	0.00054	0.00007	0.00035		0.94110
Methionine, DL- (2TMS)	0.00062	0.00027	0.00012	0.00005		0.01997
Octadecanoic acid, n- (1TMS)	0.01521	0.01961	0.00057	0.00225		0.08691
Palatinose (1MEOX) (8TMS)	0.00006	0.00046	0.00001	0.00023		0.10521
Phenylalanine, DL- (2TMS)	0.00137	0.00105	0.00014	0.00020		0.21099
Proline, L- (2TMS)	0.05118	0.02673	0.01198	0.00544		0.09278
Psicose, D- (1MEOX) (5TMS)	0.00051	0.00050	0.00003	0.00020		0.97438
Putrescine (4TMS)	0.00240	0.00522	0.00014	0.00039		0.00004
Pyroglutamic acid, DL- (2TMS)	0.02322	0.01981	0.00482	0.00267		0.58017
Pyruvic acid (1MEOX) (1TMS)	0.00044	0.00020	0.00006	0.00003		0.00468
Raffinose (11TMS)	0.00108	0.00894	0.00024	0.00184		0.00174
Serine, DL- (3TMS)	0.04721	0.07747	0.00134	0.00669		0.00126
Succinic acid (2TMS)	0.00147	0.00076	0.00016	0.00017		0.01233
Sucrose, D- (8TMS)	0.03024	0.04072	0.00212	0.00746		0.20611
Threonic acid (4TMS)	0.00195	0.00136	0.00012	0.00021		0.03284
Threonine, DL- (3TMS)	0.01211	0.01588	0.00095	0.00185		0.09999
Trehalose, alpha, alpha'-, D- (8TMS)	0.00016	0.00067	0.00002	0.00058		0.40472
Tryptophan, L- (3TMS)	0.00007	0.00019	0.00001	0.00007		0.19512
Tyrosine, DL- (3TMS)	0.00037	0.00062	0.00003	0.00020		0.24603
Urea (2TMS)	0.00052	0.00093	0.00008	0.00015		0.03147
Valine, DL- (2TMS)	0.00485	0.01115	0.00053	0.00175		0.00628
Xylose, D- (1MEOX) (4TMS)/Lyxose, D- (1MEOX) (4TMS)	0.00021	0.00014	0.00001	0.00002		0.02280

Suppl. data 3 Raw data of leaf metabolites of *sir1-1* and WT plants after transfer to -S.

6-week-old wild-type and *sir1-1* plants were used to extract soluble metabolites which were detected via GC/MS as described in 2.7.2.

Meatabolite	average		SE		t-test
	Col-0	<i>sir1-1</i>	Col-0	<i>sir1-1</i>	
Alanine, DL- (2TMS)	0.15199	0.11737	0.01711	0.01092	0.11885
Asparagine, DL- (3TMS)	0.00112	0.00172	0.00017	0.00029	0.10026
Aspartic acid, L- (3TMS)	0.00821	0.00771	0.00080	0.00150	0.77385
Benzoic acid (1TMS)	0.00073	0.00074	0.00006	0.00007	0.93933
Butyric acid, 4-amino- (3TMS)	0.00456	0.00790	0.00037	0.00101	0.01135
Citric acid (4TMS)	0.00203	0.01022	0.00014	0.00152	0.00031
Dehydroascorbic acid dimer (TMS)	0.00234	0.00067	0.00018	0.00005	0.00000
Erythritol (4TMS)	0.00080	0.00075	0.00003	0.00005	0.44947
Fructose, D- (1MEOX) (5TMS)	0.00230	0.00093	0.00031	0.00014	0.00259
Fucose, DL- (1MEOX) (4TMS)	0.00029	0.00018	0.00001	0.00002	0.00051
Fumaric acid (2TMS)	0.13110	0.13113	0.00704	0.01000	0.99851
Galactinol (9TMS)	0.00266	0.01676	0.00029	0.00180	0.00002
Galactonic acid-1,4-lactone, D(-)- (4TMS)	0.00048	0.00029	0.00002	0.00002	0.00005
Glucoheptose (1MEOX) (6TMS)	0.00072	0.00145	0.00007	0.00016	0.00173
Glucose, 1,6-anhydro, beta-D- (3TMS)	0.00799	0.00473	0.00111	0.00041	0.09130
Glucose, D- (1MEOX) (5TMS)	0.00554	0.00226	0.00098	0.00044	0.01220
Glutamic acid, DL- (3TMS)	0.01413	0.01260	0.00126	0.00216	0.55558
Glutamine, DL- (4TMS)	0.00419	0.00377	0.00127	0.00104	0.80584
Glutaric acid, 2-oxo- (1MEOX) (2TMS)	0.00010	0.00008	0.00002	0.00002	0.45881
Glyceric acid, DL- (3TMS)	0.00091	0.00064	0.00009	0.00011	0.08406
Glycerol (3TMS)	0.00364	0.00289	0.00044	0.00033	0.20121
Glycine (3TMS)	0.02769	0.00767	0.00519	0.00107	0.00361
Glycolic acid (2TMS)	0.00016	0.00030	0.00002	0.00002	0.00069
Guanidine (3TMS)	0.00049	0.00113	0.00012	0.00011	0.00303
Gulonic acid, 2-oxo-, DL- (1MEOX) (5TMS)	0.00016	0.00019	0.00001	0.00001	0.07022
Inositol, myo- (6TMS)	0.02701	0.02676	0.00146	0.00134	0.90233
Isoleucine, L- (2TMS)	0.00185	0.00207	0.00013	0.00021	0.38950
Isomaltose (1MEOX) (8TMS)	0.00008	0.00025	0.00001	0.00002	0.00002
Lyxose, D- (1MEOX) (4TMS)	0.00023	0.00012	0.00001	0.00001	0.00019
Malic acid, 2-methyl-, DL- (3TMS)	0.00010	0.00033	0.00000	0.00002	0.00000
Malic acid, DL- (3TMS)	0.01164	0.01662	0.00172	0.00187	0.07844
Maltose, D- (1MEOX) (8TMS)	0.00008	0.00008	0.00000	0.00001	0.82649
Melezitose (11TMS)	0.00016	0.00051	0.00004	0.00012	0.02301
Methionine, DL- (2TMS)	0.00039	0.00031	0.00010	0.00005	0.45119
Octadecanoic acid, n- (1TMS)	0.00632	0.00671	0.00057	0.00086	0.71440
Ornithine, DL- (4TMS)	0.00024	0.00016	0.00002	0.00002	0.03114
Phenylalanine, DL- (2TMS)	0.00244	0.00185	0.00023	0.00020	0.07711
Proline, 4-hydroxy-, DL-, trans- (3TMS)	0.00062	0.00054	0.00003	0.00004	0.11708
Proline, L- (2TMS)	0.08570	0.02697	0.01586	0.00257	0.00442
Psicose, D- (1MEOX) (5TMS)	0.00010	0.00007	0.00000	0.00000	0.00116
Putrescine (4TMS)	0.00352	0.00407	0.00026	0.00065	0.45084
Pyroglutamic acid, DL- (2TMS)	0.03666	0.04363	0.00550	0.00778	0.48105
Pyruvic acid (1MEOX) (1TMS)	0.00056	0.00019	0.00009	0.00003	0.00246
Raffinose (11TMS)	0.00251	0.00963	0.00063	0.00170	0.00284
Serine, DL- (3TMS)	0.05855	0.06087	0.00293	0.00387	0.64287
Shikimic acid (4TMS)	0.00457	0.00592	0.00027	0.00052	0.04426
Sorbose, D- (1MEOX) (5TMS)	0.00106	0.00043	0.00015	0.00007	0.00392
Spermidine (5TMS)	0.00173	0.00004	0.00018	0.00001	0.00006
Succinic acid (2TMS)	0.00200	0.00101	0.00011	0.00010	0.00005
Sucrose, D- (8TMS)	0.03088	0.02936	0.00195	0.00212	0.60886
Threonic acid (4TMS)	0.00230	0.00180	0.00022	0.00018	0.11296
Threonine, DL- (3TMS)	0.01509	0.01241	0.00093	0.00095	0.07171
Trehalose, alpha, alpha', D- (8TMS)	0.00017	0.00006	0.00001	0.00001	0.00002
Tryptophan, L- (3TMS)	0.00014	0.00035	0.00004	0.00007	0.02983
Turanose, D- (1MEOX) (8TMS)	0.00038	0.00031	0.00001	0.00003	0.12219
Tyrosine, DL- (3TMS)	0.00075	0.00079	0.00009	0.00010	0.77690
Urea (2TMS)	0.00045	0.00074	0.00003	0.00009	0.01160
Valine, DL- (2TMS)	0.00768	0.01253	0.00059	0.00094	0.00137

Suppl. data 4 Raw data of root metabolites of *sir1-1* and WT plants grown hydroponically on +S.

6-week-old wild-type and *sir1-1* plants were used to extract soluble metabolites which were detected via GC/MS as described in 2.7.2.

Metabolite	average		SE		t-test
	Col-0	<i>sir1-1</i>	Col-0	<i>sir1-1</i>	
Alanine, DL- (2TMS)	0.005626	0.008989	0.000234	0.001449	0.044934
Asparagine, DL- (3TMS)	0.000439	0.000210	0.000083	0.000022	0.023667
Aspartic acid, L- (3TMS)	0.003945	0.002787	0.000316	0.000144	0.007559
Benzoic acid, 4-hydroxy- (2TMS)	0.000010	0.000016	0.000002	0.000002	0.068507
Butyric acid, 4-amino- (3TMS)	0.011259	0.006485	0.001041	0.000482	0.001941
Citric acid (4TMS)	0.002971	0.003185	0.000606	0.000360	0.767060
Erythrose, D- (1MEOX) (3TMS)	0.000038	0.000067	0.000005	0.000004	0.000738
Fructose, D- (1MEOX) (5TMS)	0.000508	0.000826	0.000042	0.000224	0.192931
Fructose-6-phosphate (1MEOX) (6TMS)	0.000056	0.000048	0.000003	0.000005	0.198539
Fucose, DL- (1MEOX) (4TMS)	0.000279	0.000284	0.000010	0.000009	0.744590
Fumaric acid (2TMS)	0.001500	0.001819	0.000091	0.000348	0.396551
Galactinol (9TMS)	0.000052	0.000098	0.000009	0.000017	0.036285
Galactonic acid (6TMS)	0.000156	0.000185	0.000005	0.000008	0.012254
Galactose, D- (1MEOX) (5TMS)	0.000073	0.000066	0.000004	0.000003	0.161740
Glucoheptose (1MEOX) (6TMS)	0.000094	0.000057	0.000007	0.000005	0.002110
Glucose, 1,6-anhydro, beta-D- (3TMS)	0.001769	0.001410	0.000270	0.000058	0.222520
Glucose, D- (1MEOX) (5TMS)	0.001639	0.001611	0.000163	0.000186	0.912702
Glucose-6-phosphate (1MEOX) (6TMS)	0.000034	0.000024	0.000002	0.000004	0.053263
Glutamic acid, DL- (3TMS)	0.005068	0.002951	0.000651	0.000207	0.011292
Glutamine, DL- (4TMS)	0.000185	0.000149	0.000016	0.000015	0.147110
Glutaric acid, 2-oxo- (1MEOX) (2TMS)	0.000149	0.000091	0.000008	0.000002	0.000051
Glyceric acid, DL- (3TMS)	0.000042	0.000120	0.000004	0.000050	0.148617
Glycerol (3TMS)	0.000414	0.000897	0.000055	0.000093	0.001210
Glycerol-3-phosphate, DL- (4TMS)	0.000141	0.000219	0.000011	0.000025	0.016895
Glycine (3TMS)	0.001039	0.001316	0.000089	0.000059	0.026426
Glycolic acid (2TMS)	0.000026	0.000047	0.000002	0.000005	0.004559
Guanidine (3TMS)	0.000150	0.000245	0.000042	0.000058	0.215697
Inositol, myo- (6TMS)	0.002128	0.002625	0.000117	0.000174	0.039730
Inositol-1-phosphate, myo- (7TMS)	0.000024	0.000037	0.000002	0.000007	0.125539
Isoleucine, L- (2TMS)	0.000341	0.000429	0.000022	0.000016	0.008464
Kestose, 1- (11TMS)	0.000110	0.000097	0.000021	0.000012	0.617913
Lyxose, D- (1MEOX) (4TMS) or Xylose, D- (1MEOX) (4TMS)	0.000030	0.000024	0.000002	0.000003	0.107297
Malic acid, DL- (3TMS)	0.002597	0.001920	0.000140	0.000176	0.013132
Malonic acid (2TMS)	0.000064	0.000171	0.000009	0.000059	0.139536
Maltose, D- (1MEOX) (8TMS)	0.000085	0.000058	0.000007	0.000005	0.008608
Melezitose (11TMS)	0.000315	0.000497	0.000037	0.000056	0.021155
Methionine, DL- (2TMS)	0.000176	0.000096	0.000009	0.000005	0.000014
Nicotinic acid (1TMS)	0.000040	0.000017	0.000005	0.000002	0.002056
Octadecanoic acid, n- (1TMS)	0.000176	0.000854	0.000028	0.000114	0.000174
Phenylalanine, DL- (2TMS)	0.000217	0.000166	0.000009	0.000009	0.002575
Phosphoric acid (3TMS)	0.010935	0.012190	0.001627	0.001529	0.586421
Proline, L- (2TMS)	0.000137	0.000059	0.000021	0.000007	0.006111
Putrescine (4TMS)	0.000163	0.000264	0.000015	0.000011	0.000275
Pyroglutamic acid, DL- (2TMS)	0.015106	0.012649	0.001080	0.000554	0.070458
Pyruvic acid (1MEOX) (1TMS)	0.000143	0.000231	0.000011	0.000024	0.007535
Serine, DL- (3TMS)	0.002127	0.005461	0.000095	0.000653	0.000496
Serine, O-acetyl-, DL- (2TMS)	0.000025	0.000070	0.000002	0.000004	0.000002
Succinic acid (2TMS)	0.000317	0.000264	0.000012	0.000017	0.029228
Sucrose, D- (8TMS)	0.006264	0.009236	0.000630	0.000570	0.005741
Threonine, DL- (3TMS)	0.001122	0.000913	0.000083	0.000027	0.037220
Trehalose, alpha, alpha'-, D- (8TMS)	0.000027	0.000034	0.000002	0.000003	0.083392
Tyrosine, DL- (3TMS)	0.000166	0.000171	0.000011	0.000006	0.713201
Uracil (2TMS)	0.000027	0.000044	0.000004	0.000007	0.085779
Urea (2TMS)	0.000396	0.000640	0.000047	0.000065	0.012556
Valine, DL- (2TMS)	0.001016	0.001162	0.000069	0.000070	0.168442

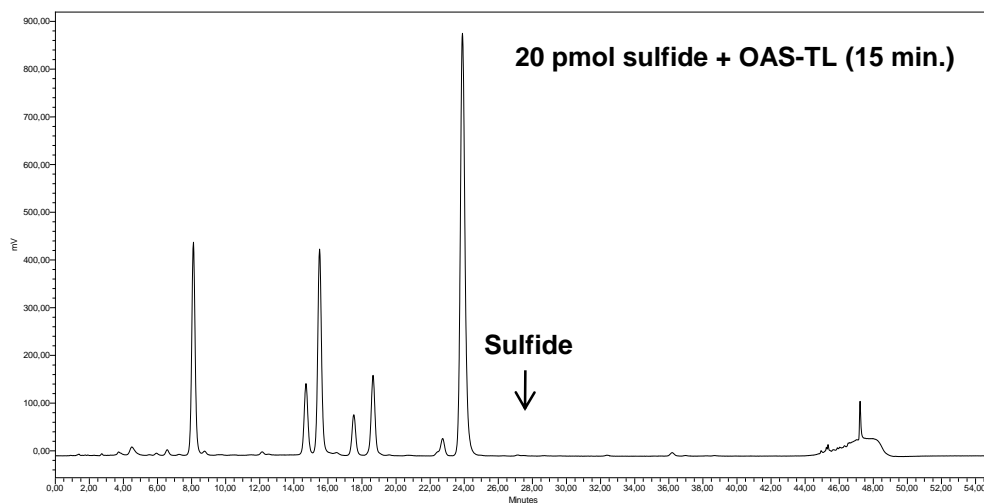
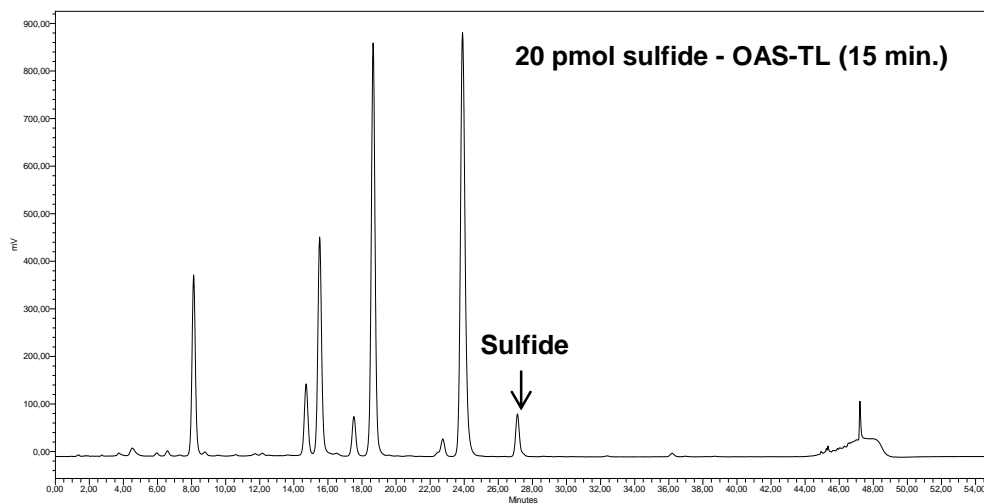
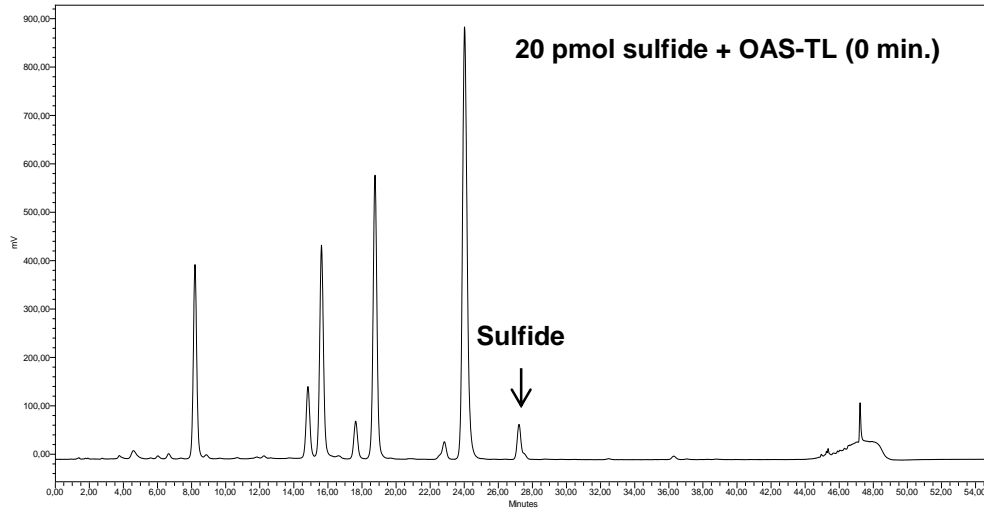
Suppl. data 5 Raw data of root metabolites of *sir1-1* and WT plants after transfer to -S.

6-week-old wild-type and *sir1-1* plants were used to extract soluble metabolites which were detected via GC/MS as described in 2.7.2.

Metabolite	average		SE		t-test
	Col-0	<i>sir1-1</i>	Col-0	<i>sir1-1</i>	
Alanine, beta- (3TMS)	0.000336	0.000258	0.000035	0.000058	0.251518
Alanine, DL- (2TMS)	0.018750	0.013501	0.003275	0.001722	0.258384
Asparagine, DL- (3TMS)	0.002187	0.001847	0.000376	0.000141	0.501348
Aspartic acid, L- (3TMS)	0.012467	0.009775	0.000751	0.002664	0.276485
Benzoic acid (1TMS)	0.000214	0.000374	0.000030	0.000059	0.028349
Butyric acid, 4-amino- (3TMS)	0.024546	0.020064	0.001911	0.004547	0.329396
Butyric acid, 4-hydroxy- (2TMS)	0.000050	0.000100	0.000005	0.000015	0.016871
Calystegine B2 (1MEOX) (4TMS)	0.000125	0.000152	0.000009	0.000042	0.453981
Citric acid (4TMS)	0.003445	0.007855	0.000876	0.001256	0.017520
Erythritol (4TMS)	0.000014	0.000035	0.000001	0.000004	0.000371
Fructose, D- (1MEOX) (5TMS)	0.000903	0.001182	0.000088	0.000117	0.088115
Fructose-6-phosphate, D- (1MEOX) (6TMS)	0.000158	0.000172	0.000015	0.000017	0.568821
Fumaric acid (2TMS)	0.002825	0.004184	0.000434	0.000675	0.111881
Galactinol (9TMS)	0.000070	0.000311	0.000027	0.000052	0.001960
Glucose, D- (1MEOX) (5TMS)	0.006850	0.008655	0.000900	0.001151	0.247491
Glucose-6-phosphate (1MEOX) (6TMS)	0.000215	0.000203	0.000030	0.000010	0.780937
Glutamic acid, DL- (3TMS)	0.015673	0.020697	0.000852	0.004006	0.171083
Glutamine, DL- (3TMS)	0.012986	0.009905	0.001413	0.001214	0.163796
Glutaric acid (2TMS)	0.000147	0.000118	0.000030	0.000046	0.595592
Glutaric acid, 2-oxo- (1MEOX) (2TMS)	0.000549	0.001097	0.000036	0.000252	0.027688
Glyceric acid, DL- (3TMS)	0.000107	0.000175	0.000016	0.000044	0.126519
Glycerol (3TMS)	0.001181	0.002710	0.000115	0.000425	0.003085
Glycerol-3-phosphate, DL- (4TMS)	0.000318	0.000685	0.000023	0.000117	0.005236
Glycine (3TMS)	0.003204	0.005548	0.000580	0.002668	0.323880
Guanidine (3TMS)	0.000134	0.000237	0.000035	0.000096	0.272989
Inositol, myo- (6TMS)	0.005000	0.004399	0.000287	0.000981	0.501578
Isoleucine, L- (2TMS)	0.000873	0.000718	0.000070	0.000109	0.243213
Lactic acid, DL- (2TMS)	0.004312	0.015363	0.000393	0.003194	0.002629
Lysine, L- (4TMS)	0.000625	0.000376	0.000063	0.000091	0.047631
Maleic acid (2TMS)	0.000482	0.000688	0.000103	0.000165	0.353823
Malic acid, DL- (3TMS)	0.006104	0.012362	0.000440	0.003980	0.085781
Maltose, D- (1MEOX) (8TMS)	0.000172	0.000312	0.000036	0.000033	0.027887
Melezitose (11TMS)	0.000883	0.000400	0.000154	0.000141	0.061924
Melibiose (1MEOX) (8TMS)	0.000027	0.000016	0.000006	0.000002	0.232467
Nicotinic acid (1TMS)	0.000251	0.000091	0.000029	0.000016	0.003143
Ornithine, DL- (4TMS)	0.000342	0.000521	0.000029	0.000160	0.210289
Phenylalanine, DL- (2TMS)	0.000775	0.000632	0.000036	0.000105	0.168958
Phosphoric acid (3TMS)	0.020326	0.033586	0.002064	0.010477	0.164912
Putrescine (4TMS)	0.000614	0.001081	0.000052	0.000407	0.191580
Pyroglutamic acid, DL- (2TMS)	0.046034	0.039065	0.002266	0.008165	0.351802
Pyruvic acid (1MEOX) (1TMS)	0.000414	0.000728	0.000050	0.000141	0.040063
Raffinose (11TMS)	0.000265	0.000434	0.000100	0.000116	0.308987
Serine, DL- (3TMS)	0.006152	0.010305	0.000354	0.001627	0.015739
Serine, O-acetyl-, DL- (2TMS)	0.000100	0.000320	0.000007	0.000050	0.000582
Sorbose, D- (1MEOX) (5TMS)	0.000614	0.000860	0.000060	0.000086	0.040229
Succinic acid (2TMS)	0.000858	0.001727	0.000078	0.000479	0.057056
Sucrose, D- (8TMS)	0.007898	0.017932	0.000733	0.004248	0.020431
Tagatose, D- (1MEOX) (5TMS)	0.000198	0.000315	0.000038	0.000148	0.380747
Threonine, DL- (3TMS)	0.003417	0.002059	0.000203	0.000393	0.009583
Trehalose, alpha,alpha'-, D- (8TMS)	0.000849	0.003498	0.000396	0.000708	0.007574
Tryptophan, L- (3TMS)	0.000470	0.000479	0.000033	0.000083	0.916286
Tyrosine, DL- (3TMS)	0.000728	0.000674	0.000035	0.000162	0.701805
Uracil (2TMS)	0.000075	0.000111	0.000011	0.000036	0.285905
Valine, DL- (2TMS)	0.002997	0.002318	0.000288	0.000287	0.149781
Xylose, D- (1MEOX) (4TMS)	0.000045	0.000030	0.000004	0.000003	0.026860

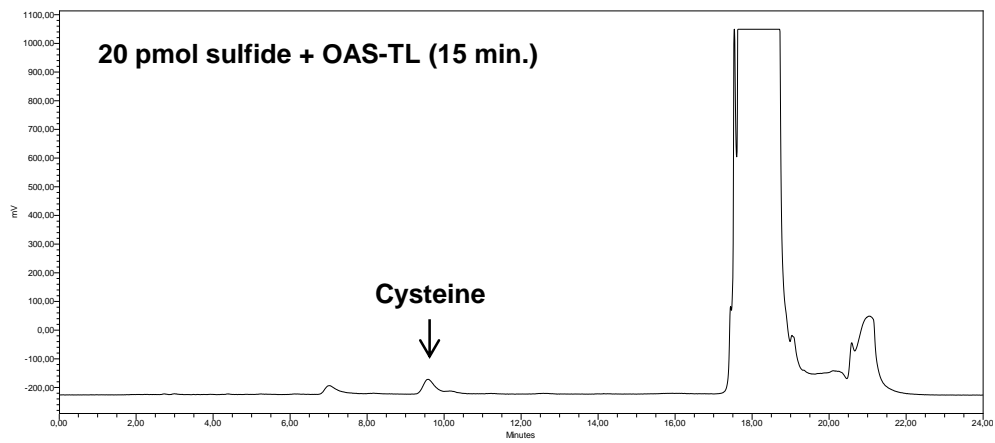
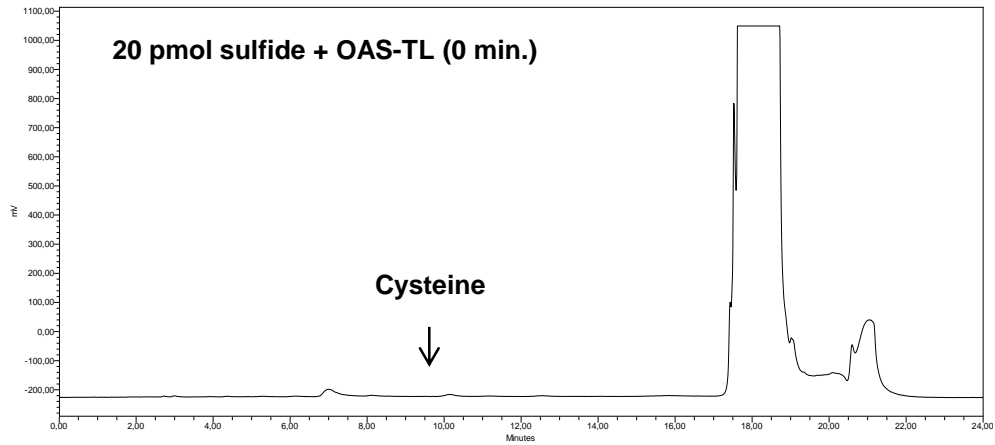
Suppl. data 6 In vitro detection of sulfide via HPLC using OAS-TL activity.

A reaction was carried out in 0.1 ml containing 0.1 mM HEPES, pH 7.5, 0.2 mM sulfide, 10 mM OAS, 5 mM DTT and 2 U OAS-TL A. Thereby, sulfide is converted in cysteine. As a negative control reaction was immediately stopped with 50 μ l trichloroacetic acid. As a second negative control the reaction was carried out without enzyme. The reaction was stopped with 50 μ l trichloroacetic acid after 15 min. An aliquot of 75 μ l was subjected to sulfide derivatization (2.7.3), the second aliquot of 75 μ l to cysteine derivatization (2.7.3 and Suppl. data 7).



Suppl. data 7 In vitro detection of cysteine via HPLC using OAS-TL activity.

A reaction was carried out in 0.1 ml containing 0.1 mM HEPES, pH 7.5, 0.2 mM sulfide, 10 mM OAS, 5 mM DTT and 2 U OAS-TL A. Thereby, sulfide is converted in cysteine. As a negative control reaction was immediately stopped with 50 μ l trichloroacetic acid. The reaction was carried out for 15 min and was stopped with 50 μ l trichloroacetic acid. An aliquot of 75 μ l was subjected to sulfide derivatization (2.7.3 and Suppl. data 6), the second aliquot of 75 μ l to cysteine derivatization (2.7.3).



Suppl. data 8 399 genes that were altered in 7-week-old *sir1-1* in comparison to wild-type of same age.

Only genes with p < 0.05 and 1 < 2log-fold-change > -1 were listed.

Table with 12 columns: ATG, Gene symbol, Difference (L506% (10W) / -506% (7W)) (FV), Difference (L506% (10W) / -V (7W)) (FV), Difference (L506% (7W) / -V (7W)) (FV), p (L506% (10W) / -506% (7W)) (FV), p (L506% (10W) / -V (7W)) (FV), p (L506% (7W) / -V (7W)) (FV), and 6 columns of p-values for various genes.

(Table continues on following page.)

Suppl. data 10 Mutation-specific regulated genes in *sir1-1*.

Genes were categorized and listed, when they were altered in the same manner in 7- and 10-week-old *sir1-1* plants (both up- or down-regulated), but remained unchanged during *sir1-1* development; ($p < 0.05$; $1 < 2\log\text{-fold-change} > -1$).

Locus	Gene title	Category	Difference (<i>sir1-1</i> (10w)- WT(7w))	Difference (<i>sir1-1</i> (7w)- WT(7w))
AT3G30775	ERD5 (EARLY RESPONSIVE TO DEHYDRATION 5); PROLINE DEHYDROGENASE	amino acid metabolism	1.6	1.3
AT2G13810	ALD1 (AGD2-LIKE DEFENSE RESPONSE PROTEIN1); CATALYTIC	amino acid metabolism	-1.2	-1.2
AT3G22740	HMT3; HOMOCYSTEINE S-METHYLTRANSFERASE	amino acid metabolism	1.1	1.6
AT3G19710	BCAT4 (BRANCHED-CHAIN AMINOTRANSFERASE4)	amino acid metabolism + secondary metabolism	2.1	1.3
AT2G38400	AGT3 (ALANINE:GLYOXYLATE AMINOTRANSFERASE 3)	amino acid metabolism	1.8	1.0
AT1G36370	SHM7 (SERINE HYDROXYMETHYLTRANSFERASE 7); CATALYTIC/ GLYCINE HYDROXYMETHYLTRANSFERASE	C1-metabolism	-1.4	-1.8
AT5G44130	FLA13 (FASCICLIN-LIKE ARABINO GALACTAN PROTEIN 13 PRECURSOR)	cell wall	-1.4	-1.0
AT1G35230	AGP5 (ARABINO GALACTAN-PROTEIN 5)	cell wall	-1.8	-1.8
AT4G03450	ANKYRIN REPEAT FAMILY PROTEIN	cell	-1.2	-1.8
AT1G10340	ANKYRIN REPEAT FAMILY PROTEIN	cell	-1.0	-1.5
AT1G02820	LATE EMBRYOGENESIS ABUNDANT 3 FAMILY PROTEIN / LEA3 FAMILY PROTEIN	development	-1.1	-1.2
AT1G28330	DYL1 (DORMANCY-ASSOCIATED PROTEIN-LIKE 1)	development	1.1	1.4
AT4G22530	EMBRYO-ABUNDANT PROTEIN-RELATED	development	-1.0	-1.4
AT2G35980	YLS9 (YELLOW-LEAF-SPECIFIC GENE 9)	development	-1.5	-1.7
AT3G13610	OXIDOREDUCTASE, 2OG-FE(II) OXYGENASE FAMILY PROTEIN	DNA	-1.4	-2.0
AT5G13320	PBS3 (AVRPPHB SUSCEPTIBLE 3)	hormone metabolism	-1.1	-2.0
AT1G22400	UGT85A1; UDP-GLYCOSYLTRANSFERASE/ CIS-ZEA TIN O-BETA-D-GLUCOSYLTRANSFERASE	hormone metabolism	-1.7	-1.3
AT5G44070	CAD1 (CADMIUM SENSITIVE 1)	metal handling	-1.0	-1.4
AT2G47180	ATGOLS1 (ARABIDOPSIS THALIANA GALACTINOL SYNTHASE 1)	minor CHO metabolism	1.1	1.1
AT2G04450	ATNUDT6 (ARABIDOPSIS THALIANA NUDIX HYDROLASE HOMOLOG 6); ADP-RIBOSE DIPHOSPHATASE	nucleotide metabolism	-2.2	-2.3
AT2G04430	ATNUDT5 (ARABIDOPSIS THALIANA NUDIX HYDROLASE HOMOLOG 5); HYDROLASE	nucleotide metabolism	-1.1	-1.1
AT1G20823	ZINC FINGER (C3HC4-TYPE RING FINGER) FAMILY PROTEIN	protein	-1.1	-1.2
AT4G11890	PROTEIN KINASE FAMILY PROTEIN	protein	-1.6	-1.8
AT1G48920	ATNUC-L1; NUCLEIC ACID BINDING / NUCLEOTIDE BINDING	protein	1.1	1.1
AT1G30900	VACUOLAR SORTING RECEPTOR, PUTATIVE	protein	-1.1	-1.6
AT1G03850	GLUTAREDOXIN FAMILY PROTEIN	redox	-1.4	-1.2
AT1G64380	AP2 DOMAIN-CONTAINING TRANSCRIPTION FACTOR, PUTATIVE	RNA	-1.3	-1.1
AT5G62920	ARR6 (RESPONSE REGULATOR 6); TRANSCRIPTION REGULATOR/ TWO-COMPONENT RESPONSE REGULATOR	RNA	-1.3	-1.5
AT3G48100	ARR5 (ARABIDOPSIS RESPONSE REGULATOR 5); TRANSCRIPTION REGULATOR/ TWO-COMPONENT RESPONSE REGULATOR	RNA	-1.3	-1.1
AT1G19050	ARR7 (RESPONSE REGULATOR 7)	RNA	-1.3	-1.7
AT1G74890	ARR15 (RESPONSE REGULATOR 15); TRANSCRIPTION REGULATOR	RNA	-1.3	-1.6
AT4G13850	GR-RBP2 (GLYCINE-RICH RNA-BINDING PROTEIN 2); ATP BINDING / RNA BINDING / DOUBLE-STRANDED DNA BINDING / SINGLE-STRANDED DNA BINDING	RNA	1.0	1.1
AT2G21660	CCR2 (COLD, CIRCADIAN RHYTHM, AND RNA BINDING 2); RNA AND DNA BINDING	RNA	1.9	1.3
AT5G24120	SIGE (SIGMA FACTOR E); DNA BINDING / DNA-DIRECTED RNA POLYMERASE/ SIGMA FACTOR/ TRANSCRIPTION FACTOR	RNA	-1.1	-1.7
AT5G04590	SIR; SULFITE REDUCTASE (FERREDOXIN)	S-assimilation	-1.3	-1.3
AT5G42830	TRANSFERASE FAMILY PROTEIN	secondary metabolism	-1.1	-1.4
AT3G16390	NSP1 (NITRILE SPECIFIER PROTEIN 1)	secondary metabolism + hormone metabolism	1.3	2.1
AT5G23010	MAM1 (METHYLTHIOALKYLALATE SYNTHASE 1); 2-ISOPROPYLMALATE SYNTHASE/ METHYLTHIOALKYLALATE SYNTHASE	secondary metabolism	1.6	1.1
AT5G52810	ORNITHINE CYCLODEAMINASE/MU-CRYSTALLIN FAMILY PROTEIN	secondary metabolism	-1.5	-1.5
AT1G52410	TSA1 (TSK-ASSOCIATING PROTEIN 1)	signalling	1.4	2.3
AT1G01560	ATMPK11	signalling	-1.2	-1.7
AT1G09080	BIP3; ATP BINDING	stress	-1.2	-1.3
AT3G50480	HR4 (HOMOLOG OF RPW8 4)	stress	-1.3	-1.5
AT3G47540	CHITINASE, PUTATIVE	stress	-1.2	-1.4
AT1G75040	PR5 (PATHOGENESIS-RELATED GENE 5)	stress	-2.2	-2.6
AT2G14610	PR1 (PATHOGENESIS-RELATED GENE 1)	stress	-1.8	-2.8
AT1G57630	DISEASE RESISTANCE PROTEIN (TR CLASS), PUTATIVE	stress	-1.2	-1.9
AT3G11010	ATRLP34 (RECEPTOR LIKE PROTEIN 34); KINASE	stress	-1.1	-1.6
AT1G73330	ATDR4; PEPTIDASE INHIBITOR	stress	1.7	1.7
AT1G33960	AG1 (AVRRPT2-INDUCED GENE 1); GTP BINDING	stress	-1.9	-2.2

(Table continues on following page.)

Suppl. data 10 (Continued from previous page.)

AT3G52720	ACA1 (ALPHA CARBONIC ANHYDRASE 1)	TCA / org. transformation	-1.8	-1.7
AT1G15520	PDR12 (PLEIOTROPIC DRUG RESISTANCE 12); ATPASE	transport	-1.2	-1.6
AT3G56200	AMINO ACID TRANSPORTER FAMILY PROTEIN	transport	-1.4	-1.6
AT2G22500	UCP5 (UNCOUPLING PROTEIN 5); BINDING	transport	-1.0	-1.8
AT4G37370	CYP81D8; ELECTRON CARRIER/HEME BINDING / IRON ION BINDING / MONOOXYGENASE/ OXYGEN BINDING	misc	-1.1	-2.0
AT3G26210	CYP71B23; ELECTRON CARRIER/HEME BINDING / IRON ION BINDING	misc	-1.0	-1.3
AT1G02850	BGLU11 (BETA GLUCOSIDASE 11); CATALYTIC	misc	2.2	1.4
AT5G18470	CURCULIN-LIKE (MANNOSE-BINDING) LECTIN FAMILY PROTEIN	misc	-1.3	-1.8
AT4G20830	FAD-BINDING DOMAIN-CONTAINING PROTEIN	misc	-1.4	-1.2
AT1G19250	FMO1 (FLAVIN-DEPENDENT MONOOXYGENASE 1); FAD BINDING / NADP OR NADPH BINDING	misc	-1.0	-1.7
AT5G55450	PROTEASE INHIBITOR/SEED STORAGE/LIPID TRANSFER PROTEIN (LTP) FAMILY PROTEIN	misc	-1.1	-1.5
AT3G11340	UDP-GLUCORONOSYL/UDP-GLUCOSYL TRANSFERASE FAMILY PROTEIN	misc	-1.6	-1.6
AT1G55960	---	not assigned	-1.4	-1.4
AT2G26400	ATARD3 (ACIREDUCTONE DIOXYGENASE 3)	not assigned	-2.0	-2.3
AT5G48540	33 KDA SECRETORY PROTEIN-RELATED	not assigned	-1.3	-1.4
AT3G60420	---	not assigned	-1.2	-1.7
AT3G48640	---	not assigned	-1.4	-1.7
AT4G39670	GLYCOLIPID BINDING / GLYCOLIPID TRANSPORTER	not assigned	-1.3	-1.8
AT4G01870	TOLB PROTEIN-RELATED	not assigned	-1.1	-1.3
AT3G28290	AT14A	not assigned	1.2	2.2
AT3G28270	---	not assigned	1.8	1.1
ORF111D	ORF111D	not assigned	1.3	1.1
AT3G01290	BAND 7 FAMILY PROTEIN	not assigned	-1.7	-1.7
AT1G56060	---	not assigned	-1.6	-1.7
AT1G14870	---	not assigned	-1.7	-2.4

Suppl. data 11 Constantly altered genes in all three groups.

Interfacing genes were categorized and listed, when they were altered in 7- and 10-week-old *sir1-1* and 7-week-old wild-type plants; ($p < 0.05$; $1 < 2\log\text{-fold-change} > -1$).

Locus	Gene title	Category	Difference (<i>sir1-1</i> (10w)- <i>sir1-1</i> (7w))	Difference (<i>sir1-1</i> (10w)-WT(7w))	Difference (<i>sir1-1</i> (7w)-WT(7w))
AT5G06870	PGIP2 (POLYGALACTURONASE INHIBITING PROTEIN 2)	cell w all	-2.4	-1.1	1.3
AT2G17840	ERD7 (EARLY-RESPONSIVE TO DEHYDRATION 7)	development	2.3	1.3	-1.1
AT4G35770	SEN1 (SENESCENCE 1)	development	-3.5	-2.2	1.3
AT5G14920	GIBBERELLIN-REGULATED FAMILY PROTEIN	hormone metabolism	-2.4	-1.2	1.2
AT3G47340	ASN1 (GLUTAMINE-DEPENDENT ASPARAGINE SYNTHASE 1)	protein	-3.5	-1.4	2.2
AT3G48360	BT2 (BTB AND TAZ DOMAIN PROTEIN 2)	protein	-3.0	-1.1	1.9
AT1G23390	KELCH REPEAT-CONTAINING F-BOX FAMILY PROTEIN	protein	-2.3	-1.1	1.2
AT1G09070	SRC2 (SOY BEAN GENE REGULATED BY COLD-2)	protein	2.4	1.3	-1.1
AT5G22920	ZINC FINGER (C3HC4-TYPE RING FINGER) FAMILY PROTEIN	protein	-2.7	-1.6	1.1
AT2G21650	MEE3 (MATERNAL EFFECT EMBRYO ARREST 3)	RNA	3.0	1.6	-1.4
AT1G52040	MBP2 (MYROSINASE-BINDING PROTEIN 2)	secondary metabolism	-1.1	1.3	2.4
AT1G66760	MATE EFFLUX FAMILY PROTEIN	transport	-2.4	-1.1	1.4
AT3G22600	PROTEASE INHIBITOR/SEED STORAGE/LIPID TRANSFER PROTEIN (LTP) FAMILY PROTEIN	misc	1.3	-1.7	-2.9
AT1G64360	---	not assigned	2.8	1.2	-1.7
AT1G76960	---	not assigned	2.4	1.3	-1.1
AT2G05540	---	not assigned	-3.0	-2.0	1.0
AT2G18690	---	not assigned	1.1	-1.1	-2.1
AT3G07350	---	not assigned	-2.7	-1.5	1.2
AT3G15450	---	not assigned	-3.9	-2.3	1.6
AT3G15630	---	not assigned	-2.4	-1.3	1.0
AT5G52760	HEAVY-METAL-ASSOCIATED DOMAIN-CONTAINING PROTEIN	not assigned	1.1	-1.2	-2.3

Suppl. data 12 GSEA results for gene set 'nucleobase, nucleoside and nucleic acid metabolic process'.

Genes from the significantly affected gene set 'nucleobase, nucleoside and nucleic acid metabolic process' between *sir1-1* (7-week-old) vs. wild-type and *sir1-1* (10-week-old) were listed. Redundant genes were highlighted in italic.

Locus	Gene	Description	Rank in gene list	Rank metric score	Running Es	Core enrichment
Nucleobase, nucleoside, nucleotide and nucleic acid metabolic process						
<i>sir1-1</i> (7W) vs WT						
AT1G77470	<i>RFC3</i>	replication factor C subunit 3	116	1.045	0.096	Yes
AT3G57610	<i>ADSS</i>	adenylosuccinate synthetase	797	0.526	0.178	Yes
AT2G01170	<i>BAT1</i>	bidirectional amino acid transporter 1	1010	0.462	0.213	Yes
AT2G34710	<i>PHB</i>	homeobox-leucine zipper protein ATHB-14	1166	0.430	0.248	Yes
AT5G61770	<i>PPAN</i>	Peter Pan-like protein	1477	0.378	0.270	Yes
AT3G48190	<i>ATM</i>	serine/threonine-protein kinase	1519	0.371	0.304	Yes
AT2G31970	<i>RAD50</i>	DNA repair protein RAD50	1765	0.339	0.326	Yes
AT1G73960	<i>TAF2</i>	TBP-associated factor 2	2225	0.290	0.332	Yes
AT2G29680	<i>CDC6</i>	cell division control 6	2332	0.279	0.354	Yes
AT5G44740	<i>POLH</i>	DNA polymerase eta subunit	2571	0.259	0.368	Yes
AT5G42540	<i>XRN2</i>	5'-3' exoribonuclease 2	2594	0.257	0.392	Yes
AT4G02460	<i>PMS1</i>	DNA mismatch repair protein PMS2	2818	0.242	0.405	Yes
AT5G44750	<i>REV1</i>	DNA repair protein REV1	2900	0.236	0.424	Yes
AT4G09140	<i>MLH1</i>	DNA mismatch repair protein MLH1	2974	0.231	0.443	Yes
AT1G54390	<i>ING2</i>	PHD finger protein-like protein	3275	0.213	0.450	Yes
AT3G18524	<i>MSH2</i>	DNA mismatch repair protein Msh2	3339	0.209	0.467	Yes
AT2G42120	<i>POLD2</i>	DNA polymerase delta subunit 2	3552	0.196	0.476	Yes
AT5G62810	<i>PEX14</i>	peroxin 14	3642	0.191	0.491	Yes
AT2G45640	<i>SAP18</i>	histone deacetylase complex subunit SAP18	3676	0.189	0.507	Yes
AT2G34520	<i>RPS14</i>	small subunit ribosomal protein S14	3977	0.174	0.510	Yes
AT3G22880	<i>DMC1</i>	meiotic recombination protein DMC1-like protein	4760	0.140	0.487	Yes
AT1G20693	<i>HMGB2</i>	high mobility group B2 protein	4764	0.140	0.500	Yes
AT1G09815	<i>POLD4</i>	DNA polymerase delta subunit 4	5101	0.126	0.497	Yes
AT3G51880	<i>HMGB1</i>	high mobility group protein B1	5297	0.119	0.499	Yes
AT2G24490	<i>RPA2</i>	replicon protein A2	5494	0.112	0.501	Yes
AT2G36010	<i>E2F3</i>	E2F transcription factor 3	5514	0.111	0.510	Yes
<i>sir1-1</i> (10W) vs WT						
AT1G20693	<i>HMGB2</i>	high mobility group B2 protein	86	1.521	0.116	Yes
AT5G58760	<i>DDB2</i>	DNA damage-binding protein 2	675	0.685	0.142	Yes
AT2G01170	<i>BAT1</i>	bidirectional amino acid transporter 1	839	0.615	0.182	Yes
AT5G44750	<i>REV1</i>	DNA repair protein REV1	1108	0.544	0.213	Yes
AT5G62810	<i>PEX14</i>	peroxin 14	1455	0.471	0.233	Yes
AT3G51880	<i>HMGB1</i>	high mobility group protein B1	1510	0.460	0.267	Yes
AT2G42120	<i>POLD4</i>	DNA polymerase delta subunit 2	1531	0.457	0.302	Yes
AT1G08600	<i>ATR</i>	DEAD-like helicase domain-containing protein	1868	0.400	0.318	Yes
AT1G73960	<i>TAF2</i>	TBP-associated factor 2	1898	0.396	0.347	Yes
AT2G31970	<i>RAD50</i>	DNA repair protein RAD50	2161	0.363	0.364	Yes
AT4G26840	<i>SUMO1</i>	small ubiquitin-related modifier 1	2229	0.356	0.388	Yes
AT5G61770	<i>PPAN</i>	Peter Pan-like protein	2277	0.350	0.414	Yes
AT3G48190	<i>ATM</i>	serine/threonine-protein kinase	2590	0.320	0.424	Yes
AT1G77470	<i>RFC3</i>	replication factor C subunit 3	3019	0.281	0.451	Yes
AT1G54390	<i>ING2</i>	PHD finger protein-like protein	3126	0.273	0.467	Yes
AT5G44740	<i>POLH</i>	DNA polymerase eta subunit	3318	0.257	0.478	Yes
AT4G09140	<i>MLH1</i>	DNA mismatch repair protein MLH1	3638	0.233	0.481	Yes
AT3G05210	<i>ERCC1</i>	DNA excision repair protein ERCC-1	3720	0.228	0.496	Yes
AT4G02460	<i>PMS1</i>	DNA mismatch repair protein PMS2	3895	0.218	0.505	Yes

Suppl. data 13 GSEA results for gene set 'DNA metabolic process'.

Genes from the significantly affected gene set 'DNA metabolic process' between *sir1-1* (7-week-old) vs. wild-type and *sir1-1* (10-week-old) were listed. Redundant genes were highlighted in italic.

Locus	Gene	Description	Rank in gene list	Rank metric score	Running Es	Core enrichment
DNA metabolic process						
<i>sir1-1</i> (7W) vs WT						
AT1G77470	<i>RFC3</i>	replication factor C subunit 3	116	1.045	0.207	Yes
AT3G48190	<i>ATM</i>	serine/threonine-protein kinase	1519	0.371	0.216	Yes
AT2G31970	<i>RAD50</i>	DNA repair protein RAD50	1765	0.339	0.273	Yes
AT2G29680	<i>CDC6</i>	cell division control 6	2332	0.279	0.303	Yes
AT5G44740	<i>POLH</i>	DNA polymerase eta subunit	2571	0.259	0.344	Yes
AT5G42540	<i>XRN2</i>	5'-3' exoribonuclease 2	2594	0.257	0.395	Yes
AT4G02460	<i>PMS1</i>	DNA mismatch repair protein PMS2	2818	0.242	0.434	Yes
AT5G44750	<i>REV1</i>	DNA repair protein REV1	2900	0.236	0.478	Yes
AT4G09140	<i>MLH1</i>	DNA mismatch repair protein MLH1	2974	0.231	0.521	Yes
AT3G18524	<i>MSH2</i>	DNA mismatch repair protein Msh2	3339	0.209	0.546	Yes
AT2G42120	<i>POLD2</i>	DNA polymerase delta subunit 2	3552	0.196	0.576	Yes
AT3G22880	<i>DMC1</i>	meiotic recombination protein DMC1-like protein	4760	0.140	0.547	Yes
AT1G20693	<i>HMGB2</i>	high mobility group B2 protein	4764	0.140	0.576	Yes
AT1G09815	<i>POLD4</i>	DNA polymerase delta subunit 4	5101	0.126	0.585	Yes
AT3G51880	<i>HMGB1</i>	high mobility group protein B1	5297	0.119	0.600	Yes
AT2G24490	<i>RPA2</i>	replicon protein A2	5494	0.112	0.614	Yes
AT1G08600	<i>ATRX</i>	DEAD-like helicase domain-containing protein	5728	0.104	0.624	Yes
AT3G20475	<i>MSH5</i>	DNA mismatch repair protein MSH5	6089	0.091	0.625	Yes
<i>sir1-1</i> (10W) vs WT						
AT1G20693	<i>HMGB2</i>	high mobility group B2 protein	86	1.521	0.197	Yes
AT5G58760	<i>DDB2</i>	DNA damage-binding protein 2	675	0.685	0.259	Yes
AT5G44750	<i>REV1</i>	DNA repair protein REV1	1108	0.544	0.311	Yes
AT3G51880	<i>HMGB1</i>	high mobility group protein B1	1510	0.460	0.353	Yes
AT1G09815	<i>POLD4</i>	DNA polymerase delta subunit 4	1531	0.457	0.412	Yes
AT1G08600	<i>ATRX</i>	DEAD-like helicase domain-containing protein	1868	0.400	0.449	Yes
AT2G31970	<i>RAD50</i>	DNA repair protein RAD50	2161	0.363	0.483	Yes
AT4G26840	<i>SUMO1</i>	small ubiquitin-related modifier 1	2229	0.356	0.527	Yes
AT3G48190	<i>ATM</i>	serine/threonine-protein kinase	2590	0.320	0.552	Yes
AT1G77470	<i>RFC3</i>	replication factor C subunit 3	3019	0.281	0.569	Yes
AT5G44740	<i>POLH</i>	DNA polymerase eta subunit	3318	0.257	0.589	Yes
AT4G09140	<i>MLH1</i>	DNA mismatch repair protein MLH1	3638	0.233	0.604	Yes
AT3G05210	<i>ERCC1</i>	DNA excision repair protein ERCC-1	3720	0.228	0.631	Yes
AT4G02460	<i>PMS1</i>	DNA mismatch repair protein PMS2	3895	0.218	0.651	Yes

Suppl. data 14 GSEA results for gene set 'DNA repair'.

Genes from the significantly affected gene set 'DNA repair' between *sir1-1* (7-week-old) vs. wild-type and *sir1-1* (10-week-old) were listed. Redundant genes were highlighted in italic.

Locus	Gene	Description	Rank in gene list	Rank metric score	Running Es	Core enrichment
DNA repair						
<i>sir1-1</i> (7W) vs WT						
AT1G77470	<i>RFC3</i>	replication factor C subunit 3	116	1.045	0.269	Yes
AT3G48190	<i>ATM</i>	serine/threonine-protein kinase	1519	0.371	0.301	Yes
AT2G31970	<i>RAD50</i>	DNA repair protein RAD50	1765	0.339	0.378	Yes
AT5G44740	<i>POLH</i>	DNA polymerase eta subunit	2571	0.259	0.408	Yes
AT4G02460	<i>PMS1</i>	DNA mismatch repair protein PMS2	2818	0.242	0.460	Yes
AT5G44750	<i>REV1</i>	DNA repair protein REV1	2900	0.236	0.519	Yes
AT4G09140	<i>MLH1</i>	DNA mismatch repair protein MLH1	2974	0.231	0.576	Yes
AT3G18524	<i>MSH2</i>	DNA mismatch repair protein Msh2	3339	0.209	0.613	Yes
<i>sir1-1</i> (10W) vs WT						
AT1G20693	<i>HMGB2</i>	high mobility group B2 protein	86	1.521	0.240	Yes
AT5G58760	<i>DDB2</i>	DNA damage-binding protein 2	675	0.685	0.323	Yes
AT5G44750	<i>REV1</i>	DNA repair protein REV1	1108	0.544	0.390	Yes
AT3G51880	<i>HMGB1</i>	high mobility group protein B1	1510	0.460	0.445	Yes
AT1G08600	<i>ATR</i>	DEAD-like helicase domain-containing protein	1868	0.400	0.492	Yes
AT2G31970	<i>RAD50</i>	DNA repair protein RAD50	2161	0.363	0.537	Yes
AT4G26840	<i>SUMO1</i>	small ubiquitin-related modifier 1	2229	0.356	0.591	Yes
AT3G48190	<i>ATM</i>	serine/threonine-protein kinase	2590	0.320	0.625	Yes
AT1G77470	<i>RFC3</i>	replication factor C subunit 3	3019	0.281	0.650	Yes
AT5G44740	<i>POLH</i>	DNA polymerase eta subunit	3318	0.257	0.678	Yes
AT4G09140	<i>MLH1</i>	DNA mismatch repair protein MLH1	3638	0.233	0.700	Yes
AT3G05210	<i>ERCC1</i>	DNA excision repair protein ERCC-1	3720	0.228	0.733	Yes
AT4G02460	<i>PMS1</i>	DNA mismatch repair protein PMS2	3895	0.218	0.760	Yes

Suppl. data 15 GSEA results for gene set 'response to endogenous stimulus'.

Genes from the significantly affected gene set 'response to endogenous stimulus' between *sir1-1* (7 week-old) vs. wild-type and *sir1-1* (10-week-old) were listed. Redundant genes were highlighted in italic.

Locus	Gene	Description	Rank in gene list	Rank metric score	Running Es	Core enrichment
Response to endogenous stimulus						
<i>sir1-1</i> (7W) vs WT						
AT1G77470	<i>RFC3</i>	replication factor C subunit 3	116	1.045	0.269	Yes
AT3G48190	<i>ATM</i>	serine/threonine-protein kinase	1519	0.371	0.301	Yes
AT2G31970	<i>RAD50</i>	DNA repair protein RAD50	1765	0.339	0.378	Yes
AT5G44740	<i>POLH</i>	DNA polymerase eta subunit	2571	0.259	0.408	Yes
AT4G02460	<i>PMS1</i>	DNA mismatch repair protein PMS2	2818	0.242	0.460	Yes
AT5G44750	<i>REV1</i>	DNA repair protein REV1	2900	0.236	0.519	Yes
AT4G09140	<i>MLH1</i>	DNA mismatch repair protein MLH1	2974	0.231	0.576	Yes
AT3G18524	<i>MSH2</i>	DNA mismatch repair protein Msh2	3339	0.209	0.613	Yes
<i>sir1-1</i> (10W) vs WT						
AT1G20693	<i>HMGB2</i>	high mobility group B2 protein	86	1.521	0.240	Yes
AT5G58760	<i>DDB2</i>	DNA damage-binding protein 2	675	0.685	0.323	Yes
AT5G44750	<i>REV1</i>	DNA repair protein REV1	1108	0.544	0.390	Yes
AT3G51880	<i>HMGB1</i>	high mobility group protein B1	1510	0.460	0.445	Yes
AT1G08600	<i>ATR</i>	DEAD-like helicase domain-containing protein	1868	0.400	0.492	Yes
AT2G31970	<i>RAD50</i>	DNA repair protein RAD50	2161	0.363	0.537	Yes
AT4G26840	<i>SUMO1</i>	small ubiquitin-related modifier 1	2229	0.356	0.591	Yes
AT3G48190	<i>ATM</i>	serine/threonine-protein kinase	2590	0.320	0.625	Yes
AT1G77470	<i>RFC3</i>	replication factor C subunit 3	3019	0.281	0.650	Yes
AT5G44740	<i>POLH</i>	DNA polymerase eta subunit	3318	0.257	0.678	Yes
AT4G09140	<i>MLH1</i>	DNA mismatch repair protein MLH1	3638	0.233	0.700	Yes
AT3G05210	<i>ERCC1</i>	DNA excision repair protein ERCC-1	3720	0.228	0.733	Yes
AT4G02460	<i>PMS1</i>	DNA mismatch repair protein PMS2	3895	0.218	0.760	Yes

Suppl. data 16 GSEA results for gene set response to 'DNA damage stimulus'.

Genes from the significantly affected gene set 'response to DNA damage stimulus' between *sir1-1* (7 week-old) vs. wild-type and *sir1-1* (10-week-old) were listed. Redundant genes were highlighted in italic.

Locus	Gene	Description	Rank in gene list	Rank metric score	Running Es	Core enrichment
Response to DNA damage stimulus						
<i>sir1-1</i> (7W) vs WT						
AT1G77470	<i>RFC3</i>	replication factor C subunit 3	116	1.045	0.269	Yes
AT3G48190	<i>ATM</i>	serine/threonine-protein kinase	1519	0.371	0.301	Yes
AT2G31970	<i>RAD50</i>	DNA repair protein RAD50	1765	0.339	0.378	Yes
AT5G44740	<i>POLH</i>	DNA polymerase eta subunit	2571	0.259	0.408	Yes
AT4G02460	<i>PMS1</i>	DNA mismatch repair protein PMS2	2818	0.242	0.460	Yes
AT5G44750	<i>REV1</i>	DNA repair protein REV1	2900	0.236	0.519	Yes
AT4G09140	<i>MLH1</i>	DNA mismatch repair protein MLH1	2974	0.231	0.576	Yes
AT3G18524	<i>MSH2</i>	DNA mismatch repair protein Msh2	3339	0.209	0.613	Yes
<i>sir1-1</i> (10W) vs WT						
AT1G20693	<i>HMGB2</i>	high mobility group B2 protein	86	1.521	0.240	Yes
AT5G58760	<i>DDB2</i>	DNA damage-binding protein 2	675	0.685	0.323	Yes
AT5G44750	<i>REV1</i>	DNA repair protein REV1	1108	0.544	0.390	Yes
AT3G51880	<i>HMGB1</i>	high mobility group protein B1	1510	0.460	0.445	Yes
AT1G08600	<i>ATR</i>	DEAD-like helicase domain-containing protein	1868	0.400	0.492	Yes
AT2G31970	<i>RAD50</i>	DNA repair protein RAD50	2161	0.363	0.537	Yes
AT4G26840	<i>SUMO1</i>	small ubiquitin-related modifier 1	2229	0.356	0.591	Yes
AT3G48190	<i>ATM</i>	serine/threonine-protein kinase	2590	0.320	0.625	Yes
AT1G77470	<i>RFC3</i>	replication factor C subunit 3	3019	0.281	0.650	Yes
AT5G44740	<i>POLH</i>	DNA polymerase eta subunit	3318	0.257	0.678	Yes
AT4G09140	<i>MLH1</i>	DNA mismatch repair protein MLH1	3638	0.233	0.700	Yes
AT3G05210	<i>ERCC1</i>	DNA excision repair protein ERCC-1	3720	0.228	0.733	Yes
AT4G02460	<i>PMS1</i>	DNA mismatch repair protein PMS2	3895	0.218	0.760	Yes

Suppl. data 17 Detailed information about LC-MS/MS protein identification.

This table includes detailed information about protein digestion, mass spectrometry, data acquisition, MASCOT search parameters, peptide sequences and scores.

Databank

NCBI nr 20100104 (10274250 sequences; 3505793397 residues)
taxonomy: Arabidopsis thaliana (thale cress) (62387 sequences)

search parameters

Type of search : MS/MS Ion Search
Enzyme : Trypsin
Variable modifications : Carbamidomethyl (C), Oxidation (M)
Mass values : Monoisotopic
Protein Mass : Unrestricted
Peptide Mass Tolerance : ± 0.1 Da
Fragment Mass Tolerance : ± 0.2 Da
Max Missed Cleavages : 2
Instrument type : ESI-QUAD-TOF

validation:

significant score > 35 (for proteins)
at least two different peptides
if a single peptide score > 50 and at least 5 consecutive y or b ions

spots	protein accession	protein description	% coverage	score > 35	MW	Pi	m/z	mass (exp)	sequence
22	gi15238686	AT5G17920 ATMS1;5-methyltetrahydropteroyltriglutamate-homocysteine S-methyltransferase/ copper ion binding/ methionine synthase	3	59	84304	6.09	437.7249	873.4352	R.VTNEGQVK.A
mascot-22									
24									
mascot-24									
29	gi15235321	AT4G28520 CRU3 (CRUCIFERIN3); nutrient reservoir [Arabidopsis thaliana]	2	139	58199	6.53	668.9776	1335.9406	K.ISYVQGTGISGR.V
	gi162319667	AT5G44120 legumin-like protein [Arabidopsis thaliana]	10	50	13066	9.8	672.4567	1342.8988	K.TNANAQNTLAGR.T
	gi166676	12S storage protein CRA1 [Arabidopsis thaliana]	4	49	52592	7.68	596.8552	1191.6958	R.CTDNLDDPSR.A + Carbamidomethyl (C)
	gi13430632	AT3G24170 putative glutathione reductase [Arabidopsis thaliana]	2	35	53807	6.36	672.4567	1342.8988	K.TNANAQNTLAGR.T
							549.3806	1096.7466	R.VWGPNEVEVR.Q
mascot-26									
31	gi14916970	RecName: Full=ATP synthase subunit alpha, mitochondrial	16	212	55011	6.23	438.8233	875.6320	R.QMSLLLR.R + Oxidation (M)
							513.8898	1025.7650	K.AVDSLVIPIGR.G
							522.3795	1042.7444	R.TGSIVDVPAGK.A
							608.9190	1215.8234	R.VWDAMGVPIDGK.G + Oxidation (M)
							621.9212	1241.8278	K.SVHEPMTGLK.A + Oxidation (M)
							625.9326	1249.8506	R.AAELTNLFESR.I
							642.4627	1282.9108	K.QPQYAPLPIEK.Q
							665.9969	1329.9792	K.TTIAIDTLNQQ.Q
mascot-31									
35									
mascot-35									
38	gi166702	glyceraldehyde 3-phosphate dehydrogenase A subunit [Arabidopsis thaliana]	27	321	37652	7	417.3119	832.6092	K.VAINGFGR.I
							464.8549	927.6952	K.IIQVSNR.N
							519.4218	1036.8290	K.AVALVLPNLK.G
							627.9145	1253.8144	K.TFAEEVNAFR.D
							693.0063	1383.9980	R.AAALNIVPTSTGAAK.A
							729.0142	1456.0138	R.VDLADIVANNWK.-
							814.5616	1627.1086	K.DSPLDIIINDTGGVK.Q
							917.6056	1833.1966	K.GILDVCEPLVSVDFR.C + Carbamidomethyl (C)
	gi15218564	AT1G72680 cinnamyl-alcohol dehydrogenase, putative [Arabidopsis thaliana]	9	140	38646	6.67	519.3497	1036.6848	R.MLAGVDEPLVGI + Oxidation (M)
							601.4197	1200.8248	K.ISPANLNLGMR.M + Oxidation (M)
							714.0314	1426.0482	K.IYPNIEPIQK.I
	gi15235321	AT4G28520 CRU3 (CRUCIFERIN3); nutrient reservoir [Arabidopsis thaliana]	2	57	58199	6.53	668.9727	1335.9308	K.ISYVQGTGISGR.V
	gi166706	cystolic glyceraldehyde-3-phosphate dehydrogenase [Arabidopsis thaliana]	6	51	36963	6.34	417.3119	832.6092	R.IGINGFGR.I
							718.0004	1433.9862	R.AASFNIPSSSTGAAK.A
mascot-36									
1	gi15236992	AT4G27440 2S seed storage protein 1/ 2S albumin storage protein/ MMU1-2S albumin 1 [Arabidopsis thaliana]	18	56	19001	5.63	426.3240	850.6334	R.KIYQTAH
							669.4429	1336.8712	R.LQGHQPMQVR.K + Oxidation (M)
							738.4383	1474.8620	R.QEEDPCVCPCLK.Q + 2 Carbamidomethyl (C)
mascot-01									
10									
mascot-10									
9	gi15238686	ATMS1;5-methyltetrahydropteroyltriglutamate-homocysteine S-methyltransferase/ copper ion binding/ methionine synthase	19	375	84304	6.09	526.3665	1050.7184	K.AVNEYKEA.K
							548.8864	1095.7582	K.YLFAVVDGR.N
							591.3597	1180.7048	K.GVTFAGFDLVR.G
							634.4049	1266.7952	R.GNASVPAMEMTK.W + 2 Oxidation (M)
							706.4406	1410.8866	K.GGIGVQIDEALR.E
							729.5172	1457.0198	R.IPSEIADRNVK.M
							904.0234	1806.0322	K.GMLTGPVTLNWSFVR.N + Oxidation (M)
							692.4202	2074.2388	K.ALAGQKDEALFSANAALASR.R
							1070.6869	2139.3592	K.ALGDVTPVPLVGPVSYLLSK.A
							1155.7069	2309.3992	K.LNLPIPLPTTIGSFPQVELR.R
							770.8144	2309.4214	K.LNLPIPLPTTIGSFPQVELR.R
	gi15235321	AT4G28520 CRU3 (CRUCIFERIN3); nutrient reservoir [Arabidopsis thaliana]	5	186	58199	6.53	668.9803	1335.9460	K.ISYVQGTGISGR.V
	gi18403467	AT3G22640 PAP85; nutrient reservoir [Arabidopsis thaliana]	3	94	55029	6.64	1030.6011	2059.1876	R.YMEQGLYLPFTFTSPK.I
	gi998396	heat-shock Protein [Arabidopsis thaliana]	2	50	79986	4.97	764.5178	1527.0210	K.GIVDSEDLPLNISR.E
mascot-06									
b1c	gi15238686	AT5G17920 ATMS1;5-methyltetrahydropteroyltriglutamate-homocysteine S-methyltransferase/ copper ion binding/ methionine synthase	4	119	84304	6.09	904.0057	1805.9968	K.GMLTGPVTLNWSFVR.N + Oxidation (M)
							1070.6883	2139.3220	K.ALGDVTPVPLVGPVSYLLSK.A
	gi15235321	AT4G28520 CRU3 (CRUCIFERIN3); nutrient reservoir [Arabidopsis thaliana]	3	63	58199	6.53	1030.5747	2059.1348	R.YMEQGLYLPFTFTSPK.I
mascot-b1c									

(Table continues on following page.)

Suppl. data 17 (continued from previous page.)

16	gi15235321	AT4G28520	CRU3 (CRUCIFERIN3); nutrient reservoir [Arabidopsis thaliana]	12	224	58199	6.53	668.8804 927.5294 1030.5781 1035.5786	1335.7462 1853.0442 2059.1416 2069.1426	K.ISYVQGTGISGR.V R.VTSVNSYTLPILEVRL.L R.YVIEQGLYLPTFFTSFK.I R.ALPLEVISNGFQISPEEAR.K
	gi18403462	AT3G22640	PAP85; nutrient reservoir [Arabidopsis thaliana]	14	197	55029	6.64	814.4564 895.5007 1016.0629 1036.5876	1626.8982 1788.9868 2030.1112 2071.1606	R.LAQITVPVWNPQNYK.D K.EVLSTSFVNPPELLGR.L R.TFLAGEENLLSNLNPAAATR.V R.IPSGVNTINTNTQVPLR.L
	gi116215		catalase [Arabidopsis thaliana]	4	89	56849	6.75	523.2981 762.4562	1044.5816 1522.8978	K.SLLEDAIR.L R.LGPNYLQLPWNAPK.C
	gi15236375	AT4G13930	SHM4 (serine hydroxymethyltransferase 4); catalytic/ glycine hydroxymethyltransferase/ pyridoxal phosphate binding [Arabidopsis thaliana]	5	81	51685	6.8	460.2548	918.4950	R.IGAPAMTSR.G+ Oxidation (M)
mascol-16										
12	gi15219584	AT1G03890	cupin family protein [Arabidopsis thaliana]	7	138	49644	5.47	420.7626 598.7861 720.4398	839.5106 1195.5576 1438.8650	R.AVPVDVIA.K K.ASYGVNEEAK.R R.ISTLNSLNLPLVLR.L
	gi1166678		12S storage protein CRB [Arabidopsis thaliana]	12	133	50612	6.77	694.3517 738.7344 808.7634	1386.6888 2213.1814 2423.2684	K.TNENAVNTLAGR.T R.GLPLEVITNGFQISPEEAR.V R.VFDEISSQLLVVPGFSVMK.H+ Oxidation (M)
	gi1166676		12S storage protein CRA1 [Arabidopsis thaliana]	4	99	52592	7.68	1035.5640	2069.1134	R.GLPLEVITNGFQISPEEAR.R
	gi1107497	AT5G40420	oleosin type2 [Arabidopsis thaliana]	15	80	21125	9.13	505.2293 563.7734 589.3143	1008.4440 1125.5322 1176.6140	R.GQGQYEGDR.G R.MADAVYAGQK.G+ Oxidation (M) R.TVPEQLEYAK.R
	gi15235321	AT4G28520	CRU3 (CRUCIFERIN3); nutrient reservoir [Arabidopsis thaliana]	7	68	58199	6.53	1030.5453 1035.5640	2059.0760 2069.1134	R.YVIEQGLYLPTFFTSFK.I R.ALPLEVISNGFQISPEEAR.K
	gi116215		catalase [Arabidopsis thaliana]	3	58	56849	6.75	993.0142	1984.0138	R.EGNFDLVGNVFPVFR.D
mascol-12										
13	gi15229231	AT3G04120	GAPC1 (GLYCERALDEHYDE-3-PHOSPHATE DEHYDROGENASE SUBUNIT 1); glyceraldehyde-3-phosphate dehydrogenase (phosphorylating)/ glyceraldehyde-3-phosphate dehydrogenase [Arabidopsis thaliana]	26	284	36891	6.62	400.7482 406.2542 417.2307 455.7321 464.7944 495.7600 519.7797 614.3421 717.8760 1086.5190	799.4818 810.4938 832.4468 909.4496 927.5742 989.5054 1037.5448 1226.6696 1433.7374 2171.0234	K.VISAPSK.D K.VLPLALNGK.L R.IGINFGFR.I K.AATYDEIK.K K.KVISAPSK.D K.AIKEESEGL.L K.AATYDEIK.A R.VDLVHMSKA.+ Oxidation (M) R.AASFNIIPSTGAAK.A K.GILGYTEDWSTDFVGNR.S
	gi15231715	AT3G52930	fructose-bisphosphate aldolase, putative [Arabidopsis thaliana]	15	183	38516	6.05	415.2061 531.2592 744.9029 777.0735 1165.1191	828.3976 1060.5038 1487.7912 2328.1987 2328.2236	K.YYEAGAR.F R.NLNAMNQLK.T+ Oxidation (M) K.GILADESTGTIGR.L R.TVPAAPVAVIVLSSGGQSEEEATR.N R.TVPAAPVAVIVLSSGGQSEEEATR.N
	gi15219721	AT1G04410	malate dehydrogenase, cytosolic, putative [Arabidopsis thaliana]	9	76	35548	6.11	409.2212 472.2766 825.5084	816.4278 942.5386 1649.0022	K.SQAALAK.H R.LSVPDVK.N K.VLWNPANTNALIK.E
	gi15235321	AT4G28520	CRU3 (CRUCIFERIN3); nutrient reservoir [Arabidopsis thaliana]	2	64	58199	6.53	668.8698	1335.7250	K.ISYVQGTGISGR.V
	gi15220051	AT1G80090	CBS domain-containing protein [Arabidopsis thaliana]	3	54	43757	6.87	668.3659	1334.7172	R.TLLFATATSTPGR.E
mascol-18										
14	gi15218868	AT1G68930	isocitrate dehydrogenase, putative / NADP+ isocitrate dehydrogenase, putative [Arabidopsis thaliana]	30	565	45717	6.13	471.7362 528.8093 560.2625 634.3323 644.3771 452.5674 678.3552 717.8230 854.8873 899.4431 1021.4985	941.4578 1055.6040 1118.5104 1266.6500 1286.7396 1354.6804 1354.6958 1433.6314 1707.7600 1796.8716 2040.9824	K.LMTFEGK.D+ Oxidation (M) R.ATDAVKGPGK.L K.CATITPDEGR.V+ Carbamidomethyl (C) R.LIDDMVAALK.S+ Oxidation (M) K.LITPFVELDIK.Y K.TIEEAAHGTVTR.H K.TIEEAAHGTVTR.H R.FADASMNNTAYEK.K+ Oxidation (M) K.VANPVMGDQDMTR.V+ 2 Oxidation (M) K.GGETSNTSISIFAWR.G R.DTYLNTFEEDIVAAELK.E
	gi15235321	AT4G28520	CRU3 (CRUCIFERIN3); nutrient reservoir [Arabidopsis thaliana]	13	185	58199	6.53	621.8503 668.8660 697.3374 927.5026 1035.5488	1241.6880 1335.7174 1392.6602 1852.9906 2069.0830	R.GVLQGNAMVLPK.Y+ Oxidation (M) K.ISYVQGTGISGR.V K.TNENAMISLAGR.T+ Oxidation (M) R.VTSVNSYTLPILEVRL.L R.ALPLEVISNGFQISPEEAR.K
	gi1166676		12S storage protein CRA1 [Arabidopsis thaliana]	8	85	52592	7.68	518.7484 596.7548 1035.5488	1035.4822 1191.4950 2069.0830	R.FEQGQSQR.F R.CTDNDDPSR.A+ Carbamidomethyl (C) R.GLPLEVITNGFQISPEEAR.R
	gi15236995	AT4G27150	2S seed storage protein 2 / 2S albumin storage protein / NMMU2-2S albumin 2	12	76	19348	6.79	454.2408 756.3920	906.4670 1510.7694	K.YLPNICK.I+ Carbamidomethyl (C) R.AVSLQGHGPFQSR.K
	gi15241945	AT5G28840	GME (GDP-D-MANNOSE 3',5'-EPIMERASE); GDP-mannose 3,5-epimerase/ NAD or NADH binding / catalytic [Arabidopsis thaliana]	3	75	42731	5.85	712.9164	1423.8182	K.WGTQAPVQLSLR.A
	gi18423187	AT5G50600	AtHSD1 (hydroxysteroid dehydrogenase 1); binding / catalytic/ oxidoreductase [Arabidopsis thaliana]	4	59	39062	5.92	458.7545	915.4944	R.IMDIPGVR.S+ Oxidation (M)
	gi1166678		12S storage protein CRB [Arabidopsis thaliana]	4	51	50612	6.77	466.7532 1029.5382	931.4918 2057.0618	R.GACLALTAR.R+ Carbamidomethyl (C) R.GLPLEVITNGFQISPEEAR.R
mascol-14										
19	gi121537178		xylose isomerase [Arabidopsis thaliana]	16	182	53642	5.54	572.3127 672.8741 682.8348 745.3558 757.3527 951.4442	1142.6108 1343.7336 1363.6550 1488.6970 1512.6908 1900.8738	K.NLDELAK.E K.ILEEGSLSELVR.K K.NGGIAPGGFNDAK.L R.DIAPDGTLEESKN.N R.EGYQTLNTDMGR.E+ Oxidation (M) K.VSSAKOELAMIFQSAM.+ 2 Oxidation (M)
	gi15227982	AT2G36530	LOS2; copper ion binding / phosphopyruvate hydratase [Arabidopsis thaliana]	11	133	47689	5.54	775.4531 942.9858 1003.0338	1548.8916 1883.9570 2004.0530	K.AVGNWNIIPALIGK.D R.LAMQFMIPLVGAASF.K.E+ 2 Oxidation (M) K.VTAAVPSGASTGYALELR.D
	gi15225782	AT2G33070	NSP2 (NITRILESPECIFIER PROTEIN 2) [Arabidopsis thaliana]	13	100	51182	5.5	482.7721 507.7826 630.3099 654.3708 972.4933	963.5296 1013.5506 1258.6052 1306.7270 1942.9720	R.SVFASAWGK.H R.GGAGLEWQK.V K.LGEEETPSIR.G K.LLTPVEQPTPR.S R.STDVLHSLGAYSSPATPK.L
	gi1150740		GDP-associated inhibitor [Arabidopsis thaliana]	4	37	49813	5.49	536.7748 582.7845	1071.5350 1163.5544	K.VPATPMEALK.S+ Oxidation (M) K.VSGTSEGETAK.C
mascol-18										

(Table continues on following page.)

Suppl. data 17 (continued from previous page.)

26	gi15235321	AT4G28520	CRU3 (CRUCIFERIN3); nutrient reservoir [Arabidopsis thaliana]	14	207	58199	6.53	424.2994 621.8536 668.8712 697.3439 927.5353 942.4949	846.5842 1241.6926 1335.7278 1392.6732 1853.0560 1882.9752	R.CVGSVVAR.Y+Carbamidomet hyl (C) R.GVLQGNAMVLPK.Y+Oxidation (M) K.ISYVVOGTGISGR.V K.TNENAMISTLAGR.T+Oxidation (M) R.VTSVNSYTLPILEYVR.L K.IDVQLAQQLNQDQSR.G
	gi166678		12S storage protein CRB [Arabidopsis thaliana]	8	88	50612	6.77	559.3494 694.3503 1029.5734	558.3421 1386.6860 2057.1322	R.LSALR.G K.TNENAOVNTLAGR.T R.GLPLEVITNGYQISPEEAK.R
	gi15232888	AT3G02360	6-phosphogluconate dehydrogenase family protein [Arabidopsis thaliana]	5	65	53544	7.02	508.2790 822.4585	1014.5434 1642.8984	K.AGSPVDQTIK.T R.NAELANLLVDPEFAK.E
	gi134222076	AT3G21380	At3g21380 [Arabidopsis thaliana]	4	54	49249		934.4749	1866.9352	R.GTPSAQTPPGSAQPTGSAGAK.K
mascol_26										
27	gi15240946	AT5G01300	phosphatidylethanolamine-binding family protein [Arabidopsis thaliana]	10	197	17812	5.34	897.4401	1792.8656	K.GLPEGYSNEDQTTGIR.E
mascol_27										
28	gi175309952	AT1G54870	RecName: Full=Glucose and ribitol dehydrogenase homolog 1	24	164	31368	6.11	471.8138 590.8221 602.8659 608.3864 627.3625 792.4485	941.6130 1179.6296 1203.7172 1214.7582 1252.7104 1582.8824	R.GLALQLAEK.G K.NFGSEVPMKR.A+Oxidation (M) R.VVDEVNAFGR.I R.VALITGDSGISGR.A K.GNASLLDYATK.G K.EGSSIINTTSVNAKY.G
	gi15235321	AT4G28520	CRU3 (CRUCIFERIN3); nutrient reservoir [Arabidopsis thaliana]	7	138	58199	6.53	424.2493 668.9099 1030.6102	846.4840 1335.8052 2059.2058	R.CVGSVVAR.Y+Carbamidomet hyl (C) K.ISYVVOGTGISGR.V R.YMEDQGLYLPTFTTSPK.I
	gi1526422		LEA protein in group 5 [Arabidopsis thaliana]	6	94	26810	5.46	780.9399	1559.8652	R.GGPAAMVMSAATTNIR.G+Oxidation (M)
	gi18778288		F14D16.30 [Arabidopsis thaliana]	7	85	38913	9.49	554.2886 835.4980	1106.5626 1668.9814	R.AEFOEQEQR.V R.IDSGLDLNLIPSER.I
mascol_28										
15	gi166678		12S storage protein CRB [Arabidopsis thaliana]	13	337	50612	6.77	487.2622 633.6906 996.1343 1011.6068	972.5098 1898.0500 1990.2540 2021.1990	R.CSGFAFER.F+Carbamidomet hyl (C) K.INVETAQQLNQODNR.G R.FVMEPQGLFLPTFLNAGK.L K.QNNIFNGFAPELAAQAF.I
	gi15226403	AT2G28490	cupin family protein [Arabidopsis thaliana]	5	178	55670	5.83	475.7651 631.8578 637.9009	949.5156 1261.7010 1273.7872	K.DKPSFDNK.Y R.YFAFCQASR.T+Carbamidomet hyl (C) R.VSVGDVFWPR.Y
	gi15220526	AT1G05510	unknown protein [Arabidopsis thaliana]	21	171	27276	6.22	639.4229 684.4334 746.9013	1276.8312 1366.8522 1491.7880	R.LIGLEIVYTEK.L R.EIDIKVSVPR.V R.OCLIVDGPDANAR.L+Carbamidomet hyl (C)
	gi15235321	AT4G28520	CRU3 (CRUCIFERIN3); nutrient reservoir [Arabidopsis thaliana]	4	67	58199	6.53	817.9868 668.9134 697.4176	1633.9590 1335.8122 1392.8206	K.GGFLFMPGVPEAIQR.Q+Oxidation (M) K.ISYVVOGTGISGR.V K.TNENAMISTLAGR.T+Oxidation (M)
	gi15221082	AT1G48130	ATPER1; antioxidant / thioredoxin peroxidase [Arabidopsis thaliana]	16	67	24066	6.12	430.2737 446.7398 532.8301 621.3832	858.5328 891.4650 1063.6456 1240.7518	K.TADLP SKK.G R.NMDVLR.A+Oxidation (M) R.ALDSLLMASK.H+Oxidation (M) K.LSFLYPTTGR.N
	gi130694455	AT5G44120	CRA1 (CRUCIFERINA); nutrient reservoir [Arabidopsis thaliana]	2	50	41007	6.62	518.7761	1035.5376	R.FEGGQSQSR.F
	gi15219584	AT1G03890	cupin family protein [Arabidopsis thaliana]	5	40	49644	5.47	417.2452 463.2640 549.8165	832.4758 924.5134 1097.6184	R.CAGVTVAR.I+Carbamidomet hyl (C) R.MFQLAGSR.T+Oxidation (M) R.ENQLDQVPR.M
mascol_15										
21	gi166678	AT1G03880	12S storage protein CRB [Arabidopsis thaliana]	3	64	50612	6.77	996.1442	1990.2738	R.FVMEPQGLFLPTFLNAGK.L
mascol_21										

I declare that I am the sole author of this submitted dissertation and that I did not make use of any sources or help apart from those specifically referred to. Experimental data or material collected from or produced by other persons is made easily identifiable.

I also declare that I did not apply for permission to enter the examination procedure at another institution and that the dissertation is neither presented to any other faculty, nor used in its current or any other form in another examination.

City, Date

Arman Allboje Samami

Acknowledgment

First of all, I would like to thank Prof. Dr. Rüdiger Hell for giving me the possibility to work in his group and for his great supervision. His great teaching raised my interest for molecular biology of plants during my studies. During my PhD he remained an inspiring source for me with his new ideas and motivating input. I would also like to thank him for his support in many matters beyond the lab and university.

My thanks are also extended to Dr. Markus Wirtz for critical reading and fast correction of my thesis and the valuable discussions. He never hesitated to share his lab skills and huge knowledge about sulfur in plants and was helpful whenever he could.

I am thankful to our cooperation partners who contributed to this thesis which would not be in this final shape without their kind support: Dr. Karine Gallardo, Dr. H el ene Zuber, Delphine H ericher (INRA, Dijon; for seed proteome analysis); Dr. Li Li and Maria Saile (ZMF, Mannheim; for microarray analysis); Dr. Stefan Hillmer, Stephanie Gold (COS, Heidelberg; for electron microscopy); Dr. Bettina Hause, Prof. Dr. Claus Wasternack (IPB, Halle; for jasmonate measurement); Dr. Adriano Nunes-Nesi (MPI, Golm; for large scale metabolite quantification); Allan Jones (DKFZ, Heidelberg; not only for TAG measurement or language correction of my thesis, but for being a good and supportive friend during our whole study time in Heidelberg - *high five!*).

Many thanks also go to all the members of Hell group for creating a friendly and work promoting atmosphere. I also like to thank current and former colleague who have become friends of mine; together we had a great time also outside the lab in the real world: Eric Lister, Anna Speiser, Dr. Florian Haas, Dr. Achim Boltz and Dr. Corinna Wolf. Thanks also go to Lili Hocke for her help during her practical course, and Michael Schulz for excellent technical assistance.

I would also like to thank my friends for their support and sharing a great time.

I am greatly thankful to my great family, specially my little sister for her positive support and kindness. My greatest thanks are extended to my father who always believed in me, encouraged me and made my education possible. I would like to thank Sara for her endless love reaching me no matter how far away we are from each other.